



**Joana Formigal
Tavares**

**Identificação de novos reguladores da fidelidade da
síntese proteica**

**Identification of novel regulators of protein
synthesis fidelity using high content genetic
screens**



**Joana Formigal
Tavares**

**Identificação de novos reguladores da fidelidade da
síntese proteica**

**Identification of novel regulators of protein synthesis
fidelity using high content genetic screens**

Tese apresentada à Universidade de Aveiro para cumprimento dos requisitos necessários à obtenção do grau de Doutor em Biomedicina, realizada sob a orientação científica da Doutora Gabriela Maria Ferreira Ribeiro de Moura, Professora Auxiliar do Departamento de Ciências Médicas da Universidade de Aveiro, e a coorientação científica do Doutor Manuel António da Silva Santos, Professor Associado do Departamento de Ciências Médicas da Universidade de Aveiro

o júri

presidente

Prof. Doutor João Filipe Colardelle da Luz Mano
Professor Catedrático, Universidade de Aveiro

Doutor Rui Miguel Pinheiro Vitorino
Professor Auxiliar Convidado, Universidade de Aveiro

Doutor Peter Dedon
Professor Catedrático, Massachusetts Institute of Technology

Doutora Cecília Maria Pais de Faria de Andrade Arraiano
Investigadora Coordenadora, Universidade Nova de Lisboa

Prof. Doutor Manuel António da Silva Santos
Professor Associado, Universidade de Aveiro

agradecimentos

acknowledgements

I would like to thank my supervisors, Prof Dr Gabriela Moura and Prof Dr Manuel Santos, for guidance and advice, and to all members of the lab, past and present, for support and fruitful discussions.

I am very grateful to Dr Peter Dedon and all members of his group, for teaching me all about quantification of RNA modifications by MS and for their support during my stay at MIT. In particular, my thanks go to Stefanie Kellner for technical and data analysis assistance, and for the interesting lunches. A big thank you to Catarina Seabra and Ana Tellechea, for making me feel at home!

I am indebted to FCT, for financial support through a PhD grant SFRH/BD/86866/2012 and project PTDC/BEX-BCM/2121/2014, and iBiMED (UID/BIM/04501/2013) and Universidade de Aveiro for technical and academic support.

As science is a highly collaborative activity, this work would not have been the same without the help of several people, to whom I would like to particularly thank: Rui Fernandes and Francisco Figueiredo, for all the help with transmission electron microscopy; Prof. Vera Afreixo, for all the statistical support; Amanda Del Rosario, Richard and Nick Davis from MIT and Eduard Sabido Aguade and Guadalupe Espadas-García from CRG, for introducing me to proteomic analysis using mass-spectrometry; and Andreia Reis, for creating all the scripts I needed, whenever I needed.

A very special thanks to my parents, for their encouragement, care and tolerance. I also want to thank all the friends and family that have always supported me. Finally, I thank Luís, for your support, listening and advising, and for being by my side at all moments.

palavras-chave

tRNA, rRNA, modificações do RNA, síntese proteica, fidelidade, misincorporação de aminoácidos, agregação de proteínas, *Saccharomyces cerevisiae*.

resumo

A síntese proteica é central para a vida e tem sido extensivamente estudada a vários níveis. Contudo, o estudo da fidelidade da tradução do mRNA tem progredido lentamente devido a dificuldades técnicas na detecção de incorporações incorretas de aminoácidos nas proteínas. Poucos genes têm sido associados com o controlo da fidelidade da síntese proteica e não é evidente quais os genes que controlam este processo biológico. Nesta tese investigámos o papel da modificação dos nucleósidos do RNA na eficiência e precisão da síntese proteica. A nossa hipótese é que as enzimas que modificam nucleósidos do tRNA (tRNAmods) têm um impacto significativo na síntese proteica através da modulação das interações codão-anticodão. A biologia das tRNAmods e das modificações do tRNA são ainda pouco conhecidas, mas estão envolvidas na estabilidade e função do RNA e mutações nos seus genes causam doenças neurodegenerativas, metabólicas, cancro, entre outras. Neste projeto realizámos um rastreio genético em levedura com o objetivo de identificar tRNAmods que asseguram a homeostase do proteoma (proteostase) e usámos espectrometria de massa para clarificar o papel das tRNAmods na fidelidade da síntese proteica.

Os resultados do estudo genético mostram que um sub-grupo de tRNAmods envolvidas na modificação de nucleósidos do anticodão do tRNA são essenciais para manter a estabilidade do proteoma. Outras tRNAmods estudadas não produziram impactos visíveis na proteostase.

Os genes de proteínas agregadas que isolámos a partir de células de levedura com tRNAs hipomodificados são enriquecidos em codões descodificados por estes tRNAs. Os nossos dados mostram também que tais proteínas participam em processos biológicos específicos e têm níveis de aminoácidos errados mais elevados que as células *wild-type*. Estes dados mostram que certas modificações do tRNA são essenciais para a fisiologia celular, estabilidade do proteoma e fidelidade da síntese proteica.

keywords

tRNA, rRNA, RNA modifications, protein synthesis, fidelity, amino acid misincorporations, protein aggregation, *Saccharomyces cerevisiae*.

abstract

Protein synthesis is central to life and is being intensively studied at various levels. The exception is mRNA translational fidelity whose study has been hampered by technical difficulties in detecting amino acid misincorporations in proteins. Few genes have so far been associated to the control of protein synthesis fidelity and it is unclear how many genes control this biological process. We investigated the role of RNA modification by RNA modifying enzymes (RNAmods) in protein synthesis efficiency and accuracy. Our hypothesis was that RNAmods that modify tRNA nucleosides (tRNAmods) have a significant impact on protein synthesis through modulation of codon-anticodon interactions. To address this issue, we focused our work on tRNAmods involved in the modification of tRNA anticodons. The biology of these enzymes is still poorly understood, but they are involved in RNA processing, stability and function and their deregulation is associated with cancer, neurodegenerative, metabolic and other diseases.

We have set up a yeast genetic screen and used mass-spectrometry methods to determine the role of tRNAmods on proteome homeostasis. Our work identified a subgroup of yeast tRNAmods that play essential roles in protein synthesis fidelity and folding.

The genes that encode insoluble proteins isolated from yeast cells lacking U₃₄ modification were enriched in codon sites that are decoded by the hypomodified tRNAs. These aggregated proteins also participate in specific biological processes, suggesting that tRNAmods are linked to specific physiological pathways. Interestingly, we detected amino acid misincorporations at the codon sites decoded by the anticodons of the hypomodified tRNAs, demonstrating that tRNA U₃₄ modifications control translational error rate.

CONTENTS

List of Tables	iv
List of Figures.....	v
List of Abbreviations	ix
1. Introduction	1
1.1 Overview	2
1.2 Transfer RNA	2
1.2.1 tRNA structure	3
1.2.2 tRNA biogenesis.....	4
1.2.3 tRNA quality control	18
1.3 The ribosome	23
1.3.1 Structure of ribosomes.....	24
1.3.2 Ribosome biogenesis	27
1.3.3 Quality control.....	42
1.4 Protein biosynthesis	44
1.4.1 Translation.....	45
1.4.2 Translation fidelity.....	53
1.5 Protein folding and misfolding	57
1.5.1 Protein aggregation	58
1.5.2 Cellular protein quality control mechanisms	60
1.6 Translational fidelity, protein aggregation and disease.....	71
1.7 Objectives of the study	75
2. Methods.....	77
2.1 Yeast strains and growth conditions.....	78
2.2 In vivo detection of protein aggregates.....	84
2.2.1 Amplification of the genes of interest by PCR.....	85
2.2.2 Yeast transformation.....	86
2.2.3 Analytical colony PCR	87
2.2.4 Fluorescence microscopy	87
2.3 Validation of gene deletions by PCR.....	88
2.3.1 DNA extraction.....	88
2.3.2 PCR	88

2.4	Transmission electron microscopy for ultrastructural analysis	89
2.5	Physiology of selected KO strains	90
2.5.1	Growth curves.....	90
2.5.2	Cell viability assays.....	90
2.5.3	Proteasome activity assay	91
2.6	Biochemical characterization of tRNAs	92
2.6.1	RNA extraction and tRNA purification	92
2.6.2	Isolation of total tRNA and total rRNA by HPLC	93
2.6.3	Quantification of ribonucleosides by LC-MS/MS.....	94
2.7	tRNA quantification using four-leaf clover qRT-PCR	98
2.7.1	Total RNA isolation	98
2.7.2	Deacylation treatment.....	98
2.7.3	Annealing and ligation of SL-adaptors to mature tRNAs.....	99
2.7.4	TaqMan qRT-PCR for mature tRNAs	99
2.8	Proteome profiling and quantification of amino acid misincorporations .	101
2.8.1	Extraction of insoluble aggregates.....	101
2.8.2	Protein sample preparation (Reduction, Alkylation and Tryptic Digestion).....	102
2.8.3	Chromatographic and mass spectrometric analysis	102
2.8.4	Data analysis	103
3.	Genetic screen to identify RNAmods required to maintain proteostasis	107
3.1	Introduction	108
3.1.1	Methyltransferases	110
3.1.2	Thiolases and mediators.....	116
3.1.3	Deaminases.....	118
3.1.4	RNA pseudouridine synthases.....	119
3.1.5	Dihydrouridine synthases	121
3.1.6	Overview of this study.....	121
3.2	Results	121
3.2.1	RNA-modifying enzymes are important for protein synthesis fidelity	121
3.2.2	Absence of RNAmods influences cellular fitness.....	133
3.2.3	Deletion of RNAmods decreases tRNA stability and modification levels	137

3.3	Discussion.....	141
3.3.1	Proteins involved in the U ₃₄ modification are critical for proteostasis	143
3.3.2	Deletion of rRNA-modifying enzymes causes protein aggregation .	149
3.3.3	Phenotypic characterization of the selected KO strains.....	151
3.3.4	Characterization of the KO strains.....	153
3.4	Conclusion	156
4.	U ₃₄ modifications of tRNA anticodons maintain proteome integrity.....	157
4.1	Introduction	158
4.1.1	The role of modified nucleosides in translation.....	158
4.1.2	The role of modified nucleosides in translational accuracy.....	161
4.1.3	Overview of this study.....	162
4.2	Results	163
4.2.1	Identification of proteins that aggregated in yeast strains lacking U ₃₄ modification.....	163
4.2.2	Codon biases in the genes of the aggregated proteins.....	172
4.2.3	U ₃₄ modifications fine tune translational accuracy	182
4.2.4	Aggregated proteins have homologues in humans.....	190
4.3	Discussion.....	191
4.3.1	U ₃₄ modification is important to maintain proteome homeostasis ...	192
4.3.2	Loss of U ₃₄ modifications affects the translation of genes enriched in specific codons	193
4.3.3	Loss of U ₃₄ modifications elevates codon mistranslation rate.....	196
4.4	Conclusion	198
5.	General discussion	199
5.1	rRNA modifications and proteostasis	200
5.2	tRNA modifications and proteostasis.....	201
5.2.1	tRNAmods that modify the body of tRNAs have little impact on proteostasis	202
5.2.2	tRNAmods that modify the tRNA anticodon loop affect proteostasis	204
5.3	Wobble uridine modification	207
5.3.1	Absence of U ₃₄ modifications increases mistranslation	209
5.3.2	Protein synthesis errors and human disease.....	210
5.4	Conclusion and future work.....	211

6. References	213
7. Annexes.....	253

LIST OF TABLES

Table 1.1. Subcellular location of the biosynthesis, processing and turnover of the cytoplasmic tRNAs in yeast and vertebrates.	6
Table 1.2. Major effects of mistranslation in <i>S. cerevisiae</i>	56
Table 1.3. Summary of the main diseases related to protein aggregation.	72
Table 1.4. tRNA-related diseases.....	74
Table 2.1. List of strains used in this study.....	78
Table 2.2. List of oligonucleotides used for GFP fusion proteins construction. ...	86
Table 2.3. Primers used for selected KO strains validation.	89
Table 2.4. Fraction collection timetable used for HPLC-based purification of tRNA and rRNA.....	93
Table 2.5. Solvent gradient used by the UPLC-MS system.....	95
Table 2.6. Dynamic MRM parameters for tRNA ribonucleosides identification based on optimizer results.	95
Table 2.7. Dynamic MRM parameters for rRNA ribonucleosides identification based on optimizer results.	96
Table 2.8. Sequences of adaptors for FL-PCR.....	99
Table 2.9. Sequences of primers for FL-PCR.....	100
Table 2.10. Synthetic peptides (Pepscan) added to insoluble fraction samples for LC-MS/MS analysis.	102
Table 3.1. KO strains grouped according their function on RNA modification. ...	122
Table 3.2. Summary of the Elongator complex protein aggregation data.	143
Table 3.3. Summary of protein aggregation data of the regulators of the Elongator complex.	145
Table 3.4. Summary of protein aggregation data of the U ₃₄ thiolases and modifiers of mt-tRNAs.	148

Table 4.1. Summary of amino acid and codon composition data of the aggregated proteins in the absence of U ₃₄ modification.	176
Table 4.2. List of human orthologues associated to disease found in the aggregated proteins in the Elp1Δ strain.	191
Table 4.3. Summary of codon usage and amino acid misincorporation observed in KO strains.....	197

LIST OF FIGURES

Figure 1.1. The structure of tRNAs.....	4
Figure 1.2. tRNA biogenesis in <i>S. cerevisiae</i>	5
Figure 1.3. Structure of yeast tRNA genes and model of tRNA transcription.	7
Figure 1.4. From tRNA precursor to mature tRNA.....	8
Figure 1.5. The 5' leader sequence from pre-tRNAs is cleaved by RNase P.	9
Figure 1.6. Model for pre-tRNA 3'-end processing. ...	10
Figure 1.7. The pre-tRNA splicing pathway in yeast.....	12
Figure 1.8. Schematic pattern of modifications found in <i>S. cerevisiae</i> tRNA.....	13
Figure 1.9. Two-step mechanism of aminoacylation by aaRS.....	16
Figure 1.10. Aminoacyl-tRNA synthetase recognition hot spots present in the three-dimensional structure of tRNA.....	17
Figure 1.11. The nuclear surveillance pathway of tRNAs.....	19
Figure 1.12. The rapid tRNA decay (RTD) pathway.	20
Figure 1.13. Quality control steps for mischarged tRNA.....	22
Figure 1.14. Secondary structure of the <i>S. cerevisiae</i> ribosomal RNA.....	26
Figure 1.15. Three-dimensional structure of the yeast ribosome.	27
Figure 1.16. Eukaryotic ribosome synthesis.....	28
Figure 1.17. Structure of rDNA in yeast.....	30
Figure 1.18. Pre-rRNA processing in <i>S. cerevisiae</i>	32
Figure 1.19. Distribution of rRNA modifications in the yeast ribosome.....	35
Figure 1.20. Three-dimensional distribution of rRNA modifications in the <i>S. cerevisiae</i> ribosome.	36
Figure 1.21. rRNA modification by snoRNPs.....	39

Figure 1.22. Maturation of pre-ribosomes to form 40S and 60S ribosomal subunits.	42
Figure 1.23. Types of errors that may affect protein synthesis and folding.	45
Figure 1.24. Eukaryotic translation initiation model.	48
Figure 1.25. Eukaryotic translation elongation model.....	50
Figure 1.26. Translation termination complex.....	52
Figure 1.27. Eukaryotic translation termination and ribosome recycling model. ...	53
Figure 1.28. Model for sorting of misfolded proteins to different quality control compartments.....	60
Figure 1.29. Protein quality control.....	62
Figure 1.30. Protein folding assisted by chaperones and co-chaperones as a protein quality control mechanism.	66
Figure 1.31. The ubiquitin-proteasome system.	68
Figure 1.32. Types of autophagy in yeast.	70
Figure 2.1. Strategy for the construction of fluorescent molecular sensors of protein aggregation.	85
Figure 2.2. Retention time and peak width of tRNA and rRNA signals recorded in the HPLC system for programmed fraction collection.	93
Figure 2.3. Method to calculate gene-specific usage patterns weighted by tRNA availability.	105
Figure 3.1. Modified bases and ribose moieties of RNAs.....	109
Figure 3.2. The holoElongator complex structure.....	112
Figure 3.3. Pathway for mcm ⁵ s ² U ₃₄ modification.....	114
Figure 3.4. Pathway for yW modification.	115
Figure 3.5. tRNA modifications synthesized by some methyltransferases.	116
Figure 3.6. Cellular sulfur trafficking related to thiouridine formation of cytoplasmic tRNA anticodon in <i>S. cerevisiae</i>	117
Figure 3.7. Thiouridine formation of mitochondrial tRNA anticodon in <i>S. cerevisiae</i>	118
Figure 3.8. Network analysis of RNAmods.....	123

Figure 3.9. Deletion of specific RNAmods induces cytoplasmic protein aggregates.	124
Figure 3.10. Effect of deletion of wobble uridine modifying enzymes on the formation of protein aggregates.	125
Figure 3.11. Effect of deletion of tRNA-modifying enzymes on the formation of protein aggregates.	126
Figure 3.12. Effect of deletion of rRNA-modifying enzymes on the formation of protein aggregates.	127
Figure 3.13. Heat-map representing the number and type of protein aggregates per cell.	128
Figure 3.14. Top 10 KO strains with protein aggregates.	130
Figure 3.15. Ultrastructure of WT and selected RNAmod KO yeast cells.	131
Figure 3.16. Deletion of RNAmods increases the level of insoluble proteins. ...	132
Figure 3.17. Deletion of selected RNAmods increases proteasome activity.	133
Figure 3.18. Growth rate and cell viability of the selected KO strains.	134
Figure 3.19. Cells lacking RNAmods are sensitive to heat stress.	136
Figure 3.20. Hierarchical cluster of the relative levels of tRNA ribonucleoside modifications in selected KO strains.....	138
Figure 3.21. Hierarchical cluster visualization of the relative levels of rRNA ribonucleoside modifications in rRNAmods KO strains.	139
Figure 3.22. Distribution of cytoplasmic <i>S. cerevisiae</i> tRNAs through the genetic code.	140
Figure 3.23. Quantification of wobble modified tRNAs in selected tRNAmods KO strains.	140
Figure 3.24. Synthesis of U ₃₄ modification by the tRNAmods analyzed in this study.	153
Figure 4.1. The standard genetic code table.	158
Figure 4.2. Codon-anticodon pairing rules (yeast).....	161
Figure 4.3. Absence of U ₃₄ modifications leads to protein aggregation in yeast..	164
Figure 4.4. Workflow for proteome analysis of insoluble fractions by LC-MS/MS.	165

Figure 4.5. Label-free quantitative mass spectrometry identification of up-regulated proteins that aggregated in mutant strains, relative to WT.	166
Figure 4.6. Biochemical characterization of up-regulated proteins that aggregated in the mutants lacking U ₃₄ modifications.	167
Figure 4.7. Functional enrichment in up-regulated proteins that aggregated in Trm9Δ.	169
Figure 4.8. Functional enrichment in up-regulated proteins that aggregated in Elp1Δ.	170
Figure 4.9. Functional enrichment in up-regulated proteins that aggregated in Slm3Δ.....	171
Figure 4.10. Heat-map of the functional enrichment in biological processes verified in the up-regulated proteins that aggregated in mutant strains.....	172
Figure 4.11. Codons affected by U ₃₄ hypomodification.	173
Figure 4.12. Amino acid and codon composition of aggregated proteins in the absence of wobble uridine modification.....	175
Figure 4.13. Hierarchical clustering analysis of gene-specific codon usage patterns (Z-scores) for genes corresponding to the aggregated proteins in Trm9Δ.	178
Figure 4.14. Hierarchical clustering analysis of gene-specific codon usage patterns (Z-scores) for genes corresponding to the aggregated proteins in Elp1Δ.	179
Figure 4.15. Hierarchical clustering analysis of gene-specific codon usage patterns (Z-scores) for genes corresponding to the aggregated proteins in Slm3Δ.	180
Figure 4.16. Codon composition of the proteins that aggregated in the absence of wobble uridine modification.	182
Figure 4.17. Mini-genetic code table with two-split codon boxes.	184
Figure 4.18. Detection of amino acid misincorporation.....	185
Figure 4.19. Amino acid misincorporations observed in up-regulated aggregated proteins in KO strains.	187
Figure 4.20. Amino acid misincorporations occurred in specific codon sites.	189
Figure 5.1. Positions of the modifications catalyzed by tRNAmods that were analyzed in this study.	202
Figure 5.2. The genetic code and tRNA wobble modifications.	208

LIST OF ABBREVIATIONS

[¹⁵ N] ⁵ -dA – [¹⁵ N] ⁵ -2-deoxyadenosine	ct ⁶ A – cyclic N ⁶ -
Å - ångström	threonylcarbamoyladenine
A – adenine	D – dihydrouridine
A (nA) – ampère (nanoampère)	Da (kDa) – Dalton (kilodalton)
A-site – aminoacyl-tRNA site	DEAE – diethylaminoethyl
aa-AMP – aminoacyl-AMP	DNA – deoxyribonucleic acid
aa-tRNA – aminoacyl-tRNA	dNTP – deoxyribonucleotide triphosphate
aaRS – aminoacyl-tRNA synthetase	DTT – dithiothreitol
ac ⁴ C – 4-acetylcytidine	DDA – data dependent acquisition
ACN – acetonitrile	E-site – exit-tRNA site
acp ³ Ψ – 3-(3-amino-3-carboxypropyl)pseudouridine	EDTA – ethylenediamine tetracetic acid
AGC – auto gain control	EF – elongator factor
Am – 2'-O-methyladenosine	ESI – electrospray ionization
AMC – 7-amino-4-methylcoumarin	FDR – false discovery rate
AMP – adenosine 5'-monophosphate	G – guanine
APS – ammonium persulphate	g (mg, µg, ng) – gram (milligram, microgram, nanogram)
Ar(p) – 2'-O-ribosyladenosine (phosphate)	GFP – green fluorescent protein
ATP – adenosine 5'-triphosphate	Gm – 2'-O-methylguanosine
BCA – bicinchoninic acid	GO – gene ontology
BHT – butylated Hydroxytoluene	GS – growth score
bp – base pair	GTP – guanosine-5'-triphosphate
C – cytosine	HCD – high-energy collision dissociation
cDNA – complementary DNA	HCl – hydrogen chloride
CID – collision-induced dissociation	HEPES – 4-(2-hydroxyethyl)-1-piperazineethanesulfonic acid
Cm – 2'-O-methylcytidine	His – histidine
cm ⁵ U – 5-carboxymethyluridine	hm ⁵ C – 5-hydroxymethylcytidine
cm ⁵ Um – 5-carboxymethyl-2'-O-methyl	HPLC – high-performance liquid chromatography
cmnm ⁵ U – 5-carboxymethylaminomethyluridine	HSP – heat shock protein
cmnm ⁵ s ² U – 5-carboxymethylaminomethyl-2-thiouridine	I – inosine
CP – crossing points	i ⁶ A – N ⁶ -isopentenyl adenosine
	IAA – iodoacetamide

IF – initiation factor
 Im – 2'-O-methylinosine
 KCl – potassium chloride
 KEGG – Kyoto Encyclopedia of Genes and Genomes
 KO – knock-out
 L (mL, μ L, nL) – liter (milliliter, microliter, nanoliter)
 LC – liquid chromatography
 Leu – leucine
 Lys – lysine
 LiAc – lithium acetate
 m (cm, mm, μ m, nm) – meter (centimeter, millimeter, micrometer, nanometer)
 M (mM, μ M, nM) – molar (millimolar, micromolar, nanomolar)
 m/z – mass-to-charge ratio
 $m^{2,2,7}G$ – N²,N²,7-trimethylguanosine
 m^2_2G – N², N²-dimethylguanosine
 m^6_2A – N⁶,N⁶-dimethyladenosine
 m^1A – 1-methyladenosine
 $m^1acp^3\Psi$ – 1-methyl-3-(3-amino-3-carboxypropyl) pseudouridine
 m^1G – 1-methylguanosine
 m^1I – 1-methylinosine
 m^2A – 2-methyladenosine
 m^2G – 2-methylguanosine
 m^3C – 3-methylcytidine
 m^3U – 3-methyluridine
 m^4C – N⁴-methylcytidine
 m^5C – 5-methylcytidine
 m^5U – 5-methyluridine
 m^5Um – 5,2'-O-dimethyluridine
 m^6A – N⁶-methyladenosine
 m^7G – 7-methylguanosine
 MAT – mating-type
 mcm^5U – 5-methoxycarbonylmethyluridine
 mcm^5s^2U – 5-methoxycarbonylmethyl-2-thiouridine
 Met – methionine
 $MgCl_2$ – magnesium chloride
 MM – minimal medium
 MM-His – minimal medium without histidine
 mmu – milli mass unit
 mol (nmol, pmol, fmol) – mole (nanomole, picomole, femtomole)
 mQ – milliQ
 MRM – multiple reaction monitoring
 mRNA – messenger ribonucleic acid
 MS – mass spectrometry
 ms – millisecond
 $ms^{2t^6}A$ – 2-methylthio-N⁶-threonyl carbamoyladenosine
 mt – mitochondrial
 MW – molecular weight
 Na – sodium
 ncm^5U – 5-carbamoylmethyluridine
 ncm^5Um – 5-carbamoylmethyl-2'-O-methyluridine
 NH_4OAc – ammonium acetate
 nt – nucleotide
 OD – optical density
 P-site – peptidyl-tRNA site
 PBS – phosphate buffered saline
 PCR – polymerase chain reaction
 PDE1 – snake venom phosphodiesterase

PEG – poly(ethylene glycol)
 PI – propidium iodide
 PIPES – piperazine-N,N'-bis(2-ethanesulfonic acid)
 PMSF – phenylmethanesulfonylfluoride
 ppm – parts-per million
 PQC – protein quality control
 qRT-PCR – quantitative reverse transcription polymerase chain reaction
 RNA – ribonucleic acid
 RNAmods – RNA-modifying enzymes
 RP – reverse phase
 Rpm – revolutions per minute
 rRNA – ribosomal ribonucleic acid
 RSCU – relative synonymous codon usage
 RT – room temperature
 s-LLVY-AMC – Succinyl-Leu-Leu-Val-Tyr-7-Amido-4-Methylcoumarin
 s²C – 2-thiocytidine
 s²U – 2-thiouridine
 SDS – sodium dodecyl sulfate
 SDS-PAGE – sodium dodecyl sulfate polyacrylamide gel electrophoresis
 snoRNA – small nucleolar ribonucleic acid
 snRNA – small nuclear ribonucleic acid
 SS – single strand
 T – thymine
 t⁶A – N⁶-threonylcarbamoyladenosine
 TBE – Tris-Borate-EDTA buffer
 TCA – Trichloroacetic acid
 TE – Tris-EDTA buffer
 TES – 2-[[1,3-dihydroxy-2-(hydroxymethyl)propan-2-yl]amino]ethanesulfonic acid
 TF – transcription factor
 THU – tetrahydrouridine
 T_m – melting temperature
 tm⁵U – 5-taurinomethyluridine
 tm⁵s²U – 5-taurinomethyl-2-thiouridine
 Tris – tris(hydroxymethyl)aminomethane
 tRNA – transfer ribonucleic acid
 rT – ribothymidine
 U – uridine
 Um – 2'-O-methyluridine
 UPLC – ultra performance liquid chromatography
 UPS – ubiquitin proteasome system
 Ura - uracil
 UTR – untranslated region
 UV – ultraviolet
 v (vol) – volume
 V (kV) – volt (kilovolt)
 w – weight
 WT – wild type
 Xm – unknown methylated base
 Ψ – pseudouridine
 Ψ_m – 2'-O-methylpseudouridine
 YPD – rich medium
 yW – wybutosine

1. INTRODUCTION

1. Introduction

1.1 OVERVIEW

This introduction is divided in four main topics: transfer RNA, ribosome, protein biosynthesis and protein folding, protein misfolding and disease. It provides an overview of protein biosynthesis processes and the respective mechanisms of quality control. Protein misfolding and aggregation are viewed as being post-translational processes, but they are affected by mRNA decoding speed and accuracy and we explain how the various types of translational errors may result in increased protein aggregation.

1.2 TRANSFER RNA

Transfer RNA (tRNA) molecules have a fundamental role in the transfer of genetic information from DNA to proteins. Indeed, tRNAs are adaptor molecules that connect the 20 canonical amino acids of proteins and mRNA codons (Crick, 1958). Each tRNA is charged with a particular amino acid by a cognate aminoacyl-tRNA synthetase (aaRS) and carries that amino acid to peptide chains being synthesized in the ribosome.

In *S. cerevisiae*, 275 nuclear-encoded tRNA genes code for 42 different cytoplasmic tRNAs (1 initiator and 41 elongator tRNAs) that pair with the 61 sense codons (Percudani *et al.* 1997; <http://gtrnadb.ucsc.edu/genomes/eukaryota/Scere3/>). The tRNA pool can be subdivided into tRNA isoacceptor families, each tRNA family is charged with a specific amino acid, but is composed by more than one tRNA which decode the different codons (synonymous codons) of that amino acid (codon family) (Goldman, 2008; Kutter *et al.*, 2011). There are 21 isoacceptor families (20 standard amino acids + selenocysteine), the number of tRNAs and the number of copies of each tRNA gene within a family are variable. In this way, there is both tRNA gene as well as codon redundancy in the genetic code. Additionally, one tRNA anticodon can pair with multiple codon triplets using wobble at the 1st anticodon position (3rd codon position) (Ikemura, 1985; Goodenbour and Pan, 2006; Marck *et al.*, 2006; Kutter *et al.*, 2011).

Apart from their main function in translation, tRNAs are also involved in other biological processes. Aminoacylated tRNAs can target proteins for degradation by donating their amino acids for the N-terminal of polypeptides to be degraded (Varshavsky, 1997). In yeast, uncharged tRNAs interact with Gcn2 (protein kinase that phosphorylates translation initiation factor eIF2), inducing the phosphorylation of eIF2 and decreasing the levels of general translation. Interestingly, the transcription regulator Gcn4 that regulates amino acid synthesis is translated more efficiently in these conditions (Wek, Zhu and Wek, 1995; Dever and Hinnebusch, 2005). tRNAs have also been implicated in the regulation of apoptosis in mammalian cells by binding and preventing the interaction of cytochrome c with Apaf-1 (the caspase activator) and avoiding its activation (Mei *et al.*, 2010). Therefore, tRNAs can function as molecular sensors, regulators of gene expression and modulators of cellular growth and proliferation (Pavon-Eternod *et al.*, 2009; Gu, Begley and Dedon, 2014; Wilusz, 2015).

1.2.1 tRNA structure

tRNA molecules have a length of 73 to 90 nucleotides. The secondary structure of tRNAs is highly conserved and form a cloverleaf structure (Figure 1.1) (Kim *et al.*, 1972; Goldman, 2008). It consists of an acceptor stem, three stem-loops (or arms) and a variable-loop, stabilized by hydrogen bonds between the stems. The stem-loops are the dihydrouridine (D) loop, the anticodon-loop and the T Ψ C-loop. Additionally, there are specific nucleotides conserved in most tRNA species that stabilize tertiary interactions. The 3'-end of tRNAs contains the CCA sequence. The acceptor stem is formed by the 5'- and 3'-ends of the molecule, with seven base pairs (bp) followed by an overhanging unpaired nucleotide at position 73 and the CCA tail. The amino acid is attached to the ribose of the 3'-terminal A residue. The D-loop (8-11 bases) is located on the left side of the cloverleaf structure and is followed by a stem of 3-4 bp. On the right-hand side of the cloverleaf structure there is the 7-base T Ψ C-loop or T-loop, which is followed by a 5-base pair stem. Below the T-loop there is the variable-loop, which is the main source of sequence variability in tRNAs and may contain 4 to 21 (or even more) bases. Finally, the anticodon-loop

1. Introduction

contains 7 unpaired bases. The anticodon, i. e. a 3-base sequence complementary to the codon, is located in the middle of the loop at positions 34-35-36. The pairing of codon-anticodon occurs in an antiparallel fashion, meaning that the 5'-anticodon base in the tRNA (nucleotide 34) pairs with the 3'-codon base in the mRNA, and the 3'-anticodon base (nucleotide 36) with the 5'-codon base (Kim *et al.*, 1972; Rich and Schimmel, 1977; Goldman, 2008). This cloverleaf structure folds into a L-shaped structure, which is the mature functional form of tRNAs (Figure 1.1).

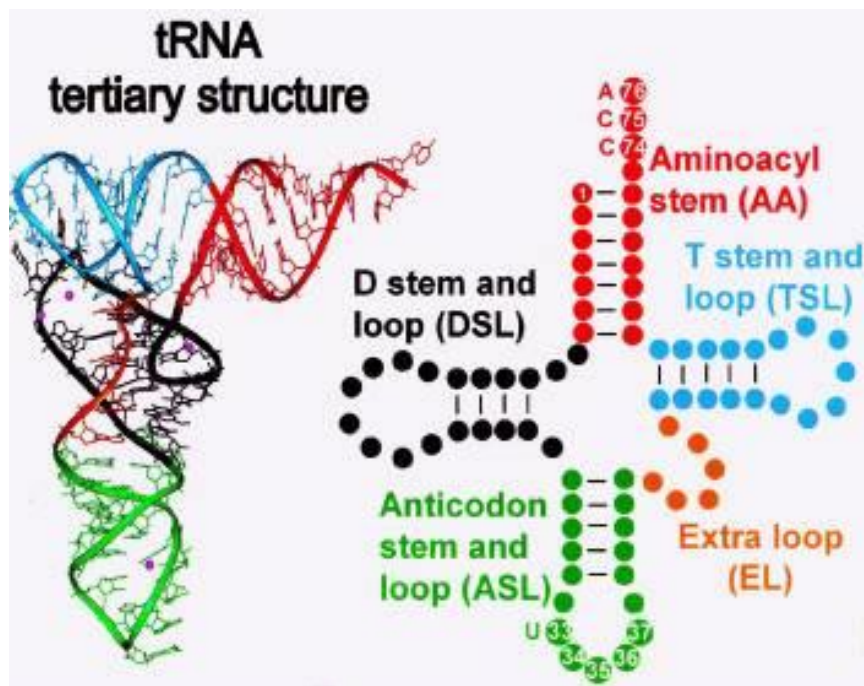


Figure 1.1. The structure of tRNAs. On the left, the crystallographic structure of yeast tRNA^{Phe} represents global three-dimensional structure of tRNA. On the right is represented the cloverleaf secondary structure. In red: amino accepting stem or aminoacyl-stem (AA); in black: dihydrouridine stem and loop domain (DSL); in green: anticodon stem and loop domain (ASL); in orange: extra loop (EL); and, in blue, the ribothymidine, or TΨC, stem and loop (TSL). Adapted from Agris, 2004.

1.2.2 tRNA biogenesis

Biogenesis of tRNAs comprises multiple processes, namely transcription, processing of the 5' leader and the 3' trailer, splicing, post-transcriptional modification of nucleoside residues, CCA addition and aminoacylation, nuclear-to-

cytoplasmic shuttling (in eukaryotes) and import into mitochondria (Figure 1.2). Furthermore, tRNA biosynthesis has multiple levels of regulation, including regulation of tRNA transcription, end maturation and splicing (Hopper and Phizicky, 2003; Goldman, 2008).

In yeast, tRNA transcription and pre-tRNA 5'-terminus processing occurs in the nucleolus (Thompson *et al.*, 2003; Phizicky and Hopper, 2010). Other tRNA processing events occur at several distinct sub-cellular locations, including nucleoplasm, inner nuclear membrane (INM), cytoplasm, and cytoplasmic surface of mitochondria (Table 1.1).

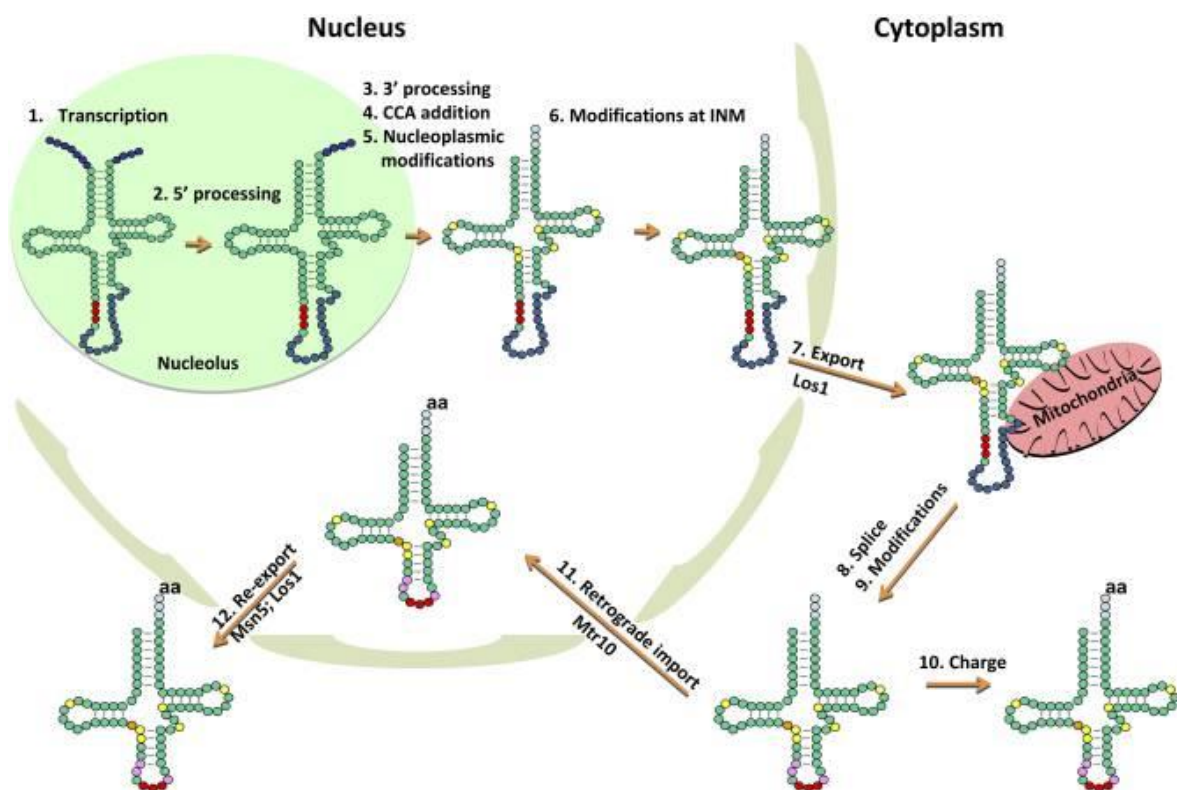


Figure 1.2. tRNA biogenesis in *S. cerevisiae*. tRNA transcription and 5'-end processing happen in the nucleolus. The 3'-end processing, CCA addition and modification steps happen in the nucleoplasm and at the inner nuclear membrane (INM). Intron-containing pre-tRNAs are exported to the cytoplasm by *Los1*, where splicing occurs on the cytoplasmic surface of mitochondria. After tRNA splicing, additional modification and aminoacylation occur to allow mature charged tRNAs to participate in protein synthesis. Cytoplasmic tRNAs are imported into nuclei *via* *Mtr10* and re-export of nuclear tRNAs is mediated by *Los1* and *Msn5*. Green circles: parts of the tRNA that are maintained in the mature structure; red circles: anticodon; purple circles: transcribed 5' leader and 3' trailer sequences; dark-blue

1. Introduction

circles: intron sequence; light-blue circles: CCA end; yellow, orange, and pink circles: several modifications made in the nucleoplasm, at the INM, and in the cytoplasm, respectively; aa: amino acid. Adapted from Phizicky and Hopper, 2010.

Table 1.1. Subcellular location of the biosynthesis, processing and turnover of the cytoplasmic tRNAs in yeast and vertebrates. Adapted from Hopper *et al.*, 2010. ND: not determined.

Step	Cellular compartment – yeast	Cellular sub-compartment – yeast	Cellular compartment – vertebrate cells	Cellular sub-compartment – vertebrate cells
Transcription	Nucleus	Nucleolus	Nucleus	ND
5' processing	Nucleus	Nucleolus	Nucleus	ND
3' processing	Nucleus	ND	Nucleus	ND
Splicing	Cytoplasm	Mitochondrial surface	Nucleus	Nucleoplasm
Nucleoside modification	Nucleus or cytoplasm	Nucleoplasm, nuclear membrane, ER, cytoplasm	Nucleus and ND	ND
TRAMP-mediated 3'→5' turnover	Nucleus	ND	ND	ND
RTD 5'→3' turnover	Nucleus and cytoplasm	ND	ND	ND
Half molecule production	Cytoplasm	Vacuolar enzyme	Cytoplasm	Endocytosed enzyme

1.2.2.1 tRNA transcription

tRNA genes are highly transcribed, producing 3 million tRNAs per generation in yeast (Waldron and Lacroute, 1975), where about 60 000 mRNAs are also produced (Ares, Grate and Pauling, 1999). tRNA genes are transcribed by RNA polymerase III (Pol III), whose activity is guided by two transcription factors with multi-subunits: TFIIB and TFIIC. TFIIB is a multi-subunit complex formed by B double prime 1 (BDP1), B-related factor 1 (BRF1) and TATA-binding protein (TBP) and is recruited upstream of the transcription start site. TFIIC binds to the intragenic A- and B-boxes that encode parts of the D- and T-stems and loops of tRNAs, respectively (Figure 1.3). Pol III also binds to the transcription start site and this binding is modulated by the sequence diversity among tRNA genes in their 5' upstream region, resulting in the observed variability in expression levels among tRNA isoacceptors (Ishiguro *et al.*, 2002; Kirchner and Ignatova, 2014).

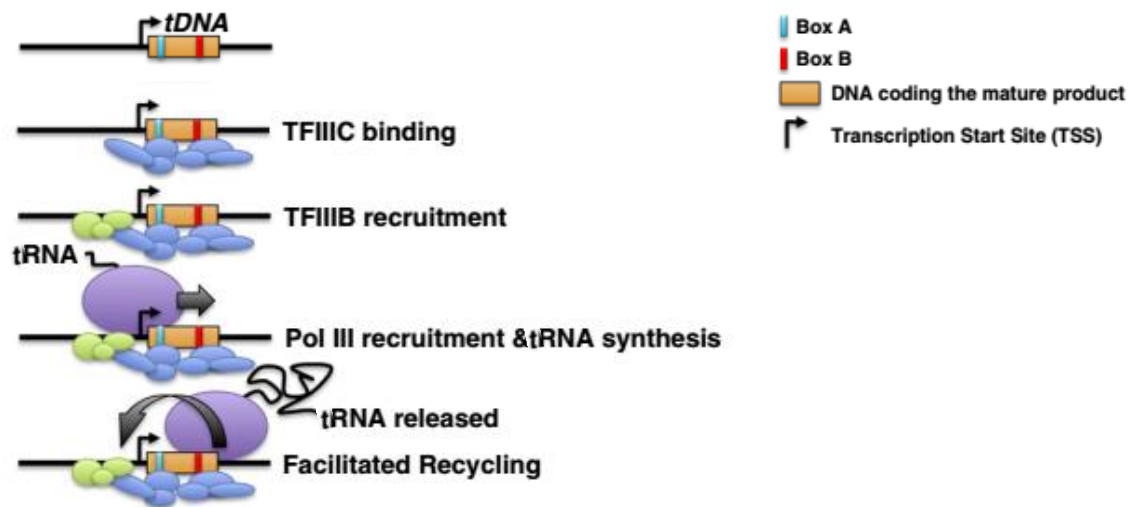


Figure 1.3. Structure of yeast tRNA genes and model of tRNA transcription. Transcription complex assembly on a yeast tRNA gene (tDNA). The solid black bar represents upstream and downstream DNA, the open orange rectangle the mature product and the blue and red rectangles the A- and B-boxes, respectively. The horizontal arrow indicates the transcription start site (TSS). The components of TFIIB and TFIIC are represented as green and blue ovals, respectively. The 17-subunits of Pol III enzyme are represented as a unique purple oval. Adapted from Acker *et al.*, 2013.

tRNA transcription by Pol III is coordinated with rRNA transcription by Pol I because tRNAs and ribosomes depend on each other to function properly. Additionally, tRNA transcription is regulated in response to cellular nutrient availability and other environmental information.

At the end of transcription, a tRNA precursor is formed with a 5' leader, a U-rich 3' trailer, and occasionally an intron-sequence that experiences several processing events to produce mature tRNAs.

1.2.2.2 tRNA processing

The processing of tRNAs is complex and requires five main steps: 1) elimination of the 5' leader by RNase P; 2) elimination of the 3' trailer sequence by endonucleases and exonucleases; 3) addition of CCA; 4) splicing of introns in some tRNAs by an endonuclease and a ligase; and 5) introduction of several modifications at various

1. Introduction

residue sites (Figure 1.2 and Figure 1.4). This specific order of processing events is not mandatory; instead the trafficking of pre-tRNA through the cellular compartments seems to influence the order of maturation events.

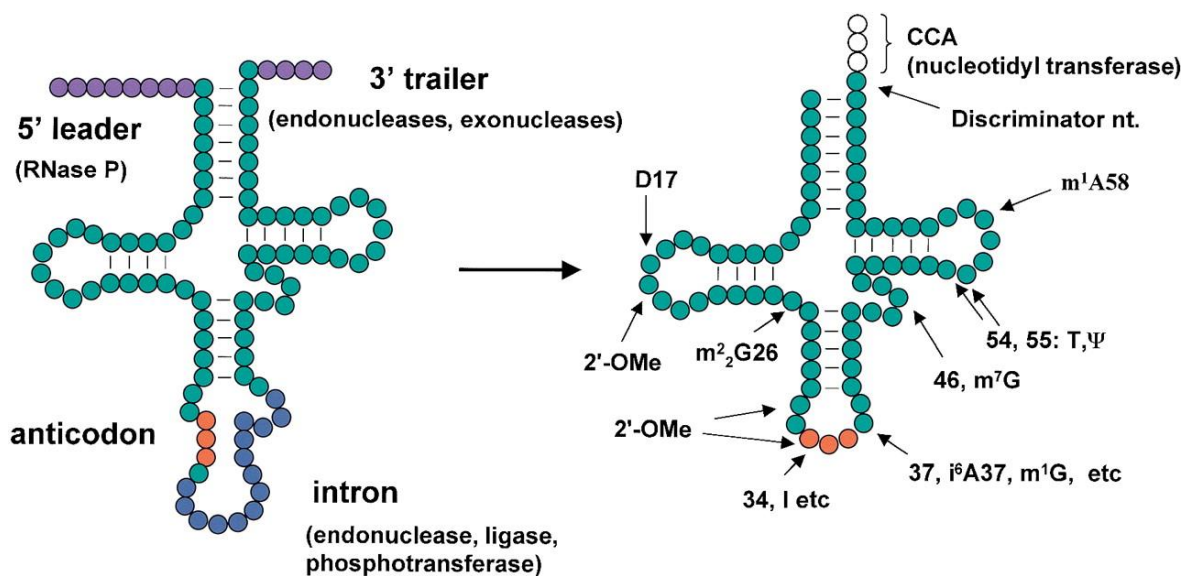


Figure 1.4. From tRNA precursor to mature tRNA. Processing of pre-tRNA (*left*) into mature tRNA (*right*) includes removal of 5' leader and 3' trailer sequences (purple circles), addition of CCA sequence (white circles), splicing of introns (blue circles) and modification of residues throughout the tRNA molecule. Green circles represent part of the mature tRNA. All processes are carried out by protein enzymes, except for 5'-end processing that is carried out by a ribonucleoprotein. Adapted from Hopper and Phizicky, 2003.

1.2.2.2.1 5'-end processing

The 5' leader sequence of tRNA transcripts is removed by endonuclease Ribonuclease P (RNase P). This processing event occurs in the nucleolus (Table 1.1) and produces a tRNA molecule with a mature 5'-end containing a phosphate, releasing the leader sequence with a 3'-OH terminus.

In yeast, the RNase P contains a RNA component (RPR1) and nine protein subunits (Pop1, Pop3, Pop4, Pop5, Pop6, Pop7, Pop8, Rpr2 and Rpp1) (Marquez *et al.*, 2005; Walker and Engelke, 2006). The RNA component is essential for substrate recognition and recognizes L-shaped tRNA substrates *via* the TΨC loop,

the acceptor stem and the CCA end (in the case of most bacteria) (Figure 1.5) (Grosjean, 2009a).

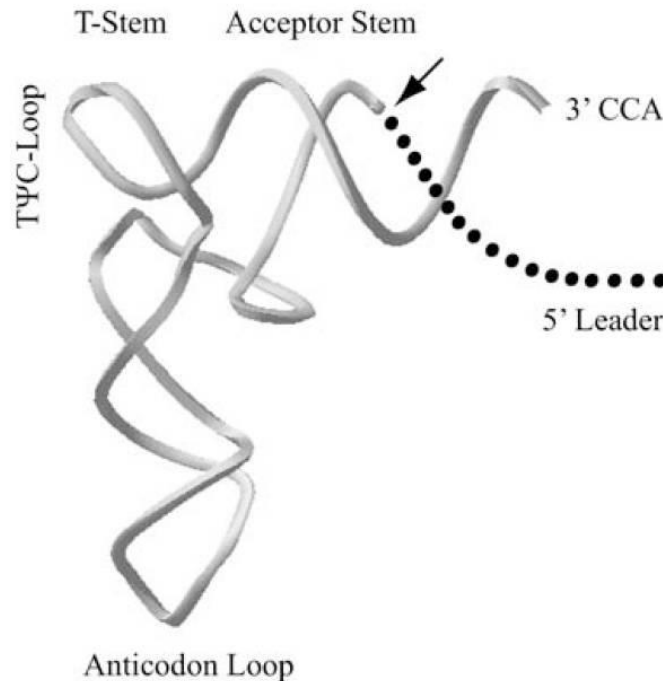


Figure 1.5. The 5' leader sequence from pre-tRNAs is cleaved by RNase P. The site of cleavage is denoted with an arrow. Substrate recognition and cleavage by RNase P requires the acceptor stem and T-stem-loop structures. Adapted from Walker and Engelke, 2006.

1.2.2.2.2 3'-end processing

Processing of the 3'-end of tRNA requires ablation of the 3' sequence from the pre-tRNA by either endonucleolytic cut at or close to the discriminator or exonucleolytic activity (Figure 1.6). This 3' endonucleolytic processing of tRNAs requires the yeast La protein, Lhp1 (Yoo and Wolin, 1997), and the endonuclease RNase Z (also tRNase Z). Lhp1 binds not only to precursors of tRNAs, but also to precursors of 5S ribosomal RNA, the spliceosomal U6 RNA, the signal recognition particle SRP RNA, and the cytoplasmic Y RNAs, since Lhp1 recognizes the sequence UUU_{OH} of the 3'-terminus of most newly synthesized RNAs (Stefano, 1984). La protein assists folding of some pre-tRNAs and also protects the 3'-terminus of precursors of RNAs from exonucleases, favoring terminus removal by an endonuclease (Yoo and Wolin,

1. Introduction

1997). So, the endonuclease RNase Z then removes the 3'-terminus of tRNAs immediately upstream of the discriminator base (N₇₃), before the addition of CCA (Schiffer, Rösch and Marchfelder, 2002).

Regarding the exonucleolytic pathway, Rex1 is the main exonuclease participating in the 3'-end processing. This enzyme is also involved in the nuclear CCA turnover (Copela *et al.*, 2008).

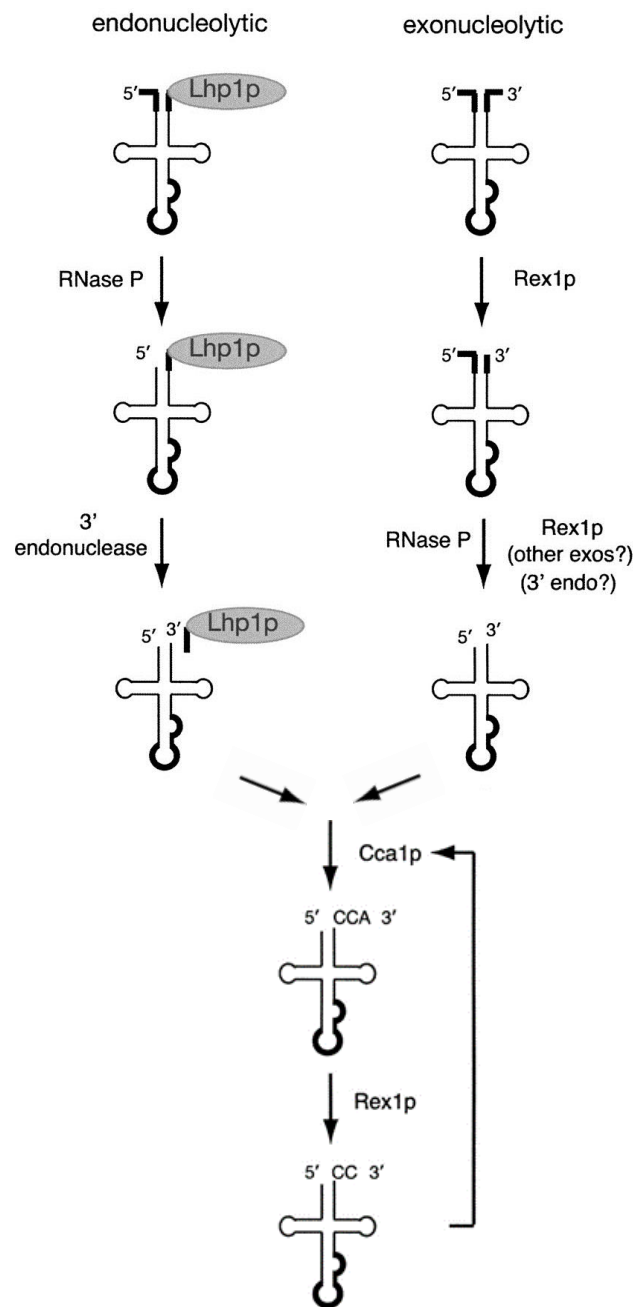


Figure 1.6. Model for pre-tRNA 3'-end processing. In the endonucleolytic pathway, Lhp1p binds to the 3'-ends of various pre-tRNAs protecting them from exonucleases.

Consequently, RNase P first cleaves the 5'-ends and, then, RNase Z removes the 3'-ends (bound to Lhp1). In the exonucleolytic pathway, pre-tRNAs free of Lhp1p are first processed at their 3'-ends by Rex1. Followed by deletion of the 5'-ends by RNase P and maturation of the 3'-ends by Rex1 and other exonucleases. In both pathways, Rex1 also participates in end turnover, after CCA addition. Adapted from Copela *et al.*, 2008.

1.2.2.2.3 Addition of CCA

All mature tRNAs must have a 3' CCA sequence to participate in protein biosynthesis since it serves to attach the amino acids. The 3' CCA terminus is added post-transcriptionally by the enzyme ATP(CTP):tRNA nucleotidyltransferase which transfers CMP and AMP from CTP and ATP to the 3'-ends of tRNA molecules (Aebi *et al.*, 1990). Although there are CCA nucleotidyltransferases located either in the nucleus and in the cytoplasm, it was demonstrated that nucleoplasmic CCA nucleotidyltransferase adds CCA to 3'-ends of end-processed intron-containing pre-tRNAs, whereas cytoplasmic CCA nucleotidyltransferase functions in tRNA end repair (Wolfe, Hopper and Martin, 1996; Phizicky and Hopper, 2010).

1.2.2.2.4 Splicing

In *S. cerevisiae*, introns occur in genes for only ten different tRNA species, totaling 61 tRNAs with introns (Hani and Feldmann, 1998; <http://gtrnadb.ucsc.edu/genomes/eukaryota/Scere3/>). tRNA introns are 14–60 nucleotides in length and are always located immediately 3' to the anticodon (between nucleotides 37 and 38) (Abelson, Trotta and Li, 1998). Introns are required for the introduction of specific nucleoside modifications in some pre-tRNAs (Johnson and Abelson, 1983). Splicing of the pre-tRNAs occurs in three steps: 1) a tRNA splicing endonuclease (4 subunits: Sen54, Sen2, Sen34, and Sen15) removes the intron, resulting in a 5' tRNA half-molecule ending in a 2'–3' cyclic phosphate and a 3' tRNA half-molecule beginning with a 5'-OH group (Peebles, Gegenheimer and Abelson, 1983); 2) a tRNA ligase (Trl1p) joins the excised exons (tRNA half-molecules) after adenylation of the 5'-P end (Phizicky *et al.*, 1992); and 3) a 2'-phosphotransferase (Tpt1p) transfers the 2'-phosphate at the splice junction to

1. Introduction

NAD⁺ to form ADP-ribose 1'-2'-cyclic phosphate (Abelson, Trotta and Li, 1998) (Figure 1.7).

In yeast, tRNA splicing endonuclease subunits are located in the cytoplasmic surface of the mitochondria and the other two enzymes required for splicing are located in the nucleus and in the cytoplasm (Yoshihisa *et al.*, 2003). In this way, tRNA splicing occurs in the cytoplasm.

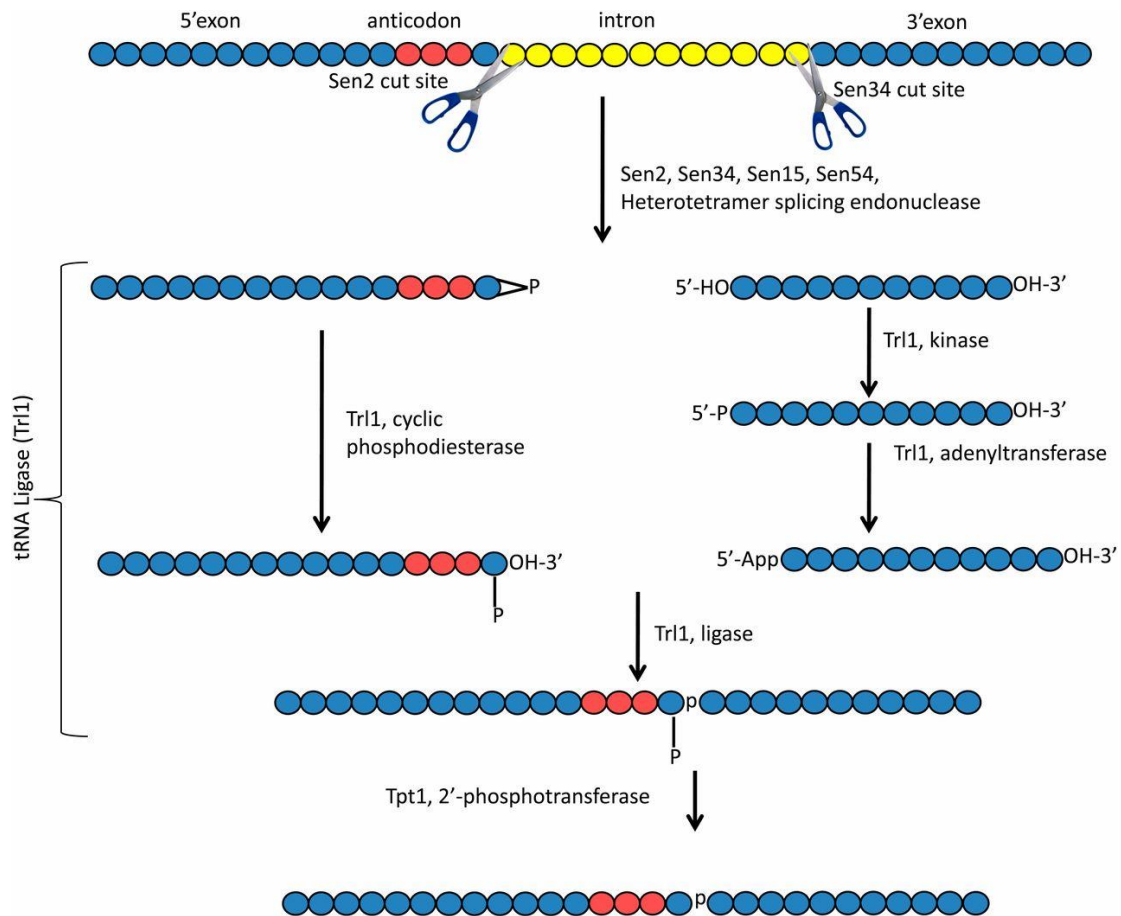


Figure 1.7. The pre-tRNA splicing pathway in yeast. Pre-tRNA sequence is shown with anticodon indicated by red circles and the intron located after residue 37 by yellow circles. The endonuclease (comprised of Sen2, Sen34, Sen15 and Sen54) removes the intron by cleaving the pre-tRNA at each exon/intron border, leaving tRNA half-molecules with a 2'-3' cyclic phosphate and a 5'-OH group at their ends. In yeast, the ligase Trl1, through its RNA 5' kinase activity, phosphorylates the 5'-OH end of the 3' half-molecule, and the ligase cyclic phosphodiesterase activity opens the 2'-3' cyclic phosphate to a 2' phosphate. Then ligase Trl1 joins the half-molecules (after activation of the 5' phosphate by the ligase adenylyltransferase activity), using the 5' phosphate as the junction phosphate, and leaving

the 2' phosphate at the splice junction. This 2' phosphate is subsequently transferred to NAD by the 2' phosphotransferase Tpt1. Adapted from Hopper, 2013.

1.2.2.2.5 tRNA modification

tRNA nucleosides are highly modified (Figure 1.8), exhibiting the largest number and the widest variety of nucleoside modifications among RNAs. The RNA Modification Database currently contains 112 modified ribonucleoside entries, distributed by RNA type and phylogenetic source (<http://mods.rna.albany.edu>). In *S. cerevisiae*, 27 different modifications were found among the sequenced tRNAs (<http://modomics.genesilico.pl>) (Annex I.1, Annex I.2 and Annex I.3). These modifications occur at 36 different positions, corresponding to 14.6% of the residues of all tRNA species, with a range of 7 to 17 modifications per cytoplasmic tRNA and 6 to 9 modifications per mitochondrial tRNA (Annex I.2 and Annex I.3).

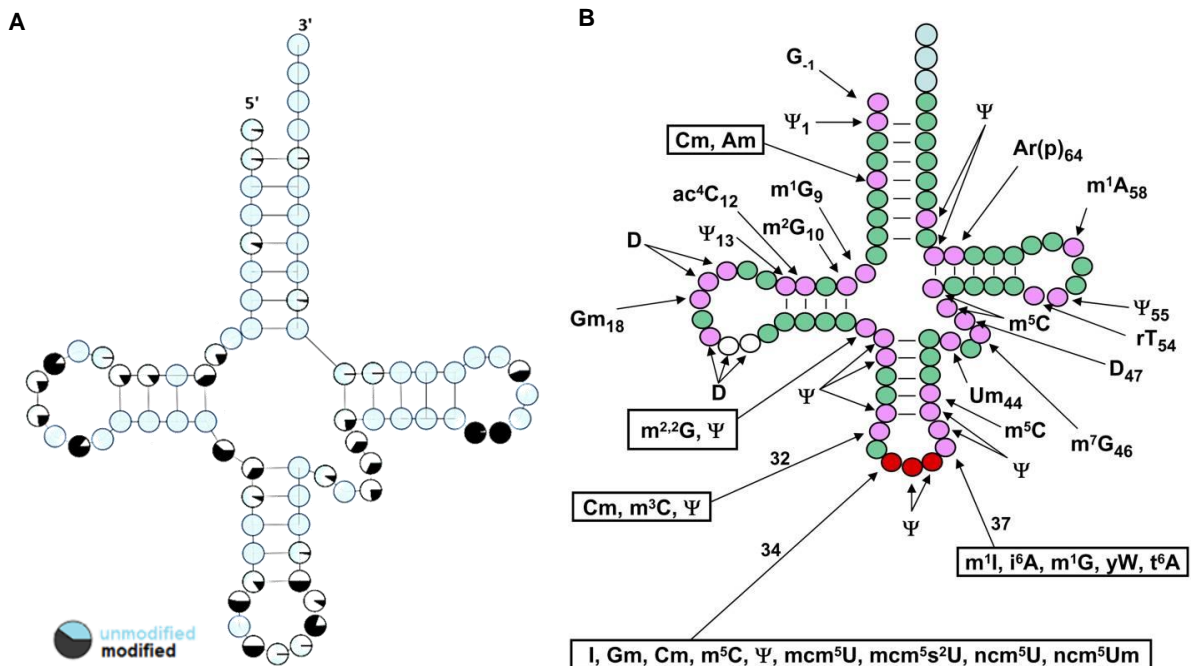


Figure 1.8. Schematic pattern of modifications found in *S. cerevisiae* tRNA. A. Localization of modified residues in tRNA with the frequency of modification observed in all tRNAs species from *S. cerevisiae*. Graph constructed in <http://modomics.genesilico.pl>. **B.** Type of modification observed in each residue of cytoplasmic tRNAs. Green circles: residues that are unmodified in all yeast tRNA species; pink circles: residues that are

1. Introduction

modified in some or all tRNA species; white circles: additional residues (20a and 20b) that are present in some tRNAs and are occasionally modified; red circles: anticodon residues, which are modified in some tRNAs; light-blue circles: the CCA end. Adapted from Phizicky and Hopper, 2010.

A substantial number of genes and energy is required for post-transcriptional modification of tRNA. The tRNA-modifying enzymes can be localized in the cytoplasm and distinct sub-nuclear compartments, namely in the nucleolus, in the nucleoplasm, or at the INM (Hopper and Phizicky, 2003). Many tRNA-modifying enzymes are highly conserved, however most of the yeast genes encoding tRNA-modifying enzymes are unessential (Phizicky and Hopper, 2010).

Generally, modified nucleosides in the structural core of the L-shaped structure of tRNA are formed by reactions, involving methylation, pseudouridylation, or dihydrouridine formation, and they are important for the correct folding of tRNA and to stabilize the L-shaped tertiary structure (Helm, 2006). On the other hand, modifications within the anticodon stem loop include methylations, pseudouridylations and more complex additions which contribute to stabilize the codon-anticodon pairing, maintain the translational reading frame and to allow translocation of the tRNA from the A-site to the P-site of the ribosome, ensuring efficiency and fidelity of translation (Agris, 2008; Gustilo, Vendeix and Agris, 2008). Additionally, tRNA modifications can function as identity elements for aminoacylation and in discrimination of tRNAs during translation (Grosjean, 1998, 2005; Motorin and Grosjean, 2005; Gustilo, Vendeix and Agris, 2008; Jühling *et al.*, 2009; Kramer and Hopper, 2013; Perrochia *et al.*, 2013). For example, the 2'-O-ribose phosphate [Ar(p)] modification at position 64 of the initiator methionine tRNA (tRNA^{Met}) interferes with Met-tRNA^{Met} binding to elongator factor 1 (eEF1 α), but not with the binding to the initiator factor 2 (eIF2), thus discriminating the role of the initiator tRNA in translation (Forster, Chakraborty and Sprinzl, 1993; Shin *et al.*, 2012).

Some tRNA positions are almost always modified (Figure 1.8A). For example, the nucleotide at position 37 is modified in > 70% of the tRNAs (Grosjean, 1998) and usually contains a modified purine nucleoside which can be a hypermodified nucleoside with N¹-methyl-guanosine (m¹G), N⁶-threonylcarbamoyladenosine (t⁶A)

or wybutosine (yW) (Noma *et al.*, 2006; Perrochia *et al.*, 2013). These modifications are important in the stabilization of the codon-anticodon pairing by base-stacking interactions and in the maintenance of the reading frame (Noma *et al.*, 2006; Kramer and Hopper, 2013). Similarly, position 34 is frequently modified and these wobble modifications stabilize codon-anticodon interactions, important for precise decoding (Yarian *et al.*, 2002; Näsval, Chen and Björk, 2007; Kramer and Hopper, 2013).

Methylation is the most extensively and prevalent tRNA modification, occurring in yeast tRNAs at the 2'-OH of specific nucleotide residues and at multiple base positions, namely the position 1 of adenine, 5 of uracil, 3 and 5 of cytosine and 1, 2, and 7 of guanine (Alexandrov, Martzen and Phizicky, 2002; Sprinzl and Vassilenko, 2005). On the other hand, pseudouridine (Ψ) is the most widely distributed modified nucleoside in tRNAs from *S. cerevisiae* and is found at 15 different positions (Annex I.2 and Annex I.3). The second most extensively distributed modified nucleoside is dihydrouridine, which is found at 6 different positions in tRNA (Annex I.2 and Annex I.3). The m⁵U residue (also known as ribothymidine – rT) at position 54 is present in all yeast tRNAs, except in the tRNA_i^{Met} and in the mitochondrial tRNA^{Phe}_{GAA} (Annex I.2 and Annex I.3). More complex nucleoside modifications are located at position 34 of tRNA^{Arg}_{UCU}, tRNA^{Gly}_{UCC}, tRNA^{Ala}_{UGC}, tRNA^{Thr}_{UGU}, tRNA^{Pro}_{UGG}, tRNA^{Ser}_{UGA}, tRNA^{Glu}_{UUC}, tRNA^{Lys}_{UUU}, tRNA^{Gln}_{UUG}, tRNA^{Val}_{UAC} and tRNA^{Leu}_{UAA}, namely ncm⁵U, ncm⁵Um, mcm⁵U and mcm⁵s²U (Annex I.2).

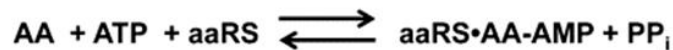
1.2.2.3 tRNA aminoacylation and aminoacyl-synthetases (aaRSs)

Mature tRNAs can then be aminoacylated at the ribose of the 3'-terminal A residue. Each family of tRNA isoacceptors is recognized by an aminoacyl-tRNA synthetase (aaRS); the cognate enzyme, i. e., each of the 20 amino acids is recognized by a specific synthetase (Schimmel, 1979; Poupiana and Schimmel, 2001; Goldman, 2008). In this reaction, each amino acid forms an ester linkage with one of the hydroxyl groups of the terminal adenosine (Schimmel, 1979). This is a two-step mechanism (Figure 1.9). In the first step, called activation step, one α -carboxylate carbon of the amino acid (AA) attacks the α -phosphorus of ATP, forming an enzyme-bound aminoacyl-adenylate (aaRS-AA-AMP) with release of pyrophosphate (PPi); in the second step, called transfer step, the 2'- or 3'-hydroxyl group of the 3'-terminal

1. Introduction

of the A₇₆ nucleotide of tRNA attacks the α-carbonyl carbon of the aminoacyl-adenylate, resulting in the 3' esterification of the aminoacyl-tRNA with release of AMP (Ibba and Soll, 2000; Schimmel, 2008b).

Step 1: Activation



Step 2: Transfer



Figure 1.9. Two-step mechanism of aminoacylation by aaRS. First, formation of the aminoacyl adenylate intermediate (upper right) and then the aminoacyl-tRNA (bottom right). The tRNA nucleophile in the second step is the oxygen atom from one of the two ribose hydroxyl groups of the 3'-A₇₆ nucleotide, depending of the structural class to which the aaRS belongs. Adapted from Kim, 2014.

The aminoacyl-tRNA synthetases can be divided in two distinct families of enzymes: class I and class II, based on the architecture of catalytic sites (Eriani *et al.*, 1990; Pouplana and Schimmel, 2001). Class I aaRSs comprise 10 families (ArgRS, CysRS, GlnRS, IleRS, LeuRS, GluRS, MetRS, TrpRS, TyrRS and ValRS) and contains a Rossmann nucleotide-binding fold in the catalytic domain, composed of five-stranded parallel β-sheets connected by α-helices (Eriani *et al.*, 1990). Most class I aaRSs bind the tRNA anticodon region by the carboxyl-terminal domains, but their structures are globally divergent. In these enzymes, the Rossmann nucleotide-binding fold binds the acceptor stem of the tRNA and the 3'-end of the tRNA adopts a hairpin structure to bind in the active site, where the amino acid is transferred onto the 2'-OH group of the ribose of the last A nucleotide of tRNA. In contrast, class II aaRSs comprise other 10 families (AlaRS, AsnRS, AspRS, GlyRS, HisRS, LysRS, PheRS, ProRS, SerRS and ThrRS) and the common catalytic domain is organized

as a seven-stranded β -sheets flanked by α -helices (Eriani *et al.*, 1990). This common domain binds and accurately juxtaposes the amino acid, ATP and the 3'-terminus of tRNA for the catalytic reactions. Additionally, most class II aaRSs acylate the amino acid to the 3'-OH group of the terminal ribose of the tRNA and face the tRNA from different angles (Woese *et al.*, 2000; Pouplana and Schimmel, 2001; Perona and Hadd, 2012).

aaRSs recognition of the correct tRNA involves interaction of the enzyme with discriminator base (N₇₃), the acceptor stem (helical structure formed by base pairing of 1 to 7 with 72 to 66 bases), and/or the anticodon. However, interactions with other regions in tRNA were described, namely the extra arm, the D stem, the inside of the L-shaped tRNA structure, and the phosphate backbone (Figure 1.10). As mentioned before, modified nucleotides have also been identified as strong determinants for cognate aminoacylation (Ibba and Soll, 2000).

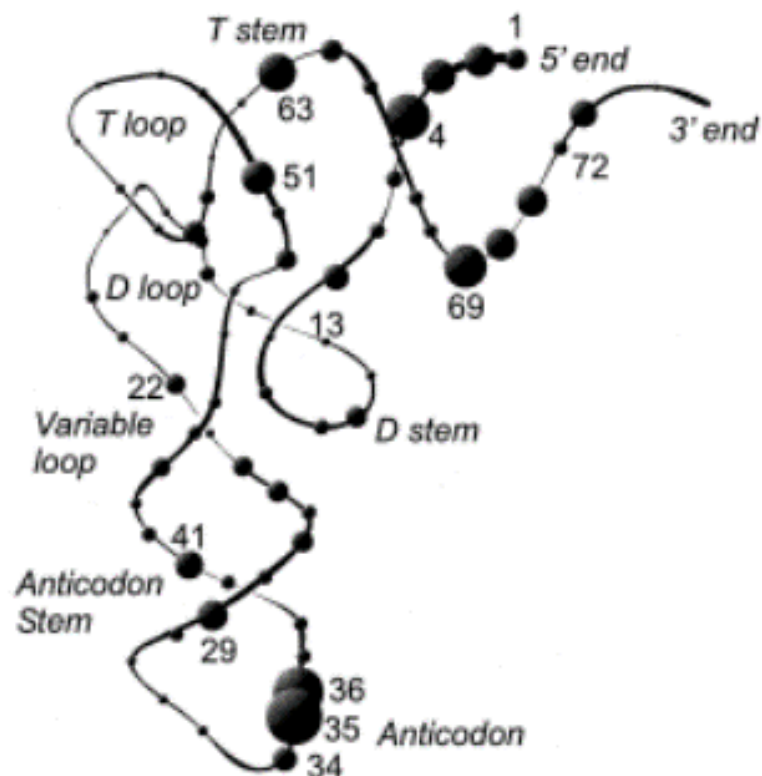


Figure 1.10. Aminoacyl-tRNA synthetase recognition hot spots present in the three-dimensional structure of tRNA. Circles indicate the position of the hot spot nucleotides and their size is related to the frequency they are used for recognition by aaRSs. Adapted from Ibba and Soll, 2000.

1. Introduction

1.2.3 tRNA quality control

Product tRNAs produced during tRNA biogenesis are not always stable and, in this way, cells have quality control mechanisms to evaluate the integrity of tRNAs during and post biosynthesis. The mechanisms ensuring that the correct levels of properly structured, modified and charged tRNAs exist in the cytoplasm involve discrimination of precursor tRNAs during tRNA export, the nuclear surveillance pathway, the rapid tRNA decay (RTD) pathway and amino acid editing by aminoacyl-tRNA synthetases.

tRNA quality control is observed during primary tRNA export, when pre-tRNAs are discriminated for export by Los1. Los1 binds and exports appropriately structured tRNAs with mature 5' and 3'-ends (Figure 1.2) (Lipowsky *et al.*, 1999). Another exportin present in yeast is Msn5, which exports tRNAs encoded by genes lacking introns, tRNAs earlier imported from the cytoplasm and aminoacylated tRNAs (Figure 1.2) (Feng and Hopper, 2002; Murthi *et al.*, 2010). Aminoacylation of mature tRNAs in the nucleus is also important for tRNA nuclear export (Sarkar, Azad and Hopper, 1999; Grosshans, Hurt and Simos, 2000).

For hypomodified pre-tRNAs and tRNAs with unprocessed 3'-ends, tRNA turnover requires proteins comprising the nuclear TRAMP complex, namely Mtr4 (a RNA-dependent helicase), Trf4 or Trf5 (poly(A) polymerases), and Air1 or Air2 (RNA binding proteins). TRAMP complex polyadenylates the misfolded forms of mature tRNAs and these activated substrates containing the TRAMP complex interact with the nuclear exosome (3' to 5' exoribonuclease), assisting the 3'-ends decay (Copela *et al.*, 2008; Hopper, 2013) as part of the nuclear surveillance pathway (Figure 1.11). The exosome is a multi-subunit complex of proteins occurring in the nucleus and cytoplasm, which is involved in the processing, degradation and retention of stable and unstable RNAs. The nuclear exosome contains two nucleases, Rrp6 and Rrp44, and other proteins. This mechanism of tRNA turnover in the nucleus was first observed in hypomodified pre-tRNA_i^{Met} that is 3' polyadenylated by Trf4 and the poly(A)-containing tRNA is degraded by the nuclear exosome (Kadaba *et al.*, 2004; Kadaba, Wang and Anderson, 2006). Similarly, 3'-5' exonuclease Rex1 has been

implicated in the degradation of pre-tRNAs with unprocessed 3'-ends (Copela *et al.*, 2008).

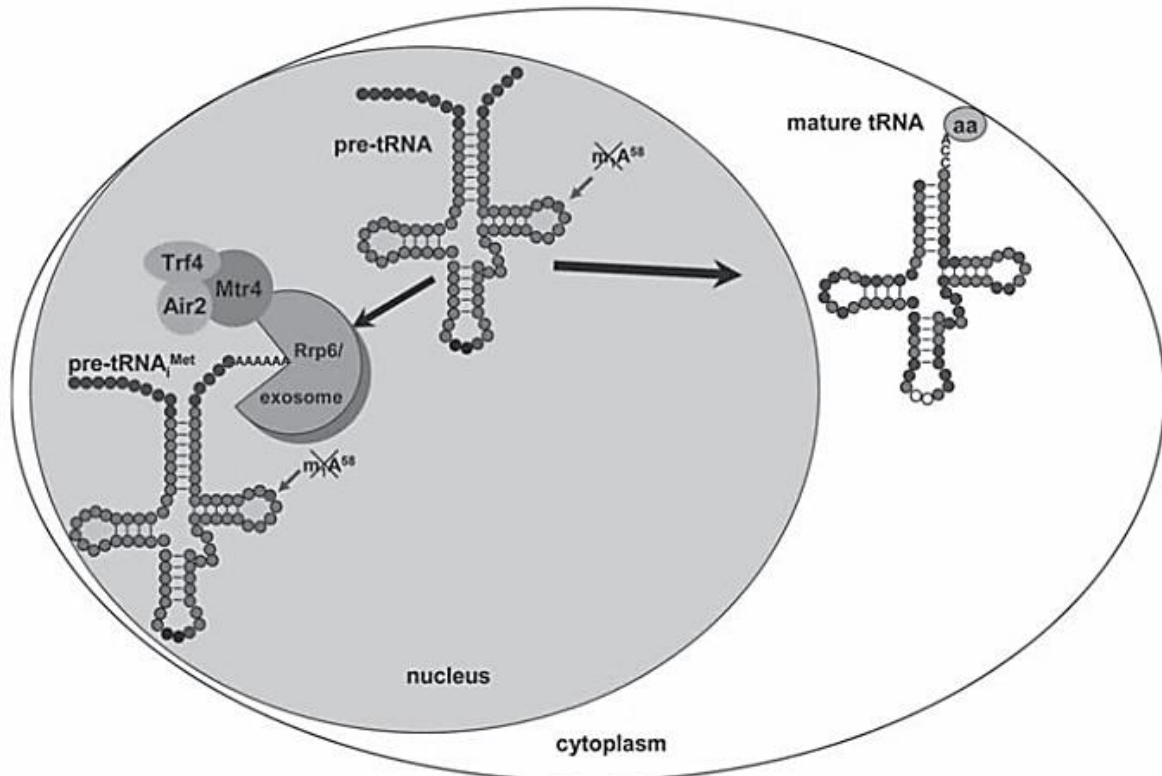


Figure 1.11. The nuclear surveillance pathway of tRNAs. Hypomodified pre-tRNA, e.g. pre-tRNA_i^{Met} lacking m¹A₅₈, is degraded by polyadenylation of the 3'-end by the TRAMP complex (Trf4, Mtr4 and Air2), followed by exonuclease digestion catalyzed by the nuclear exosome Rrp44/Rrp6. Adapted from Grosjean, 2009.

The hypomodified tRNAs and/or tRNAs with unstable acceptor and T stems that expose their 5'-ends undergo tRNA decay by the 5' to 3' exonucleases Rat1 (nuclear) and Xrn1 (cytoplasmic). This mechanism belongs to the rapid tRNA decay pathway that degrades mature tRNAs destabilized in structure, in both the nucleus and the cytoplasm (Figure 1.12) (Alexandrov *et al.*, 2006; Chernyakov *et al.*, 2008; Whipple *et al.*, 2011). Related to the RTD pathway is the retrograde tRNA nuclear import, in which abnormal tRNAs are imported into the nucleus and are repaired or eliminated, ensuring that only correctly structured and modified tRNAs are present in the cytoplasm to participate in translation (Kramer and Hopper, 2013).

1. Introduction

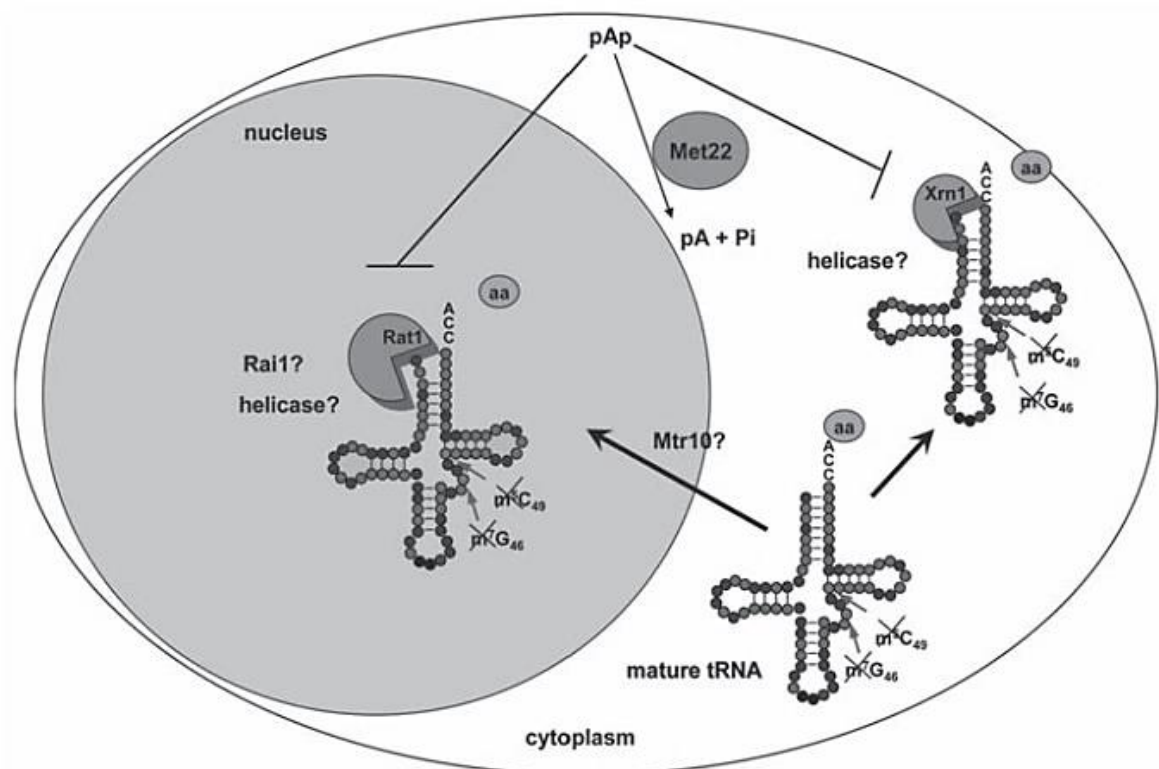


Figure 1.12. The rapid tRNA decay (RTD) pathway. The RTD pathway mediates degradation of several mature tRNAs lacking different modifications and partially unfolded tRNAs that transiently expose the 5'-end to Rat1 or Xrn1 in the nucleus or cytoplasm, respectively. Nuclear tRNA degradation mediated by Rat1 imply retrograde import of mature tRNAs by Mtr10. The metabolite pAp is hydrolyzed by Met22 to yield AMP (pA) and inorganic phosphate (Pi) and inhibits Rat1 and Xrn1. Precise activities of described enzymes and participation of others remains undefined. Adapted from Grosjean, 2009.

Another mechanism of tRNA cleavage and degradation involves the nuclease Rny1, which is a member of RNaseT2 family that is secreted and targeted to membrane-bound components, namely the vacuole. This nuclease cleaves tRNAs in the anticodon loop during stress (Macintosh *et al.*, 2001; Thompson and Parker, 2009).

Finally, errors can emerge during tRNA charging by aminoacyl-tRNA synthetases. These errors are mostly caused by the incorrect recognition of cognate tRNAs by aaRSs or by inability of the aaRSs to differentiate between similar amino acids. These errors are minimized by aaRSs editing mechanisms, responsible to reject incorrectly activated amino acids or incorrectly charged tRNAs by specific

tRNA-aaRS interaction networks (Schimmel, 2008a). Aminoacyl-tRNA synthetase editing activities can occur either before and/or after the misactivated amino acid is attached to tRNA, known as pre-transfer editing and post-transfer editing, respectively. Post-transfer editing, was first demonstrated by Eldred and Schimmel and by Yarus (Eldred and Schimmel, 1972; Yarus, 1972; Ling, Reynolds and Ibba, 2009). The pre-transfer editing involves hydrolysis of misactivated aminoacyl-adenylates (aa-AMPs) and may occur *via* 3 pathways: pathway 1 involves the dissociation of an aaRS·aa-AMP complex to free aa-AMP, which spontaneously hydrolyzes in solution; pathway 2 is the tRNA-independent hydrolysis of an aaRS·aa-AMP within the canonical aminoacylation site of the aaRS; and pathway 3 is the tRNA-dependent hydrolysis of an aaRS-bound aa-AMP without transient mischarging of tRNA (Figure 1.13A) (Jakubowski, 2012; Yadavalli and Ibba, 2012). Pre-transfer editing is utilized for the clearance of misactivated Ile by LeuRS, Ala by ProRS, Val by IleRS, and Ser by ThrRS (Jakubowski, 2012). On the other hand, the post-transfer editing requires that the 3'-end of mischarged aa-tRNAs translocate from the active site to editing site of the aaRS, where it deacylates the aminoacyl ester bond between non-cognate amino acid and tRNA. Post-transfer editing can occur by 2 proposed models: the direct translocation model that refers to the movement of the 3' CCA of the mischarged tRNA from the aminoacylation site to the editing site of the aaRS; and/or the dissociation-reassociation model that refers to the release of the mischarged tRNA into solution to be rebound by the aaRS editing site, where hydrolysis occurs, or where it is hydrolyzed by an accessory *trans*-editing factor (Figure 1.13B) (Yadavalli and Ibba, 2012). Post-transfer editing activities are associated with both class I and II aaRSs (IleRS, ValRS, LeuRS, PheRS, ThrRS, ProRS, and AlaRS) to eliminate non-cognate aminoacyl-tRNAs (Ling, Reynolds and Ibba, 2009; Jakubowski, 2012; Yadavalli and Ibba, 2012).

1. Introduction

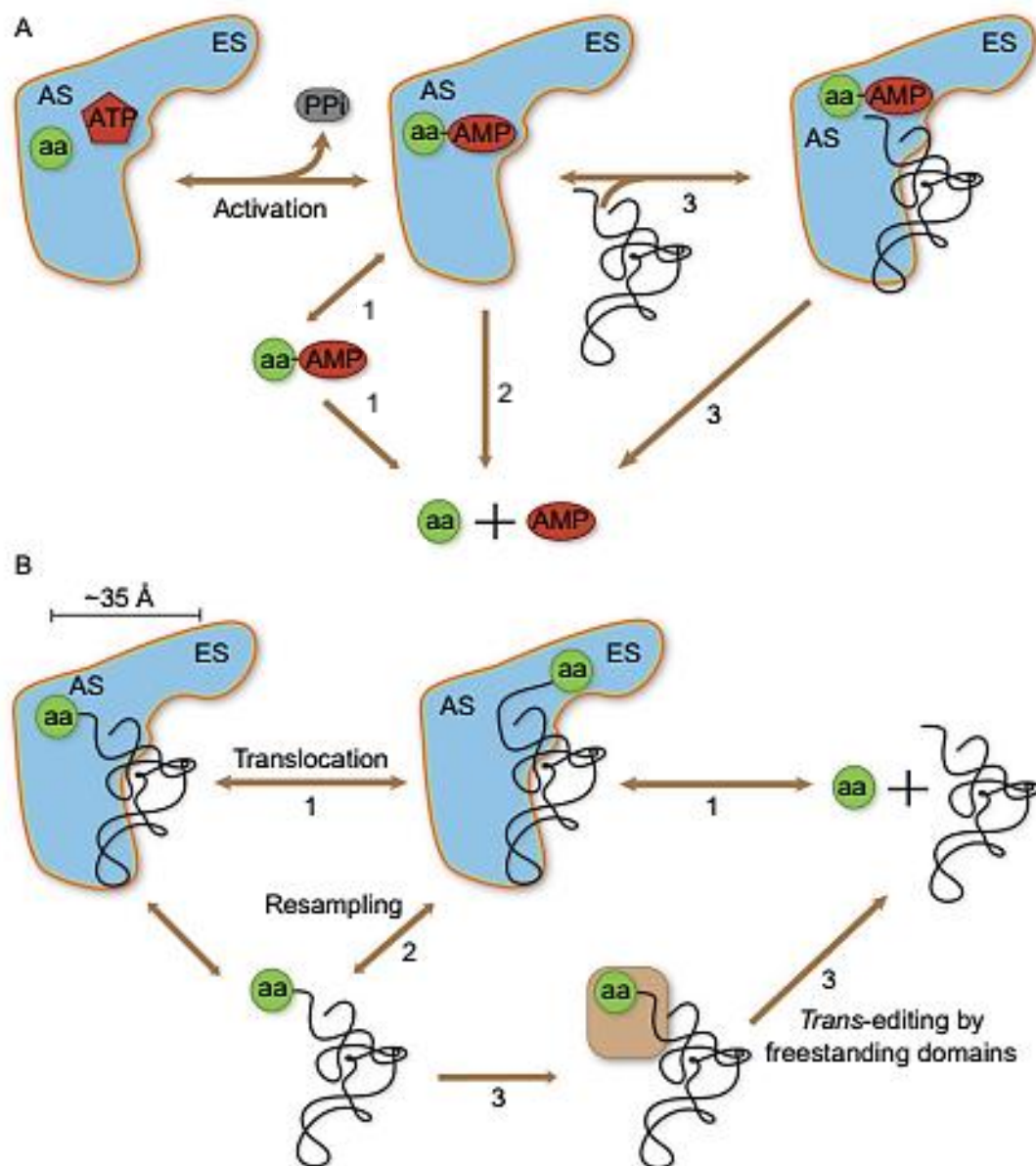


Figure 1.13. Quality control steps for mischarged tRNA. A. Pre-transfer editing pathways in aaRS. The misactivated aa-AMP may be hydrolyzed spontaneously in solution after selective release of non-cognate aa-AMP (pathway 1) or in a tRNA-independent manner through the direct catalysis of aa-AMP hydrolysis by the aminoacylation active site (pathway 2). tRNA-dependent pre-transfer hydrolysis can occur within the aminoacylation active site in some aaRS (pathway 3). **B.** Post-transfer editing pathways in aaRS. A non-cognate aminoacyl-tRNA may be translocated into the editing site of the aaRS for hydrolysis (pathway 1). If the mischarged aminoacyl-tRNA is released from the aaRS without being edited it is subjected to editing through resampling by the aaRS (pathway 2) or by *trans*-editing factors (pathway 3). Adapted from Yadavalli and Ibba, 2012.

1.3 THE RIBOSOME

Ribosomes are critical for protein synthesis since they provide the catalytic activity for the translation of the information contained in mRNA into proteins. An eukaryotic ribosome (80S) consists of two ribonucleoprotein subunits: a small subunit (SSU) – named 40S in yeast, which contains one ribosomal RNA (rRNA) (18S, 1800 nt long) and 33 ribosomal proteins (r-proteins); and a large subunit (LSU) – named 60S in yeast, which contains three rRNAs (5S, 121 nt; 5.8S, 158 nt; and 25S, 3396 nt) and 46 r-proteins, whose function seems to be the stabilization of the highly compact rRNA structures. The mRNA and aminoacylated-tRNA are brought together according to the mRNA sequence in the SSU. The peptidyltransferase reaction that catalyzes peptide bond formation occurs in the LSU.

The small subunit is responsible for the decoding process and its major functional sites are the mRNA path used to conduct mRNA during translation and the decoding center containing the tRNA binding sites (A, P and E). The A-site is where incoming aminoacyl-tRNA is bound during translation, the P-site is where the peptidyl-tRNA with the associated nascent polypeptide chain is located, and the E-site is where deacylated tRNA from the P-site can bind before leaving the ribosome (Rodnina, Beringer and Wintermeyer, 2006; Melnikov *et al.*, 2012). On the other hand, the major functional sites of the large subunit are the tRNA binding sites (A, P and E), the peptide exit tunnel that extends along the body of the LSU, and the peptidyl transferase center (PTC). The PTC is where peptide formation occurs and is located at the beginning of the peptide exit tunnel in a conserved region mainly composed of rRNA. So, as the peptide bond formation occurs in the PTC, the nascent polypeptide chain is transferred from the peptidyl-tRNA in the P-site to the aa-tRNA in the A-site and the nascent chain extends by one amino acid (Melnikov *et al.*, 2012). Additionally, the occupation of the E-site can change allosterically the affinity of the A-site during selection of in-coming aa-tRNAs and influences decoding fidelity (Wilson and Nierhaus, 2006). The ribosome experiments two conformational states during translation: pre-translocational state and post-translocational state. The former is characterized by high affinity for tRNA in A- and P-sites and low affinity in the E-site, while in the second state the P- and E-sites have high affinity for tRNA and the A-site has low affinity. Interestingly, transitions from one state to the other

1. Introduction

occur when the previous low affinity binding site is occupied (Kirillov, Makarov and Semenov YuP, 1983; Gnirke *et al.*, 1989).

80% of total RNA in cells is rRNA, followed by tRNA (15%) and then mRNA (only 5%). Cells produce around 2 000 ribosomes per min, thus, in a cell with a generation time of nearly 100 minutes, there are approximately 200 000 ribosomes per cell (Warner, 1999). Ribosome assembly is a major task for cells, requiring a significant number of resources. For example, it is supported by the three RNA polymerases: RNA Pol I and III transcribe the rRNAs, and RNA Pol II transcribes the mRNA encoding r-proteins (at least 60% of its transcripts). Additionally, ribosome assembly is subjected to quality control simultaneous to nuclear export of pre-rRNPs.

Production of ribosomes is closely related to the growth and proliferation of cells and deregulation of ribosome assembly has a high impact on cell physiology and disease (ribosomopathies).

1.3.1 Structure of ribosomes

The structure of ribosomes has been elucidated by both X-ray crystallography and cryo-EM (Armache *et al.*, 2010; Klinge *et al.*, 2011, 2012; Jenner *et al.*, 2012; Weisser *et al.*, 2013). These studies reveal that the core of each ribosomal subunit contains RNA with the r-proteins (15 conserved proteins in the SSU and 19 in the LSU) assembled on the surface and occasionally projecting into the rRNA core, mentioned above (Spahn *et al.*, 2001; Melnikov *et al.*, 2012). Besides the core, the ribosome contains domain-specific proteins, insertions and extensions of conserved proteins and expansion segments of rRNAs located mostly on the solvent-exposed surface of the subunits (Melnikov *et al.*, 2012). This composition of ribosomes may vary slightly under different conditions of growth and stress.

In the 40S ribosomal subunit the 18S rRNA sequences form four secondary structural domains: the 5', central, 3' major and 3' minor domains (Figure 1.14A). These domains fold into tertiary structures and together with r-proteins form the head, beak, platform, body, shoulder regions of the SSU (Figure 1.15B) (Klinge *et al.*, 2012; Melnikov *et al.*, 2012; Woolford and Baserga, 2013). The mRNA-binding

site is located at the 40S subunit interface and each subunit contains the three tRNA-binding sites (A, P and E) at the 40S/60S interface. The incoming aminoacylated tRNAs bind to their matching codons in the A-site, but the methionyl initiation tRNA binds directly to the P-site. The deacylated tRNAs bind to the E-site (Mahoney, Dempsey and Blenis, 2009) prior to leaving the ribosome. The mRNA enters the ribosome through a tunnel located between the head and the shoulder of the 40S subunit and wraps around the neck of the SSU, while its exit site (5'-end of the mRNA) is located between the head and the platform (Figure 1.15B) (Melnikov *et al.*, 2012). The decoding center of the SSU is located at the 40S/60S interface, where the codons and anticodons pair, conveying fidelity to mRNA decoding (Jenner *et al.*, 2010; Melnikov *et al.*, 2012).

In the large subunit of the ribosome, the 25S rRNAs are arranged into six domains (I-VI) and the 5.8S rRNAs base pair with domain-I of the 25S rRNAs (Figure 1.14B). The central protuberance that contains 5S rRNA is one of the features of the LSU (Figure 1.15A, C, D) (Melnikov *et al.*, 2012; Woolford and Baserga, 2013). The 60S subunit contains 27 eukaryote-specific proteins, multiple insertions and extensions of conserved proteins and a variety of rRNA expansion segments that are concentrated on the periphery of the subunit forming a partial ring-shaped assembly involving the core (Figure 1.15D) (Melnikov *et al.*, 2012). Located at the 40S/60S interface side of the LSU are also the peptidyl transferase center where the peptide bond formation is catalyzed. This PTC is adjacent to the entrance of the polypeptide exit tunnel along which nascent polypeptides progress before they emerge from the ribosome on the solvent side (Melnikov *et al.*, 2012).

The two ribosomal subunits interact through several contact points of the interface, named bridges. Seven bridges connect the ribosomal core and a few bridges are distinct in prokaryotic and eukaryotic ribosomes. Those distinct bridges are formed by a ribosomal protein of the LSU, which binds to the SSU (Melnikov *et al.*, 2012). The two subunits of the ribosome rotate and swivel relative to each other during translation in order to allow translocation of tRNAs and mRNA along the subunit interface (Jenner *et al.*, 2012).

1. Introduction

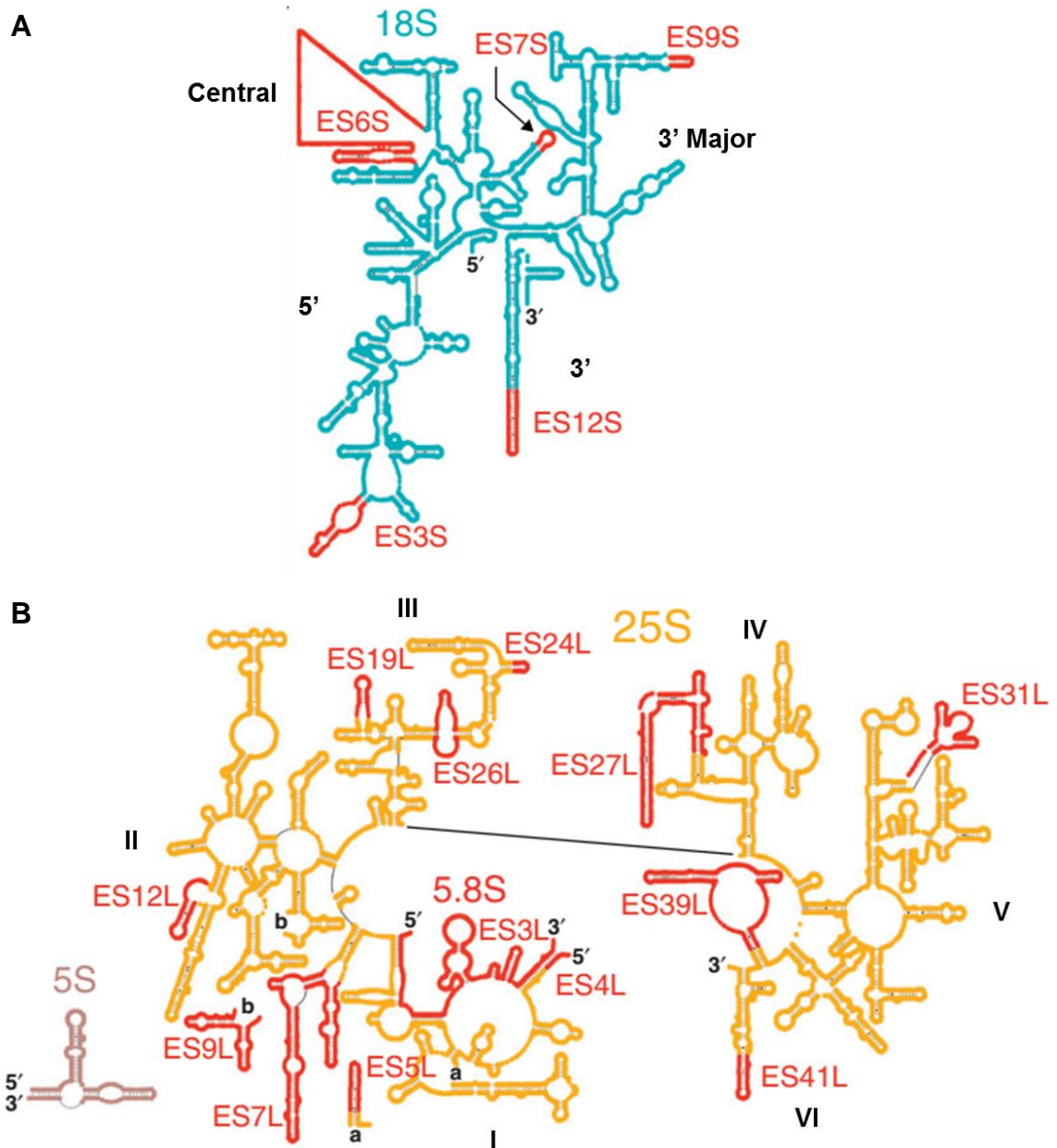


Figure 1.14. Secondary structure of the *S. cerevisiae* ribosomal RNA. **A.** Secondary structure of SSU rRNA: 18S rRNA – blue. The 18S rRNA secondary structure has four domains: 5', central, 3' major, and 3' domains. **B.** Secondary structure of LSU rRNAs: 25S rRNA – orange, 5.8S rRNA – red and 5S rRNA – violet. The 25S rRNA contains six domains (I-VI) of the secondary structure. The 5.8S rRNA (red) base pairs with domain I of 25S rRNA. In red are shown the eukaryote expansion segments (ES). Adapted from Jenner *et al.*, 2012.

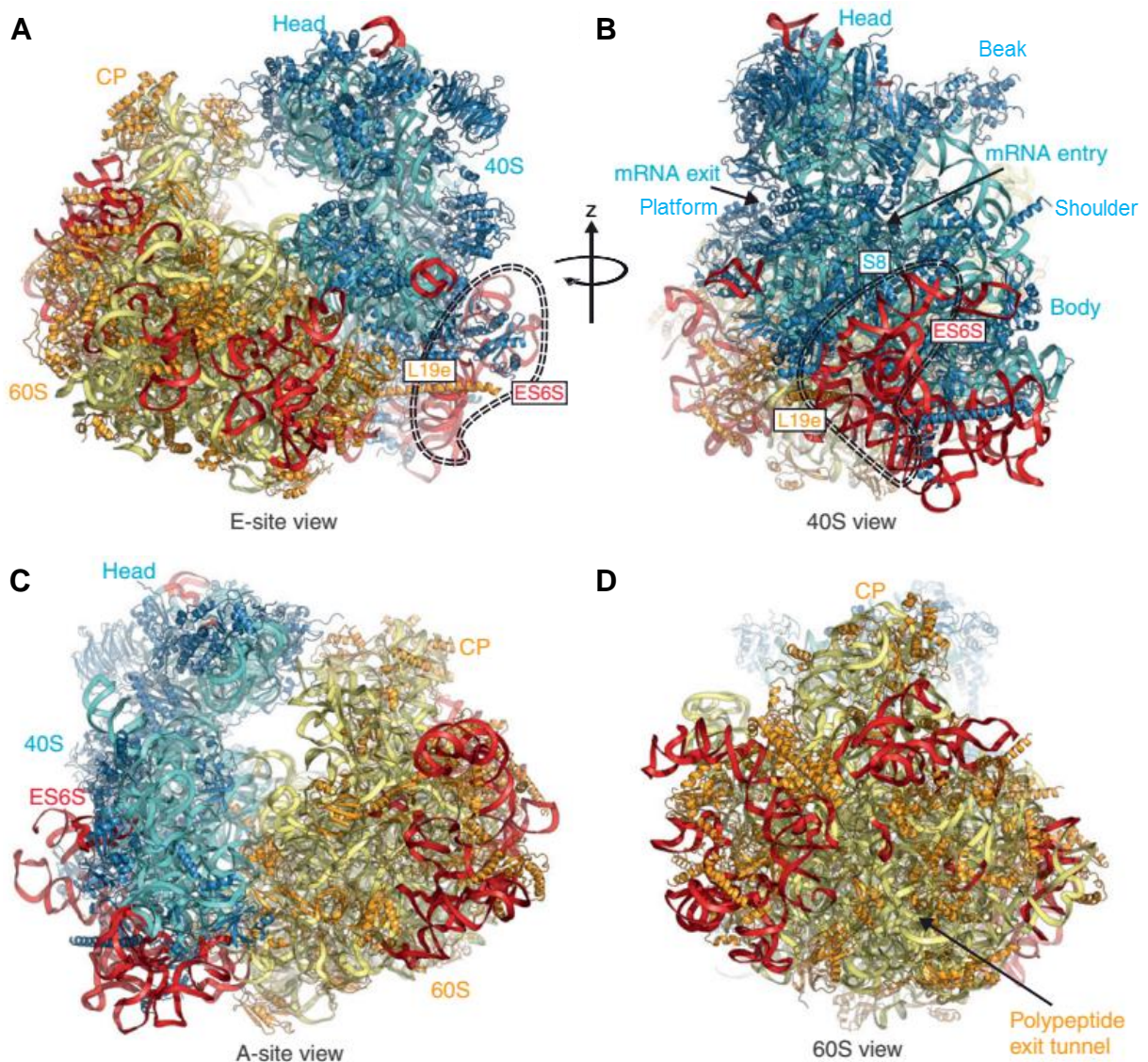


Figure 1.15. Three-dimensional structure of the yeast ribosome. A-D. Views from the E-site, small subunit site, A-site and large subunit site. **B**, **C** and **D** were rotated 90° , 180° and 270° around the z-axis relative to **A**. The LSU is shown in yellow with orange proteins and the SSU in cyan with blue proteins. In red are shown the eukaryote expansion segments (ES), that are located on the surface of the ribosome and concentrated in two large clusters. CP, central protuberance. Adapted from Jenner *et al.*, 2012.

1.3.2 Ribosome biogenesis

The synthesis of ribosomes is one of the major cellular activities that takes place primarily in the eukaryotic nucleolus, a non-membrane-bound sub-compartment of the cell nucleus. It comprises transcription of the rDNA, processing of the pre-rRNA

1. Introduction

transcript, covalent modification of the mature rRNA regions of the pre-rRNA, assembly of the rRNAs with the ribosomal proteins imported from the cytoplasm, and export of the ribosomal subunits from the nucleolus to the cytoplasm (Figure 1.16) (Mélèse and Xue, 1995; Lafontaine and Tollervy, 2001). As mentioned previously, ribosomes are composed of one small (40S) and one large (60S) subunits, which contain rRNA and protein components. Ribosome biogenesis is a complex mechanism involving all three RNA polymerases and translation.

The transcription of the large precursor occurs at the limit of the nucleolar fibrillar center (FC) and dense fibrillar component (DFC) of the nucleolus. Initial processing and assembly happens in the DFC of the nucleolus and late processing in the granular component (GC) and then in the nucleoplasm, before exporting of the pre-ribosomal particles through nuclear pores to the cytoplasm (Sandmeier *et al.*, 2002; Nazar, 2004). In *S. cerevisiae*, the maturation process is completed in the cytoplasm (Figure 1.16).

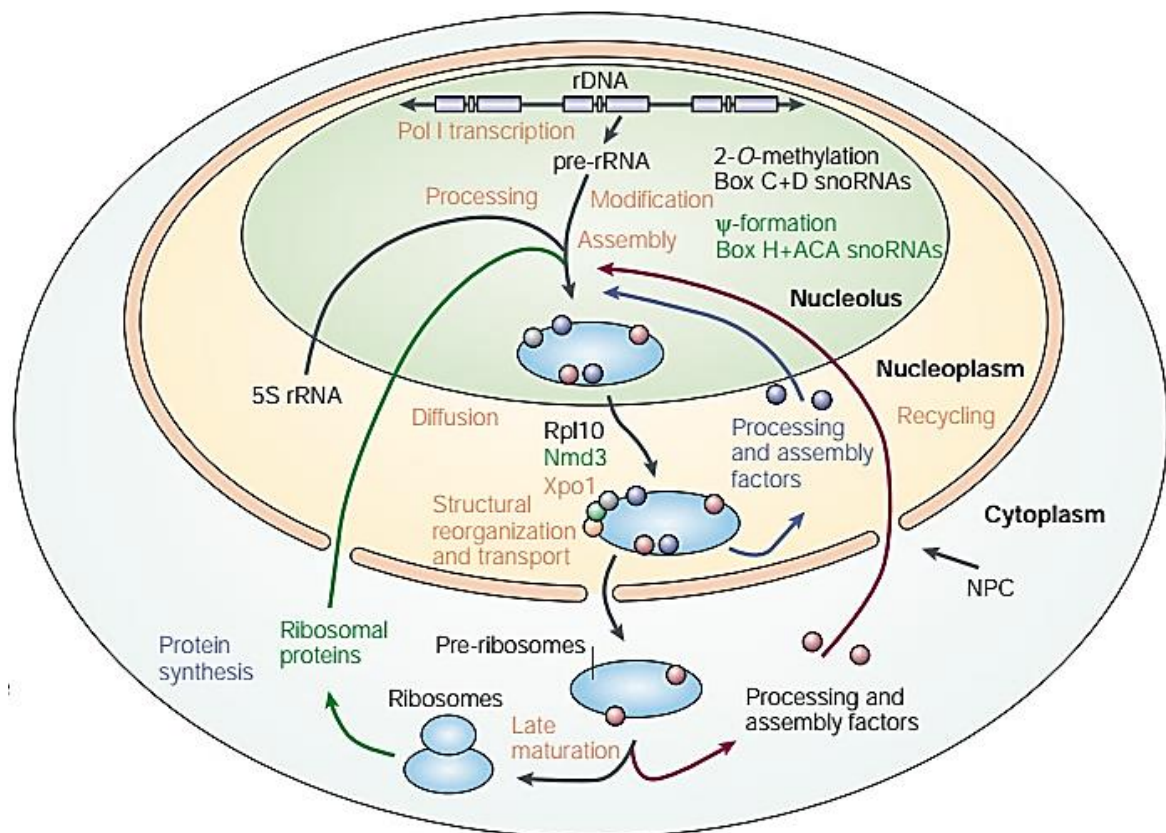


Figure 1.16. Eukaryotic ribosome synthesis. Most steps of pre-rRNA processing occur within the nucleolus, where the pre-rRNAs yield the mature rRNAs that also undergo

extensive covalent modification. In eukaryotes, most modification involves methylation of the sugar 2' hydroxyl group (2'-O-methylation) or pseudouridine formation, which are mediated by small nucleolar ribonucleoprotein (snoRNP) particles. During pre-rRNA processing many of the r-proteins assemble into the mature rRNA regions of the rRNA. During maturation, the pre-ribosomal particles diffuse to the nuclear pore complex (NPC), mediated by the small GTPase Ran and the export factor Xpo1, which binds to the ribosomal protein Rpl10 through an adaptor protein, Nmd3 in the case of pre-60S subunit. Export of the pre-40S subunit only requires Ran. In the cytoplasm, structural rearrangements occur that convert the pre-ribosomal particles to the mature ribosomal subunits. Adapted from Lafontaine and Tollervey, 2001.

1.3.2.1 Transcription of pre-rRNAs

In *S. cerevisiae*, the genes coding for the 35S rRNA precursor are organized in one cluster containing 100-200 tandem repeats separated by short spacers (non-transcribed spacer – NTS) containing also the 5S rRNA gene (transcribed in the opposite direction by RNA Pol III) (Figure 1.17) and an origin of DNA replication on chromosome XII (Venema and Tollervey, 1995). Contrary to the rRNA genes, the genes for r-proteins are scattered throughout the eukaryotic genomes (Planta and Raué, 1988).

rRNA genes are highly transcribed in the nucleolus by RNA Pol I and RNA Pol III. RNA Pol I transcribes the 35S rDNA that contains the 25S, 18S, and 5.8S rRNA components separated by two internal transcribed spacers, ITS1 and ITS2, and flanked by two external transcribed spacers, the 5' ETS and 3' ETS (Figure 1.17) (Venema and Tollervey, 1995). On the other hand, Pol III transcribes the 5S rRNA as a 3'-end extended precursor (Lee and Nazar, 2003). Pre-40S ribosomal subunits contain the 18S rRNA and the pre-60S ribosomal subunits integrate the 28S, 5.8S, and 5S rRNA species. Maturation of pre-40S and pre-60S ribosomal subunits occurs in the cytoplasm (Venema and Tollervey, 1995; Mahoney, Dempsey and Blenis, 2009).

rRNA transcription is regulated by transcriptional initiation frequency and/or elongation from each open rRNA gene and by the ratio of active (opening) to inactive (closing) rDNA repeats (Sandmeier *et al.*, 2002; Woolford and Baserga, 2013).

1. Introduction

Additionally, Pol I activity depends on four transcription factors: TATA binding protein (TBP), Rrn3, upstream activating factor (UAF; comprises Rrn5, Rrn9, Rrn10, Uaf30 and histones H3 and H4) and core factor (CF; comprises Rrn6, Rrn7 and Rrn11). Additionally, rRNA synthesis is coordinated with the ribosomal proteins synthesis in order to ensure an efficient assembly of ribosomal subunits (Warner, 1999).

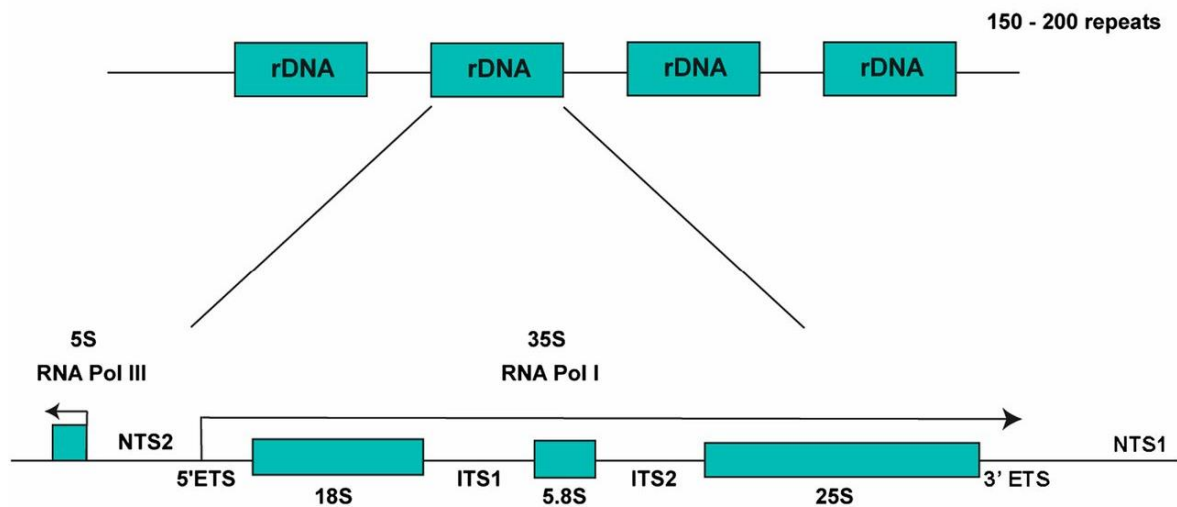


Figure 1.17. Structure of rDNA in yeast. The rDNA repeats are located on chromosome XII. RNA Pol I transcribes a single repeat unit to synthesize the 35S primary pre-rRNA transcript, whose processing produces the mature 18S, 5.8S and 25S rRNAs (arrow pointing right). RNA Pol III also transcribes a single repeat unit to synthesize the 5S rRNA (arrow pointing left). NTS: non-transcribed spacer; ETS: external transcribed spacer; ITS: internal transcribed spacer. Adapted from Woolford and Baserga, 2013.

1.3.2.2 Processing of pre-rRNAs

Maturation of the primary 35S precursor into the mature 18S, 5.8S and 25S rRNA involves a multistep pathway and requires many different *trans*-acting factors (e.g. snoRNPs, putative helicases, ribonucleases) for the removal of the four transcribed spacers by endonucleolytic and exonucleolytic processing reactions (Venema and Tollervey, 1995; Dieter Kressler *et al.*, 1999). On the other hand, processing of the pre-5S rRNA is independent of the 35S pre-rRNA processing. This precursor only

needs to be processed at its 3'-end by an exonucleolytic cleavage (Lee and Nazar, 2003).

The first pre-35S rRNA processing event is the cleavage by the endo-RNase Rnt1 in the 3' ETS followed by cleavage at the site A₀ in the 5' ETS to generate the 33S primary pre-rRNA transcript (Figure 1.18) (Hughes and Ares, 1991; Lafontaine and Tollervey, 1995; Dieter Kressler *et al.*, 1999; Venema and Tollervey, 1999). Then cleavage at A₁ site in the 5' ETS produces 32S pre-tRNA and cleavage at the A₂ site in the ITS1 generates the 20S and 27SA₂ pre-rRNAs, which can occur co-transcriptionally in 40-80% of the nascent transcripts (Hughes and Ares, 1991; Woolford and Baserga, 2013). The cleavage of the ITS1 can also be done by the RNase MRP at the A₃ site, producing instead the 23S and 27SA₃ pre-rRNAs (Tollervey, 1996; Dieter Kressler *et al.*, 1999; Woolford and Baserga, 2013). The 20S pre-rRNA undergoes endonucleolytic cleavage by Rio1/Rrp10 at D site to remove the remaining ITS1 sequences, producing mature 18S rRNA, a step which occurs after export to the cytoplasm (Vanrobays *et al.*, 2001). On the other hand, 27SA₂ pre-rRNA processing can occur by two alternative pathways (Figure 1.18). Most frequently (85-90%), 27SA₂ pre-rRNA is first processed to 27A₃ pre-rRNA *via* MRP RNase at the A₃ site in the ITS1, and then 5'-3' exonucleases Rat1 and Rrp17 (or Xrn1) eliminate the remaining ITS1 spacer sequences from 27A₃ pre-rRNA, stopping at the B_{1S} site and forming the 5'-end of 27SB_S pre-rRNA. The alternative pathway (10-15%) of 27SA₂ pre-rRNA processing involves direct cleavage at the B_{1L} site in 27SA₂ pre-rRNA (by an unknown endonuclease), generating 27SB_L pre-rRNA. Either the 27SB_S and 27SB_L pre-rRNAs are endonucleolytic cleaved at the C₂ site of the ITS2 spacer to form the 25.5S and 7S_S/7S_L pre-rRNAs. Finally, the 5'-end of 25.5S pre-rRNA is trimmed by Rat1 to generate mature 25S rRNA. And, the 3'-ends of 7S pre-rRNAs are processed *via* a 3'-5' exonucleolytic processing mechanism requiring the exosome (composed of three 3'-5' exonucleases – Rrp4, Rrp41/Ski6, Rrp44 – and eight putative ones – Csl4, Mtr3, Rrp40, Rrp42, Rrp43, Rrp45, Rrp46 and Rrp6), and producing mature 5.8S_S and 5.8S_L rRNAs, which differ by 6 nucleotides at their 5'-ends (Dieter Kressler *et al.*, 1999; Venema and Tollervey, 1999; Woolford and Baserga, 2013).

1. Introduction

Some of the removed pre-rRNA spacer fragments, namely A₀-A₁, D-A₂, and A₂-A₃ fragments, are degraded by Rat1 and Xrn1 (Dieter Kressler *et al.*, 1999).

rRNA processing and ribosome biogenesis require interaction with snoRNA-protein complexes (snoRNPs), such as U3 snoRNA. Interestingly, a 10-nucleotide sequence, 250 nucleotides before the A₁ cleavage site, is complementary to the 5'-end of the U3 snoRNA and acts as a binding site for a U3 snoRNA, whose binding directs nuclease activities. A few other snoRNAs also participate in pre-rRNA cleavage (U8, U14, U22, snR10 and snR30) (Nazar, 2004). For instance, pre-18S processing requires U3, U14, snR30 and snR10, in addition to RNase MRP (Lemay *et al.*, 2011; Woolford and Baserga, 2013).

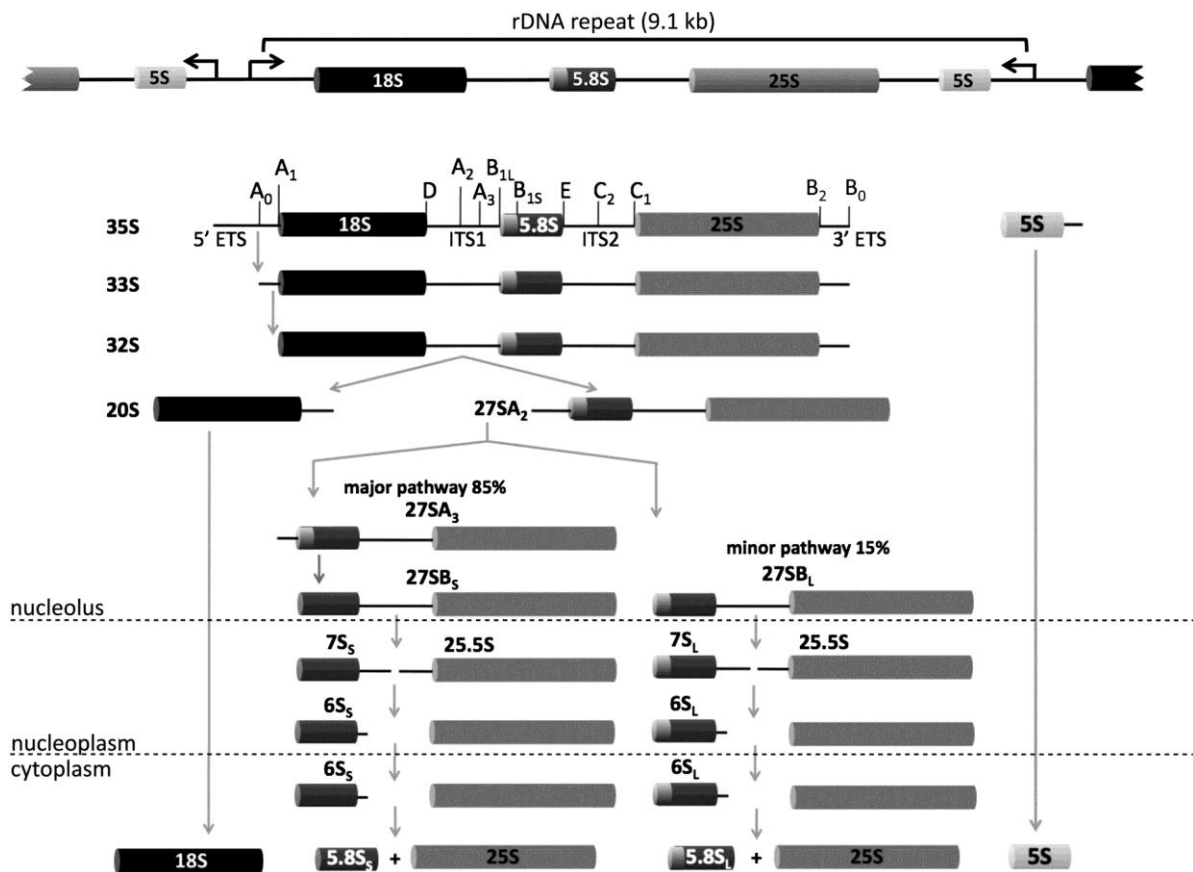


Figure 1.18. Pre-rRNA processing in *S. cerevisiae*. An rDNA repeat unit contains a large operon encoding the 35S pre-rRNA, which is transcribed by RNA Pol I and comprises sequences for 18S, 5.8S and 25S rRNAs (black, dark gray, and light gray cylinders), and an RNA Pol III-transcribed 5S rRNA gene (white cylinder). Processing steps to generate each rRNA are indicated and include removal of spacer sequences in a series by

endonucleases and exonucleases. rRNA processing begins in the nucleolus of the cell, but later phases occur in the nucleoplasm and cytoplasm. Adapted from Woolford and Baserga, 2013.

1.3.2.3 Modification of pre-rRNAs

Many specific nucleotides within the rRNA also undergo covalent modification during rRNA maturation and even co-transcriptionally. The modifications include isomerization of uridine to pseudouridine by base rotation (Ψ ; 45 modified nucleotides), methylation of the 2'-hydroxyl group of sugar residues (2'-O-ribose methylation – Nm; 67 modified nucleotides) and base methylation (mN; approximately 10 modified nucleotides) (Dieter Kressler *et al.*, 1999; Woolford and Baserga, 2013). Little is known about the functional roles of nucleotide modification in rRNA: pseudouridine residues seem to alter base stacking and has an extra hydrogen bond donor (relative to uridine), contributing to RNA stability (Charette and Gray, 2000; Helm, 2006); Nm residues seem to alter RNA structure and protect from hydrolysis by nucleases and bases (Decatur and Fournier, 2002; Helm, 2006; Baxter-Roshek, Petrov and Dinman, 2007). However, rRNA modifications do not seem to be positioned arbitrarily. Those modifications occur at sites that cluster near the active core of the ribosome, namely in the ribosomal large subunit, where modifications cluster in highly conserved regions of the ribosome dedicated to peptidyl transfer, sites of tRNA binding (A- and P-sites – domain V of LSU), the peptide exit tunnel and inter-subunit bridges (Figure 1.19 and Figure 1.20), and help the tight packing of the rRNAs through tertiary interactions (Decatur and Fournier, 2002). In yeast, the sites of modification in the SSU are concentrated in the area where the head and upper body regions converge, particularly in A- and P-sites and in the mRNA-channel latch region, which could affect its function in mRNA binding (Figure 1.20A, B). Also, modifications are concentrated at the subunit interface, particularly for the Nm nucleotides in the yeast SSU (Figure 1.20B), and are present in inter-subunit bridges, suggesting their influence in subunit interactions (Decatur and Fournier, 2002). In turn, almost all modifications in the LSU occur at domains II, IV and V (Figure 1.19B). Interestingly, domain V is at the center of the subunit interface, including the PTC, and is surrounded by domains II and IV. So, almost all

1. Introduction

modifications in the yeast LSU cluster near the core of the subunit and define a shell around the regions for the A- and P-sites tRNAs. In fact, modified nucleotides at the A- and P-sites, particularly Nm modified nucleotides, are predicted to base pair with nucleotides of the tRNA acceptor end to modulate tRNA binding (Decatur and Fournier, 2002). The overall effect of rRNA modification could be associated with changes in rRNA structure that could enhance rRNA folding, rRNA assembly, or ribosome activity, trafficking and half-life (Decatur and Fournier, 2003). Additionally, defects in rRNA modification were shown to have influence in ribosome integrity and translation rates (Baxter-Roshek, Petrov and Dinman, 2007).

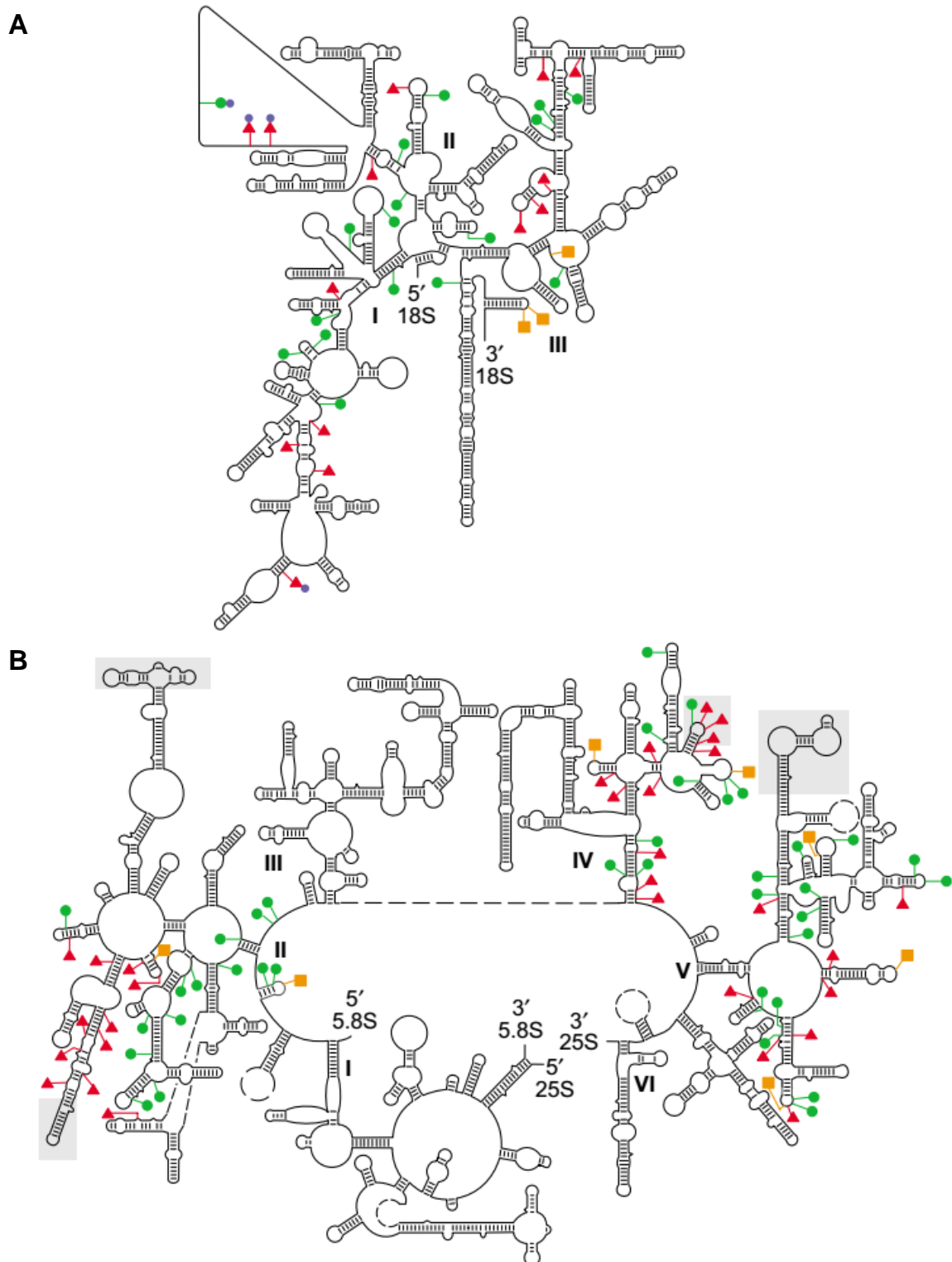


Figure 1.19. Distribution of rRNA modifications in the yeast ribosome. Secondary structure maps showing modification sites for the 18S (**A**) and 25S-5.8S (**B**) rRNAs. RNA domains are identified with Roman numerals. The color scheme for modifications is red

1. Introduction

triangle for Ψ , orange square for mN and green circle for Nm. Adapted from Decatur and Fournier, 2002.

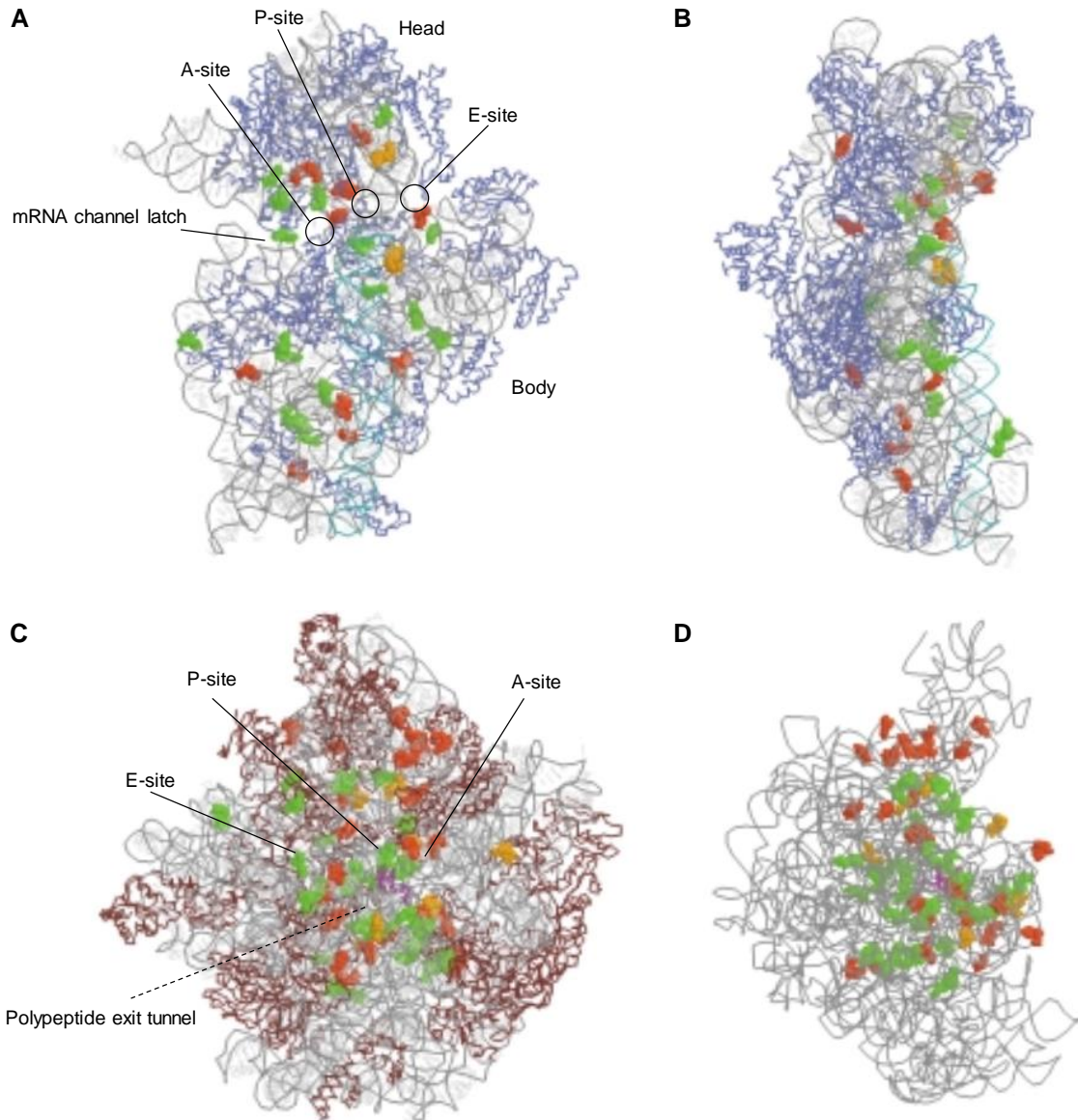


Figure 1.20. Three-dimensional distribution of rRNA modifications in the *S. cerevisiae* ribosome. **A, B.** Sites of yeast modification in two views of the SSU. **C, D.** Positions of yeast modifications in two views of the LSU. Predicted sites for modifications are shown in the three-dimensional subunits for 44 (of 45) pseudouridines (red), 54 (of 67) 2'-O-methylations (green) and 10 (of ~10) base methylations (orange). The distribution of these modifications within the SSU and the LSU are: Ψ – 14/30, mN – 3/7 and Nm – 17/37. Unmodified nucleotides in the rRNA of the ribosomal subunits are represented in grey,

whereas protein chains are represented in blue for SSU and in maroon for LSU. Adapted from Decatur and Fournier, 2002.

Covalent modifications are first introduced on the 35S pre-rRNA (Figure 1.21A), which is extensively modified particularly by 2'-O-ribose methylation and pseudouridylation at sites that are selected by small ribonucleoprotein particles (snoRNPs) (Venema and Tollervey, 1999). The snoRNPs are complexes comprising nuclear proteins and snoRNAs, whose function is to guide the modification by enzymatic activities associated with the protein complex. The snoRNAs (75-100 different in yeast) are divided into two families called C/D box and H/ACA box snoRNAs (Nazar, 2004). Each class of guide snoRNAs and snoRNPs is both modification type-specific and site-specific. Members of the H/ACA box family contain guide sequences for pseudouridylation, while those of the C/D box family are complementary to targets of rRNA for methylation. Each box H/ACA snoRNA has two hairpins separated by a short single stranded sequence (hinge) (Figure 1.21C), thus binding to one or two sites of pseudouridine formation, where it forms short base-paired regions with the rRNA sequence (guide sequences of 4-8 nt) to modify uracil in the pseudouridylation pocket (Venema and Tollervey, 1999; Decatur and Fournier, 2002; Reichow *et al.*, 2007). The H/ACA snoRNPs box comprises four protein components: Cbf5 (dyskerin in humans), that is the catalytic pseudouridine synthase; Gar1, Nop10, and Nhp2, which perform structural functions, stabilizing the tertiary fold of the RNA and ensuring correct positioning of the target nucleotide in the Cbf5 active site (Figure 1.21C) (Henras *et al.*, 2004; Normand *et al.*, 2006). On the other hand, each C/D snoRNA box base-pairs to one or two 2'-O-ribose methylation sites. At those sites, the C/D snoRNA box forms an extended region of complementarity, where the D box region is placed five base pairs from the nucleotide to be modified (Venema and Tollervey, 1999; Gagnon, Qu and Maxwell, 2009). The box C/D guide RNAs comprise the box C (RUGAUGA, where R is purine) and box D (CUGA) sequence elements located at the 5' and 3' RNA ends, respectively, and the internal box C' and D' elements. Those terminal and internal boxes create the box C/D and C'/D' motifs, respectively. Both motifs fold into RNA elements known as kink-turns (K-turns), which are characterized by

1. Introduction

an asymmetric bulge flanked by two stems and stabilized by tandem, shared G:A pairs (Figure 1.21B) (Reichow *et al.*, 2007; Grosjean, 2009a). The four protein components of C/D snoRNA box are fibrillarin/Nop1, the methyltransferase that catalyzes nucleotide modification; Snu13, that binds to the K-turn in the C/D snoRNA box; Nop58 and Nop56, which have extensive coiled-coil domains with which they heterodimerize (Figure 1.21B) (Watkins *et al.*, 2000; Gagnon, Qu and Maxwell, 2009; Woolford and Baserga, 2013).

However, a pseudouridine (Ψ_{50}) present in yeast 5S rRNA and a 2'-O-methylation (Gm₂₉₂₂) in the 25S rRNA are generated by protein-only enzymes (Pus7 and Spb1, respectively) that recognize the U₅₀ and G₂₉₂₂ and catalyze their modification, respectively (Lapeyre and Purushothaman, 2004; Decatur and Schnare, 2008). Similarly, base methylation is mediated by specific protein enzymes.

As verified in tRNAs, rRNA modifications can be a source of ribosome heterogeneity that may alter ribosome function in response to distinct environmental conditions (Sloan *et al.*, 2016).

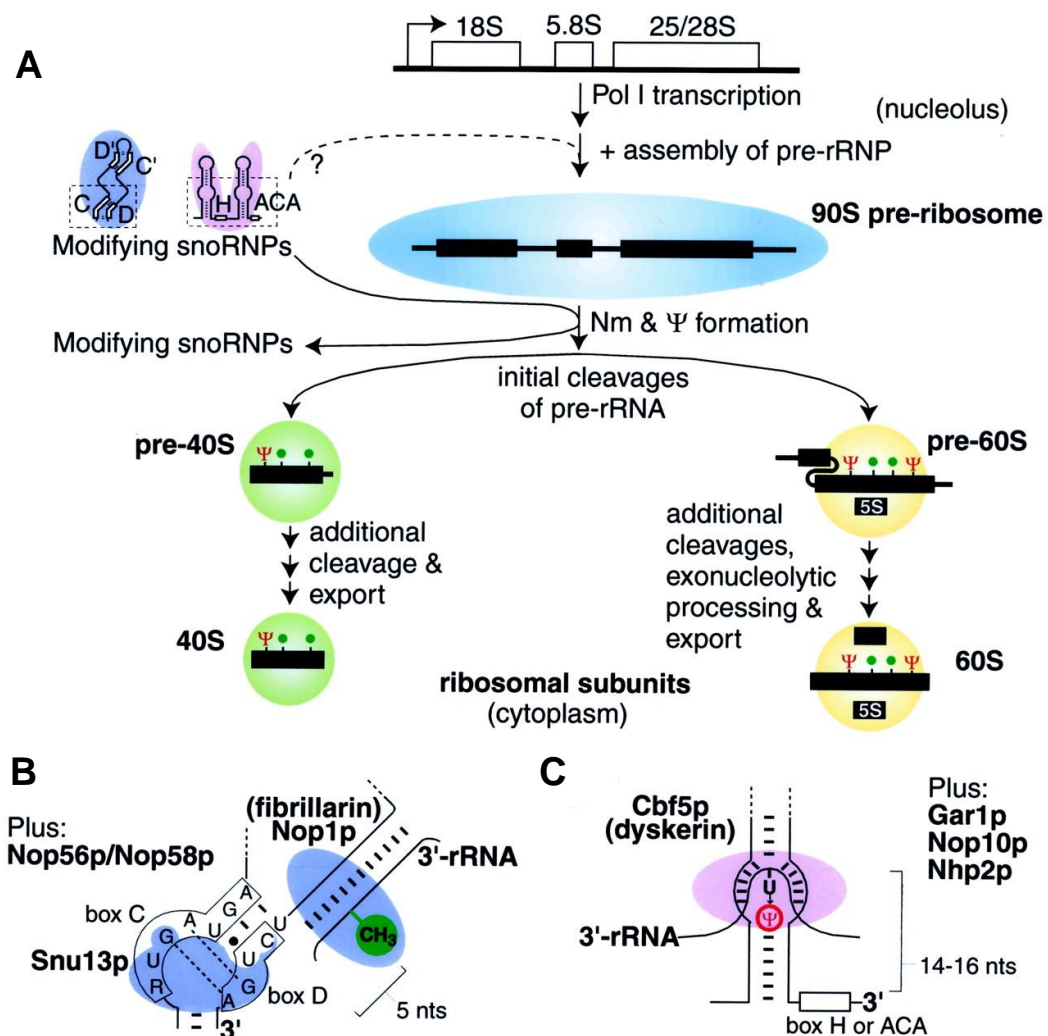


Figure 1.21. rRNA modification by snoRNPs. **A.** Overview of ribosome synthesis. snoRNPs modify pre-rRNA in the nucleolus during or post transcription. **B.** The diagram shows the interaction of C/D snoRNA box with its target rRNA. **C.** The diagram shows the interaction of H/ACA snoRNA box with its target rRNA. Adapted from Decatur and Fournier, 2003.

1.3.2.4 Ribosome assembly

Assembly of the 4 rRNAs and 79 r-proteins into ribosomes requires 76 small nucleolar RNAs and >200 assembly factors and occurs concomitantly with maturation and folding of the pre-rRNA (Nazar, 2004; Woolford and Baserga, 2013). In yeast, many r-proteins associate with pre-ribosomes at the earliest events of subunits assembly to initiate assembly. Some r-proteins enter into the rRNA core, but part of them has also extensions that overpass the RNA surface to function as

1. Introduction

binding site for assembly or translation factors. r-proteins located in the body of 40S subunits, bound near the 5' domain of 18S rRNA, are important for early steps in pre-rRNA processing. Contrary, r-proteins relevant for later steps (S10, S25, S27, S31, S32, S33 and S34) are mainly located in the head of the SSU, bound to 3' domain of 18S rRNA (Kruiswijk, Planta and Krop, 1978). Similarly, LSU r-proteins bound to domains I and II in the 5'-end of 25S/5.8S rRNA are required for early steps, the processing of 27SA₂ and 27SA₃ pre-rRNA. r-proteins bound to domains I and III, located near the polypeptide exit tunnel, are required for a middle step of pre-rRNA processing, cleavage of 27SB pre-rRNA. Finally, r-proteins involved in late steps (L6, L7, L8, L9, L11, L15, L16, L23, L24, L30, L32, L36, L40, L41, L42, L44 and L45), processing of 7S pre-rRNA and nuclear export, are located on the interface surface of LSUs and near the central protuberance (Kruiswijk, Planta and Krop, 1978; Woolford and Baserga, 2013).

Approximately 90 proteins are in the 66S precursors of mature 60S subunits and the earliest pre-40S subunit contains the U3 snoRNA (enable correct folding) and more than 75 proteins, all participating in assembly (Grandi *et al.*, 2002; Woolford and Baserga, 2013) (Figure 1.22). Among those proteins are endo- and exonucleases (for processing), enzymes that modify RNA or proteins, RNA helicases/ATPases, AAA ATPases, GTPases, kinases and phosphatases, RNA binding proteins, putative scaffolding proteins, and few proteins with high homology to r-proteins. Each of those proteins function at a specific event(s) in pre-rRNA processing, nuclear export, and/or subunit maturation (Watkins and Bohnsack, 2012).

Assembly initiates with pre-40S and pre-60S subunits associated with some assembly factors and r-proteins. During maturation of these initial pre-ribosomes, they experience RNA-protein alterations that requires helicases and includes release of some assembly factors (Figure 1.22). In the earliest events of pre-40S maturation that follows the cleavage at the A₂ site, large number of the early-acting factors as well as the U3 subunit are discarded and a few late-acting factors assemble onto pre-rRNPs (Schafer *et al.*, 2003; Woolford and Baserga, 2013). On the other hand, maturation of 66S pre-ribosomes, to generate mature 60S subunits, involves: construction of stable early assembly intermediates containing 27SA₂ pre-

rRNA, cleavage of 27SA₂ pre-rRNA at the A₃ site and removal of ITS1 to form 27SB pre-rRNA, release of early-assembly factors, cleavage at the C₂ site in ITS2, removal of ITS2 from 25.5S and 7S pre-rRNAs, nuclear export and cytoplasmic maturation of subunits. The early pre-60S ribosomes comprising 27SA₂ or 27SA₃ pre-rRNA contains at least 45-50 assembly factors. Among those factors are proteins that form the Pwp1 complex, namely Ebp2, Brx1, Nop12, L8 and Pwp1, that function together to process 27SA₂ and 27SA₃ pre-rRNAs. Few assembly factors join these intermediates, in order to catalyze release of the early factors and elimination of the ITS2 spacer from 27SB pre-rRNA, or to ease the export of the pre-RNPs to cytoplasm. After export, the last steps in pre-rRNA processing and assembly of the late r-proteins are facilitated by 10-12 late-acting factors that bind to cytoplasmic pre-ribosomes. Finally, the last 6-8 assembly factors are released (Figure 1.22) (Nissan *et al.*, 2002; Woolford and Baserga, 2013).

Exported pre-40S particles into the cytoplasm contain seven assembly factors and lack two r-proteins (S10 and S26). Those assembly factors are important to protect pre-40S subunits from premature association with translation initiation factors and with 60S ribosomal subunits by overlapping their respective binding sites (Strunk *et al.*, 2011). Pre-60S subunits are also prevented from participating in translation by blocking their association with 40S subunits (Gartmann *et al.*, 2010; Strunk *et al.*, 2012).

In mature ribosomes, all r-proteins directly interact with rRNA and stabilize rRNA folding (Ramaswamy and Woodson, 2009; Woodson, 2011; Woolford and Baserga, 2013).

1. Introduction

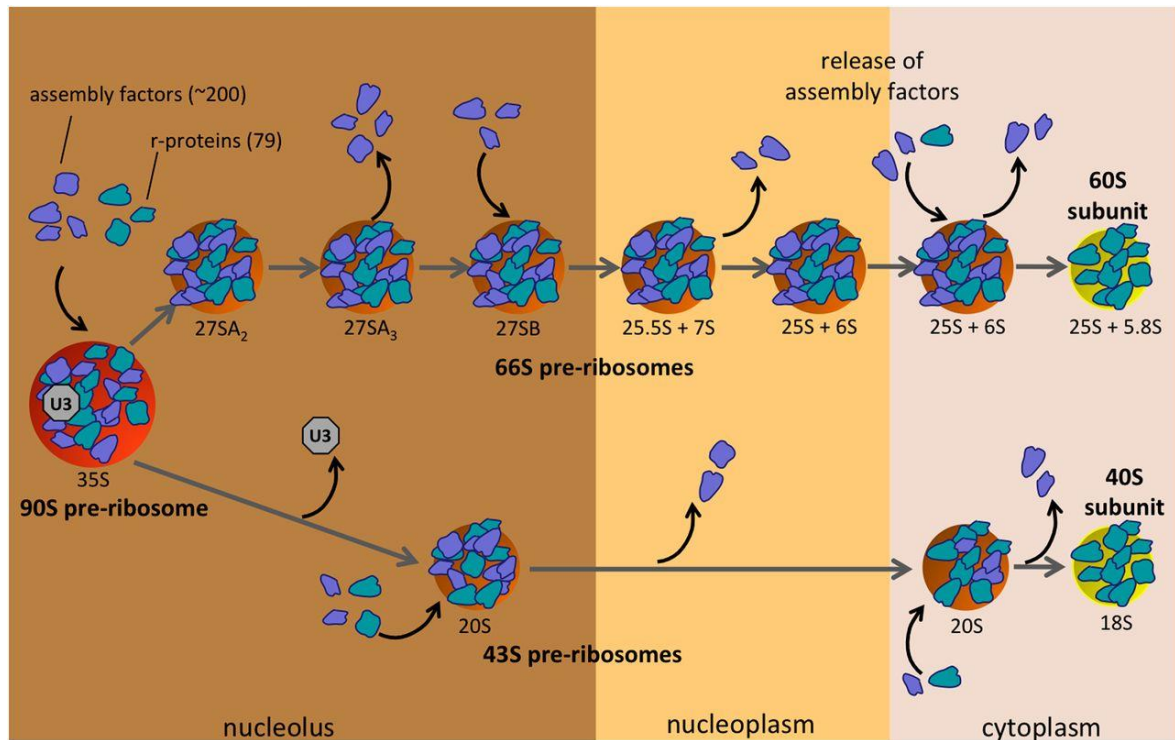


Figure 1.22. Maturation of pre-ribosomes to form 40S and 60S ribosomal subunits. Intermediates for sequential assembly are shown associated with the respective pre-rRNA processing intermediate. The early nucleolar/nuclear precursors are associated to most r-proteins (light blue) and many assembly factors (dark blue). Some other assembly factors connect pre-ribosomes in middle steps of assembly or even during late steps in the cytoplasm. During early, middle or late stages of subunit maturation assembly factors are released from pre-ribosomes. Adapted from Woolford and Baserga, 2013.

1.3.3 Quality control

Alterations in the structure and dynamics of ribosomal subunits can lead to decreased fidelity of protein synthesis. Thus, a proofreading mechanism for assembly of pre-ribosomes, assuring that only functional RNA is incorporated, and for degradation of misassembled pre-ribosomes is essential.

One quality control mechanism was attributed to the 5S rRNA-binding protein Rpl5 that binds over or caps the termini in a critical manner, protecting the nascent 5S rRNA from degradation by housekeeping nucleases. This precise binding is crucial to 5S rRNA stability and even for ribosome integrity (Lee and Nazar, 2003). Additionally, the formation of the nucleolar pre-ribosome particle comprising the two

pre-ribosomal subunits as well as a third domain with spacer elements, nucleolar proteins and snoRNAs is a process of fitting everything correctly into this large particle, acting as a kind of “checklist” to ensure that all is normal. Failure during this step makes aberrant pre-rRNA susceptible to housekeeping nucleases, which degrade the nascent rRNA, avoiding its incorporation into ribosomes (Nazar, 2004).

rRNA modification may also act as a quality control mechanism, in addition to its role on rRNA conformation and stability, protein binding, and even ribosome function. Since rRNA modifications are mediated by snoRNAs, which share long sequence complementarities and pair with the rRNA, these interactions could be a form of proofreading (Song and Nazar, 2002). In this way, altered sequences in the rRNA would not effectively pair with snoRNAs and would disrupt the modification process. Thus, modified nucleotide position would be unstable or less stable, being critical sites for nuclease attack and elimination (Song and Nazar, 2002; Nazar, 2004).

The mechanism for surveillance and degradation of misassembled ribosomes is performed by the exosome complex of exonucleases (Allmang *et al.*, 2000). For that, pre-rRNAs are adenylated at their 3'-end by nuclear TRAMP complexes, containing poly(A) polymerase Trf4 or Trf5, the RNA helicase Mtr4, and RNA-binding protein Air1 or Air2. The Mtr4 helicase help to disassemble pre-rRNAs or pre-RNPs and adenylation of pre-rRNAs may form an ideal substrate for binding and 3' degradation by the exosome (Lacava *et al.*, 2005; Houseley, LaCava and Tollervey, 2006; Woolford and Baserga, 2013). This mechanism of nucleolar surveillance can be initiated co-transcriptionally and might take place in a distinct region of the nucleolus, termed “No-body” (Dez, Houseley and Tollervey, 2006; Wery *et al.*, 2009; Woolford and Baserga, 2013).

1. Introduction

1.4 PROTEIN BIOSYNTHESIS

The translation of mRNA is divided in four main steps: initiation, elongation, termination and recycling. The goal of initiation is to position the ribosome at the start of the coding region, i. e., at the initiation codon of the mRNA with a methionyl initiator tRNA bound in the ribosomal P-site. Elongation of the peptide chain then begins with the selection of tRNAs in the acceptor A-site, and then the ribosome catalyzes the formation of a peptide bond. The tRNAs and mRNA are translocated, so that the next codon can be moved into the A-site. Termination occurs when a stop codon (UAA, UAG, or UGA) arrives at the active ribosomal A-site. The finished polypeptide chain is then released from the ribosome. Finally, ribosome recycling involves the separation of the ribosomal subunits, releasing the mRNA and the deacylated tRNA (Jansen *et al.*, 1995; Kapp and Lorsch, 2004). These fundamental events sometimes differ between bacteria, eukaryote, and archaea (Kapp and Lorsch, 2004).

As mentioned before, the small unit is responsible for the decoding process, where aminoacylated tRNAs are selected according to the mRNA sequence, and the large subunit is responsible for the peptide bond formation.

Gene expression is regulated at different levels, namely chromatin structure (histones modifications and DNA methylation), transcription of the gene into mRNA, processing and modification of mRNA transcripts, transport of the mRNA from the nucleus to the cytoplasm, stability/decay of mRNA transcripts, binding of the mRNA to ribosomes, initiation, elongation and termination of translation, and processing of proteins to their final and functional conformation (Lodish, 1976; Adeli, 2011). At the translation level, the main control point is the initiation step, but elongation and termination are also important. Furthermore, eukaryotic mRNAs have structural *cis*-acting elements such as 5'- and 3'-UTRs facilitating specific regulation by *trans*-acting RNA binding proteins. mRNA stability and its rate of translation is also controlled by small microRNAs (miRNAs) that hybridize to mRNA sequences within the 3'-UTR or other regions. On the other hand, translational efficiency could be determined by motifs within mRNA, namely the presence of start-site consensus sequence, secondary structure, upstream open reading frames (uORFs), the canonical end modification of mRNA molecules – the cap structure and the poly(A)

tail, and internal ribosomal entry sites (IRES) (Gebauer and Hentze, 2004; Adeli, 2011). Since mRNAs are translationally active by default, those regulatory mechanisms are mostly inhibitory (Gebauer and Hentze, 2004). Deregulation of one of those steps could lead to errors during protein synthesis that are summarized in Figure 1.23.

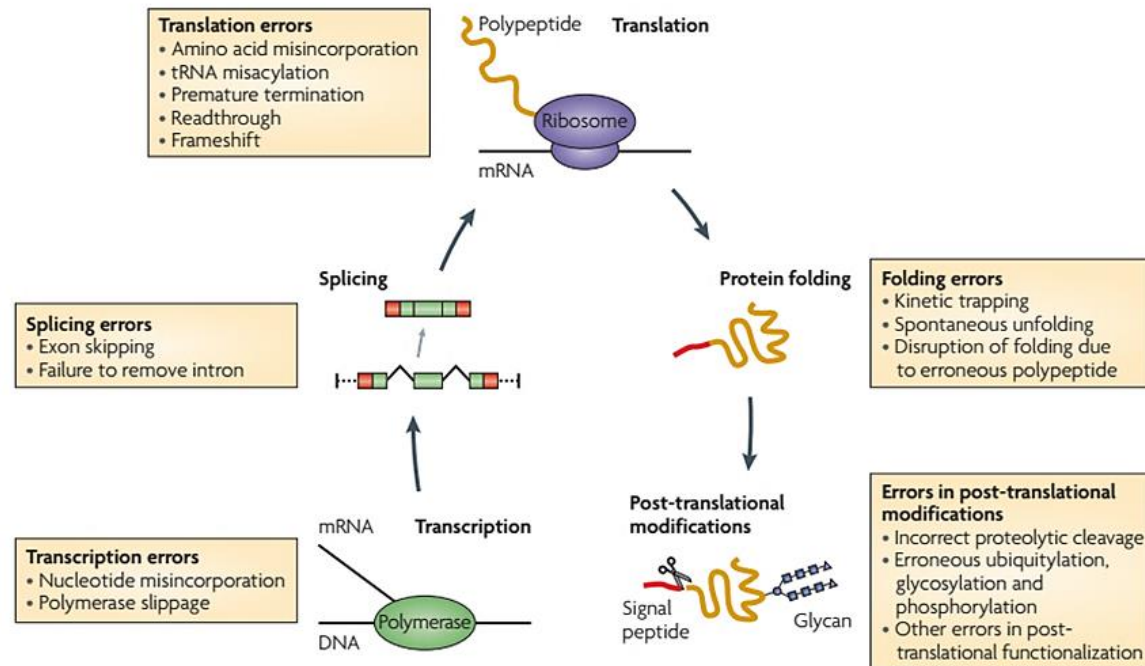


Figure 1.23. Types of errors that may affect protein synthesis and folding. Errors could occur at many steps of protein synthesis, namely during transcription, splicing, translation, folding and during post-translational modification of the proteins. Adapted from Allan Drummond and Wilke, 2009.

1.4.1 Translation

1.4.1.1 Initiation

During transcription in the nucleus, mRNA loses its introns and acquires a cap structure at its 5'-end and a poly(A)-tail at the 3'-end. The mature strand of RNA can be divided into three domains, namely the 5'-untranslated region (5'-UTR), the protein encoding region (ORF – open reading frame), and the 3'-UTR or 3'-tail (Jansen *et al.*, 1995).

1. Introduction

The translation initiation process begins when the eukaryotic initiation factor (eIF) 2·GTP·Met-tRNA_i ternary complex is assembled. The formation of this complex is assisted by eIF2B to recycle the eIF2·GDP complex after each initiation cycle: eIF2 is a G protein and has higher affinity for GDP than GTP (Kapp and Lorsch, 2004). After the formation of eIF2·GTP·Met-tRNA_i ternary complex, eIF2·GDP helps the association of Met-tRNA_i to the P-site of the small ribosomal subunit (40S), forming the 43S pre-initiation complex. The formation of this complex is mainly assisted by eIF1, eIF1A and eIF3 (Dever, 1999; Kapp and Lorsch, 2004; Mahoney, Dempsey and Blenis, 2009). The Met-tRNA_i binds to the P-site of the ribosome, in contrast to the delivery of specific aa-tRNA to the A-site of the ribosome during elongation (Dever, 2002).

The 5'-cap of the mRNA is used to assemble the eIF4F complex that opens secondary structures present in the 5'-UTR. eIF4F complex contains a cap-binding protein – eIF4E, a DEAD-box RNA helicase responsible for unwinding the secondary structure at the 5'-UTR – eIF4A, and eIF4G that serves as a scaffold for eIF4A, poly(A)-binding proteins (PABPs), and eIF3 (or probably eIF5 in yeast). Additionally, eIF4F and eIF4B, together with the PABP bound to the 3'-poly(A) tail and eIF3 bring the mRNA onto the 43S pre-initiation complex, forming the 48S pre-initiation complex. The opening of the mRNA entry tunnel latch is stabilized by the closed orientation of the helix 16 of the SSU altered with the help of eIF1 and eIF1A factors. This allows the 48S pre-initiation complex to scan the message in the 5' to 3' direction until the initiation codon is found (Passmore *et al.*, 2007; Mahoney, Dempsey and Blenis, 2009; Jackson, Hellen and Pestova, 2010). As soon as the 43S complex finds the proper start AUG codon (with a purine at position -3 and a G at position +4 relative to the A of the AUG codon) on the mRNA it stops due to the interaction of the AUG codon with the anticodon of the initiator tRNA in the ternary complex (Kozak, 1991; Jackson, Hellen and Pestova, 2010). This leads to the hydrolysis of GTP by eIF2, facilitated by eIF5, the GTPase-activating protein (GAP). Then, eIF2·GDP releases the Met-tRNA_i into the P-site of the 40S subunit and dissociates from the complex, as well as eIF1, eIF1A, eIF3 and eIF5 (Kapp and Lorsch, 2004). Simultaneously, eIF5B·GTP binds to the complex, and facilitates the binding of the large ribosomal subunit (60S) to the 40S·Met-tRNA_i·mRNA complex,

generating a translationally competent ribosome (Figure 1.24) (Dever, 2002; Kapp and Lorsch, 2004). This event is the signal for GTP hydrolysis by eIF5B, followed by its dissociation from the complex, due to the low affinity of the GDP-bound form for the ribosome (Kapp and Lorsch, 2004).

This first translational event depends on the binding of eIFs to the 5'-cap and 5'-UTR scanning to identify the AUG initiation codon, whose recognition is dependent on the context and position of the first AUG codon (as mentioned above). However, changes in the phosphorylation state of initiation factors or their interacting partners are the key elements of global control of protein synthesis. One example is the phosphorylation of residue Ser51 of the α -subunit of the eIF2, blocking the GTP-exchange reaction (Gebauer and Hentze, 2004).

1. Introduction

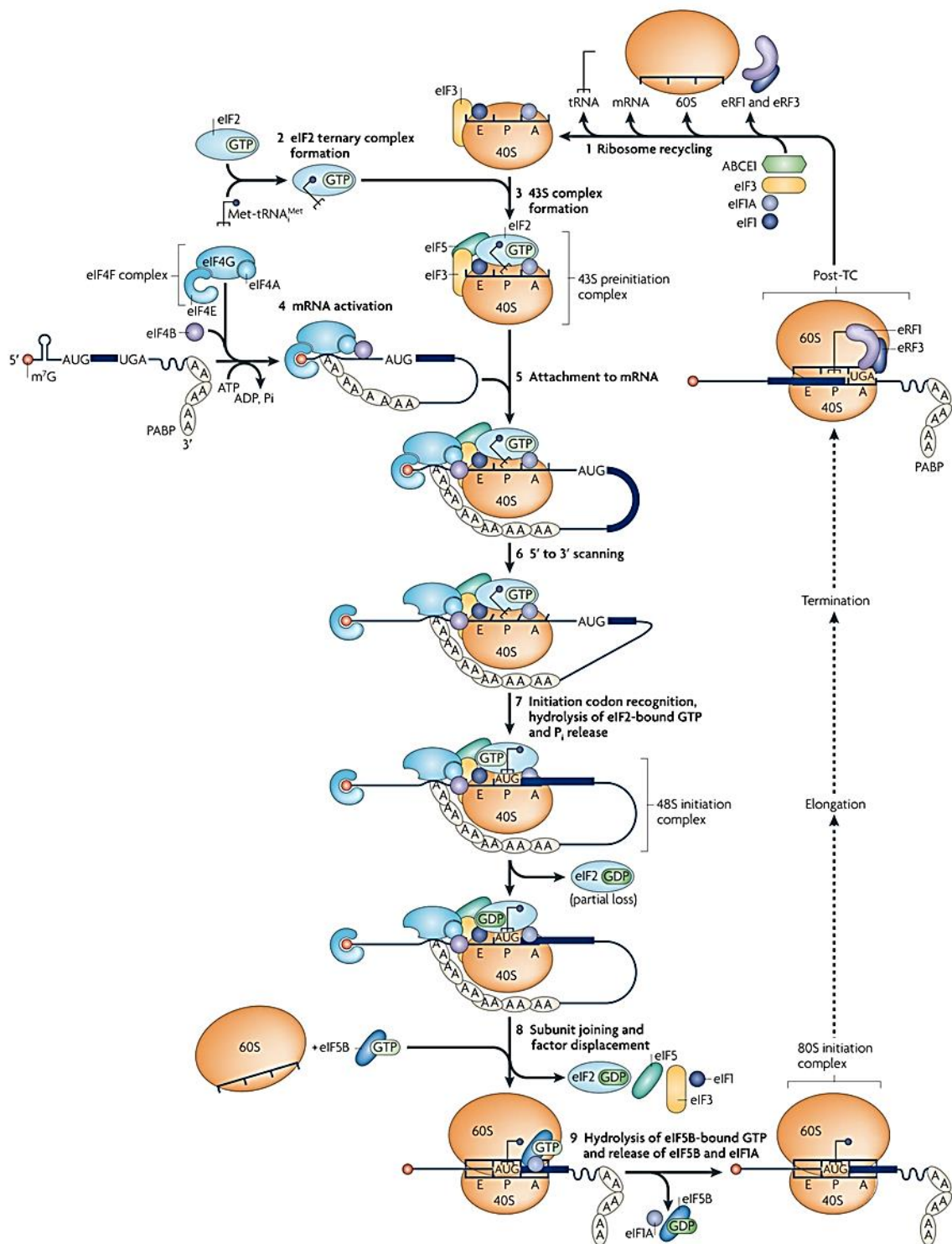


Figure 1.24. Eukaryotic translation initiation model. The pathway of eukaryotic initiation follows the recycling of post-termination complexes (post-TC; 1), where 40S and 60S ribosomal subunits are separated. Then the eukaryotic translation initiation involves eIF2·GTP·Met-tRNA_i ternary complex formation (2); generation of the 43S pre-initiation complex (40S subunit, eIF1, eIF1A, eIF3, eIF2-GTP-Met-tRNA_i^{Met} and probably eIF5) (3);

mRNA activation by eIF4F and eIF4B (4); binding of the 43S complex to the unwound mRNA region (5); 5'-UTR mRNA scanning in a 5' to 3' direction by 43S complex (6); formation of the 48S initiation complex after recognition of the initiation codon (7); 60S subunits joins 48S complex with release of eIF2-GDP and other factors (eIF1, eIF3, eIF4B, eIF4F and eIF5) mediated by eIF5B (8); and hydrolysis of eIF5B-bound GTP and release of eIF1A and eIF5B from the assembled 80S ribosome (9). Translation is a cyclic process, in which elongation and termination follows initiation and leads to recycling (1), resulting in detached ribosomal subunits. Adapted from Jackson *et al.*, 2010.

1.4.1.2 Elongation

Translation elongation uses a conserved machinery to the three kingdoms of life. During elongation an aminoacyl-tRNA is transferred to the ribosomal A-site as a ternary complex with GTP and the elongation factor (eEF1A) (Kapp and Lorsch, 2004). This eEF1A-GTP-aa-tRNA ternary complex binds to the matching codon in the A-site of the ribosome (Figure 1.25) (Agris, 2004; Kapp and Lorsch, 2004; Mahoney, Dempsey and Blenis, 2009). In order to ensure that only the cognate tRNA is selected for the next stage of elongation the codon-anticodon base pairings between the mRNA and the tRNA are checked and conformational changes in the decoding center of the small ribosomal subunit and GTP hydrolysis by eEF1A provide additional proofreading of that interaction. In the first step, codon-anticodon base pairing induces a conformational change of the three bases (G₅₆₇, A₁₇₅₅ and A₁₇₅₆) in the 40S subunit to interact with the minor groove of the codon-anticodon helix and monitor the stereochemical correctness of that base pairing *via* hydrogen-bond interactions. The correct interaction between SSU and the mRNA-tRNA duplex is likely to activate eEF1A's GTPase activity, resulting in the release of the aminoacyl-tRNA into de A-site by eEF1A-GDP (Agris, 2004; Kapp and Lorsch, 2004; Ogle and Ramakrishnan, 2005). Then, the formation of a peptide bond between the incoming amino acid and the peptidyl-tRNA is catalyzed by the ribosomal peptidyl transferase center of the 60S subunit at the A-site. Thus, a deacylated tRNA in a hybrid state is formed with its anticodon in the P-site of the 40S subunit and its acceptor terminal in the E-site of the 60S subunit of the ribosome. At the same time, the peptidyl-tRNA is in a similar hybrid conformation with its anticodon in the A-site

1. Introduction

of the small subunit and its acceptor terminal in the P-site of the large subunit. For progression of elongation, this complex is translocated so that the deacylated tRNA is in the E-site only, the peptidyl-tRNA in the P-site only, and the mRNA moves three nucleotides downstream to place the next codon of the mRNA into the A-site. These steps require elongation factor 2 (eEF2), which is responsible for the hydrolysis of GTP that facilitates translocation. After the hydrolysis of GTP and the discharge of aminoacyl-tRNA onto the ribosome, eEF1A-GDP is also released and recycled to its GTP-bound form, mediated by eEF1B (a multifactor complex); to participate in further cycles of polypeptide elongation (Figure 1.25). This process is repeated until a stop codon enters the A-site, leading to the beginning of the termination of translation (Kapp and Lorsch, 2004).

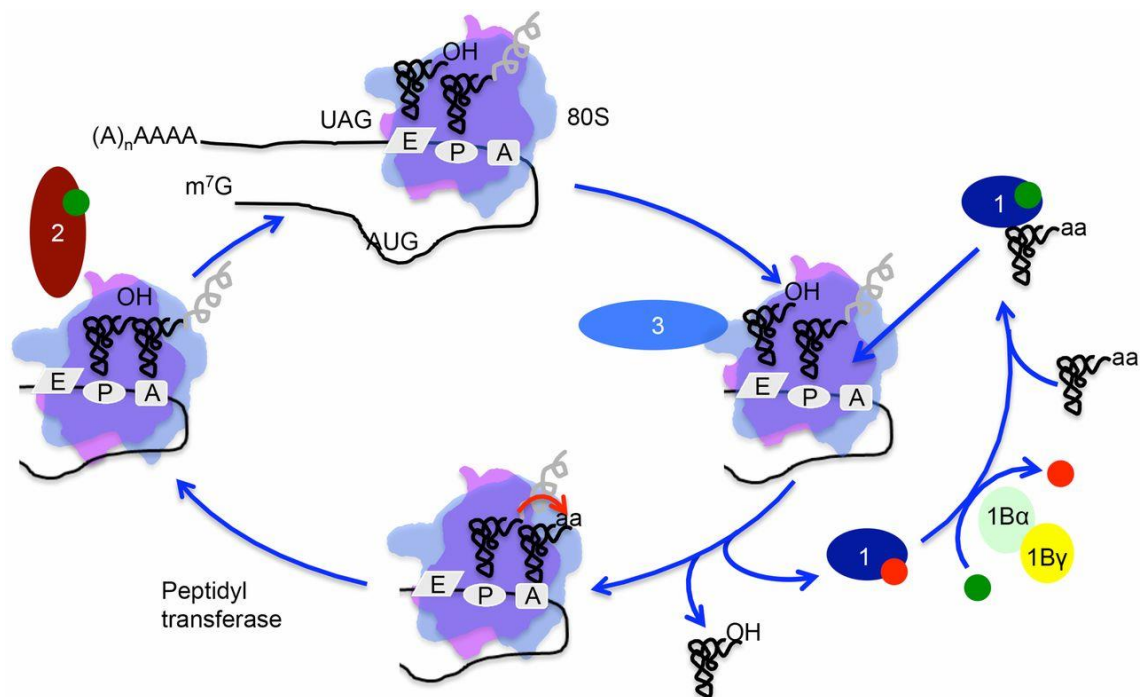


Figure 1.25. Eukaryotic translation elongation model. After initiation, an elongating ribosome is characterized by containing a peptidyl-tRNA in the P-site and a deacylated tRNA in the E-site (*top*). The aa-tRNA for the cognate codon in the A-site is delivered when it is bound to eEF1A (1)·GTP (green circle). The codon-anticodon pairing in the A-site induces conformational changes in eEF1A, GTP hydrolysis, and release of eEF1A·GDP (red circle), whereas the aa-tRNA stays in the A-site to form the peptide bond catalyzed by the ribosome. Simultaneously, eEF1A interacts with eEF3 (3) to assist the release of the E-site tRNA. Then, eEF2 (2)·GTP is involved in the movement of the A-site peptidyl-tRNA to

the P-site and of the now deacylated tRNA in the P-site to the E-site. The mRNA also moves three nucleotides downstream to place the next codon into the A-site to allow another cycle of elongation. Adapted from Dever, Kinzy and Pavitt, 2016.

1.4.1.3 Termination

As referred above, the presence of a stop codon in the ribosomal A-site leads to the termination of translation. This happens because a stop codon located in the A-site is recognized by a release factor (RF) or release factor complex. In eukaryotes, termination is mediated by a heterodimer of release factors eRF1 and eRF3 (Figure 1.27). eRF1 recognizes the three stop codons and induces peptidyl-tRNA hydrolysis by the ribosome, releasing the nascent polypeptide (Inge-Vechtomov, Zhouravleva and Philippe, 2003). eRF3 is a GTPase that stimulates the activity of eRF1 bound to the stop codon, enhancing termination efficiency (Inge-Vechtomov, Zhouravleva and Philippe, 2003). In response to a stop codon in the ribosomal A-site, formation of a quaternary complex comprising the ribosome, eRF1, GTP and eRF3 triggers GTP hydrolysis and the peptidyl transferase center of the ribosome catalyzes the hydrolysis of the ester bond, linking the polypeptide chain to the P-site tRNA, which results in the release of the completed polypeptide (Figure 1.26) (Bertram *et al.*, 2001; Kapp and Lorsch, 2004).

1.4.1.4 Recycling

The last stage of translation is the recycling of the ribosomal subunits, for another cycle of translation. In eukaryotes, ribosome recycling requires eIF3, which binds to the small ribosomal subunit opposite to the interface. In this way, eIF3 induces a conformational change in the 40S subunit, increasing the rate of subunit dissociation and lowering the rate of association. Another model for ribosomal recycling posits that termination and recycling may not discharge the 40S subunit back into the cytoplasm, instead this subunit may be transferred over or across the poly(A)-tail back to the 5'-end of the mRNA, mediated by the interaction of eRF3 and PABP with initiation factor eIF4G (Figure 1.26). These events facilitate the re-initiation of translation eliminating the need of the first initiation event (Kapp and Lorsch, 2004).

1. Introduction

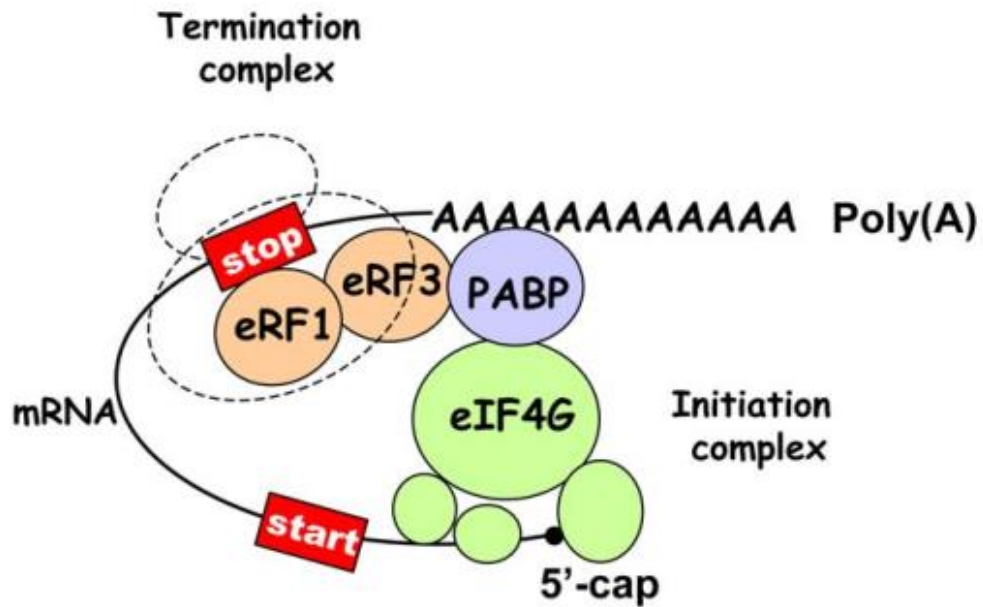


Figure 1.26. Translation termination complex. The finding of a termination codon (“stop”) by the ribosome elongation machinery (dotted) begins translation termination. The eRF1 interacts with the stop codon, resulting in the hydrolysis of the peptidyl-tRNA bond with consequent formation of eRF1/eRF3 complex with PABP. Thus, ribosome recycling and re-initiation of translation at a “start” codon is mediated by the interaction of PABP with translation factors (green circles). Adapted from Inge-Vechtsov *et al.*, 2003.

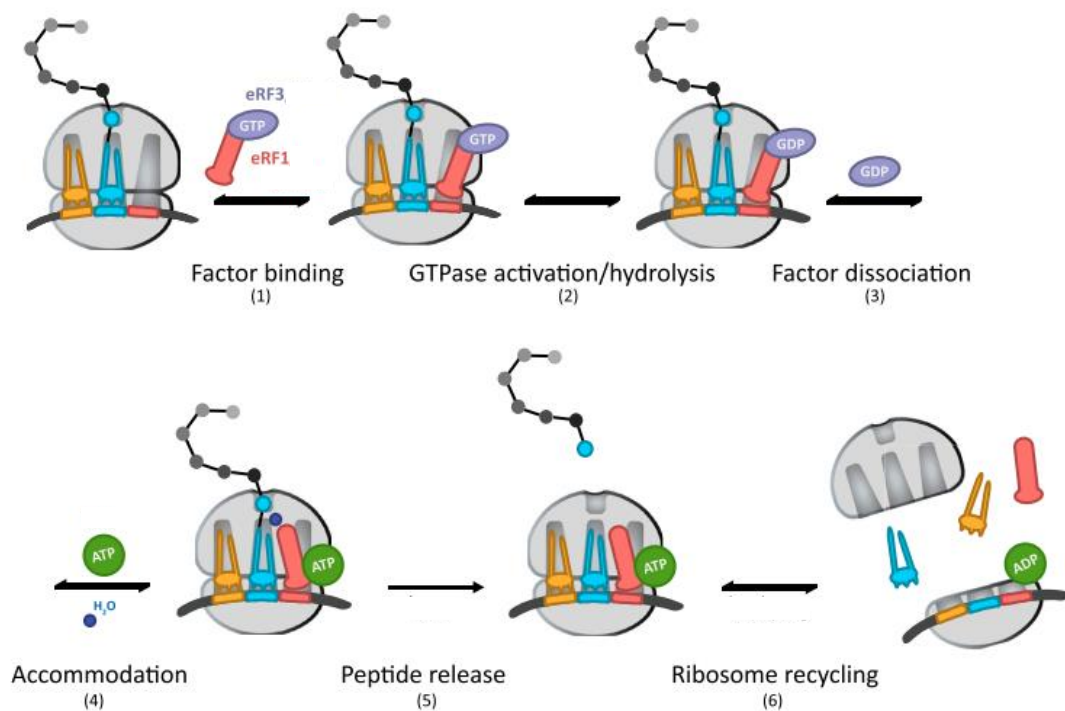


Figure 1.27. Eukaryotic translation termination and ribosome recycling model.

Translation termination occurs when eRF1-eRF3 initially bind to the ribosome, as a heterodimer (1). The GTPase hydrolysis of eRF3 occurs as a consequence of stop codon recognition (2). Following GTP hydrolysis, eRF3 in the GDP bound state dissociate from the eRF1-eRF3 complex (3). Then, eRF1 accommodates into the active site, analogous to accommodation of the aminoacyl-tRNA (4). After accommodation, peptide release occurs promoted by an ATP-independent process (5). Post-accommodation complexes then proceed to the final step, which initiates recycling in an ATP-dependent manner (6). Adapted from Shoemaker and Green, 2011.

1.4.2 Translation fidelity

Translation fidelity relies deeply on discrimination between complementary Watson-Crick, wobble base pairs and non-complementary base pairing. However, translation is the most error-prone event of gene expression with an observed fidelity of 1 error in 10^3 - 10^4 polymerized amino acids (Cochella and Green, 2005). Translation errors can emerge during tRNA charging by aminoacyl-tRNA synthetases and when mRNA is decoded by the ribosome (Figure 1.23). In terms of aminoacylation errors, these are mostly caused by the incorrect recognition of non-cognate tRNAs by aaRSs or by the inability of the aaRSs to differentiate between

1. Introduction

similar amino acids. These errors are minimized by aaRS editing mechanisms, responsible to reject incorrectly bound amino acids, and by specific tRNA-aaRS interaction networks, as described previously (Figure 1.13), reducing error frequencies to a range of 1 in 10^4 - 10^5 . At the ribosome level, mRNA decoding can be affected by four major types of errors: missense errors, which cause incorrect amino acid incorporation into polypeptide chains, resulting in the synthesis of mutant proteins (Bouadloun, Donner and Kurland, 1983); nonsense errors, which cause readthrough of stop codons, producing proteins with extended C-ends; frameshifting errors that alter the mRNA reading frame, resulting in out-of-frame truncated proteins (Björk *et al.*, 1999); and, processivity errors that stop translation early, producing truncated proteins. Two mechanisms of correction of the errors that occur at the ribosome level were described. The kinetic proofreading model states that the ribosome distinguishes between cognate and non-cognate tRNAs by the kinetics of their association or dissociation from the ribosome (Farabaugh and Björk, 1999). Thus, during the encounter between the eEF1A·GTP·aa-tRNA ternary complex and the ribosome (initial selection), a cognate ternary complex is more likely to induce GTP hydrolysis than to dissociate, whereas a near-cognate ternary complex is more likely to dissociate (Cochella and Green, 2005). And, in the following step of proofreading, the cognate aa-tRNA is more likely to “accommodate” into the A site and participate in peptide bond formation, while the near cognate aa-tRNAs are more likely to be rejected from the ribosome (Cochella and Green, 2005). In an alternative model, the discrimination between cognate and non-cognate tRNAs is achieved by an allosteric interaction between tRNAs in the E-site and the A-site of the ribosome, reducing the rate of incorrect tRNAs binding to the A-site. In fact, the E-site of the ribosome has a role in reducing the effects of misincorporation and in the maintenance of the translational reading frame (Wilson and Nierhaus, 2006), as the accuracy of selection of the aa-tRNA at the A-site is dependent on the E-site occupation. The E-site influences the affinity state of the A-site by monitoring codon-anticodon interaction (Wilson and Nierhaus, 2006). Those models also point out that a determinant element for translation accuracy is the concentration of cognate-tRNA relative to all other incorrect tRNAs, also demonstrated in the no more than 10-fold (approximately) difference between the most and the least abundant tRNAs

(Ikemura, 1985; Farabaugh and Björk, 1999; Kramer and Farabaugh, 2007; Shah and Gilchrist, 2010).

The most frequent translational errors correspond to mistakes in selecting the correct aa-tRNA at the A-site and consequently misincorporation of the incorrect aminoacyl residue. Amino acid misincorporation occurs in about 10^{-3} to 10^{-4} amino acid incorporations, but only one in 400 misincorporations affects the structure and/function of proteins (Bouadloun, Donner and Kurland, 1983; Parker, 1989; Ogle and Ramakrishnan, 2005; Wilson and Nierhaus, 2006). On the other hand, frameshifting errors occurs only once in at least 3×10^4 amino acid incorporations (Jørgensen and Kurland, 1990), but are more detrimental; resulting in the synthesis of erroneous and most frequently incomplete polypeptides. Various models exist to explain these errors. A dual error model states that low number or slow entry of an aa-tRNA into the A-site could induce pausing during the acceptance of a near-cognate tRNA (first error), and even after a normal three nucleotide translocation the near-cognate tRNA then slips into the +1 or -1 frame due to an aberrant anticodon-codon interaction in the P-site (second error). In contrast, altered tRNAs, for instance hypomodified tRNAs, may be accepted into the A-site instead of a near-cognate tRNA, which may be prone to frameshift in the P-site after translocation depending on the sequence of the mRNA (Qian *et al.*, 1998; Björk *et al.*, 1999). A great number of frameshifting events were associated to tRNA hypomodification (Björk, Wikström and Byström, 1989; Esberg *et al.*, 1997; Qian *et al.*, 1998; Björk *et al.*, 1999), since the presence of modified nucleosides in tRNA improves the aa-tRNA selection rate and optimizes the fitness of the tRNA in the P-site.

Most processivity errors occur by a process denominated ribosome editing. In this process erroneously decoding non-cognate peptidyl-tRNAs dissociate spontaneously from the P-site of the ribosome (“drop-off”), due to their weak interaction with the mRNA (Menninger, 1977).

Translational errors often interfere with protein folding, leading to misfolded molecules that could be toxic. For instance, a single mutation in the editing domain of an Ala-tRNA synthetase causes misacylation with consequent general translation errors and protein misfolding. This was observed in the mouse cerebellum associated with degeneration of Purkinje cells, ataxia and death (Lee *et al.*, 2006).

1. Introduction

Protein synthesis errors (mistranslation) have a major impact on yeast biology (Table 1.2), and most likely in the biology of all organisms, but its relevance for protein misfolding/aggregation and proteotoxic stress is still poorly understood.

Table 1.2. Major effects of mistranslation in *S. cerevisiae* (Santos *et al.*, 1999; Gomes *et al.*, 2007; Silva *et al.*, 2007; Moura, Paredes and Santos, 2010).

Effects of CUG mistranslation in <i>S. cerevisiae</i>
<ul style="list-style-type: none">- Increased ploidy (up to 4N);- Large chromosomal rearrangements;- Blocking mating and sexual reproduction;- Altered sporulation;- Altered expression of molecular chaperones and carbohydrate metabolism;- Increased proteasome activity;- Up-regulation of cell wall structural proteins;- Down-regulation of protein synthesis and amino acid metabolism;- Alterations in genome and gene expression → phenotypic alterations:<ul style="list-style-type: none">- Morphology and cell shape and size heterogeneous;- Formation of pseudohyphae and hyphae;- Increased resistance to several agents (e. g. nutrient starvation, cadmium, H₂O₂);- Accumulation of glycogen and trehalose;- Increased secretion of extracellular hydrolases: lipases and proteases;- Strong effect on cell adhesion.

1.5 PROTEIN FOLDING AND MISFOLDING

After biosynthesis and in order to become active the newly synthesized protein chains must be converted into folded compact structures, based on the information encoded in their amino acids sequence (Barral *et al.*, 2004; Dobson, 2004). The term protein folding is universally recognized as the process responsible for the acquisition of the native structure, starting from a completely or partially unfolded state. This folding process occurring within the cells is assisted by a large number of auxiliary factors, including molecular chaperones and folding catalysts, enabling polypeptide chains to fold efficiently (Barral *et al.*, 2004; Dobson, 2004; Outeiro, 2004). This hypothesis of a relationship between the primary amino acid sequence of a protein and its conformation was initially proposed in 1973 (Anfinsen, 1973). There are various forces involved in the folding process, such as Van der Waals force, electrostatic force, hydrogen bonding, and hydrophobic force, but there are evidences that the hydrophobic force is a dominant force, determining the overall folded structure (Dobson, 2004; Outeiro, 2004). Protein folding is now considered a stochastic process and involves the hypothesis of an “energy landscape” for each protein. And, there is a limited possibility for proteins to misfold and adopt non-native states, still being transiently stable (kinetic traps) (Dobson, 2004; Outeiro, 2004; Hartl, Bracher and Hayer-Hartl, 2011).

Protein folding can begin while a nascent chain is still attached to the ribosome (Kosolapov and Deutsch, 2009), some proteins fold in the cytoplasm after release from the ribosome, or in specific compartments such as the endoplasmic reticulum (ER). The environment in which protein folding takes place influences the folding process (Dobson, 2001). The folding energy landscape and folding outcome can also be influenced by ribosome effects, polypeptide elongation rate, molecular crowding and co-translational interactions with cellular chaperones (Berg, Ellis and Dobson, 1999; Zhang, Hubalewska and Ignatova, 2009; Kaiser *et al.*, 2011; Lin *et al.*, 2012; Mashaghi *et al.*, 2013; Sander, Chaney and Clark, 2014). These mechanisms are known as translational tuning (Kim *et al.*, 2015), which is regulated by elongation rates, tRNA abundance, codon content and mRNA secondary structure. Thus, decreasing these rates can affect the folding efficiency of newly synthesized proteins (Kaiser *et al.*, 2011). Co-translational limitations can bias

1. Introduction

kinetically competing folding events to generate alternate stable structures with different functional properties (Kim *et al.*, 2015).

Protein misfolding describes processes that result in the acquirement of a number of persistent non-native interactions that biologically affect protein's architecture and/or its properties, leading to the formation of insoluble protein aggregates (Dobson, 2004; Salomons *et al.*, 2009). Protein synthesis errors frequently disrupt folding of proteins. The accumulation of misfolded proteins generates proteotoxic stress, which can occur under a variety of conditions, including hypoxia, hyperthermia, and exposure to denaturing agents or drugs that inhibit chaperone or proteasome activities. Misfolded proteins can be toxic, most likely due to the presence of oligomeric species that interfere with cellular processes (Walter and Buchner, 2002; Salomons *et al.*, 2009; Neznanov *et al.*, 2011). Fortunately, living systems have elaborated strategies that prevent interactions of misfolded proteins with other molecules (Walter and Buchner, 2002; Dobson, 2004). One of these strategies involves the presence of molecular chaperones, which associate with unfolded protein chains, avoiding aggregation and supporting a more efficient folding in an ATP-dependent manner (Walter and Buchner, 2002). Additionally, there are folding catalysts, whose function is to accelerate potentially slow steps in the folding process. Peptidylprolyl isomerases and protein disulphide isomerases (PDI) are the most important folding catalysts. The first ones amplify the rate of *cis/trans* isomerization of peptide bonds involving proline residues and, the second ones, improve the rate of formation and reorganization of disulphide bonds within proteins (Dobson, 2001, 2004). Additionally, in cases of proteotoxic stress, cells also activate an adaptive response, known as the heat shock response (HSR) (Neznanov *et al.*, 2011).

1.5.1 Protein aggregation

Protein aggregates are oligomeric complexes that arise from non-native interactions among structured intermediates in protein folding or assembly. They have poor solubility in aqueous or detergent solvents, non-native secondary structure and abnormal sub-cellular or extracellular localization (Kopito, 2000). There are different

types of protein aggregates: 1) amyloid fibrils – ordered (or structured) aggregates and 2) inclusion bodies – disordered (or amorphous) aggregates (Fink, 1998; Kopito, 2000). In both cases, aggregates are insoluble and stable in physiological conditions (Kopito, 2000).

The formation and structure of protein aggregates imply specific intermolecular interactions between hydrophobic surfaces of structural subunits in partially folded intermediates. Thus, initial stages of aggregation involve the interaction between surface elements of one molecule and hydrophobic surface areas of structural subunits of neighboring molecules. When a great number of interactions occur, the formation of large aggregates becomes possible. Probably, these aggregates (dimers and tetramers) will be soluble in the beginning, but with the formation of larger aggregates will exceed the solubility limit, and then accumulate over time in distinct compartments (Fink, 1998). In yeast, protein accumulation occurs at two major sites that have distinctive properties: 1) a juxtannuclear quality control compartment (JUNQ) and 2) perivacuolar insoluble protein deposits (IPODs) (Figure 1.28) (Kaganovich, Kopito and Frydman, 2008). The JUNQ seems to serve as temporary storage domain for misfolded and/or ubiquitinated proteins and concentrates disaggregating chaperones and proteasomes, during stress or ageing. IPODs consist of aggregated, mostly non-ubiquitinated, proteins that are sequestered from the cytosol to protect the cell from their potential toxicity (Kaganovich, Kopito and Frydman, 2008; Buchberger, Bukau and Sommer, 2010). Both the JUNQ and the IPOD are retained in the mother cell during cell division, clearing daughter cells from potentially harmful misfolded or aggregated proteins (Sontag, Vonk and Frydman, 2014).

1. Introduction

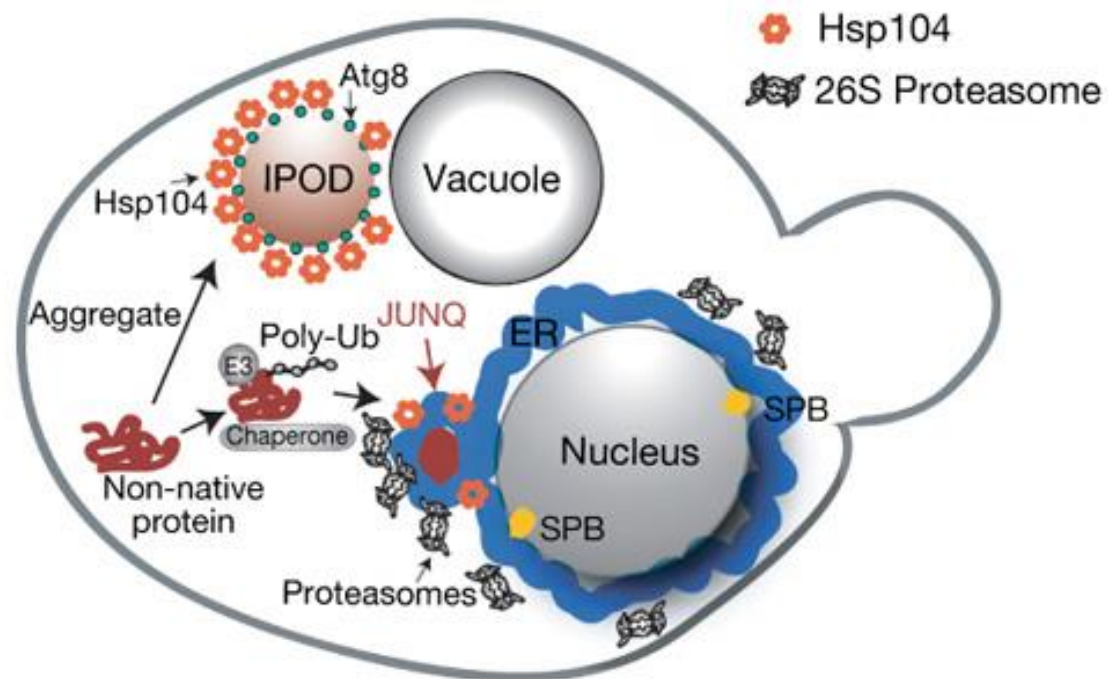


Figure 1.28. Model for sorting of misfolded proteins to different quality control compartments. Adapted from Kaganovich *et al.*, 2008.

The main factors that influence protein aggregation, the rate and the extent of the aggregation are: the amino acid sequence, pH, temperature and ionic strength, concentration of the protein, presence of co-solutes (for instance denaturants), and the presence/absence of molecular chaperones (Fink, 1998). However, environmental conditions, mutations, RNA hypomodification or translational amino acid misincorporation can also lead to differential destabilization of the native state relative to the partially folded intermediate (Fink, 1998; Kopito, 2000).

Protein aggregates are more stable than the intermediate conformers from which they are originated, so the destiny of misfolded proteins will be determined by kinetic competition between proteasomal degradation and aggregation into high molecular weight oligomers (Kopito, 2000).

1.5.2 Cellular protein quality control mechanisms

The production of aberrant proteins occurs in cells even in physiological conditions, so cellular protein quality control mechanisms are required to deal with non-native

proteins at all times (Figure 1.29). This machinery avoids the formation of aggregates by ensuring the fidelity of transcription and translation, by chaperoning nascent or unfolded proteins, and by degrading improperly folded polypeptides before they can aggregate (Kopito, 2000). In fact, protein folding is rarely achieved autonomously. As mentioned before, the nascent polypeptide chain in the ribosome needs help to reach its translation end, and many proteins (20-30%) also need assistance to reach their folding state. Thus, the protein quality control (PQC) network is able to maintain cellular protein homeostasis (proteostasis) by maximizing cellular protein folding capacity (by the chaperone system), minimizing intrinsic and extrinsic attacks and degrading misfolded proteins (by proteases, the ubiquitin-proteasome system (UPS) and lysosome) (Figure 1.29) (Outeiro, 2004; Lindner and Demarez, 2009). Aberrant or misfolded proteins are marked by protein quality control mechanisms and tagged for degradation *via* the UPS (Salomons *et al.*, 2009). Some molecular chaperones are linked to the UPS and bind to non-native proteins, mediating their refolding or degradation (Berke and Paulson, 2003). Also, most misfolded soluble proteins are favorably degraded by autophagy if the proteasome capacity is exceeded. But, aggregates can only be degraded by autophagy (Lilienbaum, 2013).

The endoplasmic reticulum (ER) also has a PQC compartment, which in yeast is a membrane-bound ER-Associated Compartment (ERAC), where soluble misfolded proteins concentrate for ER-Associated Degradation (ERAD) by the UPS. Aggregated proteins are also cleared from the ER by autophagy (Sontag, Vonk and Frydman, 2014).

1. Introduction

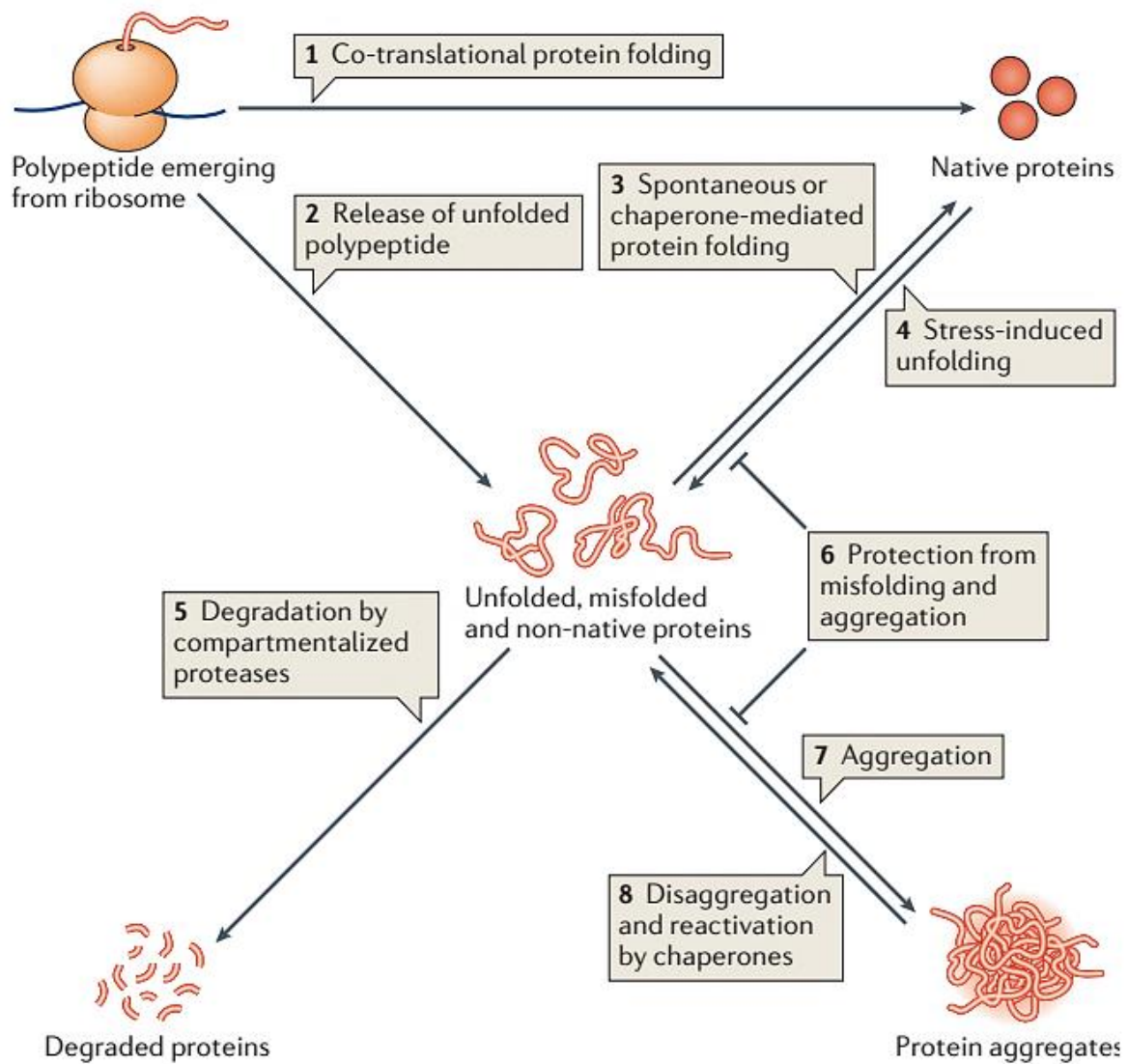


Figure 1.29. Protein quality control. Chaperones help in the co-translational folding of newly synthesized polypeptides (1), the folding of unfolded proteins released from the ribosome (2) and the refolding of non-native proteins (3), which are usually caused by stress conditions (4). Moreover, non-native proteins may be targeted for degradation (5). Some chaperones prevent protein misfolding and aggregation (6). During stress, chaperone network could be overwhelmed and non-native proteins may aggregate (7). However, other chaperones can unfold polypeptides from aggregates (8), being another opportunity for correct folding (3). Adapted from Doyle *et al.*, 2013.

1.5.2.1 Chaperones

The first evidence of the existence and function of molecular chaperones occurred during proteotoxic stress conditions. Many chaperones are known as Hsps (heat shock proteins), and this phenomenon of cells responding to insults by producing increased amounts of specific protective proteins is referred as heat-shock response or stress response (Walter and Buchner, 2002; Dobson, 2004; Lindner and Demarez, 2009). Chaperones help to avoid and reverse non-functional conformations; to facilitate co- and post-translational folding and to assist in assembly and disassembly of protein complexes (Morimoto, 2008; Lindner and Demarez, 2009). They often support the folding process *via* cycles of substrate binding and release, regulated by ATPase activity (Barral *et al.*, 2004). The chaperone expression is also controlled by specific transcription factors (TF), namely RpoH and heat shock factor (HSF) variants. Under native conditions the TF are retained as monomers by chaperones to be separated from their chromosomal targets. Misfolding proteins titrate chaperones, releasing the TF to trimerize, translocate to the nucleus and induce chaperones expression (Lindner and Demarez, 2009; Buchberger, Bukau and Sommer, 2010). Depending on the molecular chaperone, misfolded proteins, exposing buried hydrophobic amino acid residues, can be rescued by chaperones to enable their correct fold, or be solubilized to some form of aggregates (Dobson, 2004). Additionally, chaperones can act together and in synergy within the chaperone network and with other PQC systems as the proteasome and lysosomal/vacuolar degradation pathways (Lindner and Demarez, 2009).

Molecular chaperones interact momentarily with unfolded or partially folded intermediates, covering hydrophobic surfaces from forming inappropriate intra- or intermolecular contacts (Kopito, 2000). Chaperones are also involved in other cellular processes, including protein targeting, regulation of translocation, degradation and signal transduction (Barral *et al.*, 2004; Morimoto, 2008).

Chaperones are divided into different families or classes, classified by size and actions: small Hsp (sHsp), ATP-dependent Hsp60 chaperones, ATP-dependent Hsp70 chaperones, ATP-dependent Hsp90 family, and ATPase Associated with diverse Activities (AAA+) or Hsp100 family (Figure 1.30) (Walter and Buchner, 2002;

1. Introduction

Lindner and Demarez, 2009). Each family contains multiple members, which share sequence identity and have also common functional domains (Gething and Sambrook, 1992).

The ATP-independent sHsp family has molecular mass <43 kDa and the capacity to maintain the solubility of partially unfolded proteins through binding to their exposed hydrophobic surface, functioning as “holdases” and buffering aggregation. It was suggested that sHsp destabilize the aggregates and ease their solubility, refolding, or degradation, mediated by Hsp104 and Hsp70/40 chaperones (Buchberger, Bukau and Sommer, 2010; Hartl, Bracher and Hayer-Hartl, 2011).

The Hsp60 (chaperonin) family member TRiC/CCT (TCP1-ring complex or chaperonin containing TCP1) recognizes a small range of substrates and facilitates protein folding or refolding using an isolated cavity, known as the “Anfinsen cage”. This chaperonin binds ATP with high affinity and has weak ATPase activity (Gething and Sambrook, 1992; Buchberger, Bukau and Sommer, 2010; Hartl, Bracher and Hayer-Hartl, 2011). In eukaryotes, these chaperones are present in the mitochondria.

The Hsp70 chaperones are cytosolic and in eukaryotes are also present in organelles, such as mitochondria and endoplasmic reticulum (BiP/Kar2). All members of Hsp70 family bind ATP, which cause conformational changes in Hsp70 proteins, altering their sensitivity to proteases or their oligomeric state (Gething and Sambrook, 1992). These chaperones need numerous co-factors to work efficiently in the folding of nascent polypeptides, refolding of misfolded proteins, translocation of proteins targets through membrane for organelles and secretion, and controlling the function and life-time of signaling and regulatory proteins (Hartl, Bracher and Hayer-Hartl, 2011; Doyle, Genest and Wickner, 2013; Willmund *et al.*, 2013).

The ATP-dependent Hsp90 family has similar functions to Hsp70 to avoid non-specific aggregation of generic proteins, and is subjected to complex regulation by many co-chaperones, such as p23/Sba1, Hop/Sti1 (inhibitors) and Aha1 (activator) (Hessling, Richter and Buchner, 2009). The Hsp90 binds ATP in a cation-dependent manner and undergoes autophosphorylation, in contrast with Hsp70 and chaperonins that catalyze the hydrolysis of ATP (Gething and Sambrook, 1992). Besides that, Hsp90 possesses a wide range of substrates, among them are

proteins involved in signal transduction, cell cycle, meiosis, transport, secretion and chromatin remodeling, epigenetic gene regulation and viral replication. Moreover, Hsp90 can mediate conformational changes of folded proteins to ensure their stabilization, activation or degradation (Buchberger, Bukau and Sommer, 2010; Jarosz and Lindquist, 2010).

The Hsp104 proteins are members of the ring-shaped Hsp100 AAA+ family and are highly induced by external stress conditions, conferring resistance to them. Their functions are to prevent misfolding and, mainly, to disaggregate proteins (Lindner and Demarez, 2009). However, activity of the members of this family is dependent of the prior activity of Hsp70, co-chaperoned by Hsp40 and a nucleotide exchange factor (NEF), to present aggregated polypeptides to the central core of the Hsp100 unfoldase (Buchberger, Bukau and Sommer, 2010; Doyle, Genest and Wickner, 2013; Houry *et al.*, 2015).

Interestingly, the different classes of molecular chaperones cooperate in the cell and all chaperones can suppress the aggregation of folding proteins. In this way, all chaperones are overproduced simultaneously in stress conditions (Walter and Buchner, 2002).

Chaperones are regulated by co-chaperones; proteins that interact with chaperones to modulate their activity and to provide substrate selectivity. For example, members of the Hsp40 co-chaperone family stimulate the ATPase activity of Hsp70, stabilizing substrate interactions, and interact directly with unfolded proteins to assist folding. Other co-chaperones function as nucleotide exchange factors (NEFs), releasing bound ADP from Hsp70 and re-binding of ATP, which in turn triggers release of bound substrate. Additionally, co-chaperones function to manage interactions between chaperones to promote protein folding or degradation (Buchberger, Bukau and Sommer, 2010; Voisine, Pedersen and Morimoto, 2010).

Moreover, ribosome-binding chaperones, namely ribosome-associated complex (RAC) and nascent-chain-associated complex (NAC), interact first with the polypeptide, followed by chaperones that have no direct affinity for the ribosome, including the Hsp70/Hsp40 system (Balchin, Hayer-Hartl and Hartl, 2016).

1. Introduction

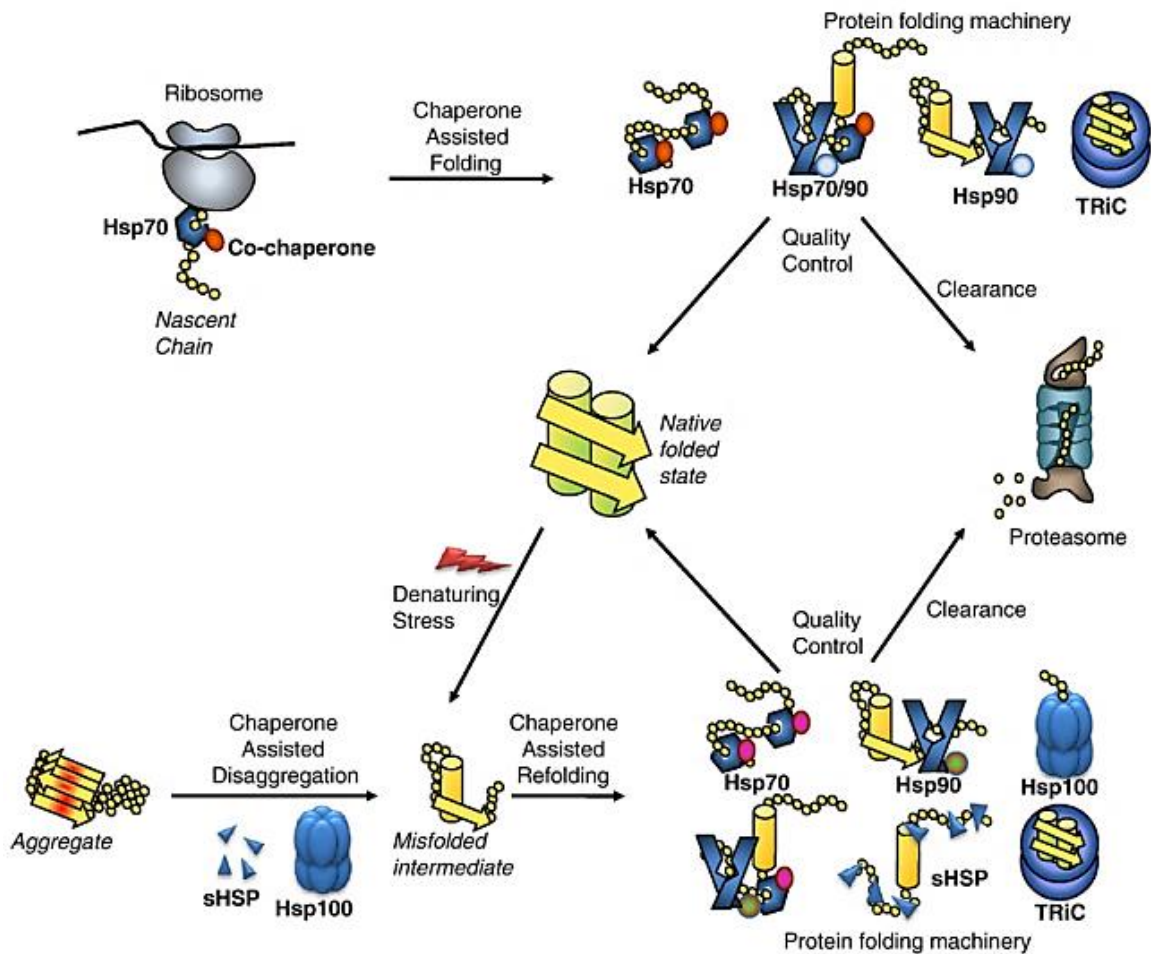


Figure 1.30. Protein folding assisted by chaperones and co-chaperones as a protein quality control mechanism. Chaperones guide folding of proteins from the initial steps of protein synthesis and protect native folded protein during stresses. As a newly nascent polypeptide chain exits the ribosome tunnel, various chaperones bind to and interact with the protein during its maturation. Folding is assisted by the core chaperone families, Hsp70, Hsp90 and chaperonin, which are modulated by specific co-chaperones depending of the substrate and the step in the folding pathway. Protein aggregation is avoided by Hsp100s and sHsps, which work with other chaperones to refold denatured proteins. The chaperone quality system also guides the aberrant proteins for refolding or degradation *via* the UPS. Adapted from Voisine *et al.*, 2010.

1.5.2.2 Ubiquitin-proteasome system

With respect to the UPS, it is known that this is the major non-lysosomal/vacuolar degradation pathway for cytosolic and nuclear proteins (including short-lived,

misfolded and damaged polypeptides) and is ubiquitin-dependent. So, proteins destined to degradation must be ubiquitinated for proteasome recognition. Ubiquitinated proteins (with at least four ubiquitin moieties) selectively bind to proteasome, which in turn unfolds and translocates ubiquitinated proteins into a proteolytic chamber where proteins are hydrolyzed into short peptide fragments. Further, deubiquitinating enzymes present in the proteasome convert ubiquitin chains into monomers that can be used in a new ubiquitination process. Beyond its proteolytic function, ubiquitination may function as a post-translational modification that regulates target protein localization and activity, being involved in membrane trafficking, cell-cycle progression, differentiation, synaptic plasticity, apoptosis, endocytosis, DNA repair and transcriptional regulation (Berke and Paulson, 2003; Salomons *et al.*, 2009).

Aberrant proteins for degradation are marked with ubiquitin in an ATP-consuming process using a catalytic cascade of E1 (ubiquitin-activating enzyme), E2 (ubiquitin-conjugating enzyme) and E3 (ubiquitin protein ligase) activities (Hershko and Ciechanover, 1998). In a first step, the C-terminal glycine residue of ubiquitin is activated by E1, forming an intermediate ubiquitin adenylate, with the release of PPi, followed by the binding of ubiquitin to a cysteine residue of E1 in a thioester linkage, with release of AMP. Activated ubiquitin is next transferred to an active site cysteine residue of E2 and then is linked by its C-terminus in an amide isopeptide linkage to an internal lysine residue of the substrate protein, mediated by E3 (Hershko and Ciechanover, 1998; Mogk, Schmidt and Bukau, 2007). Substrate selectivity is mainly determined by E3 enzymes. E4 enzyme is another component of the ubiquitination machinery that is involved in the elongation of short ubiquitin chains, since in eukaryotes most substrates are polyubiquitinated (Koege *et al.*, 1999; Lilienbaum, 2013).

On the other hand, the 26S proteasome is a large protein complex composed of 2 different sub-complexes: the 20S proteolytic core and a 19S complex (Figure 1.31). The 20S core complex is arranged in a hollow cylinder, composed of four heptameric rings with α - or β -subunits. The proteolytic active sites are in the interior chamber of the 20S complex. The 19S complex is located at either end of the proteolytic 20S complex and contains six AAA+ proteins that promote the ATP-

1. Introduction

dependent unfolding. Additionally, the 19S cap cleaves ubiquitin moieties from the substrate, unfolds the polypeptide and introduces it through the proteolytic chamber of the 20S core, where the polypeptide is cleaved into short peptides by three distinct peptidase activities (Mogk, Schmidt and Bukau, 2007).

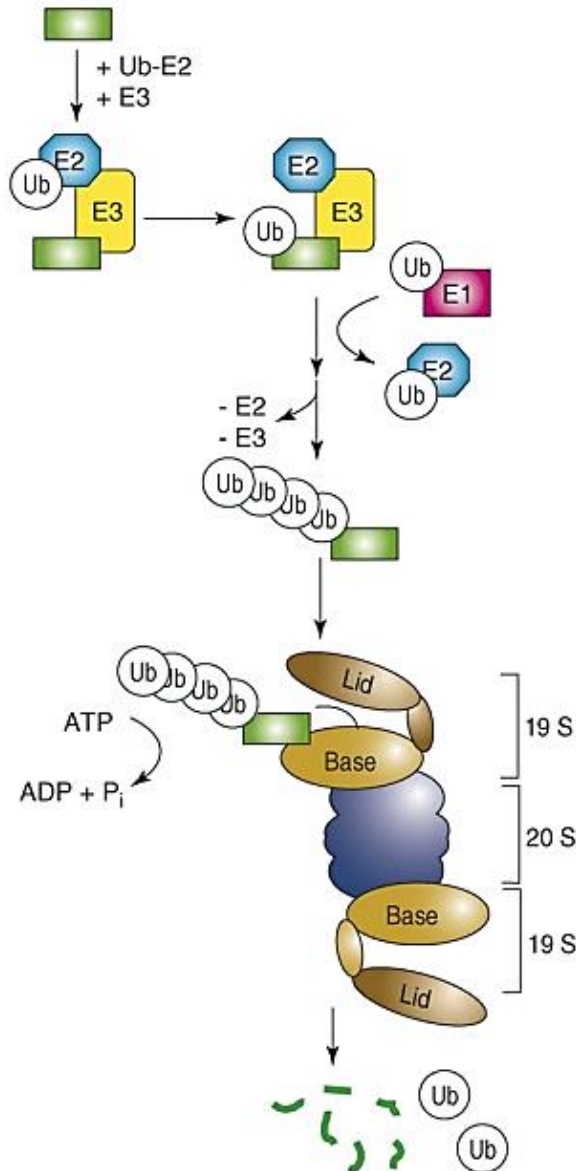


Figure 1.31. The ubiquitin-proteasome system. Misfolded or non-native proteins (green) are mainly recognized by E3 ligases, which mediate the covalent labeling of bound substrates with ubiquitin (Ub), with associated E2 ubiquitinating enzymes. After the initial Ub attachment, a substrate-linked polyubiquitin chain is formed and recognized by components of the 19S cap complex of the proteasome. AAA+ proteins within the base of the 19S complex facilitate the ATP-dependent unfolding and translocation of bound

substrates into the core of the proteolytic 20S complex. Finally, ubiquitin is released from the substrate by deubiquitinating enzymes present in the 19S complex prior polypeptide degradation. Adapted from Mogk *et al.*, 2007.

1.5.2.3 Autophagy

The autophagy clearance of aggregated proteins also requires ubiquitination of their substrates by the ubiquitin-binding proteins p62 and NBR1 (ATG19 in yeast). This process of intracellular lysosomal or vacuolar degradation is characterized by the formation of autophagosomes (double-membrane vesicles). There are three types of autophagy: macroautophagy or only autophagy, which requires the formation of the phagophore (PAS) that expands to form the double-membrane autophagosome needed for the fusion with the lysosome or vacuole; microautophagy, in which lysosomes or vacuoles invaginate and sequester cytosolic components; and chaperone-mediated autophagy (CMA), in which translocation of unfolded proteins occurs throughout the lysosomal membrane (only in higher eukaryotes) (Figure 1.32) (Kirkin *et al.*, 2009; Lilienbaum, 2013). Additionally, in yeast there is a cytoplasm-to-vacuole targeting (Cvt) pathway, in which an autophagy-related constitutive transport system delivers some vacuolar enzymes, such as α -mannosidase (Ams1) and aminopeptidase I (Ape1) (Figure 1.32) (Lynch-Day and Klionsky, 2010).

In macroautophagy, the autophagosome encloses a portion of cytoplasm or organelle, such as mitochondria, peroxisome (macropexophagy) or aggregates, for delivery to the lysosome or vacuole (Figure 1.32). This type of autophagy is believed to be the major mode of autophagy, allowing cells to degrade aggregated proteins as well as organelles with the final release of building blocks into cytosol for reuse in biosynthetic processes (Huang and Klionsky, 2002; Lilienbaum, 2013).

1. Introduction

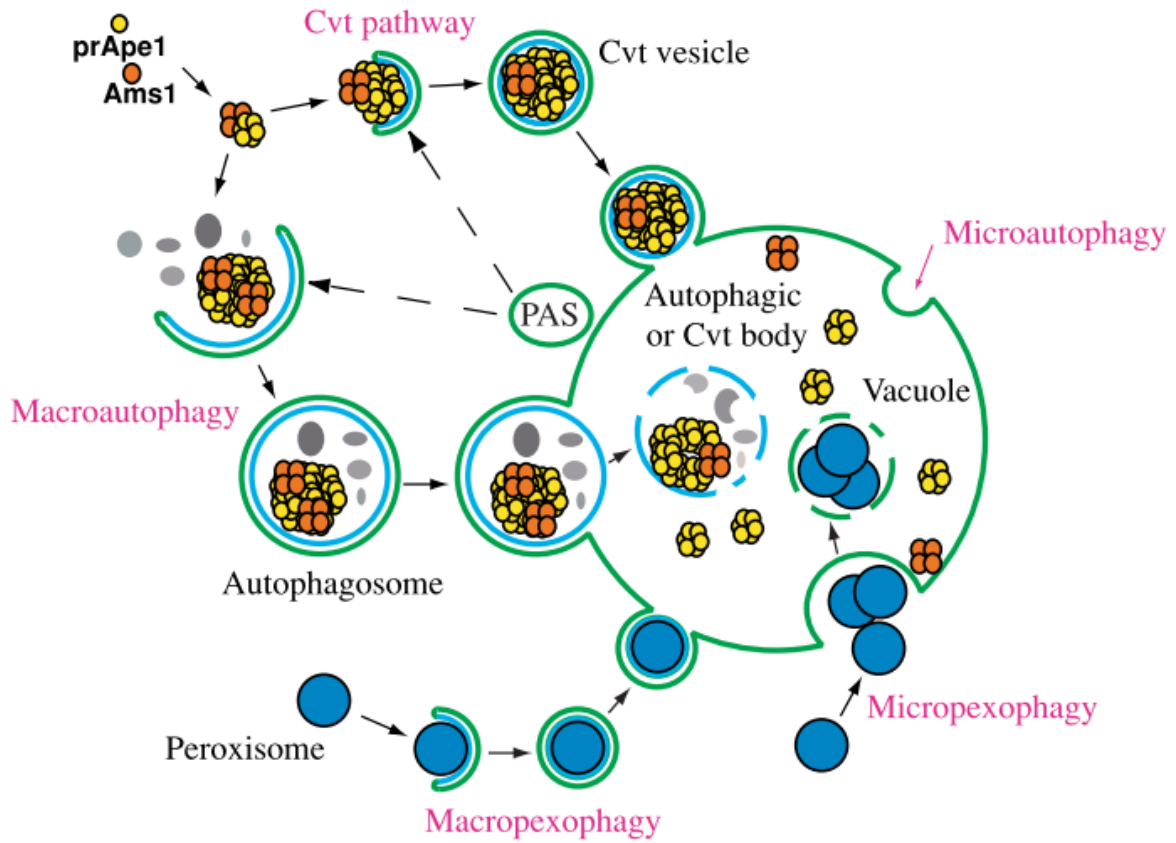


Figure 1.32. Types of autophagy in yeast. Morphology of Cvt pathway, micro- and macroautophagy, and micro- and macropexophagy. The pre-autophagosomal structure (PAS) is needed for Cvt vesicle and autophagosome formation as donor membrane. Microautophagy and micropexophagy involve uptake at the vacuole surface. Adapted from Huang and Klionsky, 2002.

1.6 TRANSLATIONAL FIDELITY, PROTEIN AGGREGATION AND DISEASE

Errors during protein synthesis as well as limitations and malfunction of chaperones, UPS and autophagy are risk factors for many diseases; collectively called protein conformation diseases. In such diseases, protein aggregates cause proteotoxicity, resulting in cellular pathology due to toxicity, incorrect trafficking or premature degradation (Morimoto, 2008). Additionally, the most typical feature of many of the aggregation diseases is the final deposition of proteins in the form of amyloid fibrils and plaques. Such deposits can form in vital organs, such as brain, liver and spleen, or in the skeletal tissue, depending on the disease type (Dobson, 2004). Conformational diseases include CAG-repeat/polyglutamine (polyQ) expansion diseases (Huntington's disease, HD; Kennedy's disease; spinocerebellar ataxias, SCAs) and non-CAG diseases (Parkinson's disease, PD; prion disease, such as Creutzfeldt–Jakob disease, CJD; amyotrophic lateral sclerosis, ALS; and, Alzheimer's disease, AD) (Barral *et al.*, 2004; Morimoto, 2008). These diseases are characterized by an age-dependent onset and a progressive fatal clinical endpoint (Morimoto, 2008). The presence of aggregation and formation of fibrils can be toxic (but not always) and frequently is caused by mutations in the disease proteins, resulting in cellular dysfunction and pathology (Morimoto, 2008). Other examples of diseases due to the presence of aberrant proteins are cystic fibrosis and hypertrophic cardiomyopathy (Barral *et al.*, 2004). Additionally, several other protein deposition diseases involve non-ordered proteins deposits, such as inclusion body myositis, light-chain deposition disease and cataracts (Fink, 1998). A summary of the main diseases related to protein aggregation is present in Table 1.3. Proteins involved in the group of aggregation disorders do not have sequence similarities; instead the amyloid fibrils into which they can form are similar in morphology. To the formation of these fibrils, misfolded monomers may oligomerize into pre-fibrillar assemblies, giving rise to mature fibrillar structures (Barral *et al.*, 2004). The exact mechanism by which protein misfolding and aggregation are related to disease is still unclear. In the case of systemic disease, insoluble proteins may physically disrupt the functioning of specific organs. In the other cases, it is the loss of functional protein that leads to the failure of some essential cellular process (Barral *et al.*, 2004; Dobson, 2004).

1. Introduction

Table 1.3. Summary of the main diseases related to protein aggregation (Dobson, 2001; Barral *et al.*, 2004; Stefani, 2004).

Clinical syndrome	Proteins peptides involved
Alzheimer's disease	APP β -peptide
Scrapie/Creutzfeldt-Jakob's disease	Prion protein
Polyglutamine expansion disease:	Various polyQ proteins:
Huntington's disease	Huntingtin
Dentatorubto-pallido-Luysian atrophy	Atrophin 1
Cerebellar ataxias	Ataxins
Kennedy disease	Androgen receptor
Spino cerebellar ataxia 17	TATA box-binding protein
Familial amyloidosis	Transthyretin/lysozyme
Cystic fibrosis	CFTR
Familial hypercholesterolemia	LDL receptor
Phenylketonuria	Phenylalanine hydroxylase
MCAD deficiency	Medium-chain acyl-CoA dehydrogenase
Hypertrophic cardiomyopathy	Various sarcometric proteins
<i>Osteogenesis imperfecta</i>	Collagens
<i>Epidermolysis bullosa simplex</i>	Keratins
Hereditary spastic paraplegia	Mitochondrial Hsp60
Desmin-related myopathy	α B-Crystallin
Sanjad-Sakati and Kenny-Caffrey	TBCE
Marfan syndrome	Fibrillin
Sickle cell anaemia	Haemoglobin
α 1-antitrypsin deficiency	α 1-antitrypsin
Tay-Sachs disease	β -hexosaminidase

Molecular chaperones play fundamental roles in the pathogenesis of these diseases since the accumulation of toxic misfolded proteins may only occur if the folding capacity of chaperones is exceeded. Therefore, the frequency of these diseases increases with age; due to reduced efficiency of the quality control machinery. In this situation, there is an imbalance between the production of toxic misfolded species and the protective capacity of the chaperone machinery (Barral *et al.*, 2004; Dobson, 2004; Voisine, Pedersen and Morimoto, 2010). Moreover, the ubiquitin-proteasome system targets disease aggregates for degradation. But, there

is an overall reduction in proteolytic activity of the proteasome in diseased tissues, so proteasomal function is compromised during aggregation disease pathogenesis (Barral *et al.*, 2004).

Another type of diseases characterized by the presence of misfolded proteins occur due to an imbalance of some mediators of proteins synthesis, namely ribosomes and tRNAs. For instance, absence of RNA modifications could have an impact on protein translation fidelity and many studies have shown a link between defects in tRNA modifications and human diseases, such as neurological disorders, cancer, type 2 diabetes and mitochondrial disorders (Table 1.4) (Kirino and Suzuki, 2005; Shimada *et al.*, 2009; Nguyen *et al.*, 2010; Igoillo-Esteve *et al.*, 2013; Torres, Batlle and Ribas de Pouplana, 2014). Similarly, rRNA modification defects are also related to human disease, such as X-linked dyskeratosis congenital (X-linked DC) and cancer (Ruggero *et al.*, 2003; Montanaro *et al.*, 2006). Defects in ribosome biogenesis are related with a diverse and heterogeneous group of disorders known as ribosomopathies (Armistead and Triggs-Raine, 2014). Some ribosomopathies are X-linked DC and Hoyeraal-Hreidarsson syndrome, in which the pseudouridine synthase dyskerin is deregulated; Diamond-Blackfan anemia, in which some ribosomal proteins have mutations (RPS7, RPS10, RPS17, RPS19, RPS24, RPS26, RPL5, RPL11, RPL26, RPL35A); Treacher Collins syndrome, in which transcription of rRNA genes is impaired; among other disorders (Ruggero *et al.*, 2003; Valdez *et al.*, 2004; Choesmel *et al.*, 2007; Armistead and Triggs-Raine, 2014).

1. Introduction

Table 1.4. tRNA-related diseases. MELAS: Mitochondrial encephalomyopathy, lactic acidosis and stroke-like episodes; MERF: Myoclonic epilepsy with ragged-red fibres; MLASA: Myopathy, lactic acidosis and sideroblastic anemia; LBSL: Leukoencephalopathy with brain stem and spinal cord involvement and lactate elevation.

Disease category	Disease	Affected gene	Pathological effect	Refs
Neurological	Intellectual disability	FTSJ1	impaired modification: 2'-O-methylribose	Ramser <i>et al.</i> , 2004; Freude <i>et al.</i> , 2004
		TRM1	impaired modification: m ² G	Najmabadi <i>et al.</i> , 2011
		NSUN2	impaired modification: m ⁵ C	Ahmad Khan <i>et al.</i> , 2012; Abbasi-Moheb <i>et al.</i> , 2012
		WDR4	impaired modification: m ⁷ G	Michaud <i>et al.</i> , 2000
		ADAT3	A-to-I editing	Alazami <i>et al.</i> , 2013
	Familial dysautonomia	IKBKAP	impaired modification: mcm ⁵ s ² U	Anderson <i>et al.</i> , 2001; Slaugenhaupt <i>et al.</i> , 2001
	Amyotrophic lateral sclerosis	ELP3	impaired modification: mcm ⁵ s ² U	Simpson <i>et al.</i> , 2009
	Rolandic epilepsy	ELP4	impaired modification: mcm ⁵ s ² U	Strug <i>et al.</i> , 2009
	Dubowitz-like	NSUN2	impaired modification of tRNA ^{Asp} _{GTC} : m ⁵ C	Martinez <i>et al.</i> , 2012
	Charcot-Marie-Tooth (CMT) syndrome	GARS	impaired aminoacylation	Sleigh <i>et al.</i> , 2014
		AARS	reduced aminoacylation and mischarging	Latour <i>et al.</i> , 2010
		KARS	impaired aminoacylation	Yao and Fox, 2013
Pontocerebellar hypoplasia	CLP1	tRNA misprocessing and reduced tRNA levels	Karaca <i>et al.</i> , 2014; Schaffer <i>et al.</i> , 2014	
Cardiac	Noonan-like syndrome	NSUN2	impaired modification: m ⁵ C	Fahiminiya <i>et al.</i> , 2014
Respiratory	Bronchial asthma	IKBKAP	impaired modification: mcm ⁵ s ² U	Takeoka <i>et al.</i> , 2001
Cancer	Skin, breast, and colorectal	NSUN2	impaired modification: m ⁵ C	Frye and Watt, 2006; Chan <i>et al.</i> , 2010
	Breast	TRMT12	impaired modification: yW	Rodriguez <i>et al.</i> , 2007
		TRMT2A	impaired modification: m ⁵ U	Bartlett <i>et al.</i> , 2010
	Colorectal	HRG9MTD2	impaired modification: m ¹ G	Berg <i>et al.</i> , 2010
	Urothelial	HABH8	impaired modification: mcm ⁵ U	Shimada <i>et al.</i> , 2009
Breast, bladder, colorectal, cervix, testicular	HTRM9L	impaired modification: mcm ⁵ U	Goll <i>et al.</i> , 2006	
Metabolic	Type 2 diabetes	CDKAL1	impaired modification: ms ² t ⁶ A	Steinthorsdottir <i>et al.</i> , 2007; Wei <i>et al.</i> , 2011
Mitochondrial-linked	MELAS	mt tRNA ^{Leu} _{UAA}	impaired modification: tm ⁵ U	Yasukawa <i>et al.</i> , 2000; Kirino <i>et al.</i> , 2005
	MERRF	mt tRNA ^{Lys} _{UUU}	impaired modification: tm ⁵ s ² U	Takehiro Yasukawa <i>et al.</i> , 2000
	Infantile liver failure	MTU1 (TRMU)	impaired modification: s ² U	Zeharia <i>et al.</i> , 2009
	Deafness	MTU1 (TRMU)	impaired modification: s ² U	Guan <i>et al.</i> , 2006
	MLASA	YARS2	reduced aminoacylation	Bonnefond <i>et al.</i> , 2007
	LBSL	DARS2	reduced aminoacylation	Scheper <i>et al.</i> , 2007
	Recessive ataxia	MARS2	reduced aminoacylation and reduced protein synthesis	Scheper <i>et al.</i> , 2007
	Myopathy and Infantile CMT syndrome	AARS2	reduced aminoacylation	Yao and Fox, 2013

1.7 OBJECTIVES OF THE STUDY

The objective of this thesis was to identify tRNA- and rRNA-modifying enzymes (RNAmods) that play a role in proteome homeostasis, using yeast as a work model. In particular, we have investigated the role of tRNA modification by tRNAmods in protein synthesis efficiency and accuracy. Our working hypothesis was that certain tRNA and rRNA modifications play a role in protein folding by fine tuning the accuracy and efficiency of codon-anticodon interactions at the ribosome decoding center. To test this hypothesis, we have combined yeast RNAmods gene knockout strains with a fluorescent sensor to identify gene knock out strains containing high level of protein aggregates, using a high throughput genetic screen that we have implemented in our laboratory. The specific objectives of the project were the following:

1. Construct a series of strains expressing a fluorescent protein aggregation sensor.
2. Set up a genetic screen, using high content microscopy, to identify RNAmods whose deletion results in increased protein aggregation.
3. Determine the tRNA modifications pattern in the candidate deletion strains, using mass spectrometry.
4. Identify the aggregated proteins associated with specific tRNA hypomodifications.
5. Identify tRNA modifications that are essential to maintain translational fidelity.

2. METHODS

2. Methods

2.1 YEAST STRAINS AND GROWTH CONDITIONS

All *S. cerevisiae* strains used are derivatives of BY4743 (MATa/α; his3Δ1/his3Δ1; leu2Δ0/leu2Δ0; LYS2/lys2Δ0; met15Δ0/MET15; ura3Δ0/ura3Δ0), here referred to as wild-type (WT), and have the gene of interest replaced by the KanMX4 cassette (EUROSCARF; Giaever et al. 2002) (Table 2.1). All yeast strains were grown at 30 °C in YPD medium (glucose: 2% (w/v), yeast extract: 0.5% (w/v), and peptone: 1% (w/v)) (Formedium) and minimal medium without histidine (MM-His; glucose: 2% (w/v), yeast nitrogen base without amino acids: 0.67% (w/v), each required amino acids (100 μg/ml)) (Formedium). BY4743 transformed cells were grown in MM-His and preserved at -80 °C in MM-His + 40% (v/v) glycerol. Solid media were performed by addition of 2% agar (Formedium). All media were heat sterilized.

Table 2.1. List of strains used in this study (from EUROSCARF).

No.	Yeast gene knockout	Systematic name	RNA-modifying Enzyme Function	Genotype
1		BY4743		MATa/α; his3Δ1/his3Δ1; leu2Δ0/leu2Δ0; LYS2/lys2Δ0; met15Δ0/MET15; ura3Δ0/ura3Δ0
2	MOD5	YOR274w	i ⁶ A ₃₇	BY4743; Mat a/α; his3Δ1/his3Δ1; leu2Δ0/leu2Δ0; lys2Δ0/LYS2; MET15/met15Δ0; ura3Δ0/ura3Δ0; YOR274w::kanMX4/YOR274w::kanMX4
3	KTI13 (ATS1, FUN28)	YAL020c	mcm ⁵ U ₃₄ , mcm ⁵ s ² U ₃₄ , ncm ⁵ U ₃₄ , ncm ⁵ Um ₃₄	BY4743; Mat a/α; his3Δ1/his3Δ1; leu2Δ0/leu2Δ0; lys2Δ0/LYS2; MET15/met15Δ0; ura3Δ0/ura3Δ0; YAL020c::kanMX4/YAL020c
4	MTR10 (KAP111)	YOR160w	Retrograde import	BY4743; Mat a/α; his3Δ1/his3Δ1; leu2Δ0/leu2Δ0; lys2Δ0/LYS2; MET15/met15Δ0; ura3Δ0/ura3Δ0; YOR160w::kanMX4/YOR160w
5	PUS7	YOR243c	Ψ ₁₃ , Ψ ₃₅	BY4743; Mat a/α; his3Δ1/his3Δ1; leu2Δ0/leu2Δ0; lys2Δ0/LYS2; MET15/met15Δ0; ura3Δ0/ura3Δ0; YOR243c::kanMX4/YOR243c::kanMX4
6	PUS8	YOL066C	Ψ ₃₂	BY4743; Mat a/α; his3Δ1/his3Δ1; leu2Δ0/leu2Δ0; lys2Δ0/LYS2; MET15/met15Δ0; ura3Δ0/ura3Δ0; YOL066c::kanMX4/YOL066c
7	TRM112	YNR046c	mcm ⁵ U ₃₄ and mcm ⁵ s ² U ₃₄ , m ⁵ G ₁₀	BY4743; Mat a/α; his3Δ1/his3Δ1; leu2Δ0/leu2Δ0; lys2Δ0/LYS2; MET15/met15Δ0; ura3Δ0/ura3Δ0; YNR046w::kanMX4/YNR046w
8	TRM4 (NCL1)	YBL024w	m ⁵ C ₃₄ , m ⁵ C ₄₀ , m ⁵ C ₄₈ , m ⁵ C ₄₉	BY4743; Mat a/α; his3Δ1/his3Δ1; leu2Δ0/leu2Δ0; lys2Δ0/LYS2;

				MET15/met15Δ0; ura3Δ0/ura3Δ0; YBL024w::kanMX4/YBL024w::kanMX4
9	TAD1	YGL243w	l ₃₇	BY4743; Mat a/α; his3Δ1/his3Δ1; leu2Δ0/leu2Δ0; lys2Δ0/LYS2; MET15/met15Δ0; ura3Δ0/ura3Δ0; YGL243w::kanMX4/YGL243w::kanMX4
10	NBP35	YGL091c	mcm ⁵ s ² U ₃₄	BY4743; Mat a/α; his3Δ1/his3Δ1; leu2Δ0/leu2Δ0; lys2Δ0/LYS2; MET15/met15Δ0; ura3Δ0/ura3Δ0; YGL091c::kanMX4/YGL091c
11	ISU2 (NUA2)	YOR226c	mcm ⁵ s ² U ₃₄	BY4743; Mat a/α; his3Δ1/his3Δ1; leu2Δ0/leu2Δ0; lys2Δ0/LYS2; MET15/met15Δ0; ura3Δ0/ura3Δ0; YOR226c::kanMX4/YOR226c::kanMX4
12	CFD1 (DRE3)	YIL003w	mcm ⁵ s ² U ₃₄	BY4743; Mat a/α; his3Δ1/his3Δ1; leu2Δ0/leu2Δ0; lys2Δ0/LYS2; MET15/met15Δ0; ura3Δ0/ura3Δ0; YIL003w::kanMX4/YIL003w
13	KTI14 (HRR25)	YPL204w	mcm ⁵ U ₃₄ , mcm ⁵ s ² U ₃₄ , ncm ⁵ U ₃₄ , ncm ⁵ Um ₃₄	BY4743; Mat a/α; his3Δ1/his3Δ1; leu2Δ0/leu2Δ0; lys2Δ0/LYS2; MET15/met15Δ0; ura3Δ0/ura3Δ0; YPL204w::kanMX4/YPL204w
14	TYW3	YGL050w	yW ₃₇	BY4743; Mat a/α; his3Δ1/his3Δ1; leu2Δ0/leu2Δ0; lys2Δ0/LYS2; MET15/met15Δ0; ura3Δ0/ura3Δ0; YGL050w::kanMX4/YGL050w::kanMX4
15	ISU1 (NUA1)	YPL135w	mcm ⁵ s ² U ₃₄	BY4743; Mat a/α; his3Δ1/his3Δ1; leu2Δ0/leu2Δ0; lys2Δ0/LYS2; MET15/met15Δ0; ura3Δ0/ura3Δ0; YPL135w::kanMX4/YPL135w::kanMX4
16	ELP2 (TOT2, KTI3)	YGR200c	mcm ⁵ U ₃₄ , mcm ⁵ s ² U ₃₄ , ncm ⁵ U ₃₄ , ncm ⁵ Um ₃₄	BY4743; Mat a/α; his3Δ1/his3Δ1; leu2Δ0/leu2Δ0; lys2Δ0/LYS2; MET15/met15Δ0; ura3Δ0/ura3Δ0; YGR200c::kanMX4/YGR200c::kanMX4
17	TRM3	YDL112w	Gm ₁₈	BY4743; Mat a/α; his3Δ1/his3Δ1; leu2Δ0/leu2Δ0; lys2Δ0/LYS2; MET15/met15Δ0; ura3Δ0/ura3Δ0; YDL112w::kanMX4/YDL112w::kanMX4
18	NCS6 (TUC1, YGL210w- A)	YGL211w	mcm ⁵ s ² U ₃₄	BY4743; Mat a/α; his3Δ1/his3Δ1; leu2Δ0/leu2Δ0; lys2Δ0/LYS2; MET15/met15Δ0; ura3Δ0/ura3Δ0; YGL211w::kanMX4/YGL211w::kanMX4
19	DUS4	YLR405w	D _{20a} , D _{20b}	BY4743; Mat a/α; his3Δ1/his3Δ1; leu2Δ0/leu2Δ0; lys2Δ0/LYS2; MET15/met15Δ0; ura3Δ0/ura3Δ0; YLR405w::kanMX4/YLR405w::kanMX4
20	TRM9 (KY11)	YML014w	mcm ⁵ U ₃₄ , mcm ⁵ s ² U ₃₄	BY4743; Mat a/α; his3Δ1/his3Δ1; leu2Δ0/leu2Δ0; lys2Δ0/LYS2; MET15/met15Δ0; ura3Δ0/ura3Δ0; YML014w::kanMX4/YML014w::kanMX4
21	SUA5	YGL169w	t ⁶ A ₃₇	BY4743; Mat a/α; his3Δ1/his3Δ1; leu2Δ0/leu2Δ0; lys2Δ0/LYS2; MET15/met15Δ0; ura3Δ0/ura3Δ0; YGL169w::kanMX4/YGL169w
22	ELP6 (HAP3,	YMR312w	mcm ⁵ U ₃₄ , mcm ⁵ s ² U ₃₄ ,	BY4743; Mat a/α; his3Δ1/his3Δ1; leu2Δ0/leu2Δ0; lys2Δ0/LYS2;

2. Methods

	TOT6, KTI4)		ncm ⁵ U ₃₄ , ncm ⁵ Um ₃₄	MET15/met15Δ0; ura3Δ0/ura3Δ0; YMR312w::kanMX4/YMR312w::kanMX4
23	TRM2 (NUC2, NUD1, RNC1)	YKR056w	m ⁵ U ₅₄	BY4743; Mat a/α; his3Δ1/his3Δ1; leu2Δ0/leu2Δ0; lys2Δ0/LYS2; MET15/met15Δ0; ura3Δ0/ura3Δ0; YKR056w::kanMX4/YKR056w::kanMX4
24	TRM44	YPL030w	m ⁵ C ₃₄ , m ⁵ C ₄₀ , m ⁵ C ₄₈ , m ⁵ C ₄₉	BY4743; Mat a/α; his3Δ1/his3Δ1; leu2Δ0/leu2Δ0; lys2Δ0/LYS2; MET15/met15Δ0; ura3Δ0/ura3Δ0; YPL030w::kanMX4/YPL030w::kanMX4
25	TUM1	YOR251c	mcm ⁵ s ² U ₃₄	BY4743; Mat a/α; his3Δ1/his3Δ1; leu2Δ0/leu2Δ0; lys2Δ0/LYS2; MET15/met15Δ0; ura3Δ0/ura3Δ0; YOR251c::kanMX4/YOR251c::kanMX4
26	CIA1	YDR267c	mcm ⁵ s ² U ₃₄	BY4743; Mat a/α; his3Δ1/his3Δ1; leu2Δ0/leu2Δ0; lys2Δ0/LYS2; MET15/met15Δ0; ura3Δ0/ura3Δ0; YDR267c::kanMX4/YDR267c
27	ELP1 (IKI3, TOT1, KTI7)	YLR384c	mcm ⁵ U ₃₄ , mcm ⁵ s ² U ₃₄ , ncm ⁵ U ₃₄ , ncm ⁵ Um ₃₄	BY4743; Mat a/α; his3Δ1/his3Δ1; leu2Δ0/leu2Δ0; lys2Δ0/LYS2; MET15/met15Δ0; ura3Δ0/ura3Δ0; YLR384c::kanMX4/YLR384c::kanMX4
28	PUS6	YGR169c	Ψ ₃₁	BY4743; Mat a/α; his3Δ1/his3Δ1; leu2Δ0/leu2Δ0; lys2Δ0/LYS2; MET15/met15Δ0; ura3Δ0/ura3Δ0; YGR169c::kanMX4/YGR169c::kanMX4
29	UBA4 (YHR1)	YHR111c	mcm ⁵ s ² U ₃₄	BY4743; Mat a/α; his3Δ1/his3Δ1; leu2Δ0/leu2Δ0; lys2Δ0/LYS2; MET15/met15Δ0; ura3Δ0/ura3Δ0; YHR111w::kanMX4/YHR111w::kanMX4
30	TYW4 (PPM2)	YOL141w	yW ₃₇	BY4743; Mat a/α; his3Δ1/his3Δ1; leu2Δ0/leu2Δ0; lys2Δ0/LYS2; MET15/met15Δ0; ura3Δ0/ura3Δ0; YOL141w::kanMX4/YOL141w::kanMX4
31	DUS2 (SMM1)	YNR015w	D ₂₀	BY4743; Mat a/α; his3Δ1/his3Δ1; leu2Δ0/leu2Δ0; lys2Δ0/LYS2; MET15/met15Δ0; ura3Δ0/ura3Δ0; YNR015w::kanMX4/YNR015w::kanMX4
32	MSN5 (KAP142, STE21)	YDR335w	Re-export	BY4743; Mat a/α; his3Δ1/his3Δ1; leu2Δ0/leu2Δ0; lys2Δ0/LYS2; MET15/met15Δ0; ura3Δ0/ura3Δ0; YDR335w::kanMX4/YDR335w::kanMX4
33	NFS1 (SPL1)	YCL017c	mcm ⁵ s ² U ₃₄	BY4743; Mat a/α; his3Δ1/his3Δ1; leu2Δ0/leu2Δ0; lys2Δ0/LYS2; MET15/met15Δ0; ura3Δ0/ura3Δ0; YCL017c::kanMX4/YCL017c
34	TRM1	YDR120c	m ² ₂ G ₂₆	BY4743; Mat a/α; his3Δ1/his3Δ1; leu2Δ0/leu2Δ0; lys2Δ0/LYS2; MET15/met15Δ0; ura3Δ0/ura3Δ0; YDR120c::kanMX4/YDR120c::kanMX4
35	DUS3	YLR401c	D ₄₇	BY4743; Mat a/α; his3Δ1/his3Δ1; leu2Δ0/leu2Δ0; lys2Δ0/LYS2; MET15/met15Δ0; ura3Δ0/ura3Δ0; YLR401c::kanMX4/YLR401c::kanMX4
36	LOS1	YKL205w	Export, re-export	BY4743; Mat a/α; his3Δ1/his3Δ1; leu2Δ0/leu2Δ0; lys2Δ0/LYS2;

				MET15/met15 Δ 0; ura3 Δ 0/ura3 Δ 0; YKL205w::kanMX4/YKL205w::kanMX4
37	ELP3	YPL086c	mcm ⁵ U ₃₄ , mcm ⁵ s ² U ₃₄ , ncm ⁵ U ₃₄ , ncm ⁵ Um ₃₄	BY4743; Mat a/ α ; his3 Δ 1/his3 Δ 1; leu2 Δ 0/leu2 Δ 0; lys2 Δ 0/LYS2; MET15/met15 Δ 0; ura3 Δ 0/ura3 Δ 0; YPL086c::kanMX4/YPL086c::kanMX4
38	TYW1	YPL207w	yW ₃₇	BY4743; Mat a/ α ; his3 Δ 1/his3 Δ 1; leu2 Δ 0/leu2 Δ 0; lys2 Δ 0/LYS2; MET15/met15 Δ 0; ura3 Δ 0/ura3 Δ 0; YPL207w::kanMX4/YPL207w::kanMX4
39	TRM7	YBR061c	Cm ₃₂ , Cm ₃₄ , Gm ₃₄ , ncm ⁵ Um ₃₄	BY4743; Mat a/ α ; his3 Δ 1/his3 Δ 1; leu2 Δ 0/leu2 Δ 0; lys2 Δ 0/LYS2; MET15/met15 Δ 0; ura3 Δ 0/ura3 Δ 0; YBR061c::kanMX4/YBR061c
40	NCS2 (TUC2)	YNL119w	mcm ⁵ s ² U ₃₄	BY4743; Mat a/ α ; his3 Δ 1/his3 Δ 1; leu2 Δ 0/leu2 Δ 0; lys2 Δ 0/LYS2; MET15/met15 Δ 0; ura3 Δ 0/ura3 Δ 0; YNL119w::kanMX4/YNL119w::kanMX4
41	URM1	YIL008w	mcm ⁵ s ² U ₃₄	BY4743; Mat a/ α ; his3 Δ 1/his3 Δ 1; leu2 Δ 0/leu2 Δ 0; lys2 Δ 0/LYS2; MET15/met15 Δ 0; ura3 Δ 0/ura3 Δ 0; YIL008w::kanMX4/YIL008w::kanMX4
42	TRM8	YDL201w	m ⁷ G ₄₆	BY4743; Mat a/ α ; his3 Δ 1/his3 Δ 1; leu2 Δ 0/leu2 Δ 0; lys2 Δ 0/LYS2; MET15/met15 Δ 0; ura3 Δ 0/ura3 Δ 0; YDL201w::kanMX4/YDL201w::kanMX4
43	TYW2 (TRM12)	YML005w	yW ₃₇	BY4743; Mat a/ α ; his3 Δ 1/his3 Δ 1; leu2 Δ 0/leu2 Δ 0; lys2 Δ 0/LYS2; MET15/met15 Δ 0; ura3 Δ 0/ura3 Δ 0; YML005w::kanMX4/YML005w::kanMX4
44	SAP190	YKR028w	mcm ⁵ U ₃₄ , mcm ⁵ s ² U ₃₄ , ncm ⁵ U ₃₄ , ncm ⁵ Um ₃₄	BY4743; Mat a/ α ; his3 Δ 1/his3 Δ 1; leu2 Δ 0/leu2 Δ 0; lys2 Δ 0/LYS2; MET15/met15 Δ 0; ura3 Δ 0/ura3 Δ 0; YKR028w::kanMX4/YKR028w::kanMX4
45	KTI12	YKL110c	mcm ⁵ U ₃₄ , mcm ⁵ s ² U ₃₄ , ncm ⁵ U ₃₄ , ncm ⁵ Um ₃₄	BY4743; Mat a/ α ; his3 Δ 1/his3 Δ 1; leu2 Δ 0/leu2 Δ 0; lys2 Δ 0/LYS2; MET15/met15 Δ 0; ura3 Δ 0/ura3 Δ 0; YKL110c::kanMX4/YKL110c::kanMX4
46	PUS3 (DEG1, HRM3)	YFL001w	Ψ ₃₈ , Ψ ₃₉	BY4743; Mat a/ α ; his3 Δ 1/his3 Δ 1; leu2 Δ 0/leu2 Δ 0; lys2 Δ 0/LYS2; MET15/met15 Δ 0; ura3 Δ 0/ura3 Δ 0; YFL001w::kanMX4/YFL001w::kanMX4
47	PUS1	YPL212c	Ψ ₂₆ , Ψ ₂₇ , Ψ ₂₈ , Ψ ₃₄ , Ψ ₍₃₅₎ , Ψ ₃₆ , Ψ ₆₅ , Ψ ₆₇	BY4743; Mat a/ α ; his3 Δ 1/his3 Δ 1; leu2 Δ 0/leu2 Δ 0; lys2 Δ 0/LYS2; MET15/met15 Δ 0; ura3 Δ 0/ura3 Δ 0; YPL212c::kanMX4/YPL212c::kanMX4
48	ELP4	YPL101w	mcm ⁵ U ₃₄ , mcm ⁵ s ² U ₃₄ , ncm ⁵ U ₃₄ , ncm ⁵ Um ₃₄	BY4743; Mat a/ α ; his3 Δ 1/his3 Δ 1; leu2 Δ 0/leu2 Δ 0; lys2 Δ 0/LYS2; MET15/met15 Δ 0; ura3 Δ 0/ura3 Δ 0; YPL101w::kanMX4/YPL101w::kanMX4
50	TRM10	YOL093w	m ¹ G ₉	BY4743; Mat a/ α ; his3 Δ 1/his3 Δ 1; leu2 Δ 0/leu2 Δ 0; lys2 Δ 0/LYS2; MET15/met15 Δ 0; ura3 Δ 0/ura3 Δ 0; YOL093w::kanMX4/YOL093w::kanMX4
51	TRM5	YHR070w	m ¹ G ₃₇ , m ¹ I ₃₇ , yW ₃₇	BY4743; Mat a/ α ; his3 Δ 1/his3 Δ 1; leu2 Δ 0/leu2 Δ 0; lys2 Δ 0/LYS2;

2. Methods

				MET15/met15 Δ 0; ura3 Δ 0/ura3 Δ 0; YHR070w::kanMX4/YHR070w
52	TRM82	YDR165w	m ⁷ G ₄₆	BY4743; Mat a/ α ; his3 Δ 1/his3 Δ 1; leu2 Δ 0/leu2 Δ 0; lys2 Δ 0/LYS2; MET15/met15 Δ 0; ura3 Δ 0/ura3 Δ 0; YDR165w::kanMX4/YDR165w::kanMX4
53	RIT1	YMR283c	Ar(p)64, tRNA _i ^{Met}	BY4743; Mat a/ α ; his3 Δ 1/his3 Δ 1; leu2 Δ 0/leu2 Δ 0; lys2 Δ 0/LYS2; MET15/met15 Δ 0; ura3 Δ 0/ura3 Δ 0; YMR283c::kanMX4/YMR283c::kanMX4
54	PUS4	YNL292w	Ψ ₅₅	BY4743; Mat a/ α ; his3 Δ 1/his3 Δ 1; leu2 Δ 0/leu2 Δ 0; lys2 Δ 0/LYS2; MET15/met15 Δ 0; ura3 Δ 0/ura3 Δ 0; YNL292w::kanMX4/YNL292w::kanMX4
55	SAP185	YJL098w	mcm ⁵ U ₃₄ , mcm ⁵ s ² U ₃₄ , ncm ⁵ U ₃₄ , ncm ⁵ Um ₃₄	BY4743; Mat a/ α ; his3 Δ 1/his3 Δ 1; leu2 Δ 0/leu2 Δ 0; lys2 Δ 0/LYS2; MET15/met15 Δ 0; ura3 Δ 0/ura3 Δ 0; YJL098w::kanMX4/YJL098w::kanMX4
56	SIT4	YDL047w	mcm ⁵ U ₃₄ , mcm ⁵ s ² U ₃₄ , ncm ⁵ U ₃₄ , ncm ⁵ Um ₃₄	BY4743; Mat a/ α ; his3 Δ 1/his3 Δ 1; leu2 Δ 0/leu2 Δ 0; lys2 Δ 0/LYS2; MET15/met15 Δ 0; ura3 Δ 0/ura3 Δ 0; YDL047w::kanMX4/YDL047w
57	TAN1	YGL232w	ac ⁴ C ₁₂	BY4743; Mat a/ α ; his3 Δ 1/his3 Δ 1; leu2 Δ 0/leu2 Δ 0; lys2 Δ 0/LYS2; MET15/met15 Δ 0; ura3 Δ 0/ura3 Δ 0; YGL232w::kanMX4/YGL232w::kanMX4
58	TRM11	YOL125w	m ² G ₁₀	BY4743; Mat a/ α ; his3 Δ 1/his3 Δ 1; leu2 Δ 0/leu2 Δ 0; lys2 Δ 0/LYS2; MET15/met15 Δ 0; ura3 Δ 0/ura3 Δ 0; YOL124c::kanMX4/YOL124c::kanMX4
59	TRM13	YOL125w	Am ₄ , Gm ₄ , Cm ₄	BY4743; Mat a/ α ; his3 Δ 1/his3 Δ 1; leu2 Δ 0/leu2 Δ 0; lys2 Δ 0/LYS2; MET15/met15 Δ 0; ura3 Δ 0/ura3 Δ 0; YOL125w::kanMX4/YOL125w::kanMX4
60	SLM3 (MTO2, MTU1)	YDL033c	mcm ⁵ s ² U ₃₄ in mt tRNAs	BY4743; Mat a/ α ; his3 Δ 1/his3 Δ 1; leu2 Δ 0/leu2 Δ 0; lys2 Δ 0/LYS2; MET15/met15 Δ 0; ura3 Δ 0/ura3 Δ 0; YDL033c::kanMX4/YDL033c::kanMX4
61	MSS1	YMR023c	mcm ⁵ U ₃₄ in mt tRNAs	BY4743; Mat a/ α ; his3 Δ 1/his3 Δ 1; leu2 Δ 0/leu2 Δ 0; lys2 Δ 0/LYS2; MET15/met15 Δ 0; ura3 Δ 0/ura3 Δ 0; YMR023c::kanMX4/YMR023c::kanMX4
62	PUS2	YGL063w	Ψ ₂₇ , Ψ ₂₈ in mt tRNA	BY4743; Mat a/ α ; his3 Δ 1/his3 Δ 1; leu2 Δ 0/leu2 Δ 0; lys2 Δ 0/LYS2; MET15/met15 Δ 0; ura3 Δ 0/ura3 Δ 0; YGL063w::kanMX4/YGL063w::kanMX4
63	PUS9	YDL036c	Ψ ₃₂ in mt tRNA	BY4743; Mat a/ α ; his3 Δ 1/his3 Δ 1; leu2 Δ 0/leu2 Δ 0; lys2 Δ 0/LYS2; MET15/met15 Δ 0; ura3 Δ 0/ura3 Δ 0; YDL036c::kanMX4/YDL036c
64	Bud32	YGR262c	t ⁶ A	BY4743; Mat a/ α ; his3 Δ 1/his3 Δ 1; leu2 Δ 0/leu2 Δ 0; lys2 Δ 0/LYS2; MET15/met15 Δ 0; ura3 Δ 0/ura3 Δ 0; YGR262c::kanMX4/YGR262c::kanMX4
65	Cgi121	YML036w	t ⁶ A	BY4743; Mat a/ α ; his3 Δ 1/his3 Δ 1; leu2 Δ 0/leu2 Δ 0; lys2 Δ 0/LYS2;

				MET15/met15Δ0; ura3Δ0/ura3Δ0; YML036w::kanMX4/YML036w::kanMX4
67	Tad2 (ADAT2)	YJL035c	l ₃₄	BY4743; Mat a/α; his3Δ1/his3Δ1; leu2Δ0/leu2Δ0; lys2Δ0/LYS2; MET15/met15Δ0; ura3Δ0/ura3Δ0; YJL035c::kanMX4/YJL035c
68	Tad3 (ADAT3)	YLR316c	l ₃₄	BY4743; Mat a/α; his3Δ1/his3Δ1; leu2Δ0/leu2Δ0; lys2Δ0/LYS2; MET15/met15Δ0; ura3Δ0/ura3Δ0; YLR316c::kanMX4/YLR316c
69	Trm140	YOR239w	m ³ C	BY4743; Mat a/α; his3Δ1/his3Δ1; leu2Δ0/leu2Δ0; lys2Δ0/LYS2; MET15/met15Δ0; ura3Δ0/ura3Δ0; YOR239w::kanMX4/YOR239w::kanMX4
70	Trm61	YJL125c	m ¹ A	BY4743; Mat a/α; his3Δ1/his3Δ1; leu2Δ0/leu2Δ0; lys2Δ0/LYS2; MET15/met15Δ0; ura3Δ0/ura3Δ0; YJL125c::kanMX4/YJL125c
71	NOP1 (LOT3)	YDL014w	Xm	BY4743; Mat a/a; his3Δ1/his3Δ1; leu2Δ0/leu2Δ0; lys2Δ0/LYS2; MET15/met15Δ0; ura3Δ0/ura3Δ0; YDL014w::kanMX4/YDL014w
72	NOP58	YOR310c	Cofactor (Xm)	BY4743; Mat a/a; his3Δ1/his3Δ1; leu2Δ0/leu2Δ0; lys2Δ0/LYS2; MET15/met15Δ0; ura3Δ0/ura3Δ0; YOR310c::kanMX4/YOR310c
73	NOP56 (SIK1)	YLR197w	Cofactor (Xm)	BY4743; Mat a/a; his3Δ1/his3Δ1; leu2Δ0/leu2Δ0; lys2Δ0/LYS2; MET15/met15Δ0; ura3Δ0/ura3Δ0; YLR197w::kanMX4/YLR197w
74	SNU13	YEL026w	Cofactor (Xm)	BY4743; Mat a/a; his3Δ1/his3Δ1; leu2Δ0/leu2Δ0; lys2Δ0/LYS2; MET15/met15Δ0; ura3Δ0/ura3Δ0; YEL026w::kanMX4/YEL026w
75	NOP2 (YNA1)	YNL061w	m ⁵ C	BY4743; Mat a/a; his3Δ1/his3Δ1; leu2Δ0/leu2Δ0; lys2Δ0/LYS2; MET15/met15Δ0; ura3Δ0/ura3Δ0; YNL061w::kanMX4/YNL061w
76	DIM1 (CDH1)	YPL266w	m ⁶ A, m ⁶ ₂ A	BY4743; Mat a/a; his3Δ1/his3Δ1; leu2Δ0/leu2Δ0; lys2Δ0/LYS2; MET15/met15Δ0; ura3Δ0/ura3Δ0; YPL266w::kanMX4/YPL266w
77	MRM1	YOR201c	Gm	BY4743; Mat a/a; his3Δ1/his3Δ1; leu2Δ0/leu2Δ0; lys2Δ0/LYS2; MET15/met15Δ0; ura3Δ0/ura3Δ0; YOR201c::kanMX4/YOR201c::kanMX4
78	MRM2	YGL136c	Um	BY4743; Mat a/a; his3Δ1/his3Δ1; leu2Δ0/leu2Δ0; lys2Δ0/LYS2; MET15/met15Δ0; ura3Δ0/ura3Δ0; YGL136c::kanMX4/YGL136c::kanMX4
79	SPB1	YCL054w	Gm, Um	BY4743; Mat a/a; his3Δ1/his3Δ1; leu2Δ0/leu2Δ0; lys2Δ0/LYS2; MET15/met15Δ0; ura3Δ0/ura3Δ0; YCL054w::kanMX4/YCL054w
80	CBF5	YLR175w	ψ	BY4743; Mat a/a; his3Δ1/his3Δ1; leu2Δ0/leu2Δ0; lys2Δ0/LYS2;

2. Methods

				MET15/met15 Δ 0; ura3 Δ 0/ura3 Δ 0; YLR175w::kanMX4/YLR175w
81	NOP10	YHR072w	Cofactor(Ψ)	BY4743; Mat a/a; his3 Δ 1/his3 Δ 1; leu2 Δ 0/leu2 Δ 0; lys2 Δ 0/LYS2; MET15/met15 Δ 0; ura3 Δ 0/ura3 Δ 0; YHR072w::kanMX4/YHR072w
82	NHP2	YDL208w	Cofactor(Ψ)	BY4743; Mat a/a; his3 Δ 1/his3 Δ 1; leu2 Δ 0/leu2 Δ 0; lys2 Δ 0/LYS2; MET15/met15 Δ 0; ura3 Δ 0/ura3 Δ 0; YDL208w::kanMX4/YDL208w
83	MTO1 (IPS1)	YGL236c	cmnm ⁵ U, cmnm ⁵ s ² U	BY4743; Mat a/a; his3 Δ 1/his3 Δ 1; leu2 Δ 0/leu2 Δ 0; lys2 Δ 0/LYS2; MET15/met15 Δ 0; ura3 Δ 0/ura3 Δ 0; YGL236c::kanMX4/YGL236c::kanMX4
84	PUS5	YLR165c	Ψ	BY4743; Mat a/a; his3 Δ 1/his3 Δ 1; leu2 Δ 0/leu2 Δ 0; lys2 Δ 0/LYS2; MET15/met15 Δ 0; ura3 Δ 0/ura3 Δ 0; YLR165c::kanMX4/YLR165c::kanMX4
85	NAF1	YNL124w	Cofactor(Ψ)	BY4743; Mat a/a; his3 Δ 1/his3 Δ 1; leu2 Δ 0/leu2 Δ 0; lys2 Δ 0/LYS2; MET15/met15 Δ 0; ura3 Δ 0/ura3 Δ 0; YNL124w::kanMX4/YNL124w
86	SHQ1	YIL104c	Cofactor(Ψ)	BY4743; Mat a/a; his3 Δ 1/his3 Δ 1; leu2 Δ 0/leu2 Δ 0; lys2 Δ 0/LYS2; MET15/met15 Δ 0; ura3 Δ 0/ura3 Δ 0; YIL104c::kanMX4/YIL104c

2.2 *IN VIVO* DETECTION OF PROTEIN AGGREGATES

Protein aggregates were analyzed as described previously (Erjavec *et al.*, 2007). Briefly, a molecular sensor of protein aggregation was constructed by fusing the Hsp104 and GFP genes under the control of the yeast Hsp104 promoter (Figure 2.1). Since Hsp104 is a molecular chaperone that recognizes and binds aggregated proteins the Hsp104-GFP chimera permits visualizing the cellular localization of the aggregates by monitoring GFP fluorescence emission using epifluorescence or confocal microscopy. Cells containing soluble proteins have GFP fluorescence homogeneously distributed throughout the cytoplasm, while cells containing protein aggregates have it concentrated in foci.

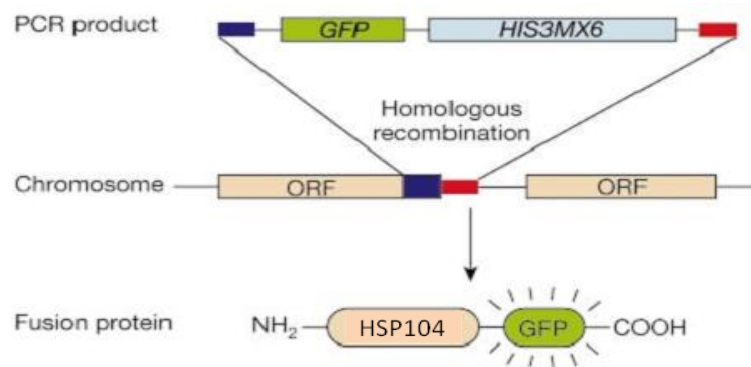


Figure 2.1. Strategy for the construction of fluorescent molecular sensors of protein aggregation. PCR products containing the GFP tag and a selectable marker gene (plasmid pKT128 – pFA6a-GFP(S65T)-His3MX6) were fused in-frame to the C-terminal coding region of the Hsp104 gene through homologous recombination, yielding an Hsp104-GFP fusion protein. Adapted from Huh *et al.*, 2003.

2.2.1 Amplification of the genes of interest by PCR

The Hsp104-GFP fusion protein was constructed following the method described previously by Huh *et al.*, 2003. For this, two oligonucleotides (oUA2403 and oUA2404, Table 2.2) were designed to share complementary sequences to the GFP tag-marker cassette at the 3'-end and contain 40 bp of homology to the C-terminal coding region of Hsp104 gene in order to construct a fusion cassette where the GFP tag was in-frame fused to the C-terminal coding region of the Hsp104 gene. The fusion cassette was generated by PCR using the plasmid pKT128 (pFA6a–GFP(S65T)–His3MX6) as template. This plasmid also contains the *S. pombe* His5 gene which is important for the selection of transformants in histidine-free media. PCR reactions were performed with 500 ng of plasmid pKT128, 1x DreamTaq DNA polymerase buffer, 0.5 μ M of each specific forward and reverse primer, 0.2 μ M of each dNTP and 1.25 units of DreamTaq DNA Polymerase (Fermentas) in a final volume of 50 μ l. PCR reactions were carried out in a thermal cycler (BioRad or Eppendorf) using a standard DNA amplification program of 94 °C for 2 min followed by 30 cycles (94 °C for 30 sec, 54 °C for 30 sec, 72 °C for 3 min) and a final extension of 72 °C for 7 min. PCR products were purified using the QIAquick PCR purification

2. Methods

kit (QIAGEN), according to the manufacturer instructions, and 3 µg of purified product was transformed into each yeast strain (Table 2.1).

Table 2.2. List of oligonucleotides used for GFP fusion proteins construction.

Name	T _m (°C)	Sequence 5'-3'
Hsp104-GFP fusion construction		
oUA2403	57	GACGATAATGAGGACAGTATGGAAATTGATGATGACCTA GATGGTGACGGTGCTGGTTTA
oUA2404	57	GATTCTTGTTTCGAAAGTTTTTAAAAATCACACTATATTTAA TCGATGAATTTCGAGCTCG
Hsp104-GFP confirmation of fusion integration		
oUA2405	53	CTTGAACATAACCTTCTGGC
oUA2406	53	GACTTCTTGCCAAATATGG

2.2.2 Yeast transformation

The transformation of yeast was performed using the LiAc/SS Carrier DNA/PEG method (Gietz and Woods, 2006). Yeast cells were inoculated onto YPD and incubated overnight at 30 °C, with 180 rpm shaking, until an OD₆₀₀ of 0.4-0.5. Cells were then centrifuged (5 000 rpm; 1 minute) in 1.5 mL microcentrifuge tubes. The supernatant was discarded and the transformation reagents were added to the pellet in the following order: 240 µL of PEG 3 500 (50% [w/v]), 36 µL of 1.0 M LiAc, 50 µL of boiled single-stranded carrier DNA (2.0 mg/mL), and 34 µL of an aqueous solution of the amplified DNA (containing 3 µg of DNA). Microcentrifuge tubes were vortexed until a homogeneous suspension was obtained, followed by incubation at 42 °C for 40 minutes, in a Thermomixer comfort (Eppendorf). Cells were then centrifuged at maximum speed for 1 minute, the transformation mixture (supernatant) was discarded, and pellets were carefully resuspended in 200 µL of sterile mQ water. Each cell suspension was plated in selective medium plates (MM-His) and incubated at 30 °C until isolated transformant colonies were visible (2-4 days).

Strains more difficult to transform were manipulated using a different protocol. Yeast cultures grown overnight were diluted into fresh YPD (OD₆₀₀ of 0.3) and were grown for an additional 4 h period to an OD₆₀₀ of 0.8 – 1.2. Cells were then centrifuged (3 220 x g; 5 min) in 50 mL falcons and were washed with sterile water. Cell pellets were resuspended in 600 µL of LiAc-sol (0.1 M LiAc pH 7.5, 1X TE) and

aliquoted in 200 μ L each. To each 200 μ L aliquot were added 50 μ L of an aqueous solution of the amplified DNA (containing 5 μ g of DNA), 100 μ g of boiled single-stranded carrier DNA and 600 μ L of PEG/LiAc-sol (50% PEG 3500, 50% LiAc-sol). Microcentrifuge tubes were vortexed until a homogeneous suspension was obtained and incubated at 30 °C for 1 h, followed by a heat shock of 20 min at 42 °C, in a Thermomixer comfort (Eppendorf) with agitation. Cells were then incubated on ice for about 2 min, centrifuged (4 000 rpm; 15 sec) and gently resuspended in 230 μ L of MM-His. Each cell suspension was plated in selective medium plates (MM-His) and incubated at 30 °C, until isolated transformant colonies were visible (2-3 days).

2.2.3 Analytical colony PCR

Insertion of the fusion cassette by homologous recombination was confirmed by colony PCR using a primer internal to the GFP tag and a primer specific to Hsp104 (oUA2405 and oUA2406 primers, Table 2.2). PCR reactions were performed with a single colony of each KO strain (heated in a microwave for 1 min), 1x DreamTaq DNA polymerase buffer, 0.5 μ M of each specific forward and reverse primer, 0.2 μ M of each dNTP and 1.25 units of DreamTaq DNA Polymerase (Fermentas) in a final volume of 12 μ L. PCR reactions were carried out in a thermal cycler (BioRad or Eppendorf) using a standard program of 94 °C for 2 min followed by 30 cycles (94 °C for 30 sec, 50 °C for 30 sec, 72 °C for 3 min) and a final extension of 72 °C for 7 min. Positive clones were then analyzed by fluorescence microscopy.

2.2.4 Fluorescence microscopy

The cells grown overnight were immobilized on 1% agarose-coated slides in order to be visualized using an Axio Imager.Z1 (Zeiss) epifluorescence upright microscope; using a 63X oil-immersion objective and 38 HE GFP and Brightfield filters. Images were captured using AxionVision Software (Zeiss). The images were taken in one representative focal plane and were processed and analyzed using ImageJ software (<http://rsb.info.nih.gov/ij>). The presence of fluorescent foci in cells was checked and their number was counted manually. On average, 500 cells of 3 clones were analyzed.

2. Methods

2.3 VALIDATION OF GENE DELETIONS BY PCR

The gene knock outs of the strains selected from the genetic screen were validated as described below.

2.3.1 DNA extraction

Yeast cultures grown overnight were centrifuged (2 000 rpm; 5 min) and resuspended in 500 μ L of Solution I (1 M Sorbitol, 0.1 M EDTA- Na_2 , pH 7.4). After transferring to microcentrifuge tubes, 5 μ L of Lyticase (5 U/ μ L; 10 mg/mL) was added to cells and incubated at 37 °C for 60 min. Samples were then centrifuged (2 000 rpm; 1 min) and resuspended in 500 μ L of Solution II (50 mM Tris-HCl; 20 mM EDTA- Na_2 , pH 7.4) and 50 μ L of 10% SDS. Samples were vortexed before incubation at 65 °C for 30 min. 200 μ L of 5 M Potassium Acetate was added to samples and samples were incubated for 60 min on ice. Samples were centrifuged (2 000 rpm; 5 min) and the supernatants were transferred to new microcentrifuge tubes. DNA was precipitated with 2 vol of 100 % ethanol (cold) and 0.1 vol of 5 M NaCl for 2 h at -30 °C. After centrifugation and supernatant discard, DNA pellets were air-dried. DNA was resuspended in mQ water and stored at -30 °C.

2.3.2 PCR

The primers of PCR reactions carried out using DreamTaq™ DNA Polymerase (ThermoFisher Scientific) are summarized in Table 2.3. PCR reactions were performed with 500 ng of DNA of each selected KO strain, 1x DreamTaq DNA polymerase buffer, 0.5 μ M of each specific forward and reverse primer, 0.2 μ M of each dNTP and 1.25 units of DreamTaq DNA Polymerase (Fermentas) in a final volume of 12 μ L. PCR reactions were carried out in a thermal cycler (BioRad or Eppendorf) using a standard program of 95 °C for 3 min followed by 25-30 cycles (95 °C for 30 sec, T_m for 30 sec, 72 °C for 1 min) and a final extension of 72 °C for 7 min. PCR products were fractionated on agarose gels and visualized by UV exposition using a Gel Doc System (BioRad).

Table 2.3. Primers used for selected KO strains validation.

Name	T _m (°C)	Sequence 5' – 3'
ELP1 Forward Primer	62	TCCGACATTAGAGCCGTTCCG
ELP1 Reverse Primer	60	TGGCACGCACTCTTTCATCT
KTI12 Forward Primer	62	CAAGCAACCGATGGGACTCT
KTI12 Reverse Primer	62	TGTTCCGTTACTTACCCCGC
SHQ1 Forward Primer	62	GAGTGCTTGGACCATGGGAA
SHQ1 Reverse Primer	64	GTGTCTCCCACTCAGGTTCCG
SLM3 Forward Primer	62	TGCTTCACCGTACAGACCAC
SLM3 Reverse Primer	62	ACTCTCTCAGCTTGCCGAAC
SPB1 Forward Primer	62	CTGCTCCTGGTTCATGGTGT
SPB1 Reverse Primer	62	TCCTGAACCCAACCCAAACC
TRM9 Forward Primer	60	TAGCTCCGCATTTCTCGCAA
TRM9 Reverse Primer	62	ACCTCAACACGTCTCTCCCT

2.4 TRANSMISSION ELECTRON MICROSCOPY FOR ULTRASTRUCTURAL ANALYSIS

Transmission electron microscopy was performed according to the methodology described in Wright, 2000 by the HEMS group of IBMC – Porto. Briefly, cultures ($OD_{600} = 0.8-1.0$) were fixed overnight at 4 °C with fixative solution (0.1 M PIPES, pH 6.8; 0.1 M sorbitol; 1 mM MgCl₂; 1 mM CaCl₂; 2% glutaraldehyde). Samples were then washed with mQ water, post-fixed with 2% potassium permanganate, pre-stained with 1% aqueous uranyl acetate, dehydrated in graded ethanol series (25%, 50%, 75%, 95%, and 100% ethanol), and embedded in Epon 812 resin. The polymerization of the resin proceeded at 60 °C for 24 h. Thin sections (80-120 nm thickness) were prepared on a Ultramicrotome RMC PowerTome, collected in grids, and stained with Reynolds' lead citrate. Grids were observed on a JEOL JEM 1 400 (80 kV) transmission electron microscope equipped with an Orius Sc1000 Digital Camera.

2. Methods

2.5 PHYSIOLOGY OF SELECTED KO STRAINS

2.5.1 Growth curves

The growth rate of the selected KO strains was determined by analyzing the growth of three independent clones. Yeast cells were grown overnight at 30 °C in liquid MM-His medium as a pre-culture. For main cultures, fresh medium (MM-His) was inoculated with cells from the pre-culture to an initial OD₆₀₀ of 0.02. These cultures were grown at 30 °C, 180 rpm, until late stationary phase. At various time points, aliquots of the culture were removed and OD₆₀₀ was measured using a Microplate Reader (BioRad). Time dependent OD₆₀₀ values were plotted using a logarithmic scale. Specific growth rate (μ) corresponds to the growth of yeast cells in exponential phase and was determined using the following equation:

$$\mu = \frac{\ln OD_2 - \ln OD_1}{t_2 - t_1},$$

where OD₁ and OD₂ corresponds to the OD₆₀₀ measured in time (t) 1 and t₂, respectively.

2.5.2 Cell viability assays

2.5.2.1 Spotting test

To determine cell viability, 0.5 OD₆₀₀ units of yeast cells from the exponential phase culture were centrifuged and washed with sterile water. Yeast cells were resuspended in 200 μ L of sterile water and 10 μ L of each suspension was then subjected to a series of 10-fold dilutions. Samples (5 μ L) of each suspension were inoculated onto solid MM-His medium and incubated at 30 °C. Colony growth was inspected after 2 days and colonies were photographed using a Gel Doc System (BioRad). All images were imported and processed using ImageJ software. Each spot of the assay was measured and a growth score was calculated (corresponding to the ratio between the area of the spot in the KO strain and the area of the same spot in the WT strain). The growth score average of all the spots correspond to the score for that specific strain (GS).

2.5.2.2 Propidium iodide incorporation

Cell death was determined using the propidium iodide (PI) labeling. Cells were collected in different time points, washed and resuspended in 1X PBS. PI was added to cells to a final concentration of 2 μ M. Cells were incubated in the dark, at 30 °C during 30 min and analyzed by flow cytometry (BD Accuri™ C6 flow cytometer). Quantification of PI positive cells was carried out using BD Accuri C6 Software.

2.5.3 Proteasome activity assay

Chymotrypsin-like activity of the proteasome was assayed by monitoring the production of 7-amino-4-methylcoumarin (AMC) from the fluorogenic peptide succinyl-leucine-leucine-valine-tyrosine-AMC (s-LLVY-AMC) (Grune *et al.*, 1998; Demasi, Silva and Netto, 2003). As described previously in Silva *et al.*, 2007, 10 OD₆₀₀ units of cells grown at 30 °C to middle exponential phase and stationary phase were harvested by centrifugation at 4 000 rpm, 4 °C for 5 minutes, washed and frozen at -80 °C. Cell pellets were resuspended in 300 μ L of lysis buffer (10 mM HEPES, 10 mM KCl and 1.5 mM MgCl₂), disrupted with glass beads using Precellys™ 24 disrupter (2 cycles of 25 sec at 6 500 rpm; samples were kept on ice between each cycle), and centrifuged for 5 min at 5 000 rpm followed by 10 min at 13 000 rpm, 4 °C. Protein extracts were quantified using the BCA protein quantification kit (Pierce) and were kept at -80 °C until further use. 100 μ g of protein extracts were resuspended in assay buffer (10 mM Tris pH 8.0, 20 mM KCl, 5 mM MgCl₂) to a final volume of 100 μ L and were incubated at 37 °C for 15 min. The proteasome substrate N-SLLVY-AMC (Sigma) was added to a final concentration of 50 μ M, and cells were incubated at 37 °C during 60 min. Fluorescence of the proteolytically released AMC was measured using Synergy 2 (Biotek), a multi-detection microplate reader, at 360 nm (excitation) and 460 nm (emission). Relative proteasome activity was calculated by determining the increase of the amount of released AMC (difference between fluorescence emission at time 60 min and at time 0 min) relatively to control (WT) cells.

2. Methods

2.6 BIOCHEMICAL CHARACTERIZATION OF tRNAs

The function of the putative RNAmod genes selected from the genetic screen were confirmed by LCMS/MS analysis using the tRNA and rRNA substrates. This validation included total RNA extraction, tRNA purification in DEAE cellulose columns, enzymatic hydrolysis, reverse-phase HPLC resolution of ribonucleosides and identification and quantification of individual ribonucleosides by LC-MS (Su *et al.*, 2014).

2.6.1 RNA extraction and tRNA purification

For total RNA extractions, 250 mL of cultures were grown until early stationary phase (OD₆₀₀ of 1-1.5) and were harvested. Cell pellets were washed and frozen overnight at -80 °C. Cells were resuspended in 10-15 mL of acid phenol chloroform 5:1 pH 4.7 (phenol volume = culture volume x [OD₆₀₀/25]) and equal volume of TES buffer (10 mM Tris pH 7.5, 10 mM EDTA, 0.5% SDS). Cells suspension was vigorously shaken for 30 seconds and incubated at 65 °C for 1 h with agitation every 10 min. The aqueous phase containing RNAs was separated from the phenolic phase by centrifugation at 7 500 rpm for 30 min at 4 °C, and re-extracted with same volume of fresh phenol at 7 500 rpm for 20 min at 4 °C. Aqueous phases were re-extracted with the same volume of Chloroform Isoamyl Alcohol 24:1 by centrifugation at 7 500 rpm for 20 min at 4 °C. RNA was precipitated overnight at -30 °C with 3 volumes of ethanol 100% and 0.1 volumes of 3 M sodium acetate pH 5.2. RNAs were harvest by centrifugation at 7 200 rpm for 30 min at 4 °C and resuspended in 1 mL of 0.1 M sodium acetate pH 4.5. tRNAs were isolated on a 40 mL DEAE-cellulose column equilibrated with the RNA resuspension buffer (Santos, Perreau and Tuite, 1996). Samples were washed with 2.5 volumes of 0.1 M sodium acetate pH 4.5/0.3 M sodium chloride, and tRNAs were eluted with 2 volumes of 0.1 M sodium acetate pH 4.5/1 M sodium chloride. tRNAs precipitated with 2.5 volumes of 100% ethanol overnight at -30 °C were harvested by centrifugation and finally resuspended in mQ water and stored at -80 °C. tRNAs were verified at room temperature in 15% polyacrylamide-8 M urea gels, buffered with TBE.

2.6.2 Isolation of total tRNA and total rRNA by HPLC

tRNAs purified as described above were also analyzed with the Agilent RNA 6000 Pico Assay before further separation from rRNA by HPLC. HPLC-based purification of the tRNA and rRNA (25S, 18S, 5S and 5.8S) was carried out using an Agilent 1100 HPLC Series with an Agilent Bio SEC-3 300 Å column (300 mm length x 7.8 mm inner diameter) with a temperature-controlled column compartment at 60 °C with 100 mM ammonium acetate aqueous phase (isocratic gradient) at a flow rate of 1 mL/min for 15 min. tRNA and rRNA peaks were detected by measuring absorbance at 260 nm and collected with a fraction collector using their retention times (Figure 2.2 and Table 2.4). Fractions were concentrated in a SpeedVac and rehydrated with pure water.

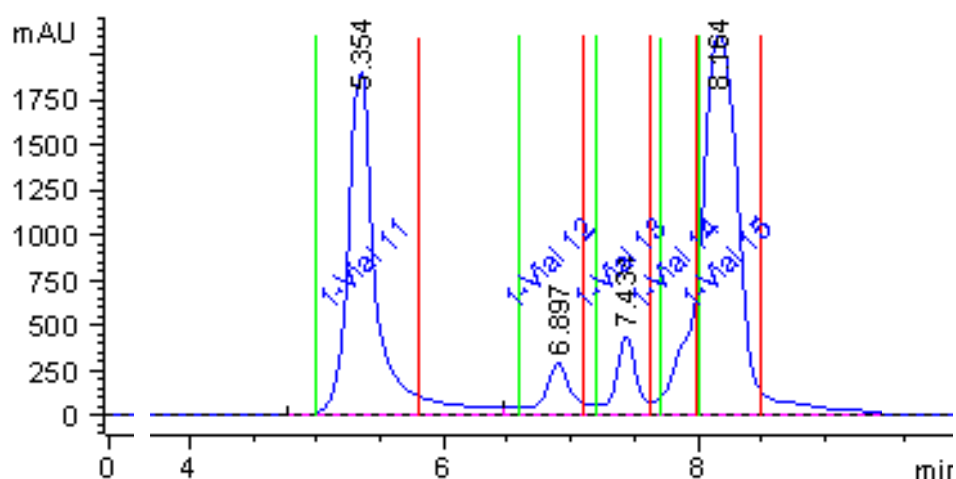


Figure 2.2. Retention time and peak width of tRNA and rRNA signals recorded in the HPLC system for programmed fraction collection.

Table 2.4. Fraction collection timetable used for HPLC-based purification of tRNA and rRNA.

Fractions	RNA isolation	Begin time (min)	End time (min)
1	25S and 18S rRNAs	4.9999	5.8001
2	5.8S rRNA	6.5999	7.0001
3	5S rRNA	7.1999	7.6001
4	tRNA	7.6999	7.9801
5	tRNA	7.9999	8.5001

2. Methods

2.6.3 Quantification of ribonucleosides by LC-MS/MS

2.6.3.1 RNA digestion

tRNAs and rRNAs (20 µg) were enzymatically hydrolyzed and dephosphorylated in a 2 h incubation at 37 °C with coformycin (50 µg/mL), tetrahydrouridine (THU; 0.3 mg/mL), MgCl₂ (0.5 mM), Tris pH 8.0 (0.2 M), alkaline phosphatase (0.05 U/µL), PDE1 (Snake venom phosphodiesterase; 0.005 U/µL), butylated hydroxytoluene (BHT; 0.3 mM) and Benzonase (0.03 U/µL). Deaminase inhibitors (coformycin and THU) and antioxidants (BHT) were present throughout the process to prevent damage artifacts (Chan *et al.*, 2010). Enzymes were removed from ribonucleosides by ultrafiltration with a 10 kDa membrane (12 000 x g, 4-10 min). Digested ribonucleosides were mixed with 5 µM of [¹⁵N]₅-deoxyadenosine ([¹⁵N]₅-dA) to function as an internal control.

2.6.3.2 Optimization of the mass spectrometer parameters

Ribonucleoside standards were used to optimize mass spectrometer parameters. 10 pmol of each ribonucleoside standard were injected into a UPLC system connected directly to a QQQ mass spectrometer with 5 mM ammonium acetate as the solvent. The UPLC system consisted in a Synergi 2.5 µm Fusion – RP 100-Å (100 x 2 mm) column with a mobile phase of 0-80% acetonitrile (ACN) in 5 mM ammonium acetate (Table 2.5) at a flow rate of 0.350 mL/min and 35 °C. The HPLC column was coupled to a 6430 Triple Quad mass spectrometer with an electrospray ionization (ESI) source operated in positive ion mode with the following parameters: gas temperature – 350 °C; gas flow – 10.0 L/min; nebulizer – 40.0 psi; capillary current – 5549 nA. Ribonucleoside standards were identified by HPLC retention time and collision-induced dissociation (CID) fragmentation pattern (Table 2.6 and Table 2.7).

Table 2.5. Solvent gradient used by the UPLC-MS system.

Time (min)	Solvent A (%) (5 mM NH ₄ OAc pH 5.3)	Solvent B (%) (ACN)
0.00	100.00	0.00
1.00	100.00	0.00
10.00	90.00	10.00
14.00	60.00	40.00
15.00	20.00	80.00
16.00	100.00	0.00
20.00	100.00	0.00

Table 2.6. Dynamic MRM parameters for tRNA ribonucleosides identification based on optimized results.

Compound Name	Precursor Ion (m/z)	Product Ion (m/z)	Fragment (V)	Collision Energy (V)	Cell Accelerator Voltage	Ret. Time (min)	Delta Ret. Time (min)
¹⁵ N-dA	257	141	90	10	2	7.3	1
ac ⁴ C	286	154	80	6	2	6.5	1
Am	282	136	100	15	2	8.3	1
Cm	258	112	80	8	2	4.2	1
cm ⁵ U	303.2	171.1	90	7	2	2.2	1
cm ⁵ Um	317	171.1	90	7	2	4.4	1
cmnm ⁵ s ² U	348	216	90	10	2	4.1	3
cmnm ⁵ U	331	200	80	5	2	1.6	3
ct ⁶ A	395	263	100	8	2	4	1
D	247	115	80	5	2	1.6	1
Gm	298	152	80	7	2	6.2	1
I	269	137	80	10	2	4.5	1
i ⁶ A	336	204	100	17	2	13.9	1
m ¹ A	282	150	100	16	2	2	2
m ¹ G	298	166	90	10	2	6.1	0.5
m ¹ I	283	151	80	10	2	5.9	1
m ^{2,2,7} G	326	194	80	10	2	6.7	1
m ² ₂ G	312	180	100	8	2	7.8	1
m ² A	282	150	100	16	2	9	0.5
m ² G	298	166	90	10	2	6.5	0.5
m ³ C	258	126	80	8	2	2.6	2
m ³ U	259	127	100	16	2	5.7	1
m ⁵ C	258	126	80	8	2	3.8	1

2. Methods

m ⁵ s ² U	275	143	80	5	2	7.2	1
m ⁵ U	259	127	80	7	2	4.9	1
m ⁵ Um	273	127	100	10	2	7.4	2
m ⁶ ₂ A	296	184	100	15	2	12.6	1
m ⁶ A	282	150	100	16	2	9.5	0.5
m ⁷ G	298	166	90	10	2	3.7	1
mcm ⁵ s ² U	333	201	100	10	2	8.8	1
mcm ⁵ U	317.2	185.1	90	8	2	6.3	2
mcm ⁵ Um	331.2	153.1	90	8	2	8.6	1
ncm ⁵ U	302	153	100	10	2	2.5	2
ncm ⁵ Um	316	170	90	7	2	5	1
s ² C	260	128	100	10	2	3.3	1
s ² U	261	129	80	5	2	5.5	1
t ⁶ A	413	281	100	8	2	8.5	1
Um	259	113	80	7	2	5.4	1
Ψ	245	191	80	10	2	1.6	1
yW	509	377	80	5	2	13	1

Table 2.7. Dynamic MRM parameters for rRNA ribonucleosides identification based on optimized results.

Compound Name	Precursor Ion (m/z)	Product Ion (m/z)	Fragment (V)	Collision Energy (V)	Cell Accelerator Voltage	Ret. Time (min)	Delta Ret. Time (min)
¹⁵ N-dA	257	141	90	10	2	7.3	1
ac ⁴ C	286	154	80	6	2	6.5	1
acp ³ Ψ	346	292	80	5	2	10.3	1
Am	282	136	100	15	2	8.4	1
Cm	258	112	80	8	2	4.2	1
cm ⁵ U	303.2	171.1	90	7	2	1.8	1
cmnm ⁵ s ² U	348	216	90	10	2	4.1	1
cmnm ⁵ U	331	200	80	5	2	1.6	1
Gm	298	152	80	7	2	6.2	1
hm ⁵ C	274	142	80	5	2	1.6	1
I	269	137	80	10	2	4.5	1
Im	283	137	80	5	2	5.5	2
m ¹ A	282	150	100	16	2	1.7	1
m ¹ acp ³ Ψ	360.1	306.1	80	5	2	11.4	1
m ¹ G	298	166	90	10	2	6.1	0.5

m ¹ Ψ	259	127	80	5	2	4.8	1
m ² ₂ G	312	180	100	8	2	7.8	1
m ² G	298	166	90	10	2	6.5	0.5
m ³ C	258	126	80	8	2	3.8	1
m ³ U	259	127	100	16	2	5.7	1
m ⁴ C	258	126	80	5	2	2.2	1
m ⁵ C	258	126	80	8	2	4.2	2
m ⁶ ₂ A	296	184	100	15	2	12.6	1
m ⁶ A	282	150	100	16	2	9.4	1
m ⁷ G	298	166	90	10	2	3.2	1
Um	259	113	80	7	2	5.4	1
Ψ	245	191	80	10	2	1.6	1
Ψm	259	113	80	5	2	4	3

2.6.3.3 Quantification of ribonucleosides by LC-MS/MS

Digested ribonucleosides (4 ug) were analyzed by the UPLC-MS/MS system and the modified nucleosides were quantified by pre-determined molecular transitions obtained with ribonucleoside standards using a dynamic multiple reaction monitoring (MRM) program (Table 2.6 and Table 2.7). After background subtraction, the signal intensity of each ribonucleoside was normalized against the signal intensity of [¹⁵N]₅-dA, in order to adjust for day-to-day fluctuations in MS sensitivity. Additionally, the signal intensity for each ribonucleoside was normalized by dividing the raw peak area for the ribonucleoside by the sum of the UV absorbance peak areas for the 4 canonical ribonucleosides, in order to adjust for variations in total tRNA in each sample. Abundance of the modified nucleosides was compared with WT. Data represent 3 independent clones with 3 technical replicates and statistical significance was determined using a Student's *t*-test. Data were transformed to log₂ ratios of modification levels in KO strains relative to WT. Hierarchical clustering analysis were performed using Cluster 3.0: average linkage algorithm based on the distance between each data set measured using Euclidean distance, with the heat map representations produced using Java TreeView.

2. Methods

2.7 tRNA QUANTIFICATION USING FOUR-LEAF CLOVER qRT-PCR

Hypomodified tRNAs in selected KO strains were quantified using a PCR-based method described in Honda *et al.*, 2015, as described below.

2.7.1 Total RNA isolation

Yeast cells were lysed in hot acidic phenol and all species of RNA were extracted by separating the lysate into two phases with chloroform, followed by the collection of the aqueous phase (Collart and Oliviero, 2001). For that, 25 OD units of yeast cultures were collected during exponential phase (OD_{600} of 0.5) and were harvested (4 000 rpm; 4 min). Cell pellets were washed and frozen overnight at -80 °C. Cells were resuspended in 500 μ L of acid phenol chloroform 5:1 pH 4.7 (warmed up at 65 °C) and an equal volume of TES buffer (10 mM Tris pH 7.5, 10 mM EDTA, 0.5% SDS). Cells suspension was vigorously shaken for 20 seconds and incubated at 65 °C for 1 h with agitation every 10 min. The aqueous phase containing RNAs was separated from the phenolic phase by centrifugation at 14 000 rpm for 20 min at 4 °C, and re-extracted twice with the same volume of acid phenol chloroform 5:1 pH 4.7 at 14 000 rpm for 10 min at 4 °C. Aqueous phases were re-extracted with the same volume of Chloroform Isoamyl Alcohol 24:1 by centrifugation at 14 000 rpm for 10 min at 4 °C. RNA was precipitated overnight at -30 °C with 3 volumes of 100% ethanol (cold) and 0.1 volumes of 3 M sodium acetate pH 5.2. RNAs were harvested by centrifugation at 14 000 rpm for 5 min, washed in 80% ethanol (cold), air-dried and resuspended in 100 μ L of mQ water. The integrity and purity of RNA were analyzed using a Bioanalyzer small RNA chip, after DNase treatment using DNase I (Amplification grade; Invitrogen™).

2.7.2 Deacylation treatment

Total RNA (1 μ g) was incubated in 20 mM Tris-HCl pH 9.0 at 37 °C for 40 min in order to remove amino acids from the mature tRNAs. Deacylated tRNAs were cleaned with RNA Clean & Concentrator™-5 (Zymo Research), according to the manufacturer instructions.

2.7.3 Annealing and ligation of SL-adaptors to mature tRNAs

Each specific adaptor (20 pmol; Table 2.8) was incubated with 100 ng of the deacylated total RNA in 9 mL mixture at 90 °C for 3 min. Annealing buffer (1X; 50 mM Tris-HCl pH 8.0, 5 mM EDTA and 100 mM MgCl₂) was added to the mixture and incubated at 37 °C for 20 min. Ligation of the annealed adaptor to mature tRNAs were performed by adding 1X reaction buffer containing 1 unit of T4 RNA ligase 2 (New England Biolabs) and the mixture was incubated at 37 °C for 1 h, and then incubated overnight at 4°C.

Table 2.8. Sequences of adaptors for FL-PCR.

Adaptor	Sequence (5'-3')
SL-Adaptor-C	/5Phos/TCGTAGGGTCCGAGGTATTCACGATGrGrC
SL-Adaptor-U	/5Phos/TCGTAGGGTCCGAGGTATTCACGATGrGrU
SL-Adaptor-A	/5Phos/TCGTAGGGTCCGAGGTATTCACGATGrGrA
SL-Adaptor-G	/5Phos/TCGTAGGGTCCGAGGTATTCACGATGrGrG

2.7.4 TaqMan qRT-PCR for mature tRNAs

Ligated RNA (10-27.5 ng) was incubated with 1 pmol of specific RT primer (Table 2.9) and 5 nmol of dNTPs in a 7 µL mixture at 90 °C for 2 min and then placed on ice for at least 1 min. Reverse transcription was performed by adding SuperScript™ III Reverse Transcriptase and its reaction buffer (Life Technologies), according to the manufacturer instructions, to create a 10 µL mixture that was incubated for 30 min at 50 °C. The resultant cDNA solution was diluted 1:5, and 3 µL of this solution was added to the Real-Time PCR mixture containing 1X Premix Ex Taq reaction solution (Clontech Lab), 400 nM TaqMan probe (5'-/56-FAM/CCATCGTAG/ZEN/GGTCCGAGGTATTC/3IABkFQ/-3'; Integrated DNA Technologies), 2 pmol of each specific forward and reverse primers (Table 2.9) and 1X ROX Reference Dye II in a final volume of 20 µL. Real-time PCR reactions were carried out in an Applied Biosystems 7 500 Real-Time PCR System using a standard program of 95 °C for 20 sec followed by 40 cycles (95 °C for 5 sec, T_m for 34 sec). All reactions were run in triplicate and the threshold cycles (C_t) were determined. 5S rRNA expression was quantified to be used as an internal control

2. Methods

using SsoFast EvaGreen Supermix (BioRad) and the primers represented in Table 2.9, according manufacturer instructions. The amplified cDNA was developed by 10% native PAGE.

For statistical evaluations of the determined CP and relative expression variations, data were analyzed for significant differences by REST-MCS© (Pfaffl, Horgan and Dempfle, 2002).

Table 2.9. Sequences of primers for FL-PCR.

Primer Name	Sequence (5'-3')	Comments
5S rRNA – Forward primer	GGTTGCGGCCATATCTACCA	20 nt; Tm: 59.89 °C; GC%: 55.00
5S rRNA – Reverse/RT primer	AGCACCTGAGTTTCGCGTAT	20 nt; Tm: 59.75 °C; GC%: 50.00
tRNA ^{Ala} _{TGC} – Reverse/RT primer	CGCTACCAACTGCGCCATGT	20 nt; Tm: 63.73 °C; GC%: 60.00
tRNA ^{Ala} _{TGC} – Forward primer	GAGGTCATCGGTTTCGATTCC	20 nt; Tm: 58.15 °C; GC%: 55.00
tRNA ^{Arg} _{TCT} – Reverse/RT primer	TCAGACGCGTTGCCATTACG	20 nt; Tm: 61.35 °C; GC%: 55.00
tRNA ^{Arg} _{TCT} – Forward primer	AGATTATGGGTTTCGACCCCC	20 nt; Tm: 58.86 °C; GC%: 55.00
tRNA ^{Gln} _{TTG} – Reverse/RT primer	CCGAAAGTGATAACCACTACAC	22 nt; Tm: 56.82 °C; GC%: 45.00
tRNA ^{Gln} _{TTG} – Forward primer	ACAACCCCGGTTTCGAATCCG	20 nt; Tm: 62.79 °C; GC%: 60.00
tRNA ^{Glu} _{TTC} – Reverse/RT primer	GATGTGATAGCCGTTACACTAT ATCG	26 nt; Tm: 59.31 °C; GC%: 42.00
tRNA ^{Glu} _{TTC} – Forward primer	GGGGTTCGACTCCCCGTATC	20 nt; Tm: 61.74 °C; GC%: 65.00
tRNA ^{Gly} _{TCC} – Reverse/RT primer	GATAACCACTACACTAACCGCC	22 nt; Tm: 58.55 °C; GC%: 50.00
tRNA ^{Gly} _{TCC} – Forward primer	ACACGGGTTTCGATTCTCGTA	20 nt; Tm: 58.83 °C; GC%: 50.00
tRNA ^{Leu} _{TAA} – Reverse/RT primer	CCTTAGACCACTCGGCCAAC	20 nt; Tm: 60.39 °C; GC%: 60.00
tRNA ^{Leu} _{TAA} – Forward primer	GCGAGTTCGAACCTCGCATC	20 nt; Tm: 61.74 °C; GC%: 60.00
tRNA ^{Lys} _{TTT} – Reverse/RT primer	CCGAAACGCTCTACCAACTGA	20 nt; Tm: 59.76 °C; GC%: 55.00
tRNA ^{Lys} _{TTT} – Forward primer	AAATGTCAGGGGTTTCGAGCC	20 nt; Tm: 60.32 °C; GC%: 55.00
mit tRNA ^{Lys} _{TTT} – Reverse/RT primer	CTGTTTTAAACCAATTAACAATA TTCTC	28 nt; Tm: 54.87 °C; GC%: 25.00
mit tRNA ^{Lys} _{TTT} – Forward primer	GCGGTTCAACTCCAGCTATT	20 nt; Tm: 58.26 °C; GC%: 50.00
tRNA ^{Pro} _{TGG} – Reverse/RT primer	GCGAGAATCATACCACTAGACC	22 nt; Tm: 58.10 °C; GC%: 50.00
tRNA ^{Pro} _{TGG} – Forward primer	AGAGGCCCTGGGTTCAATTC	20 nt; Tm: 59.67 °C; GC%: 55.00
tRNA ^{Ser} _{TGA} – Reverse/RT primer	CCTTAACCACTCGGCCATAG	20 nt; Tm: 57.76 °C; GC%: 55.00
tRNA ^{Ser} _{TGA} – Forward primer	GCTGGTTCAAATCCTGCTGG	20 nt; Tm: 58.09 °C; GC%: 55.00
tRNA ^{Thr} _{TGT} – Reverse/RT primer	GCAACGCTCTACCACTAAGC	20 nt; Tm: 59.00 °C; GC%: 55.00
tRNA ^{Thr} _{TGT} – Forward primer	GGTCGCTAGTTCAATTCTGG	20 nt; Tm: 56.24 °C; GC%: 50.00
tRNA ^{Val} _{TAC} – Reverse/RT primer	CGTCTTGAACCACTGGACCATT	22 nt; Tm: 60.81 °C; GC%: 50.00
tRNA ^{Val} _{TAC} – Forward primer	CCCGAGTTCGAACCTCGGTT	20 nt; Tm: 62.15 °C; GC%: 60.00

2.8 PROTEOME PROFILING AND QUANTIFICATION OF AMINO ACID MISINCORPORATIONS

2.8.1 Extraction of insoluble aggregates

Isolation of insoluble proteins from WT and selected KO strains was performed as described by Koplín *et al.*, 2010, with minor alterations. 50 OD₆₀₀ units of logarithmically growing cells cultivated in MM-His were harvested at 4 000 rpm and 4 °C for 10 minutes and cell pellets were frozen. For preparation of cell lysates, the cell pellets were resuspended in 500 µL of lysis buffer (20 mM Na-phosphate, pH 6.8, 10 mM DTT, 1 mM EDTA, 0.1% (v/v) Tween, 1 mM PMSF, protease inhibitor cocktail (Roche), 3 mg/mL lyticase and 1.25 U/mL benzonase) and incubated at 30 °C for 30 min. Glass beads were used to disrupt the yeast cells using a Precellys™ 24 disrupter; 2 cycles of 25 sec at 6 500 rpm; samples were kept on ice between each cycle. Cell lysates were then centrifuged for 20 min at 200 x g at 4°C, supernatants were adjusted to identical protein concentrations (4.8 mg/mL for protein gels and 4 mg/ml for LC-MS/MS analysis) and membrane and aggregated proteins were isolated at 16 000 x g for 20 min at 4 °C. Supernatants were aspirated and membrane proteins were removed by washing twice the aggregated proteins with 2% NP-40 (in 20 mM Na-phosphate, pH 6.8, 1 mM PMSF and protease inhibitor cocktail), sonicating (6 x 5 sec at cycle 0.1 and amplitude 20%) and centrifuging the extracts at 16 000 x g for 20 min at 4 °C. The final insoluble protein extracts were washed in NP-40–deficient buffer (sonication, 4 x 5 sec at cycle 0.1 and amplitude 20%), boiled in 1X laemli sample buffer, separated by SDS-PAGE (14%) and analyzed by Coomassie staining. Experiments were performed in duplicate for the three biological replicates.

Protein aggregates for mass spectrometry analysis were precipitated with TCA (100% w/v; 1 vol of TCA to 4 vol of protein sample) at 4 °C for 30 min. Samples were then washed with 200 µL ice cold acetone (9:1) and pellets were dried at RT. Protein pellets were resuspended in 50 µL of 8 M urea.

2. Methods

2.8.2 Protein sample preparation (Reduction, Alkylation and Tryptic Digestion)

Proteins were reduced with 10 mM dithiothreitol for 1 h at 56 °C and then alkylated with 55 mM iodoacetamide for 1 h at room temperature in the dark. Proteins were then digested with modified trypsin (Thermo Scientific) at an enzyme/substrate ratio of 1:50 in 100 mM ammonium acetate pH 8 at 30 °C overnight. Synthetic peptides mimicking amino acid misincorporation (designed by us) were added to each sample (1 µg of digested protein) (Table 2.10).

Peptides were desalted using MicroSpin C18 columns (The Nest Group, Inc) prior to LC-MS/MS analysis.

Table 2.10. Synthetic peptides (Pepscan) added to insoluble fraction samples for LC-MS/MS analysis.

Peptide Name	Sequence	MW (Da)	Quantity added (fmol)
WT (Q02892)	H-NVYDFLDPEIAAK-OH	1494.7	100
Mut1	H-NVY E FLDPEIAAK-OH	1508.7	1
Mut2	H-NVYD L LDPEIAAK-OH	1460.7	0.5
Mut3	H-NVYDF S DPEIAAK-OH	1468.6	0.1
Mut4	H-NVYDFLDPEI S AK-OH	1510.7	0.05

2.8.3 Chromatographic and mass spectrometric analysis

The peptide mixes were analyzed using an Orbitrap Fusion Lumos mass spectrometer (Thermo Scientific, San Jose, CA, USA) coupled to an EasyLC (Thermo Scientific (Proxeon), Odense, Denmark). Peptides were loaded directly onto the analytical column and were separated by reversed-phase chromatography using a 50 cm column with an inner diameter of 75 µm, packed with 2 µm C18 particles (Thermo Scientific, San Jose, CA, USA). Chromatographic gradients started at 95% buffer A (0.1% formic acid in water) and 5% buffer B (0.1% formic acid in acetonitrile) with a flow rate of 300 nL/min and gradually increased to 22% buffer B in 79 min and then to 35% buffer B in 11 min. After each analysis, the column was washed for 10 min with 5% buffer A and 95% buffer B.

The mass spectrometer was operated in DDA mode and full MS scans with 1 micro scans at resolution of 120 000 were used over a mass range of m/z 350-1 500 with detection in the Orbitrap. Auto gain control (AGC) was set to 1E5 and dynamic exclusion to 50 seconds. In each cycle of DDA analysis, following each survey scan Top Speed ions with charged 2 to 5 above a threshold ion count of 1E4 were selected for fragmentation at normalized collision energy of 28%. Fragment ion spectra produced *via* high-energy collision dissociation (HCD) were acquired in the Orbitrap, AGC was set to 3E4, isolation window of 1.6 m/z and maximum injection time of 80 ms was used. All data were acquired with Xcalibur software v3.0.63.

2.8.4 Data analysis

2.8.4.1 Proteome Profiling

MS/MS raw data were analyzed using PEAKS Studio (v.8.0, Bioinformatics Solutions Inc.) for peptide identification and label-free quantification. Samples were searched against a *S. cerevisiae* database available at the *Saccharomyces* Genome Database (version of July 2017), a list of common contaminants and all the corresponding decoy entries. Trypsin was chosen as the protein digestion enzyme and a maximum of three missed cleavages were allowed. Carbamidomethylation was set as a fixed modification, whereas oxidation (M) was set as a variable modification. Searches were performed using mass tolerances of 7 ppm for parent ions and 20 mmu for fragment ions. Resulting data files were filtered for FDR of 1% (or less).

2.8.4.2 Biochemical characterization of proteins

Data of the molecular weight, isoelectric point, hydrophobicity, aromaticity and protein degradation signal of the yeast proteome were collected from Lu *et al.*, 2007 and Ibstedt *et al.*, 2014. Translation rate per protein and protein abundance data were collected during non-stress conditions by Arava *et al.*, 2003 and Ghaemmaghami *et al.*, 2003, respectively. Codon adaptation index of yeast

2. Methods

proteome were calculated by our codon usage analysis software package Anaconda (Moura *et al.*, 2005) and the frequency of optimal codons were collected by Lu *et al.*, 2007. Statistical analysis was performed on the set of up-regulated aggregated proteins in each mutant strain using yeast proteome as background. Mann-Whitney U-tests were performed.

2.8.4.3 Codon usage bias and GO term analysis

The full sequences of the genes encoding the insoluble proteins identified were downloaded from the Yeast genome database (<http://www.yeastgenome.org>), with the "Gene ID" and "Associated Gene Name", in FASTA format, for uploading by our codon usage analysis software package Anaconda (Moura *et al.*, 2005). Codon usage, normalized for the amino acid usage of each protein in the whole genome (as in Begley *et al.*, 2007), and RSCU values for all genes, also normalized according to the distance between individual genes and the whole genome were determined. Normalized as described, these new RSCU values eliminate the bias effect of the amino acid frequency between proteins and also the effect of the number of synonymous codons for each amino acid. Since individual gene-specific codon frequencies can deviate significantly from genome averages, the gene-specific codon frequency for each *S. cerevisiae* gene, weighted with BY4743 gene expression from a previous study (GSE42554), was analyzed to obtain a gene-specific codon Z score also weighted by tRNA availability (Figure 2.3). The data were clustered in both dimensions using Cluster 3.0 (default settings, x/y clustering through hierarchical single linkage analysis using uncentered correlation as the similarity metric) and the resulting maps were visualized using Java TreeView to detect genes that may form specific codon clusters.

Differences in amino acid and codon composition were compared using heteroscedastic Student's *t*-test with CI 95% relative to the reference genome.

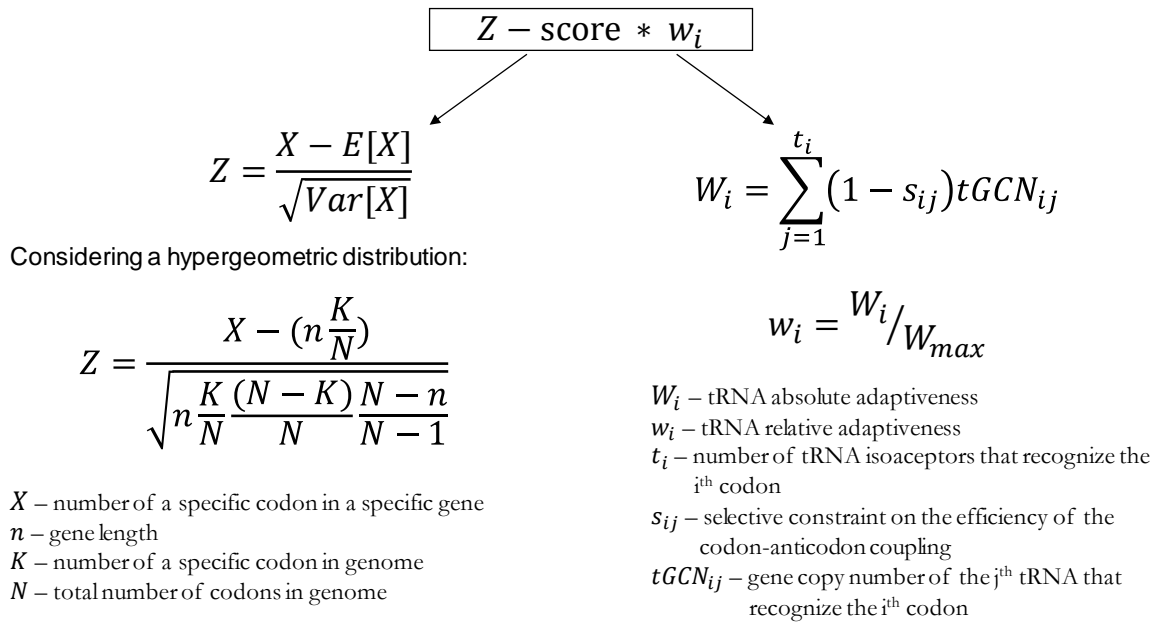


Figure 2.3. Method to calculate gene-specific codon usage patterns weighted by tRNA availability.

A GO term analysis was carried out for the gene groups belonging to each codon cluster, using GeneCodis (<http://genecodis.cnb.csic.es/>) and “GO-Biological process”, “GO-Molecular function”, “Go-Cellular component” and “KEGG Pathways”, as annotations (Carmona-Saez *et al.*, 2007; Nogales-Cadenas *et al.*, 2009; Tabas-Madrid, Nogales-Cadenas and Pascual-Montano, 2012). GO term enrichment was compiled in tables, for each annotation, and p -values were calculated with a chi-square test using 7 109 genomic genes as background. p -values were filtered with FDR < 5%.

2.8.4.4 Quantification of amino acid misincorporation

Detection of amino acid misincorporations were performed using the SPIDER algorithm present in PEAKS Studio (v.8.0, Bioinformatics Solutions Inc.). Samples were searched against a *S. cerevisiae* database from *Saccharomyces* Genome Database (version of July 2017) plus a list of common contaminants and all the corresponding decoy entries. Trypsin was chosen as enzyme and a maximum of three missed cleavages were allowed. Carbamidomethylation was set as a fixed modification, whereas oxidation (M), Asn→Lys substitution, Asp→Glu substitution,

2. Methods

His→Gln substitution, Phe→Leu substitution, and Ser→Arg substitution were set as variable modifications. Searches were performed using mass tolerances of 7 ppm for parent ions and 20 mmu for fragment ions. Additional search parameters were analyzed to identify common and unspecified post-transcriptional modifications (PTM). Resulting data files were filtered for FDR of 1% (or less). Data sets of the technical replicates were merged in a single dataset. Amino acid misincorporations were validated by bioinformatically introducing misincorporations into a new database and re-searching as in 2.8.4.1 Proteome Profiling. Only new proteins with mutant peptides identified in the second search and filtered with 1% FDR were considered as valid amino acid misincorporations. This was done to reduce the number of false positives.

Quantification of misincorporation fractional occupancy were calculated using an R script that calculated the total peak areas of all modified unique peptides that have a specific misincorporation and the total peak areas of both modified and unmodified unique peptides covering the same fragment. Fractional occupancy was calculated as the total peak area of a misincorporation site out of the total peak area of that site.

2.8.4.5 Identification of human orthologues

Identification of orthologues between yeast and human disease aggregates in Alzheimer's disease (Liao *et al.*, 2004; Wang *et al.*, 2005), Parkinson's disease (Xia *et al.*, 2009) and/or familial amyotrophic lateral sclerosis (Basso *et al.*, 2009) were identified with the OMA browser (<http://omabrowser.org/>). The level of orthology was determined by counting the number of orthologues between up-regulated aggregated proteins in each mutant strain and disease-associated aggregates and the reference genome, respectively. Significance of the analysis was achieved using Fisher's exact test.

3. GENETIC SCREEN TO IDENTIFY RNAMODS REQUIRED TO MAINTAIN PROTEOSTASIS

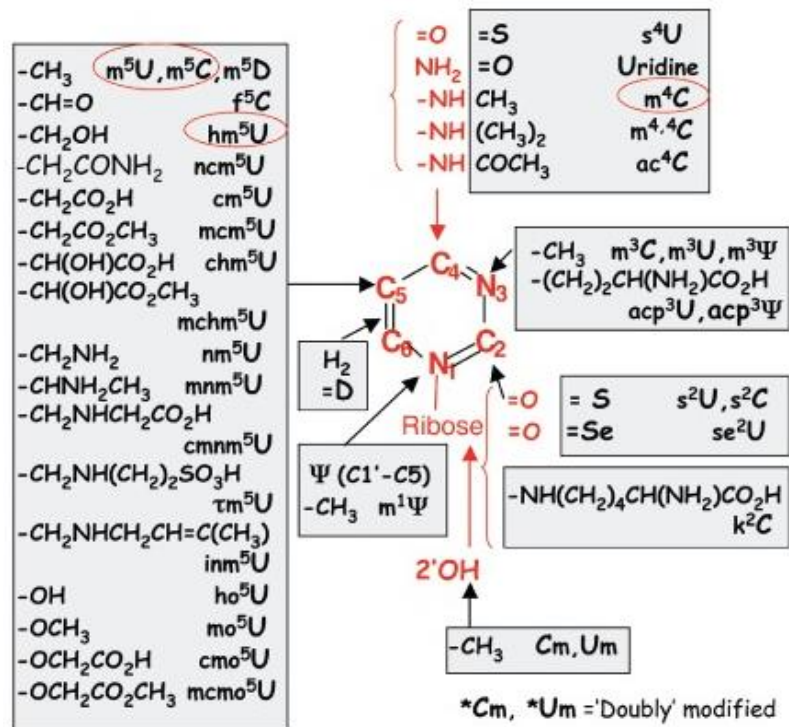
3. Genetic screen to identify RNAmods and their regulators

3.1 INTRODUCTION

During the maturation process of pre-RNAs several enzymes chemically modify ribonucleotide residues. Chemical alterations may occur at the 2'-hydroxyl group of the ribose, in the base, or both (Figure 3.1) (Grosjean, 2009b), resulting in alteration of physical and/or chemical properties of the nucleotides that generally modulate the flexibility and function of RNAs (Ishitani, Yokoyama and Nureki, 2008). The distribution, abundance and location of various types of modification diverge significantly between different RNA molecules, organisms and organelles. In fact, these post-transcriptional modifications of the four normal ribonucleosides are present in tRNA, rRNA, mRNA, snRNA, snoRNA, and tmRNA (Ishitani, Yokoyama and Nureki, 2008). Growth conditions and the physiological environment of the cell also influence RNA modification patterns (Grosjean, 2009b). Considering both tRNA and rRNA, there are more than 100 known ribonucleoside modifications across all organisms which expand the repertoire of the canonical adenosine, guanosine, cytidine and uridine nucleotides (Cantara *et al.*, 2011; Machnicka *et al.*, 2013). Beyond the well-known functions of modifications in tRNA folding, tRNA aminoacylation and translational fidelity (Motorin and Grosjean, 2005; Agris, Vendeix and Graham, 2007; Phizicky and Hopper, 2010; El Yacoubi, Bailly and de Crécy-Lagard, 2012), tRNA and rRNA modifications are critical in the responses to cellular stress (Begley *et al.*, 2007; Thompson and Parker, 2009) and cell growth (Emilsson, Näslund and Kurland, 1992; Heiss, Reichle and Kellner, 2017).

3. Genetic screen to identify RNAmods and their regulators

A



B

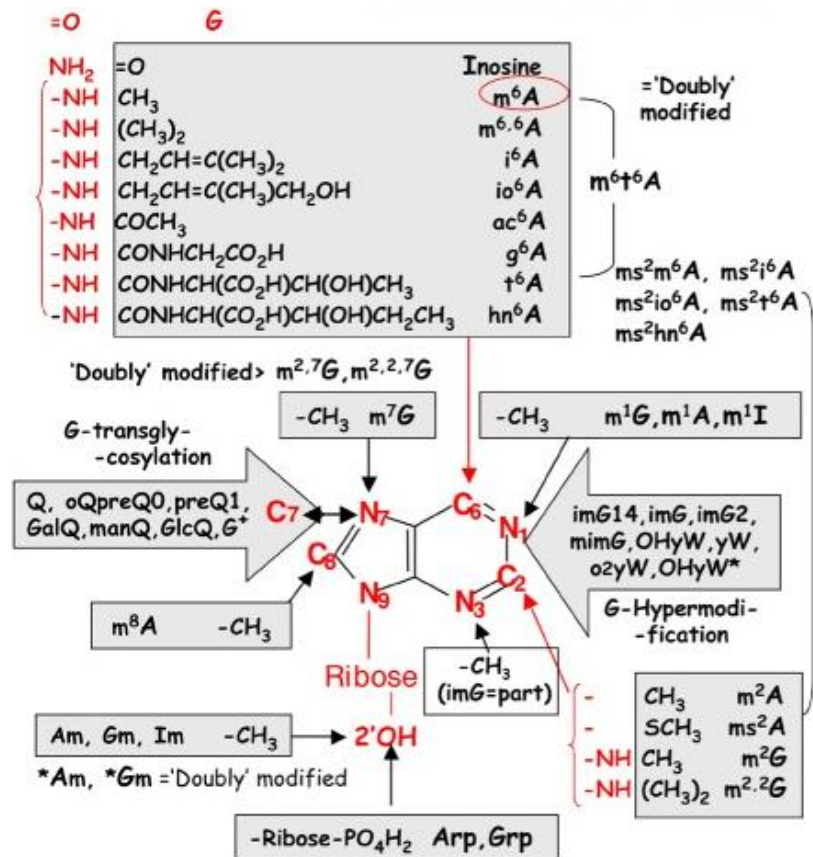


Figure 3.1. Modified bases and ribose moieties of RNAs. In the boxes are the various types of chemical groups that can be enzymatically attached to selected atoms of a

3. Genetic screen to identify RNAmods and their regulators

pyrimidine (**A**) and purine (**B**) ring (in red) during maturation of RNA precursor in Bacteria, Eukarya or Archaea. The base modifications that are also found in DNA are circled. Adapted from Grosjean, 2009.

More than 100 proteins are involved in RNA modification; both functional enzymes and protein co-factors necessary for multi-protein enzymatic processes (Czerwonec *et al.*, 2009; Machnicka *et al.*, 2013). Much progress has been made since the identification of the first RNA-modifying enzyme, a m⁵U tRNA methyltransferase (now designated Trm2 in Eukarya and TrmA in Bacteria), in 1962-63 (Fleissner and Borek, 1962; Starr, 1963; Svensson *et al.*, 1963). Most of these enzymes alter the chemical nature of the nucleosides by deamination, reduction and thiolation, or by addition of a chemical group (for instance, a methyl or an isopentenyl group) on one atom of the base or the ribose (Grosjean, 2005). Moreover, a large number of co-factors is required for these enzymatic reactions to occur, particularly metabolites from the central metabolism, such as S-adenosylmethionine (AdoMet or SAM), NADH, FAD, methylene tetrahydrofolate, ATP, GTP, isopentenyl-pyrophosphate, and/or numerous amino acids. The location of most RNA-modifying enzymes within distinct cellular compartments as well as the possible association of these enzymes with cellular and subcellular structures or commitment in multi-enzymatic complexes are crucial for the RNA maturation process. These enzymes can be site-specific (acting on the same position), multisite-specific (acting on various positions within the same RNA molecule) or dual-specific (acting on different types of RNA). Interestingly, RNA-modifying enzymes can have additional roles beyond RNA modification, as previously explained (Grosjean, 2005).

At least, five types of RNA-modifying enzymes are known, namely: methyltransferases, thiolases, deaminases, pseudouridine synthases, and dihydrouridine synthases.

3.1.1 Methyltransferases

These enzymes are responsible for methylation-based modifications of RNA. A series of methyltransferases utilize SAM as a methyl donor to methylate RNA

3. Genetic screen to identify RNAmods and their regulators

molecules (Grosjean, 2009a). In *S. cerevisiae*, there are 16 tRNA methyltransferase (Trm) genes, whose proteins are involved in the formation of more than 20 different methyl-based modifications in tRNAs, varying in nucleotide position and modification type (Cherry *et al.*, 1998). Those tRNA methyltransferases are involved in the synthesis of 5-methoxycarbonylmethyluridine (mcm⁵U), 5-methoxycarbonylmethyl-2-thiouridine (mcm⁵s²U), N², N²-dimethylguanosine (m²₂G), 5-methyluridine (m⁵U), 5-methylcytidine (m⁵C), 3-methylcytidine (m³C), 1-methylguanosine (m¹G), 1-methyladenosine (m¹A), 7-methylguanosine (m⁷G), 2-methylguanosine (m²G), 1-methylinosine (m¹I), wybutosine (yW) and 2'-O-methylated nucleosides.

In rRNA, most of the methylation at the 2'-O-ribose position is carried out by a methyltransferase of a ribonucleoprotein (RNP) complex consisting of a box C/D guide RNA and associated core proteins. Moreover, box C/D snoRNAs function in pre-rRNA processing (Hughes and Ares, 1991; Morrissey and Tollervey, 1993; Wu *et al.*, 1998), in pre-rRNA maturation (important for specific endonucleolytic cleavage, functioning as organizers for a *trans*-acting RNase) (Beltramel and Tollervey, 1995) and in pre-rRNA folding (Liang and Fournier, 1995; Gagnon, Qu and Maxwell, 2009). Eukaryotic box C/D snoRNPs contain four conserved core proteins, namely the nucleolar proteins Nop56 and Nop58, the methyltransferase Nop1 (fibrillarin) and Snu13. Nop1 is the catalytic subunit of the box C/D RNPs (Watkins *et al.*, 2000; Gagnon, Qu and Maxwell, 2009).

3.1.1.1 The Elongator complex and its regulators

The Elongator complex belongs to the methyltransferases group and is required for the synthesis of the 5-carboxymethyluridine (cm⁵U) side chain in some wobble uridines (Huang, Johansson and Byström, 2005). It consists of a core complex constituted by Elp1-Elp3 and a sub-complex formed by Elp4-Elp6 (Figure 3.2) (Krogan and Greenblatt, 2001; Winkler *et al.*, 2001). Structurally, Elp4, Elp5 and Elp6 form a heterohexamer containing two copies of each polypeptide, which interacts with two copies of an Elp1-Elp2-Elp3 sub-complex to form the holoElongator complex (Glatt *et al.*, 2012; Dauden *et al.*, 2017). Elp1 functions as a

3. Genetic screen to identify RNAmods and their regulators

scaffold for Elp2 and Elp3 and acts as the docking platform for Elp4-Elp6 sub-complex (Dauden *et al.*, 2017). Thus, Elp1, particularly its C-terminus (CTD), is essential for the assembly of the overall Elongator complex. Moreover, Elp1 contains a conserved lysine/arginine-rich basic region in its C-terminal domain that can bind tRNA with high affinity (Santo, Bandau and Stark, 2014). Elp3 is likely to catalyze the tRNA modification because in addition to the potential acetyl-CoA binding domain (KAT domain) in its C-terminal, it has an iron-sulphur (FeS) cluster in the central region, which uses SAM to catalyze various radical reactions, as other members of the Radical SAM superfamily (Wittschieben *et al.*, 1999; Paraskevopoulou *et al.*, 2006). In this way, the FeS cluster and the SAM binding regions of the radical SAM domain of Elp3 are critical for the tRNA modification reaction (Chen, Huang, Anderson, *et al.*, 2011), whereas KAT domains are critical for interaction with Elp1 (Dauden *et al.*, 2017).

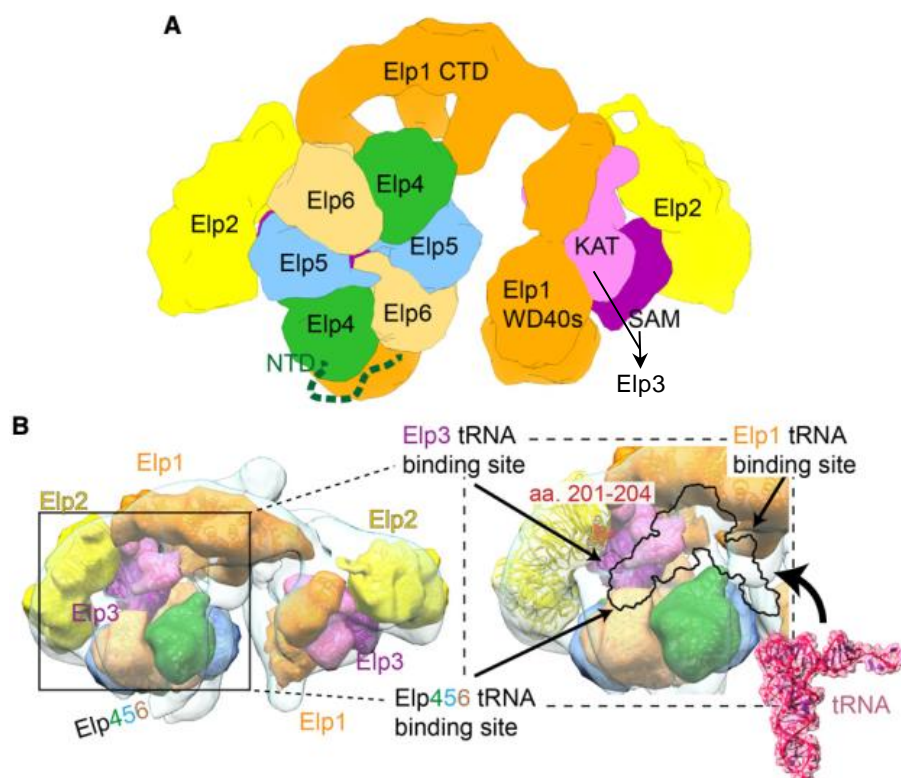


Figure 3.2. The holoElongator complex structure. A. The Elongator complex has a core complex constituted by Elp1-Elp3 and a sub-complex formed by Elp4-Elp6. Elp1 (orange), Elp2 (yellow), Elp3 (represented by its KAT and SAM domains – purple), Elp4 (green), Elp5 (blue) and Elp6 (sand) are shown in surface binding representation. **B.** View of the active site cavity

3. Genetic screen to identify RNAmods and their regulators

of the Elongator complex (*left*) and zoom-in to the tRNA binding sites and a region of Elp2 needed for tRNA modification activity (*right*). Adapted from Dauden *et al.*, 2017.

Kti11-Kti14, Sit4 or Sap185/Sap190 regulate the Elongator complex (Fichtner *et al.*, 2002, 2003, Jablonowski *et al.*, 2004, 2009; Petrakis *et al.*, 2005; Bär *et al.*, 2008; Mehlgarten *et al.*, 2009; Abdel-Fattah *et al.*, 2015; Kolaj-Robin *et al.*, 2015). Elp1 is a phosphoprotein, which is hypophosphorylated in the absence of kinases Kti12 and Hrr25 (or Kti14), and hyperphosphorylated in phosphatase Sit4 mutants (Jablonowski *et al.*, 2004; Mehlgarten *et al.*, 2009). The regulatory factor Kti12 was reported to interact with Elp2, Elp3, Elp5 (Fichtner *et al.*, 2002) and Hrr25 (Kti14) to modulate phosphorylation of Elp1 (Mehlgarten *et al.*, 2009). On the other hand, the complex Sit4-Sap185-Sap190 dephosphorylate Elp1 (Jablonowski *et al.*, 2004, 2009). Moreover, Elp1 phosphorylation is dynamic, turning wobble uridine modification by the Elongator complex up or down in response to growth conditions and protein synthesis demands as observed during the cell cycle (Mehlgarten *et al.*, 2009; Abdel-Fattah *et al.*, 2015). It is hypothesized that phosphorylation of Elp1 influences binding of tRNA during Elongator wobble uridine modification, as a regulatory mechanism.

Kti11 and Kti13 form a heterodimer that interacts with Elongator complex by binding to Elp2 and Elp5 (Bär *et al.*, 2008; Glatt *et al.*, 2015). For that, Kti11 acts as an electron donor to the FeS cluster of the Elp3 subunit and Kti13 modulates this activity of Kti11 by interacting with Elp3 (or more subunits) or by facilitating this binding by orienting Kti11 (Kolaj-Robin *et al.*, 2015).

3.1.1.2 Trm9 methyltransferase and its regulator

Trm9 (S-adenosylmethionine-dependent tRNA methyltransferase 9) is a wobble uridine methyltransferase that catalyzes the esterification of modified uridine nucleosides, resulting in the formation of 5-methoxycarbonylmethyluridine (mcm⁵U) and 5-methoxycarbonylmethyl-2-thiouridine (mcm⁵s²U) in specific tRNAs (Kalhor and Clarke, 2003). Trm9 uses SAM as the methyl donor to complete the synthesis of mcm⁵U₃₄, after the synthesis of the cm⁵U₃₄ by the Elongator complex (Figure 3.3) (Kalhor and Clarke, 2003). Like Elp3, Trm9 contains a SAM-dependent

3. Genetic screen to identify RNAmods and their regulators

methyltransferase domain that catalyzes the formation of mcm^5U_{34} modification. Trm9 forms a complex with Trm112 to catalyze the last step of the synthesis of mcm^5U_{34} (Mazauric *et al.*, 2010).

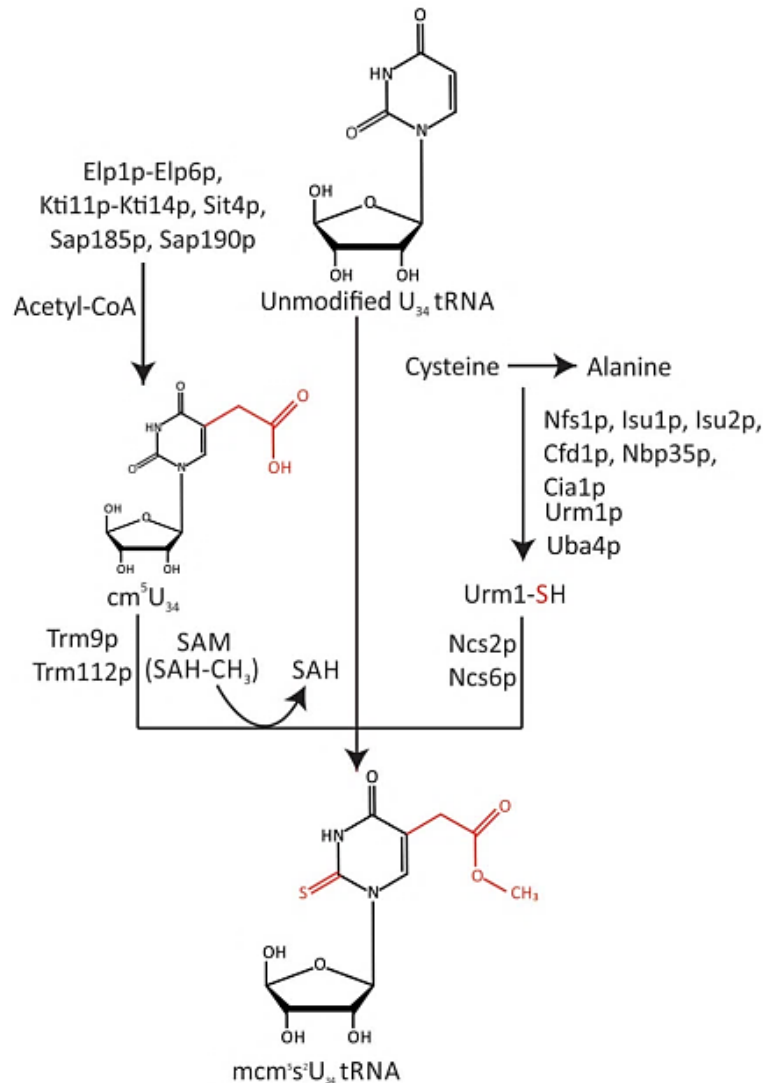


Figure 3.3. Pathway for $mcm^5s^2U_{34}$ modification. *Left:* proteins involved in the mcm^5 modification. *Right:* proteins involved in the s^2 modification. Modified side groups are in red. Adapted from Ranjan and Rodnina, 2016.

3.1.1.3 Methyltransferases in wybutosine synthesis

Wybutosine (yW) occurs at position 37 of $tRNA^{Phe}_{GAA}$ in Archaea and Eukarya, which enhances base-stacking interactions with adjacent adenosines (A_{36} and A_{38}) to reduce the flexibility of the anticodon (Stuart *et al.*, 2003). Synthesis of yW in

3. Genetic screen to identify RNAmods and their regulators

eukaryotes involves at least four sequential reactions requiring Tyw1-Tyw4 enzymes that use m^1G_{37} as precursor (Figure 3.4). These enzymes are methyltransferases that require SAM as a methyl donor (Tyw3 and Tyw4), as aminocarboxypopyl (acp) donor (Tyw2) and as a radical generator (Tyw1) (Noma *et al.*, 2006). Tyw1 (tRNA-yW synthesizing protein 1) catalyzes conversion of m^1G to imG-14 (4-demethylwyosine). Then, Tyw2 catalyzes the transfer of the acp group from SAM to the C⁷ position of the tricyclic core structure of imG-14 base, forming yW-86, which is methylated at the N³ position of the imidazo-purine ring by Tyw3 to form yW-72 (Noma *et al.*, 2006). Finally, the acp side chain at the C⁷ position of the tricyclic ring is methylated and methoxycarbonylated by Tyw4 to yield yW (Noma *et al.*, 2006; Suzuki *et al.*, 2009; Perche-Letuvée *et al.*, 2014).

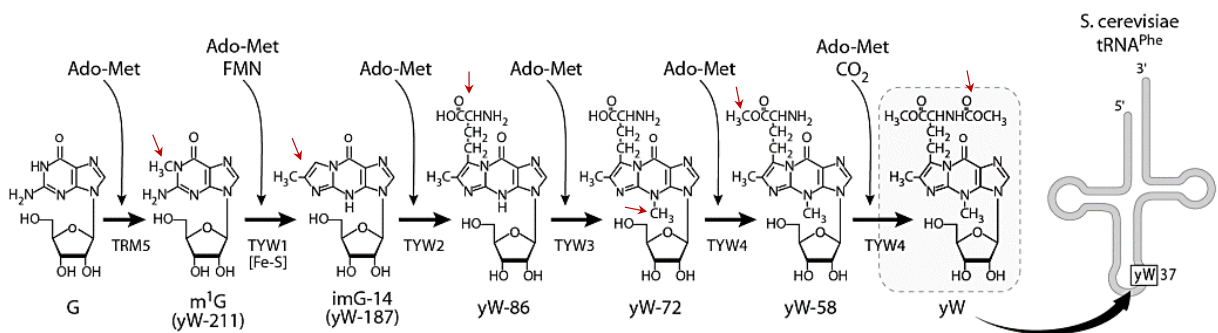


Figure 3.4. Pathway for yW modification. Detailed information in the text above. Adapted from Rodriguez *et al.*, 2012.

3.1.1.4 Other methyltransferases

Other tRNA methyltransferases (Trm) modify site-specific or multisite-specific nucleosides within the tRNA. Figure 3.5 shows the modifications catalyzed by these enzymes.

3. Genetic screen to identify RNAmods and their regulators

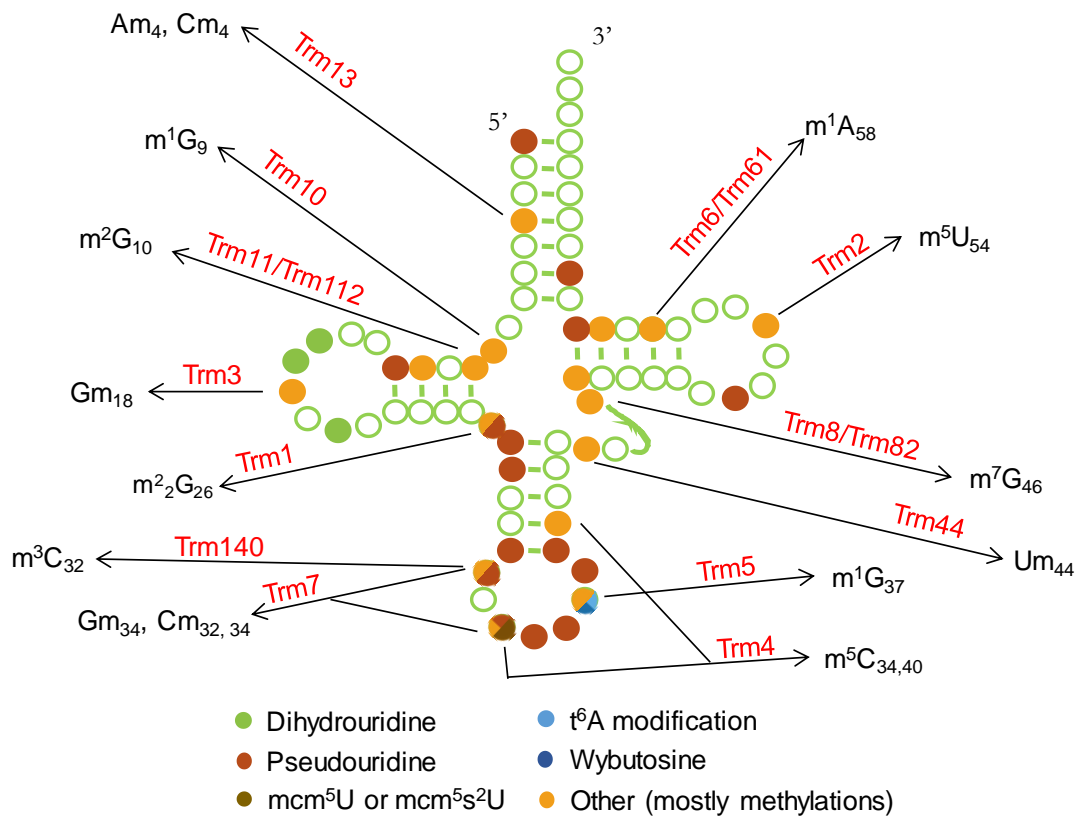


Figure 3.5. tRNA modifications synthesized by some methyltransferases.

3.1.2 Thiolases and mediators

The yeast tRNA wobble bases contain two thiouridines, 5-methoxycarbonylmethyl-2-thiouridine ($mcm^5s^2U_{34}$) in cytoplasmic tRNAs and 5-carboxymethyl-2-thiouridine ($cmnm^5s^2U_{34}$) in mitochondrial tRNAs. The biogenesis of 2-thiouridine derivatives in tRNAs requires a complicated sulfur-relay system that involves multiple sulfur mediators. The genes identified so far involved in the biosynthesis of thio-containing nucleosides in yeast are: Nfs1, Cfd1, Cia1, Nbp35, Tum1, Urm1, Uba4, Ncs2-Ncs6 (cytoplasmic tRNAs) (Figure 3.3); Nfs1, Isu1-Isu2, Mtu1, Mss1, Mto1 (mitochondrial tRNAs).

Nfs1 is a cysteine desulfurase that catalyzes the desulfuration of L-cysteine using the cofactor pyridoxal-5'-phosphate (PLP) and generating cysteine persulfide (Nfs1-S-SH) that is necessary for subsequent reactions (Noma, Sakaguchi and Suzuki, 2009). Tum1 is required to stimulate the cysteine desulfurase activity of Nfs1 and accepts persulfide sulfurs through rhodanese-like domains (RLDs); the sulfur is

3. Genetic screen to identify RNAmods and their regulators

then relayed to the RLD of Uba4 to direct the flow to 2-thiouridine formation (Noma, Sakaguchi and Suzuki, 2009). Uba4, ubiquitin-activating enzyme-like protein 4, is a sulfurtransferase that binds to its partner the ubiquitin-related modifier 1 (Urm1) via a thioester bond (Furukawa *et al.*, 2000) to provide sulfur to Urm1, forming a thiocarboxylate at the conserved C-terminal glycine of Urm1 (Nakai, Nakai and Yano, 2017). Ncs6 contains a nucleotide binding motif (PP-loop motif) and forms a heterodimer complex with Ncs2, which is thought to be important to activate the target positions of pyrimidine bases by forming acyl-adenylate intermediates (Noma, Shigi and Tsutomu, 2009; Nakai, Nakai and Yano, 2017). The specific details of the thio-modification reaction in tRNAs and the involvement of all these enzymes, namely the CIA machinery (cytosolic iron-sulfur cluster assembly) composed by Cia1 (WD40 protein), Nar1 (iron-only hydrogenase-like protein), Cdf1 and Nbp35 (NTPases), remain to be elucidated. But the mechanism proposed by Noma, Sakaguchi and Suzuki, 2009 is detailed in Figure 3.6.

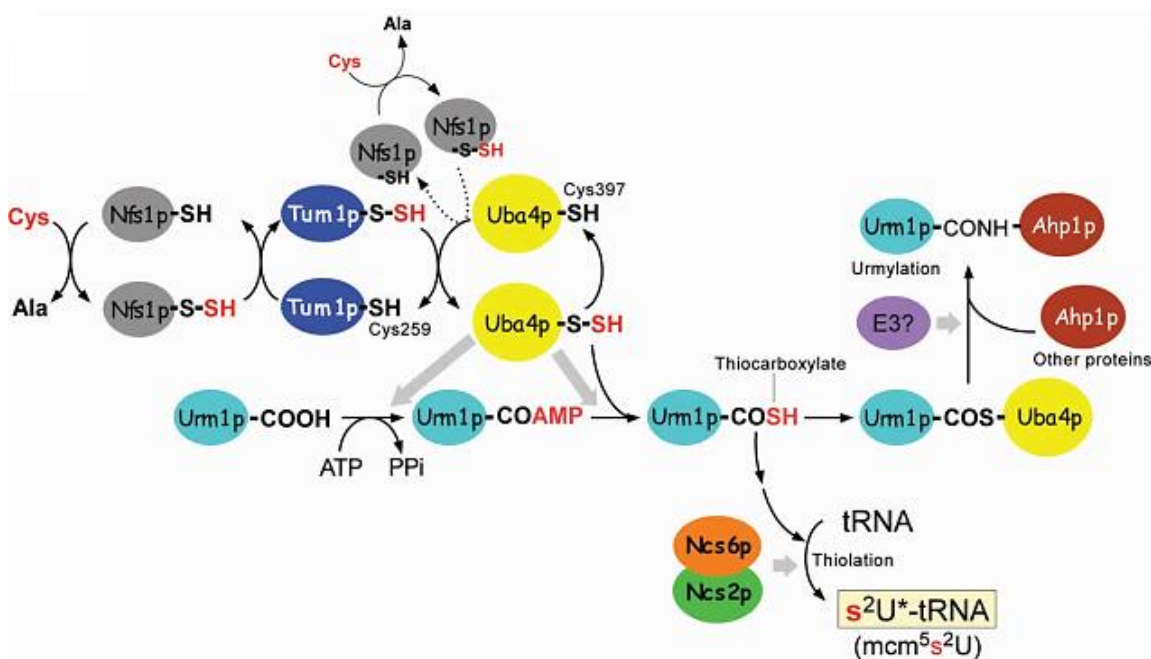


Figure 3.6. Cellular sulfur trafficking related to thiouridine formation of cytoplasmic tRNA anticodon in *S. cerevisiae*. Detailed information in the text above. Adapted from Noma, Sakaguchi and Suzuki, 2009.

3. Genetic screen to identify RNAmods and their regulators

The mitochondrial iron-sulfur cluster assembly system (ISC), contains two scaffold proteins Isu1 and Isu2. So, the sulfur atom produced by Nfs1 is transferred to Isu1 and Isu2, in which the Fe/S cluster is assembled (Lill and Uhlenhoff, 2006). These two proteins function as sulfur mediators to the thiolation of the U₃₄ of mt-tRNAs catalyzed by Mtu1 (Slm3 or Mto2), after methylation by Mss1 and Mto1 heterodimer complex (Colby, Wu and Tzagoloff, 1998; Grosjean, 2005) (Figure 3.7).

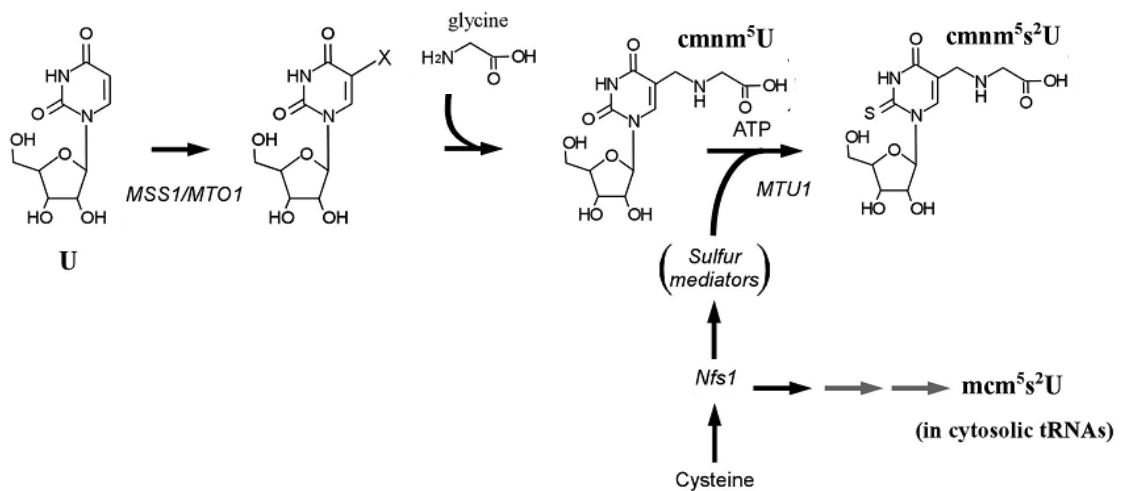


Figure 3.7. Thiouridine formation of mitochondrial tRNA anticodon in *S. cerevisiae*. Mss1 and Mto1 are involved in the first step of cmnm⁵s²U₃₄ synthesis on mt-tRNAs. In the second step, glycine is incorporated into mt-tRNAs by unknown transferases. In the third step, the sulfur from cysteine is transferred to sulfur mediators, likely Isu1 and Isu2, by Nfs1. Finally, Mtu1 (Slm3) uses the activated sulfur from the mediators to catalyze the thiolation of mt-tRNAs. Adapted from Grosjean, 2005.

3.1.3 Deaminases

Adenosine deaminases that act on RNA are known as ADARs (act on duplex coding RNA) and those acting on tRNA are named ADATs/Tads. Adenosine deaminases catalyze the hydrolytic deamination of adenosine (A) to inosine (I or 6-deaminated adenosine) in the context of folded substrates. A distant class of cytidine deaminases (CDAs) converts cytidine (C) to uridine (U) in the context of RNA or DNA (Wedekind and Beal, 2009).

3. Genetic screen to identify RNAmods and their regulators

Adenosine is deaminated to inosine in the anticodon loops of tRNAs (tRNA^{Ala}_{IGC}, tRNA^{Arg}_{ICG}, tRNA^{Ile}_{IAU}, tRNA^{Ser}_{IGA}, tRNA^{Thr}_{IGU} and tRNA^{Val}_{IAC}). Tad1 is responsible for deamination at position A₃₇ in the tRNA anticodon loop of tRNA^{Ala}_{IGC} (Gerber *et al.*, 1998). Inosine is also present at position 34 (I₃₄) in the anticodon loop of those tRNAs and its synthesis depends on the heterodimeric Tad2/Tad3 protein complex. The relevance of adenosine deamination in tRNA is emphasized by the fact that Tad2 and Tad3 are essential in *S. cerevisiae* (Auxilien *et al.*, 1996; Gerber and Keller, 1999).

3.1.4 RNA pseudouridine synthases

Pseudouridine synthases (RNA uridine transglycosylases) are enzymes responsible for the most abundant and conserved post-transcriptional modification in cellular RNAs. These enzymes catalyze an isomerization reaction of specific uridine residues of RNAs; i. e., pseudouridine synthases perform an internal transglycosylation reaction (Mueller and Ferré-D'Amaré, 2009). These enzymes are not capable of isomerizing free uridine into pseudouridine. Pseudouridine modification increases the rigidity of the sugar phosphate backbone and base stacking of tRNAs (Charette and Gray, 2000; Spenkuch, Motorin and Helm, 2015). An important characteristic of pseudouridine synthases is their substrate specificity. Several of these enzymes are highly specific and can recognize a single nucleotide in one particular RNA among the numerous different RNAs in the cell. Other interesting characteristic of pseudouridine synthases is that some enzymes (for instance, Pus4) recognize one nucleotide in the same structural context in many different substrate tRNAs, while other pseudouridine synthases recognize multiple RNAs, or multiple adjacent sites in one or a few closely related RNAs (Mueller and Ferré-D'Amaré, 2009).

In yeast, there are 9 genes encoding putative RNA pseudouridine synthases. Pus8 and Pus9 are required for the pseudouridylation of position 32 in cytoplasmic and mitochondrial tRNAs, respectively (Behm-Ansmant *et al.*, 2004). Besides Pus9, Pus3, Pus4, and Pus6 are tRNA-specific enzymes also acting on both mitochondrial and cytoplasmic tRNAs, while Pus2 only modifies mt-tRNAs at positions 27 and 28

3. Genetic screen to identify RNAmods and their regulators

(Behm-Ansmant, Branlant and Motorin, 2007). Pus3, a region-specific enzyme, is responsible for pseudouridylation at positions 38 and 39 (Lecointe *et al.*, 1998), Pus4 at position 55 (Becker *et al.*, 1997) and Pus6 at position 31 (Ansmant *et al.*, 2001). Pus5 modifies the mitochondrial 21S rRNA at position 2819 (Ansmant *et al.*, 2000) and Pus1 and Pus7 modifies both U2 snRNAs and tRNAs. Pus1 is a pseudouridine synthase with multisite specificity, modifying positions 1, 26, 27, 28, 34, 36, 65, and 67 of tRNAs and position 44 of U2 snRNA (Motorin *et al.*, 1998; Verine Massenet *et al.*, 1999; Behm-Ansmant *et al.*, 2006). On the other hand, Pus7 modifies position 35 of U2 snRNAs and positions 13 and 35 of tRNAs (Behm-Ansmant *et al.*, 2003; Ma, Zhao and Yu, 2003). The mode of target recognition for some pseudouridine synthases is yet incompletely defined. Some of those enzymes, such as Pus1 and Pus2, also modify mRNA targets and those modifications are regulated in response to environmental signals, such as nutrient starvation (Carlile *et al.*, 2014).

Other pseudouridine synthases, namely Cbf5, have a completely different mechanism of substrate recognition. Cbf5 associated with Nop10, Gar1 and Nhp2 directly binds to a guide RNA that has sequence complementarity to nucleotides contiguous to the site of the modification of its substrate RNA. Base pairing between the guide RNA and the substrate RNA brings the active site of Cbf5 to the proximity of its substrate. These guide RNAs are known as the box H/ACA RNAs (Reichow *et al.*, 2007). Shq1 and Naf1 interact with each other and also participate in the biogenesis of H/ACA snoRNP (Dez *et al.*, 2002; Yang *et al.*, 2002). Naf1 has a role in the recruitment of Cbf5 during snoRNA transcription, binding to the same site as Gar1, and in the later stages of the maturation process also recruits Gar1 to occupy its place and to activate the enzymatic activity (Fatica, Dlakic and Tollervey, 2002; Yang *et al.*, 2005; Leulliot *et al.*, 2007). Nhp2 binds to the Cbf5 and Nop10 complex and stabilizes it prior to assembly with RNA, assuring that Nhp2 binds specifically to H/ACA RNAs (Koo *et al.*, 2011). Nop10 binds to Cbf5 near the active site and has been proposed to stabilize it, but it also forms some contacts with the guide RNA as well as Cbf5 (Hamma *et al.*, 2005). Gar1 is the only protein of the box H/ACA snoRNP not directly interacting with RNA; it binds to the thumb loop of Cbf5 stabilizing it in an open conformation to modify rRNAs (Yang *et al.*, 2012; Wang *et*

3. Genetic screen to identify RNAmods and their regulators

al., 2015). In fact, thumb-Gar1 interaction is important for substrate turnover regulation, leading to a better control on the pseudouridylation reaction (Li, Duan, Li, Yang, *et al.*, 2011).

3.1.5 Dihydrouridine synthases

The enzymes required for formation of dihydrouridine (D) in six specific positions in tRNA are Dus1 (D₁₆, D₁₇), Dus2 (D₂₀), Dus3 (D₄₇), and Dus4 (D_{20A}, D_{20B}) (Xing, Martzen and Phizicky, 2002; Xing *et al.*, 2004). These enzymes reduce the 5,6-double bond of uridine residues (Madison and Holley, 1965) and are responsible for all dihydrouridine modification of cytoplasmic tRNAs in yeast. Interestingly, Dus2 and Dus3 are site-specific enzymes while Dus1 and Dus4 are region-specific enzymes; i. e. they modify more than one nucleotide in the same region of the tRNA (Xing *et al.*, 2004).

3.1.6 Overview of this study

In this thesis, we have set up a yeast genetic screen to identify tRNA and rRNA modifications that are required for proteome stability. In other words, modifications whose absence results in protein aggregation. We started with a mini-collection of 83 yeast strains containing deletions in genes coding for RNAmods and we were able to identify 6 genes whose deletions significantly increase the level of protein aggregation in yeast.

3.2 RESULTS

3.2.1 RNA-modifying enzymes are important for protein synthesis fidelity

Our main working hypothesis was that a subset of the yeast RNAmods, in particular those present in the anticodon loop of tRNAs and in the rRNA maintain proteome homeostasis by fine tuning codon-anticodon interactions, mRNA decoding accuracy and codon decoding efficiency. We postulated that perturbation of RNAmods by point mutations, deletions, environmental factors and metabolic deregulation

3. Genetic screen to identify RNAmods and their regulators

induces protein aggregation, proteotoxic stress, cell death and loss of fitness. A literature search allowed us to group RNAmods according to their function in tRNA and rRNA modification (Table 3.1).

Table 3.1. KO strains grouped according their function on RNA modification (data mining analysis).

Enzyme Function		Yeast KO strains
tRNA wobble uridine modification	Methyltransferases and regulators	Elp1Δ, Elp2Δ, Elp3Δ, Elp4Δ, Elp6Δ, Trm9Δ, Trm112Δ; Kti12Δ, Kti13Δ, Kti14Δ, Sit4Δ, Sap185Δ, Sap190Δ
	Thiolases	Cfd1Δ, Cia1Δ, Ncs2Δ, Ncs6Δ, Nbp35Δ, Tum1Δ, Uba4Δ, Urm1Δ, Isu1Δ, Isu2Δ, Nfs1Δ, Mss1Δ, Mto1Δ, Slm3Δ
Pseudouridine tRNA modification		Pus1Δ, Pus2Δ, Pus3Δ, Pus4Δ, Pus6Δ, Pus7Δ, Pus8Δ, Pus9Δ
Dihidrouridine tRNA modification		Dus2Δ, Dus3Δ, Dus4Δ
Wybutosine tRNA modification		Tyw1Δ, Tyw2Δ, Tyw3Δ, Tyw4Δ
Adenosine deaminases		Tad1Δ, Tad2Δ, Tad3Δ
t6A tRNA modification		Bud32Δ, Cgi121Δ, Sua5Δ
Other tRNA modifications		Mod5Δ, Rit1Δ, Tan1Δ, Trm1Δ, Trm10Δ, Trm11Δ, Trm13Δ, Trm140Δ, Trm2Δ, Trm3Δ, Trm4Δ, Trm44Δ, Trm5Δ, Trm61Δ, Trm7Δ, Trm8Δ, Trm82Δ
tRNA transport		Los1Δ, Msn5Δ, Mtr10Δ
rRNA modification	Pseudouridine synthases and regulators	Cbf5Δ, Naf1Δ, Nhp2Δ, Nop10Δ, Pus5Δ, Shq1Δ
	Methyltransferases and regulators	Dim1Δ, Mrm1Δ, Mrm2Δ, Nop1Δ, Nop2Δ, Nop56Δ, Nop58Δ, Snu13Δ, Spb1Δ

The studied RNA-modifying enzymes form network interactions, independently of their specific function (Figure 3.8). Network analysis of the 83 RNAmods was performed using the STRING database for known and predicted protein-protein associations (Snel *et al.*, 2000; Szklarczyk *et al.*, 2015, 2017). Network clustering was determined using a Markov Cluster (MCL) algorithm with inflation equal to 2, in order to enhance the contrast between regions of strong or weak confidence interaction (Brohée and Van Helden, 2006; Moschopoulos *et al.*, 2011). Data clustering showed five clusters (Figure 3.8); two clusters (red and green

3. Genetic screen to identify RNAmods and their regulators

clusters at Figure 3.8) were specific for most of the tRNA wobble uridine modifying enzymes; t⁶A tRNA-modifying enzymes and enzymes for tRNA transport were also found in individual clusters (brown and yellow clusters at Figure 3.8); the remaining tRNA-modifying enzymes and all rRNA-modifying enzymes were found in the blue cluster (Figure 3.8, Annex VII.1 and Annex VII.2).

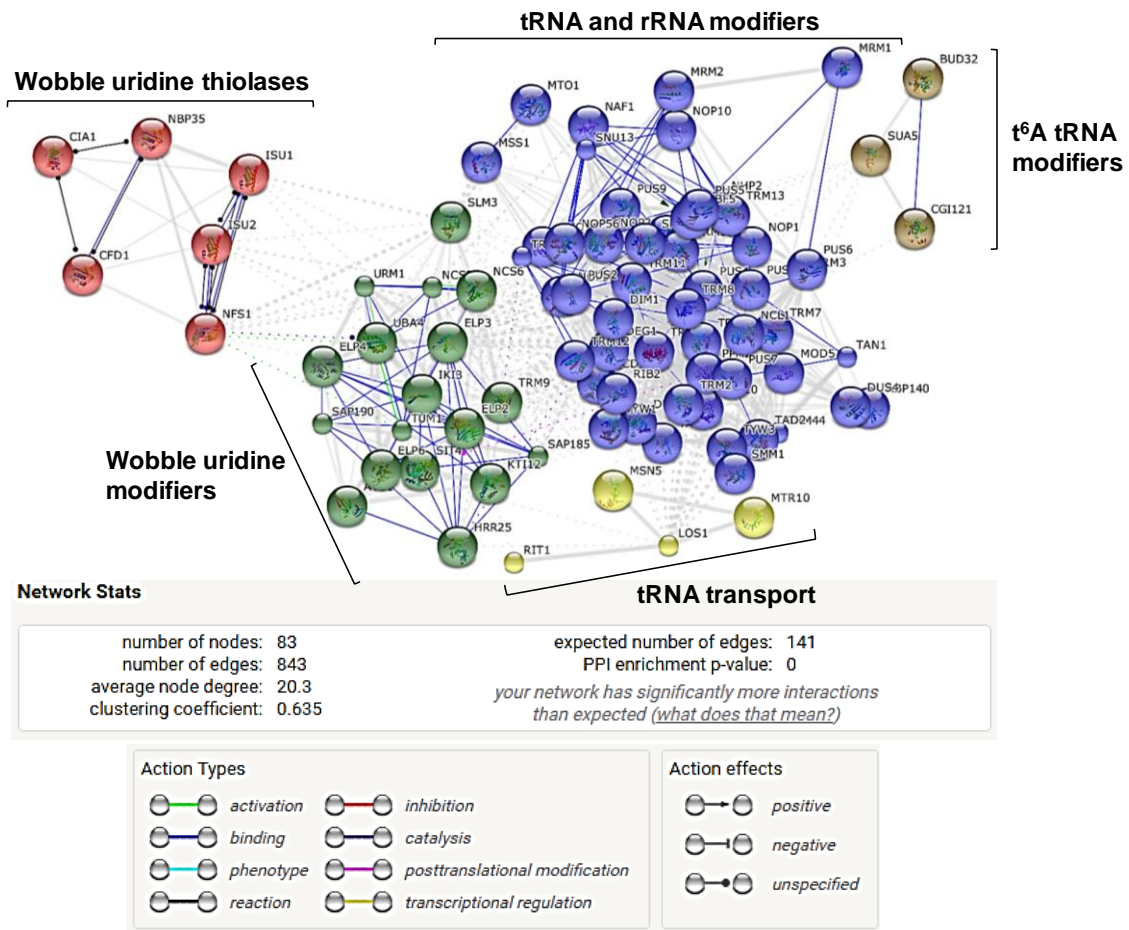


Figure 3.8. Network analysis of RNAmods. The interactome was predicted using the STRING database (version 10.0). Clustering was performed using MCL algorithm with inflation parameter = 2. Colored lines between the proteins indicate the various types of predicted mode of action. Small nodes represent proteins of unknown 3D structure; Large nodes represent some known or predicted 3D structure. Dashed lines represent inter-cluster edges.

In order to test our hypothesis, we studied *in vivo* the impact of deleting the genes encoding the tRNA and rRNA-modifying enzymes on protein aggregation

3. Genetic screen to identify RNAmods and their regulators

using Hsp104-GFP reporter system. Hsp104 is a protein disaggregase and its induction and cellular distribution are indicative of increased protein aggregation in the cell (Fujita *et al.*, 1998; Erjavec *et al.*, 2007). Yeast cells expressing the Hsp104-GFP reporter system were analyzed by epifluorescence microscopy in order to detect protein aggregates (example in Figure 3.9). The number of cells containing GFP fluorescence foci was quantified (Figure 3.10, Figure 3.11 and Figure 3.12) and the data showed significant increase in localized Hsp104-GFP in cells with deletion of Kti12, Trm9, Mto1, Dus2, Pus6, Los1, Tyw4, Tad1, Trm3, Dim1, Mrm2, Shq1, Sbp1 (*), Elp1, Cia1, Slm3 and Nop10 (**), relative to WT (Figure 3.10, Figure 3.11 and Figure 3.12).

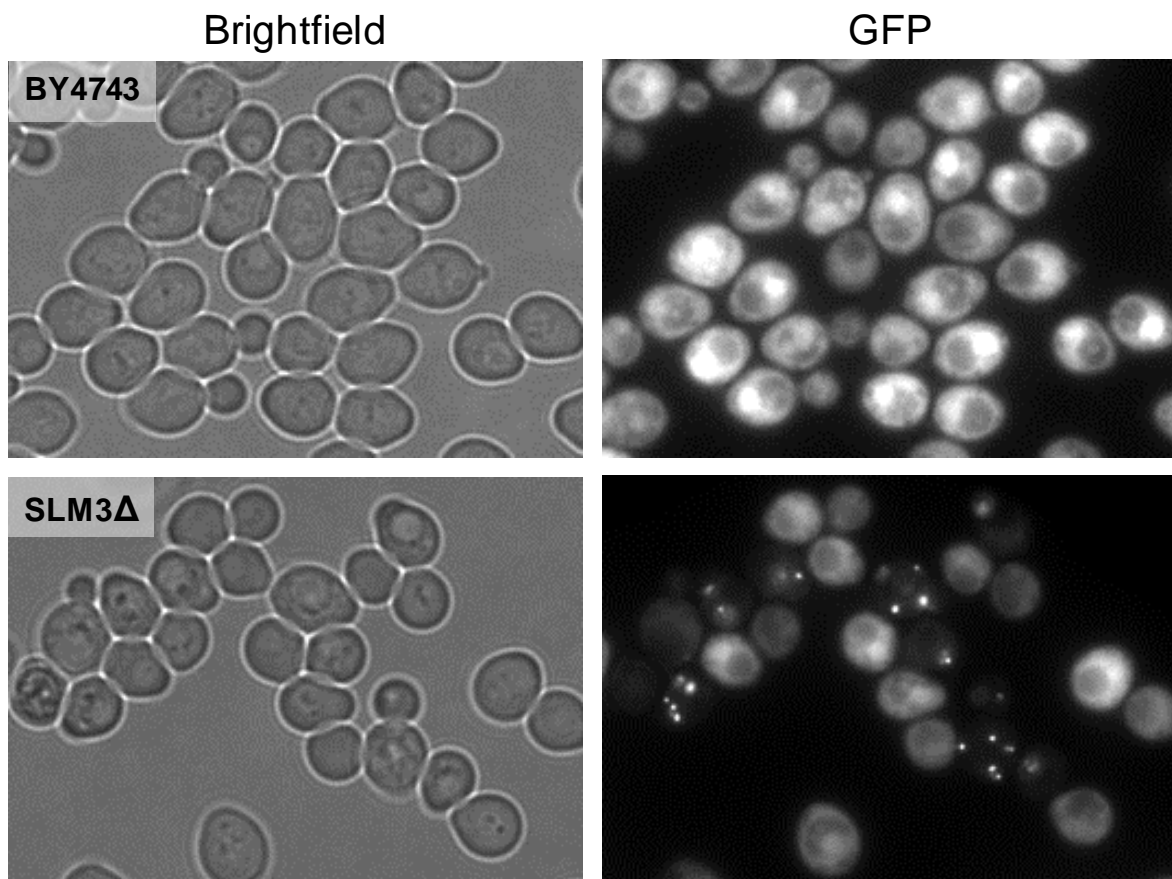


Figure 3.9. Deletion of specific RNAmods induces cytoplasmic protein aggregates. WT (BY4743) and tRNAmod gene KO yeast cells expressing the Hsp104-GFP reporter protein were collected in middle exponential growth phase and observed by fluorescence microscopy (60x objective). Cells harboring a KO in the Slm3 gene showed localized Hsp104-GFP fluorescence, indicating the presence of protein aggregates.

3. Genetic screen to identify RNAmods and their regulators

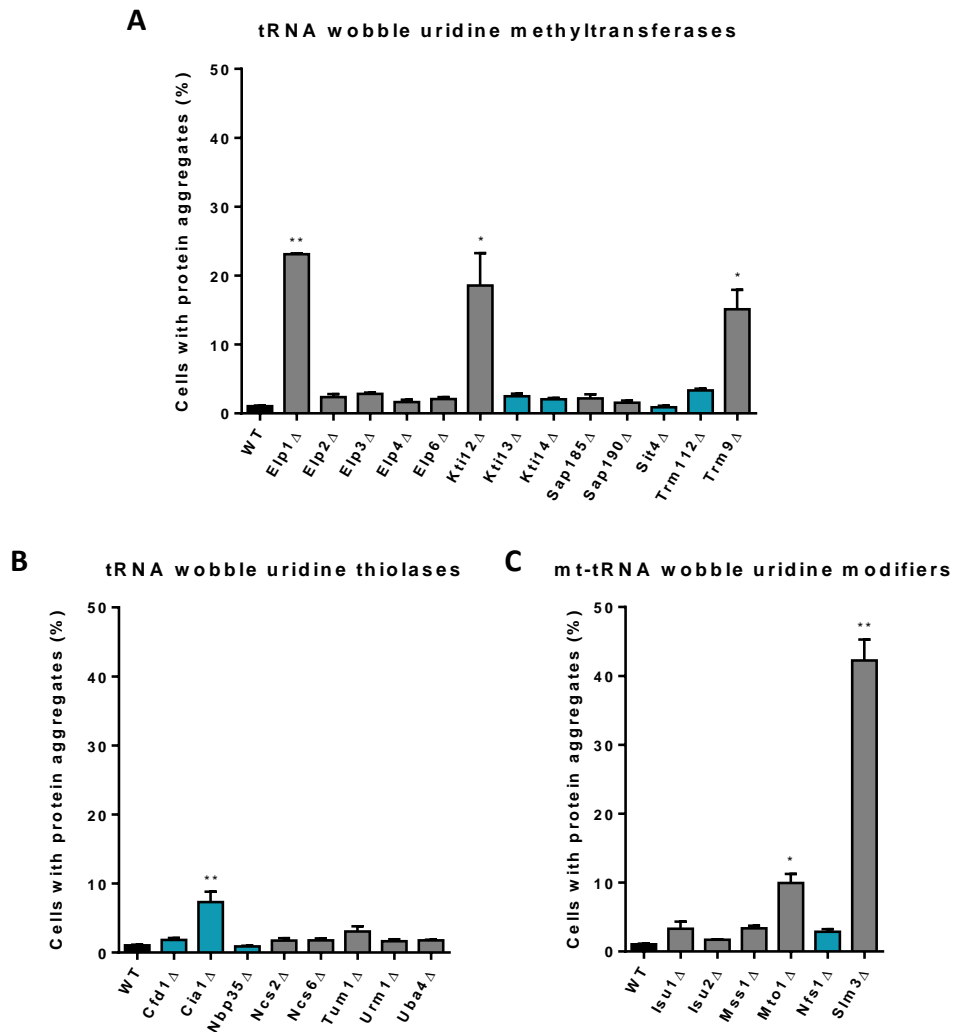


Figure 3.10. Effect of deletion of wobble uridine modifying enzymes on the formation of protein aggregates. The plots show the percentage of yeast cells containing localized Hsp104-GFP fluorescence foci. Data represent the mean \pm SEM of triplicates of three independent clones ($n = 9$) (** $p < 0.01$, * $p < 0.05$ Kruskal-Wallis post Dunn's multiple comparisons test with CI 95% relative to WT). Grey bar represents homozygous diploid KO strains; Blue bar represents heterozygous diploid KO strains; WT is represented with a black bar.

3. Genetic screen to identify RNAmods and their regulators

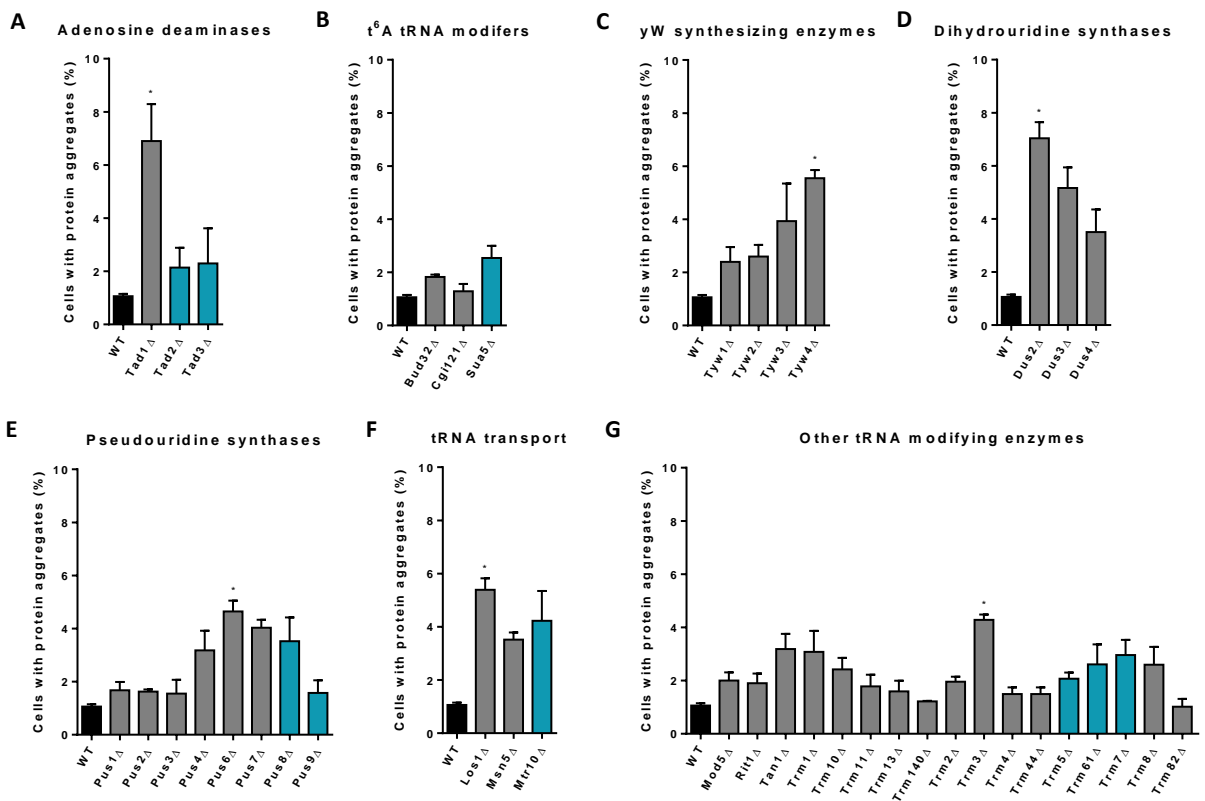


Figure 3.11. Effect of deletion of tRNA-modifying enzymes on the formation of protein aggregates. The plots show the percentage of yeast cells containing localized Hsp104-GFP fluorescence foci. Data represent the mean \pm SEM of triplicates of three independent clones ($n = 9$) (* $p < 0.05$ Kruskal-Wallis test post Dunn's multiple comparisons test with CI 95% relative to WT). Grey bar represents homozygous diploid KO strains; Blue bar represents heterozygous diploid KO strains; WT is represented with a black bar.

3. Genetic screen to identify RNAmods and their regulators

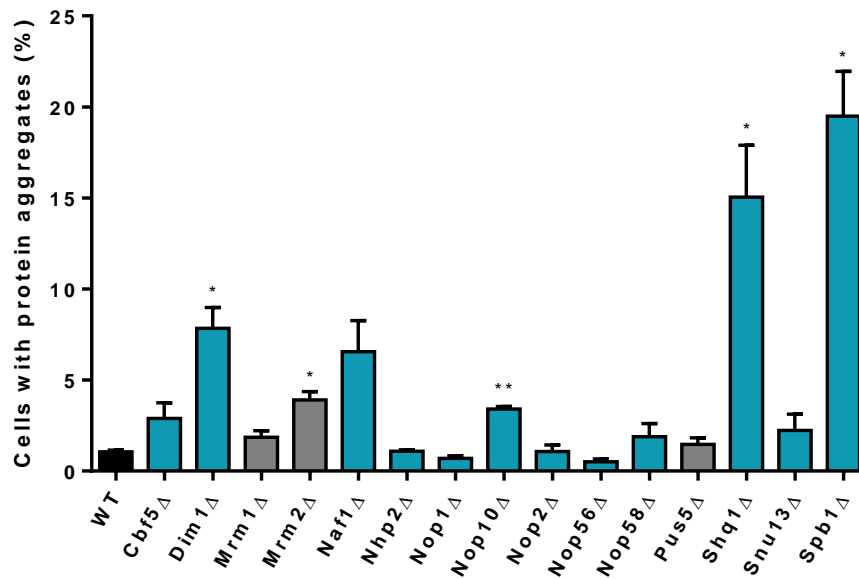


Figure 3.12. Effect of deletion of rRNA-modifying enzymes on the formation of protein aggregates. The plots show the percentage of yeast cells containing localized Hsp104-GFP fluorescence foci. Data represent the mean \pm SEM of triplicates of three independent clones ($n = 9$) (** $p < 0.01$, * $p < 0.05$ equal variances not assumed t -test with CI 95% relative to WT). Grey bar represents homozygous diploid KO strains; Blue bar represents heterozygous diploid KO strains; WT is represented with a black bar.

Besides the total number of cells with protein aggregates in each KO strain, other characteristics were studied, namely, the size of the aggregates and the number of aggregates per cell. The data show that each KO strain has slightly different protein aggregation phenotypes (Figure 3.13 and Annex II.1).

3. Genetic screen to identify RNAmods and their regulators

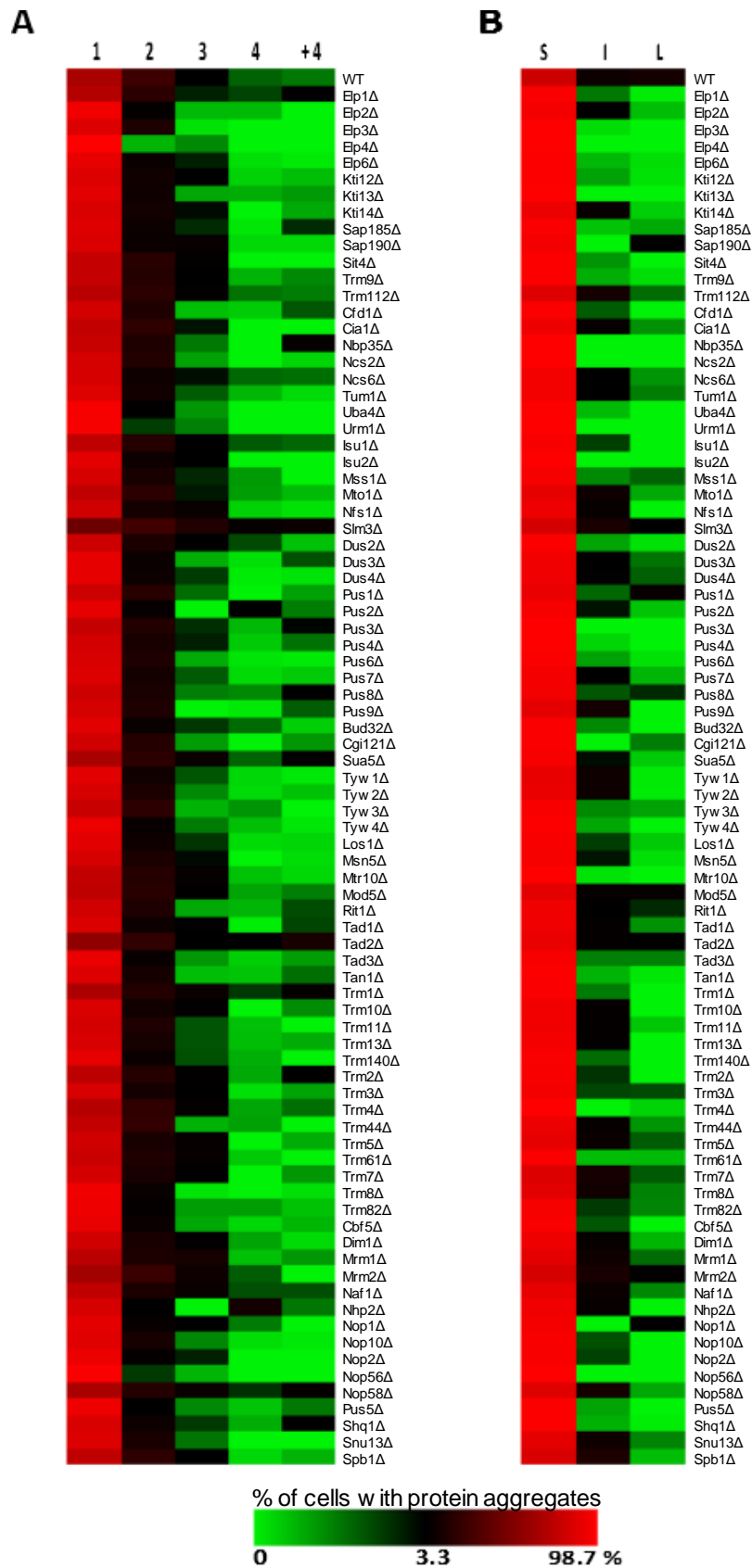


Figure 3.13. Heat-map representing the number and type of protein aggregates per cell. Yeast cells containing localized Hsp104-GFP fluorescence foci were counted and

3. Genetic screen to identify RNAmods and their regulators

differentiated according to the number (**A**) and the size (**B**) of localized Hsp104-GFP fluorescence foci per cell. Results are expressed as the percentage of positive cells (with Hsp104-GFP foci) relative to the total number of cells with protein aggregates. Data represent the mean of triplicates of three independent clones. S: small protein aggregates; I: intermediate protein aggregates; L: large protein aggregates.

The top 10 KO strains with highest level of protein aggregates were selected (Figure 3.14): six tRNAmods that modify tRNA wobble uridines, three rRNAmods and one tRNAmo that modifies nucleosides in the D-loop of tRNA. Then, a cutoff selection of <10% of cells containing protein aggregates allowed us to identify the 6 KO strains with the highest level of protein aggregation for further analysis (Figure 3.14). The selected KO strains harbor deletions in genes encoding four enzymes involved in tRNA wobble uridine modification (Trm9, Elp1, Kti12 and Slm3) and two enzymes involved in rRNA modification (Spb1 and Shq1).

Trm9 is a wobble uridine methyltransferase that catalyzes the esterification of modified uridine nucleosides, resulting in the formation of mcm^5U_{34} and $mcm^5s^2U_{34}$ in specific tRNAs (Kalhor and Clarke, 2003). Elp1 is one of the subunits in the Elongator complex, which is required for the formation of the cm^5U side chain in some wobble uridines (Huang, Johansson and Byström, 2005). Kti12 is important for the phosphorylation status of Elp1 and it is also required for the formation of mcm^5 and ncm^5 side chains at some wobble uridines (Huang, Johansson and Byström, 2005). Slm3 is known as mitochondrial tRNA-specific 2-thiouridylase 1 (Mtu1) and is responsible for the formation of the s^2 group in $cmnm^5s^2U_{34}$ -containing tRNA species (only in mitochondrial tRNAs) (Umeda *et al.*, 2005). The formation of s^2 and mcm^5 groups occurs independently of each other.

Spb1 is an essential S-adenosylmethionine-dependent methyltransferase required for 60S ribosomal subunit biogenesis (D Kressler *et al.*, 1999), which modifies the universally conserved G₂₉₂₂ located within the A loop of the catalytic center of the ribosome. This enzyme was also associated with the Um₂₉₂₁ modification in the ribosome (Lapeyre and Purushothaman, 2004). On the other hand, Shq1 enzyme is an essential assembly factor for the H/ACA particles that functions as site-specific pseudouridine synthases in a RNA-guided mechanism (Walbott *et al.*, 2011).

3. Genetic screen to identify RNAmods and their regulators

The deletion of the tRNAmods genes was validated by PCR, as described in 2.3 Validation of gene deletions by PCR, and deletion of the four tRNAmod genes was confirmed (Annex III.1). Since the two strains harboring rRNAmod deletions are heterozygous (diploid KOs), we could not validate the deletion of 1 of the alleles using one set of primers (Annex III.1). However, those strains were previously validated by the *Saccharomyces cerevisiae* Deletion Project.

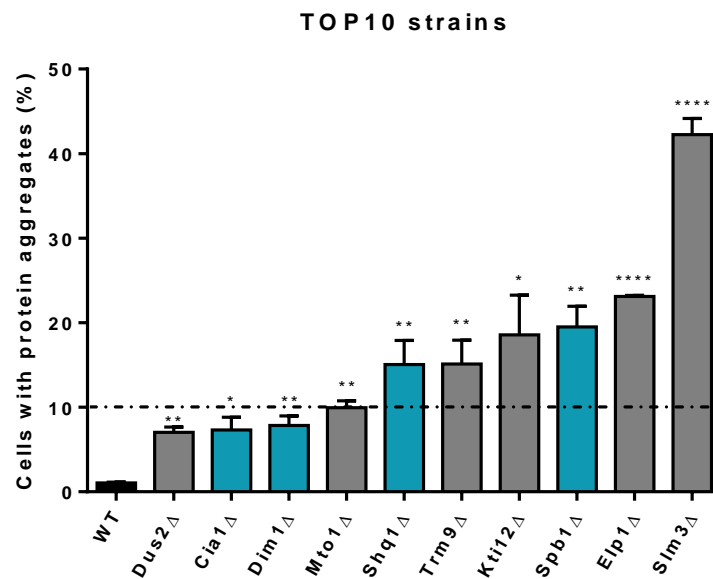


Figure 3.14. Top 10 KO strains with protein aggregates. The plots show the percentage of yeast cells containing localized Hsp104-GFP fluorescence foci. Data represent the mean \pm SEM of triplicates of three independent clones ($n = 9$) (**** $p < 0.0001$, ** $p < 0.01$, * $p < 0.05$ Student's t -test with CI 95% relative to WT). Dotted line represents the selection of more relevant KO strains (cutoff value is less than 10). Grey bar represents homozygous diploid KO strains; Blue bar represents heterozygous diploid KO strains; WT is represented with a black bar.

We have also analyzed 4 of the selected KO strains by transmission electron microscopy (TEM) to obtain a more detailed picture of the protein aggregates. Electron dense material not involved by membranes was clearly visible in the cytoplasm of the selected KO strains (Figure 3.15, red arrows), but not in the control strain, as expected. Such membrane free electron dense materials have been previously described as protein aggregates (Fujita *et al.*, 1998). We also observed

3. Genetic screen to identify RNAmods and their regulators

that vacuoles were larger and in higher number in Elp1 and Kti12 KO strains relative to control WT cells (Figure 3.15).

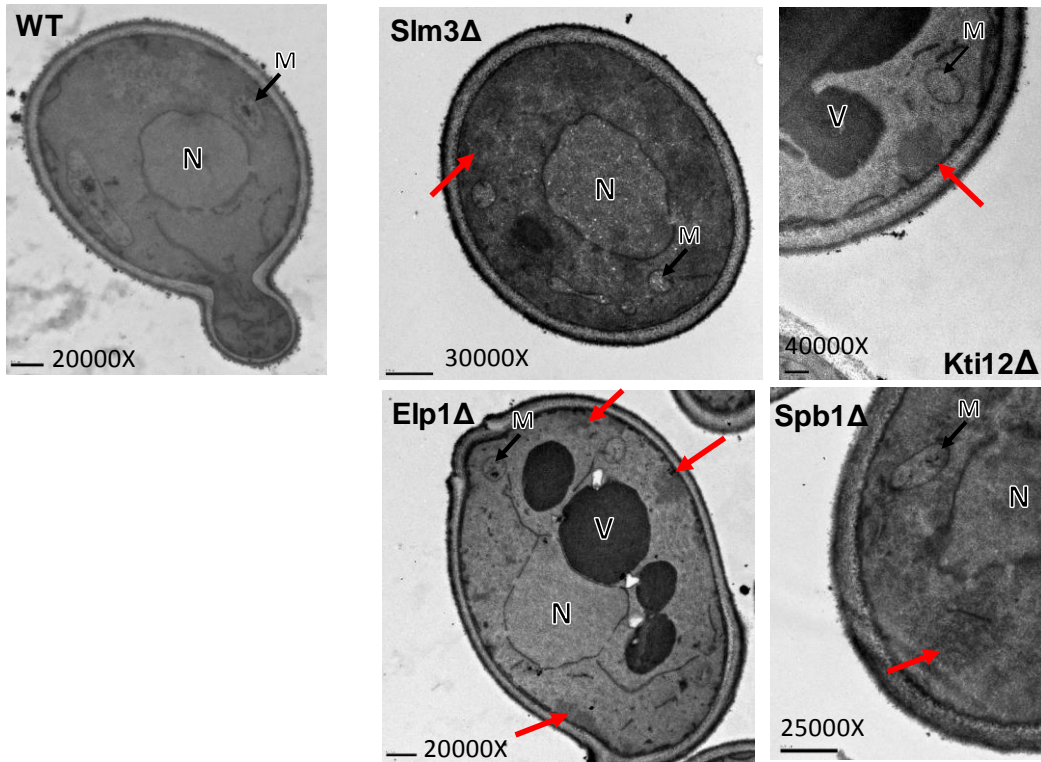


Figure 3.15. Ultrastructure of WT and selected RNAmod KO yeast cells. All cells were fixed at the same time and with the same solutions and embedded in Epon 812 resin. Electron dense materials indicated by the red arrows correspond to protein aggregates. N: nucleus; M: mitochondrion; V: vacuole.

The protein aggregates of the selected KO strains were also quantified by isolating the insoluble fraction and fractionating it by SDS-PAGE (Tomoyasu *et al.*, 2001; Jang *et al.*, 2004; Haslbeck *et al.*, 2005; Rand and Grant, 2006; Koplín *et al.*, 2010). Selected KO strains showed slightly increased levels of aggregated proteins (Figure 3.14), but the level of insoluble protein observed in the gels was relatively low (Figure 3.16). This may be explained by the fact that less than 50% of cells of each KO strain had protein aggregates and the extraction of insoluble protein was done using both types of cells. However, different SDS-PAGE band patterns were observed in different KO strains. Different aggregated protein bands were also observed for different clones from each strain.

3. Genetic screen to identify RNAmods and their regulators

Misfolded proteins may aggregate or may be degraded by the ubiquitin-proteasome system (UPS) and/or the autophagy-lysosome system (reviewed in Lindner and Demarez, 2009). To understand whether insoluble proteins were being degraded we quantified the activity of the proteasome of the selected KO strains. No significant increase in activity relative to WT strain either at exponential phase and at stationary phase was observed (Figure 3.17). Although *Trm9Δ* and *Slm3Δ* had slightly higher proteasome activity in stationary phase; these KO strains also showed high variability of proteasome activity and the increase in activity was not significantly different from WT.

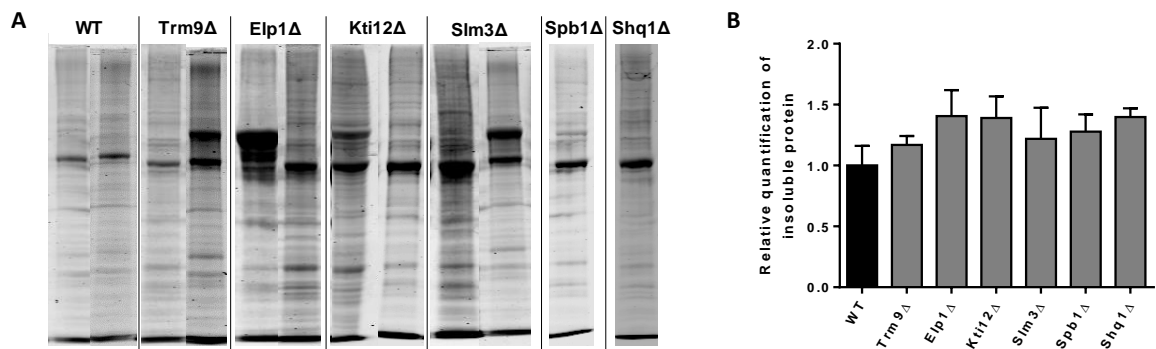


Figure 3.16. Deletion of RNAmods increases the level of insoluble proteins. A. Cells were grown to logarithmic phase in MM-His media at 30 °C and, after lysis, aggregated material was isolated, separated by SDS-PAGE and visualized by Coomassie staining. Gel lanes intensities were then quantified. Representative gel lanes showing the insoluble protein fraction of 1 or 2 clones of the selected KO and WT strains. **B.** The graph represents the relative quantification of insoluble proteins in selected KO strains relative to WT. Data represent the mean \pm SEM of duplicates of three independent clones (Kruskal-Wallis post Dunn's multiple comparisons test with CI 95% relative to WT).

3. Genetic screen to identify RNAmods and their regulators

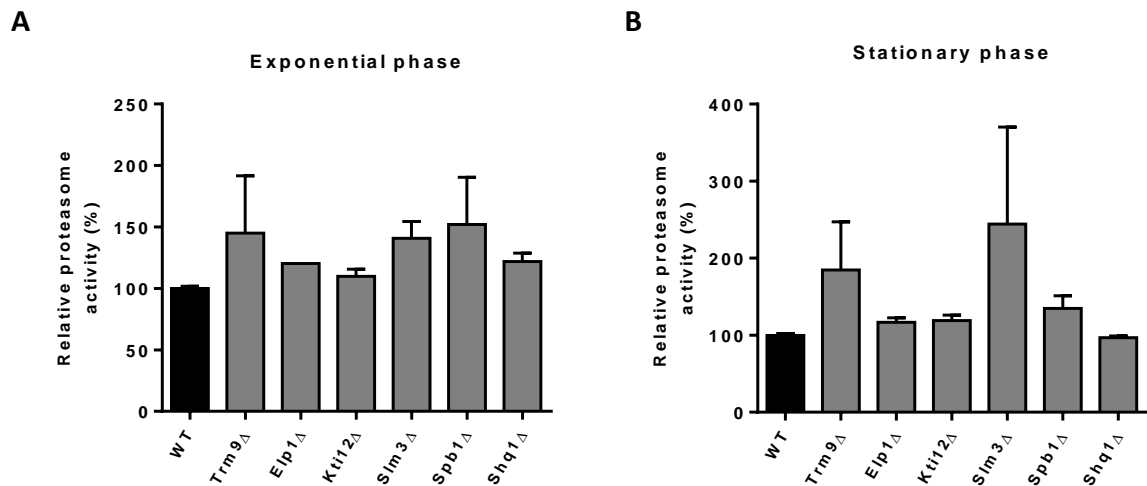


Figure 3.17. Deletion of selected RNAmods slightly increases proteasome activity.

Cells were grown in MM-His and collected at middle exponential phase (A) and stationary phase (B). Proteasome activity was quantified in total protein extracts by measuring degradation of the fluorogenic peptide Suc-LLVY-AMC (chymotrypsin-like substrate) at 37 °C for 1 h. Quantification of degraded AMC was calculated by measuring fluorescence emission intensity at 460 nm after 60 min. Values were corrected using fluorescence values at time zero. Data represent the mean \pm SEM of triplicates of three independent clones (Kruskal-Wallis post Dunn's multiple comparisons test with CI 95% relative to WT).

3.2.2 Absence of RNAmods influences cellular fitness

Since our tRNAmod KO strains had higher levels of protein aggregation than the WT control, we decided to clarify the impact of aggregation on growth rate; as a measure of fitness (Vermulst *et al.*, 2015). Surprisingly, the relative growth rate of all selected KO strains was not significantly different from that of the WT strain (Figure 3.18A, B); there was only a slight decrease in growth rate.

In order to determine whether that slight decrease in growth rate was due to increased cell death we evaluated this parameter using the propidium iodide (PI) method. The PI dye stains cells with disrupted membranes and provides an indirect measure of viability. This assay was performed at various time points of the growth curve to better understand the effect of RNAmods deletion on growth. The time points chosen for this analysis were T10h, T15h, T20h, T25h and late stationary

3. Genetic screen to identify RNAmods and their regulators

phase. Cell death was slightly increased in the *Slm3*, *Trm9*, *Spb1* and *Kti12* KO strains (Figure 3.18C).

There was good correspondence between cell death and growth rate/scores since cells lacking *Trm9*, *Slm3*, *Kti12* and *Spb1* enzymes showed the highest decrease in growth rate/scores and the highest percentage of cell death (PI incorporation).

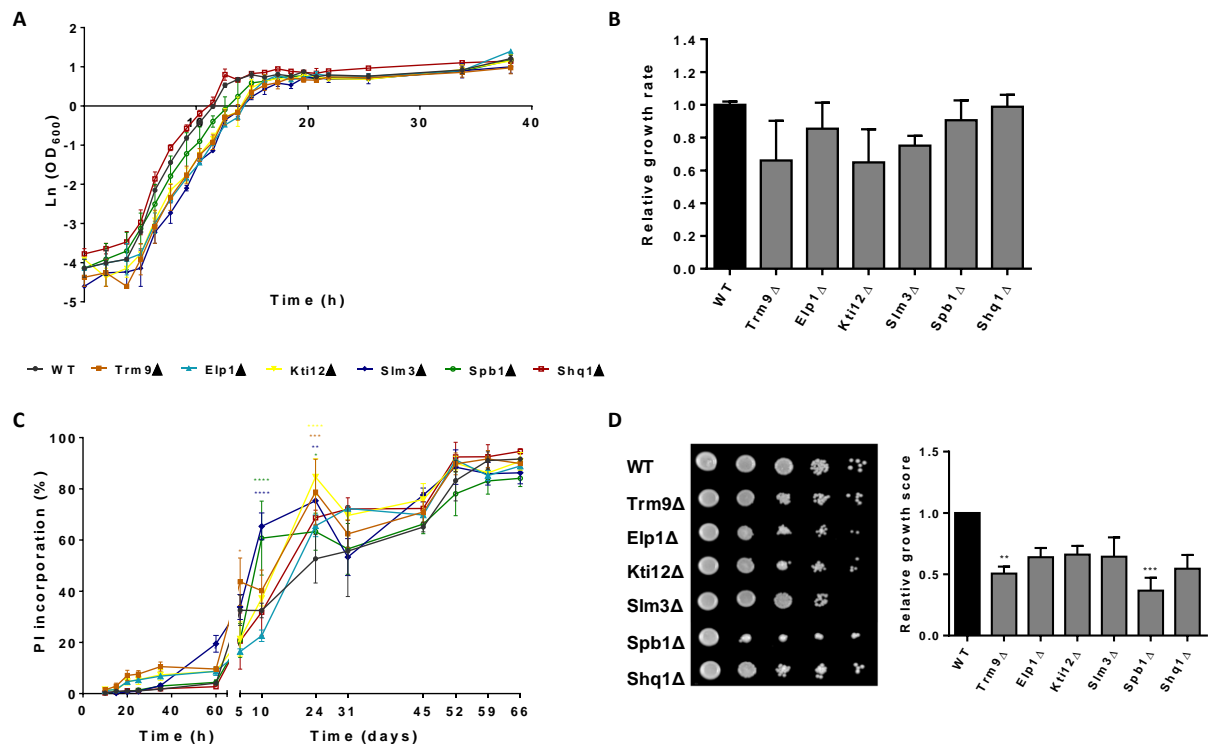


Figure 3.18. Growth rate and cell viability of the selected KO strains. **A.** Yeast cultures were inoculated at an initial OD₆₀₀ of 0.02 and were grown in selective medium (MM-His) at 30 °C and 180 rpm until stationary phase. At the indicated time points the OD₆₀₀ was measured. **B.** Relative growth rate of KO strains was determined using the growth values of the exponential growth phase, relative to WT. Data represent the mean ± SEM of duplicates of three independent clones (one-way analysis of variance post Dunnett's multiple comparison test with CI of 95%, relative to WT). **C.** Viability of selected KO strains was accessed by labeling yeast cells with propidium iodide (PI) at different time points. 10 000 cells were analyzed by flow cytometry at each time point. Data represent the mean ± SEM of three independent clones (**** p < 0.0001, * p < 0.05 Two-way RM Anova post Dunnett's multiple comparison test with CI 95% relative to WT). **D.** Colony survival of selected KO strains compared to WT strain. Equal densities of yeast cells (10 μl) grown in

3. Genetic screen to identify RNAmods and their regulators

exponential phase were serially diluted 10^1 – 10^5 -fold and were spotted onto MM-His plates and their colony-forming abilities were then analyzed after 2 days of incubation at 30 °C. The growth score represents a ratio between growth of a KO strain and growth of WT strain. Data represent mean \pm SEM of three independent clones (** $p < 0.01$, *** $p < 0.001$, Friedman post Dunn's multiple comparison test with CI 95% relative to WT).

To determine whether stress exacerbates the tRNAmod KO phenotypes under stress conditions, 10 RNAmod KO strains were exposed to stress conditions. The percentage of cells containing protein aggregates was similar to that of the WT control strain during exposure to transient heat stress 37 °C for 30 minutes (Figure 3.19A). Longer exposure to heat stress (37 °C for 120 minutes) resulted in a trend of increased protein aggregation in all KO strains relative to WT, but such increase was only statistically significant in *Elp2* Δ (Figure 3.19A).

Growth score of selected KO strains grown at 37 °C was statistically decreased in *Trm9* Δ , *Elp1* Δ and *Kti12* Δ (Figure 3.19B).

3. Genetic screen to identify RNAmods and their regulators

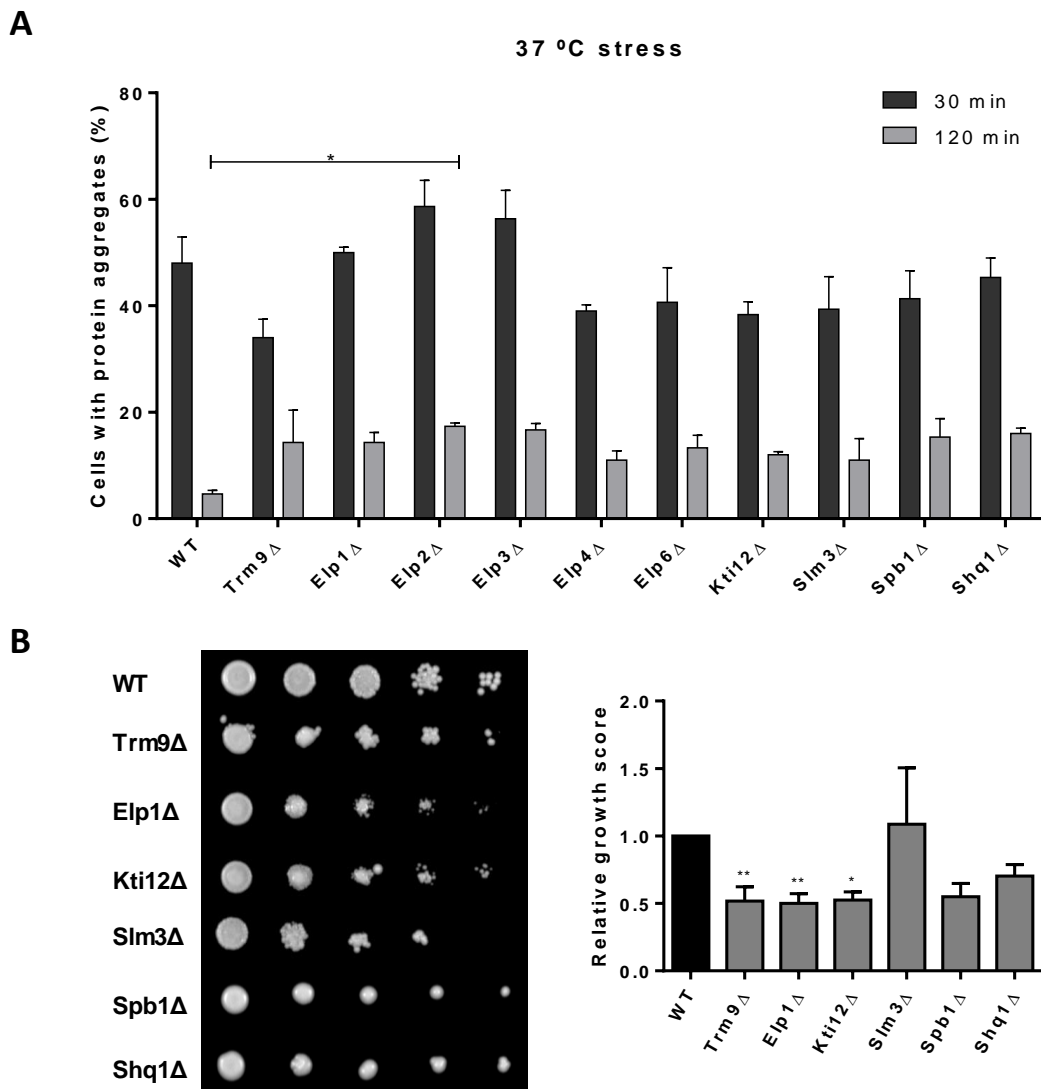


Figure 3.19. Cells lacking RNAmods are sensitive to heat stress. **A.** Yeast cells were subjected to a transient stress for 30 min at 37 °C and also for 120 min at 37 °C. The plots show the percentage of yeast cells containing localized Hsp104-GFP fluorescence foci. Data represent the mean \pm SEM of three independent clones (* $p < 0.05$ Kruskal-Wallis test post Dunn's multiple comparisons test with CI 95% relative to WT). This experiment was carried out by Margarida Ferreira, MSc, under our supervision. **B.** Colony survival of selected KO strains compared to WT strain grown at 37 °C. Equal densities of yeast cells (10 μ l) grown in exponential phase were serially diluted 10^1 – 10^5 -fold and were spotted onto MM-His plates and their colony-forming abilities were then analyzed after 2 days of incubation at 37 °C. The growth score represents a ratio between growth of a KO strain and growth of WT strain. Data represent mean \pm SEM of three independent clones (***) $p < 0.001$, ** $p < 0.01$ Friedman post Dunn's multiple comparison test with CI 95% relative to WT).

3. Genetic screen to identify RNAmods and their regulators

3.2.3 Deletion of RNAmods decreases tRNA stability and modification levels

To assess the overall dynamics of tRNA modification and validate the absence of the modified nucleosides in the KO strains, we used LC-MS/MS. This method allowed us to quantify the full set of tRNA and rRNA modifications in selected strains, after tRNA and rRNA purification using a HPLC approach. The data were used to assess population-level changes in the relative quantities of the ribonucleosides regardless of whether the changes occur by alterations in tRNA copy number, in the activity of tRNA-modifying enzymes or both. The tRNA modification patterns provided clues for subsequent analysis of individual tRNAs and tRNA copy numbers. The LC-MS/MS approach allowed us to determine the presence or absence of certain modifications in our mutant strains lacking specific modification pathways, but also to quantify changes in modification levels that result from altered regulatory pathways. We have also determined the abundance of the hypomodified tRNAs in mutant strains relative to WT, using a four-leaf clover qRT-PCR test, a method used to quantify mature tRNA (Honda *et al.*, 2015).

Regarding tRNA modified nucleosides, we observed the expected decrease in wobble uridine modifications in the tRNAmod KO strains, particularly ncm^5U , mcm^5U , and $\text{mcm}^5\text{s}^2\text{U}$ in EIp1, Kti12 and Trm9 KO strains (Figure 3.20, Annex V.1, and Annex V.2). The mutant of the SIm3 thiolase showed a significant decrease in $\text{mcm}^5\text{s}^2\text{U}$ and a significant increase in mcm^5U , as a result of the absence of uridine thiolation (Figure 3.20, Annex V.1, and Annex V.2). We also observed a statistical decrease in γW in Kti12, Trm9 and SIm3 KO strains. Modified nucleosides in rRNAmod KO strains did not change significantly relative to WT, except for a small increase in I modification (Figure 3.20, Figure 3.21 and Annex V.1 to Annex V.8).

3. Genetic screen to identify RNAmods and their regulators

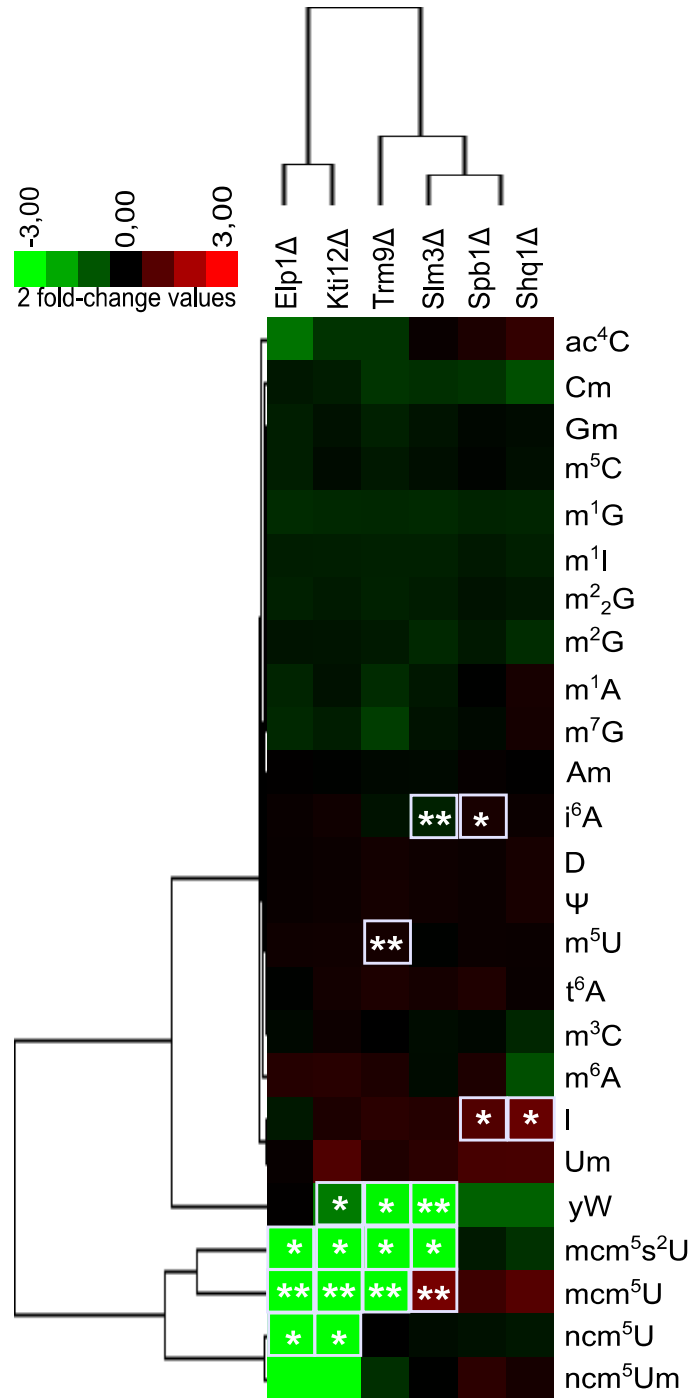


Figure 3.20. Hierarchical cluster of the relative levels of tRNA ribonucleoside modifications in selected KO strains. tRNA modification data from WT and RNAmoD KO strains were identified and quantified by mass-spectrometry. Log-based fold-change values were determined relative to WT and the ratios of ribonucleoside levels from Annex V.2 were subjected to hierarchical cluster analysis. Data represent mean of triplicates of three independent clones (n = 9) (** p < 0.01, * p < 0.05, Student's t-test with CI 95% relative to

3. Genetic screen to identify rNAMods and their regulators

WT). Red: fold increase; Green: fold decrease; according to the scale in the top-left color bar.

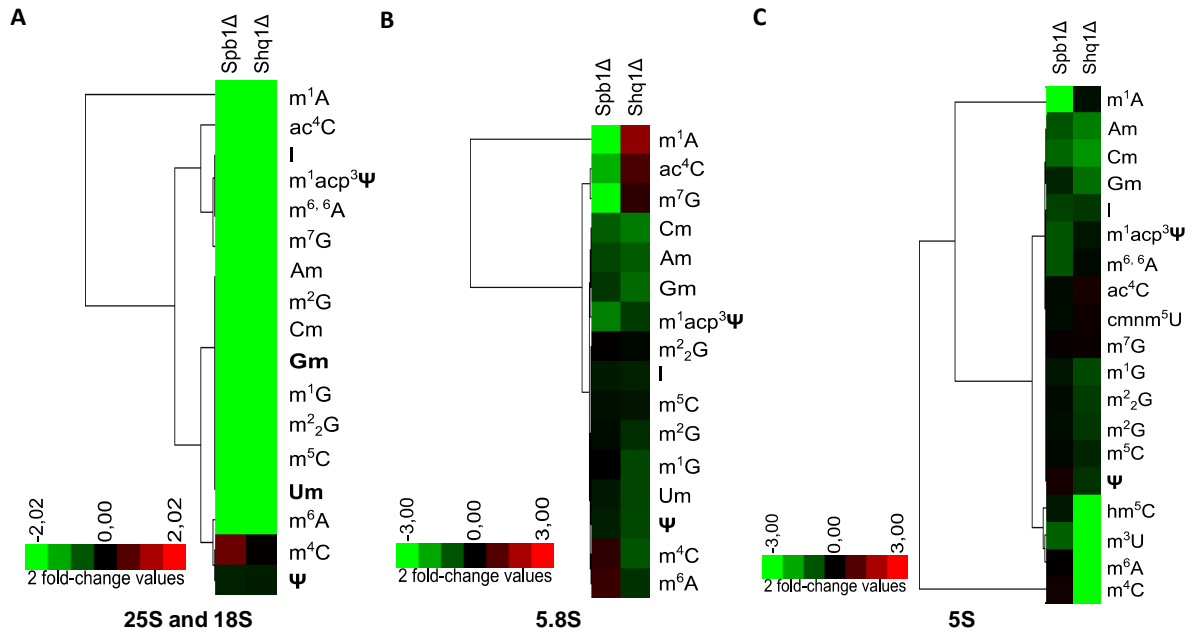


Figure 3.21. Hierarchical cluster visualization of the relative levels of rRNA ribonucleoside modifications in rNAMods KO strains. rRNA modification data from WT and rNAMod KO strains were identified and quantified by mass-spectrometry in 25 and 18s rRNAs (A), 5.8S rRNA (B) and 5S rRNA (C). Log-based fold-change values were determined relative to WT and the ratios of ribonucleoside levels from Annex V.4, Annex V.6 and Annex V.8 were subjected to hierarchical cluster analysis. Data represent mean of triplicates of three independent clones (Student's t-test with CI 95% relative to WT). Red: fold increase; Green: fold decrease, according to the scale in the bottom-left color bar in each panel.

Regarding tRNA abundance, we first selected relevant wobble uridine modified tRNAs from the tRNA pool (Figure 3.22). Eleven out of the 13 yeast cytoplasmic tRNA species that contain uridine at position 34 (U₃₄) are modified by at least two tNAMods deleted in our mutant cells. The eleven tRNA species that contain a wobble mcm⁵, ncm⁵ or mcm⁵s² side chain are the following: tRNA^{Arg}_{mcm5UCU}, tRNA^{Gly}_{mcm5UCC} (modified by Trm9, Elp1 and Kti12), tRNA^{Lys}_{mcm5s2UUU}, tRNA^{Gln}_{mcm5s2UUG}, tRNA^{Glu}_{mcm5s2UUC} (modified by Trm9, Elp1, Kti12 and Slm3), tRNA^{Val}_{ncm5UAC}, tRNA^{Ser}_{ncm5UGA}, tRNA^{Pro}_{ncm5UGG}, tRNA^{Thr}_{ncm5UGU}, tRNA^{Ala}_{ncm5UGC} and

3. Genetic screen to identify RNAmods and their regulators

tRNA^{Leu}_{ncm5UmAA} (modified by Elp1 and Kti12). We also added the mitochondrial tRNA^{Lys}_{cmnm5s2UUU}, which is thiolated by the Slm3 enzyme.

The abundance of tRNAs modified by Trm9 and Slm3 in the respective mutant cells was not significantly affected by tRNA hypomodification (Figure 3.23). However, we observed significant reduction of the abundance of tRNA^{Ala}_{ncm5UGC}, tRNA^{Thr}_{ncm5UGU} and tRNA^{Arg}_{mcm5UCU} in Elp1Δ, as well as in tRNA^{Gln}_{mcm5s2UUU}, tRNA^{Glu}_{mcm5s2UUC}, tRNA^{Thr}_{ncm5UGU} and tRNA^{Arg}_{mcm5UCU} in Kti12Δ (Figure 3.23).

codon	anticodon	amino acid	codon	anticodon	amino acid	codon	anticodon	amino acid	codon	anticodon	amino acid
UUU	-	Phe	UCU	IGA	Ser	UAU	-	Tyr	UGU	-	Cys
UUC	GmAA	Leu	UCC	-		UAC	GΨA	n.a.	UGC	GCA	Cys
UUA	ncm⁵UmAA		UCA	ncm⁵UGA		UAA	-		UGA	-	n.a.
UUG	m ⁵ CAA		UCG	CGA	UAG	-	UGG		CmCA	Trp	
CUU	-	Leu	CCU	AGG	Pro	CAU	-	CGU	ICG	Arg	
CUC	GAG		CCC	-		CAC	GUG	His	CGC		-
CUA	UAG		CCA	ncm⁵UGG		CAA	mcm⁵s²UUG	Gln	CGA		-
CUG	-		CCG	-		CAG	CUG	CGG	CCG		-
AUU	IAU	Ile	ACU	IGU	Thr	AAU	-	Asn	AGU	Ser	
AUC	-		ACC	-		AAC	GUU	AGC	GCU		GCU
AUA	ΨAΨ		ACA	ncm⁵UGU		AAA	mcm⁵s²UUU	Lys	AGA		mcm⁵UCU
AUG	CAU	Met	ACG	CGU	AAG	CUU	AGG	AGG	CCU	Arg	
GUU	IAC	Val	GCU	IGC	Ala	GAU	-	Asp	GGU	-	
GUC	-		GCC	-		GAC	GUC	GCC	GCC	GCC	Gly
GUA	ncm⁵UAC		GCA	ncm⁵UGC		GAA	mcm⁵s²UUC	Glu	GGA	mcm⁵UCC	
GUG	CAC		GCG	-		GAG	CUC	GGG	GGG	CCC	

Figure 3.22. Distribution of cytoplasmic *S. cerevisiae* tRNAs through the genetic code. The anticodon sequence of the 42 different tRNAs along with anticodon nucleosides modification. tRNAs containing wobble mcm⁵, ncm⁵ or mcm⁵s² side chains are shown in bold with the respective codon box filled in grey. Adapted from Johansson *et al.*, 2008.

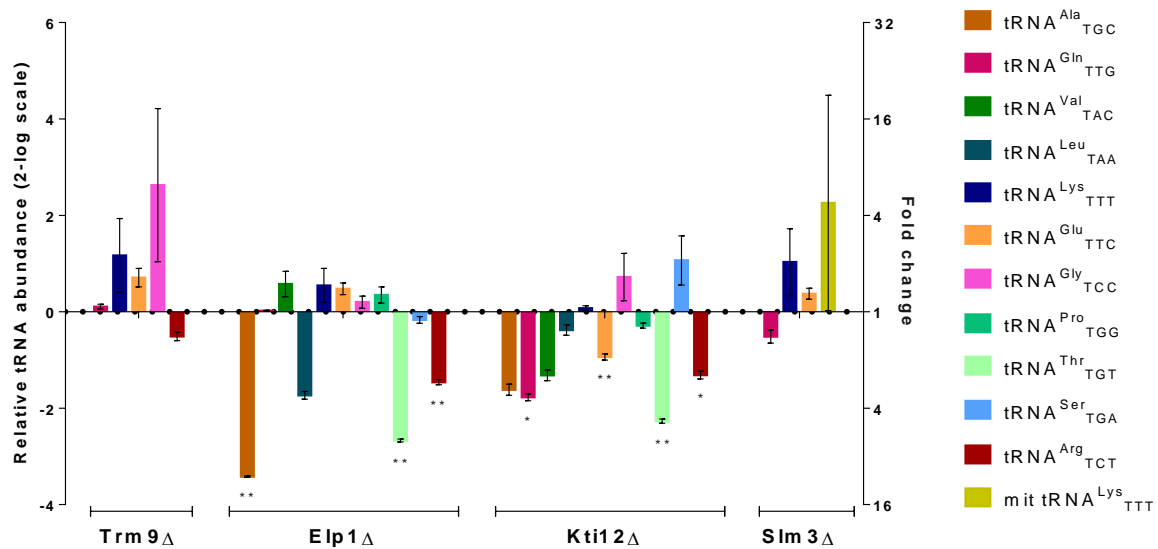


Figure 3.23. Quantification of wobble modified tRNAs in selected tRNAmoD KO strains. The plots show the level of each studied tRNA in mutant strains relative to the level

3. Genetic screen to identify RNAmods and their regulators

of the respective tRNA in WT control cells, obtained using Four-leaf clover qRT-PCR method. Data represent relative tRNA abundance \pm SD in a 2-log scale (calculated with REST software (Pfaffl, Horgan and Dempfle, 2002)).

3.3 DISCUSSION

Our genetic screen identified yeast RNAmod genes whose deletion results in increased protein aggregation. These KO strains harbor deletions in RNAmod genes whose proteins modify the wobble uridine at position 34 (U₃₄) of tRNA and some nucleosides in rRNA. These data are in line with previous results showing that modification of the anticodon loop ribonucleosides modulate translational fidelity and efficiency, namely reading frame maintenance and/or restriction or improvement of codon-anticodon interactions (Agris, Vendeix and Graham, 2007). Our data are also consistent with previous observations showing that modifications at the wobble position could affect anticodon positioning in the ribosome and allow for codon-dependent translation of specific transcripts, namely translation of DNA damage response genes (Agris, 2004, 2008; Begley *et al.*, 2007; Huang, Lu and Byström, 2008).

Most tRNA-modifying enzymes are encoded by nonessential genes whose deletion does not affect cell growth (exception for Trm1 and Bud32 KO strains) (Giaever *et al.*, 2002). Our results showed that some tRNAmod KO strains cannot be significantly differentiated from their WT parental strains in the level of cell growth or protein aggregation, but around 80% of the deletions increased protein aggregation. Previous reports showed that combined deletions decrease fitness and produce new phenotypes, indicating that tRNAmods interact (epistasis) (Alexandrov *et al.*, 2006; Chen, Tuck and Byström, 2009; Bauer *et al.*, 2012; and our bioinformatic data), which may explain the lack of visible phenotype in some of our KO strains. Conversely, most of the rRNA-modifying enzymes are encoded by essential genes and deletion of a single allele in diploid backgrounds is sufficient to produce fitness and protein aggregation phenotypes.

The lack of strong phenotypes in some of the tRNAmod KO strains, particularly in the methyltransferase-deficient strains, complicates the elucidation of the respective biological roles. As mentioned before, of the 42 cytosolic yeast tRNA

3. Genetic screen to identify RNAmods and their regulators

species, 11 have modified uridine at position 34: ncm^5U , ncm^5Um , mcm^5U or $\text{mcm}^5\text{s}^2\text{U}$ ($\text{tRNA}^{\text{Leu}}_{\text{ncm}^5\text{UmAA}}$, $\text{tRNA}^{\text{Val}}_{\text{ncm}^5\text{UAC}}$, $\text{tRNA}^{\text{Ser}}_{\text{ncm}^5\text{UGA}}$, $\text{tRNA}^{\text{Pro}}_{\text{ncm}^5\text{UGU}}$, $\text{tRNA}^{\text{Thr}}_{\text{ncm}^5\text{UGU}}$, $\text{tRNA}^{\text{Ala}}_{\text{ncm}^5\text{UGC}}$, $\text{tRNA}^{\text{Arg}}_{\text{mcm}^5\text{UCU}}$, $\text{tRNA}^{\text{Gly}}_{\text{mcm}^5\text{UCC}}$, $\text{tRNA}^{\text{Gln}}_{\text{mcm}^5\text{s}^2\text{UUG}}$, $\text{tRNA}^{\text{Lys}}_{\text{mcm}^5\text{s}^2\text{UUU}}$ and $\text{tRNA}^{\text{Glu}}_{\text{mcm}^5\text{s}^2\text{UUC}}$) (Johansson *et al.*, 2008). Synthesis of ncm^5 and mcm^5 chains at U_{34} requires at least 13 proteins (Table 2.1 and Figure 3.3), but our genetic screen showed that only deletion of Elp1, Kti12 and Trm9 had significant impact on protein aggregation (Elp1 Δ : 21.8-fold; Kti12 Δ : 17.5-fold; Trm9 Δ : 14.3-fold change relative to WT; Figure 3.10A). Other studies with Elp1 Δ -Elp6 Δ , Kti11 Δ , Kti12 Δ , Kti14 Δ , Trm9 Δ or Sit4 Δ strains confirmed the absence of $\text{mcm}^5\text{U}_{34}$ and $\text{mcm}^5\text{s}^2\text{U}_{34}$ nucleosides in total tRNAs and $\text{ncm}^5\text{U}_{34}$ was absent in one of the possible 5 tRNA isoacceptors ($\text{tRNA}^{\text{Pro}}_{\text{ncm}^5\text{UGG}}$). Deletion of the Kti13 gene resulted in reduced levels of those nucleosides (Huang, Johansson and Byström, 2005; Huang, Lu and Byström, 2008). Elp3 Δ also showed decrease in ncm^5U modification in three out of 5 tRNAs, namely $\text{tRNA}^{\text{Ala}}_{\text{ncm}^5\text{UGC}}$, $\text{tRNA}^{\text{Ser}}_{\text{ncm}^5\text{UGA}}$ and $\text{tRNA}^{\text{Thr}}_{\text{ncm}^5\text{UGU}}$ (Johansson *et al.*, 2008). We have also observed a significant decrease or complete absence of those modified nucleosides in the Elp1 Δ , Kti12 Δ and Trm9 Δ strains and also absence and significant decrease of $\text{ncm}^5\text{U}_{34}$ and $\text{ncm}^5\text{Um}_{34}$ nucleosides (Figure 3.20, Annex V.1 and Annex V.2) in Elp1 Δ and Kti12 Δ strains, respectively. Therefore, it is not clear why certain deletions produced stronger protein aggregation phenotypes than others. Elp1 and, consequently its regulator Kti12, are critical enzymes for tRNA^{Ala} and $\text{tRNA}^{\text{Thr}}_{\text{ncm}^5\text{U}_{34}}$ modification since their deletion reduces dramatically the abundance of these tRNAs (Figure 3.23), suggesting that the strong protein aggregation phenotype observed may be due to ribosome pausing at the codons lacking a cognate tRNA. It is also likely that absence of $\text{ncm}^5\text{U}_{34}$, $\text{ncm}^5\text{Um}_{34}$, $\text{mcm}^5\text{U}_{34}$ and $\text{mcm}^5\text{s}^2\text{U}_{34}$ in Elp1-Elp6, Kti11-Kti14, Trm9 and Sit4 is dependent on the genetic background of the strains. Indeed, some homozygous diploid deletions were lethal in our BY4743 yeast strains, whereas other haploid yeast strains (e. g. W303) harboring the same deletions are viable (Huang, Johansson and Byström, 2005; Björk *et al.*, 2007; Chen, Huang, Eliasson, *et al.*, 2011; Bauer *et al.*, 2012).

3. Genetic screen to identify RNAmods and their regulators

3.3.1 Proteins involved in the U₃₄ modification are critical for proteostasis

3.3.1.1 The Elongator complex

Disruption of the yeast genes encoding Elongator proteins produces similar phenotypes, namely slow growth, slow gene activation and sensitivity to temperature and various chemicals (Wittschieben *et al.*, 1999; Krogan and Greenblatt, 2001; Winkler *et al.*, 2001). However, in our genetic screen Elp1Δ produced much higher levels of protein aggregates than the other subunits of the Elongator complex (Elp1Δ: 21.8-fold; Elp2Δ: 2.2-fold; Elp3Δ: 2.7-fold; Elp4Δ: 1.6-fold; Elp6Δ: 2.0-fold change relative to WT; Figure 3.10A and Table 3.2). ELP5 is an essential gene so we could not include it in our screen. Although, in a stress condition (37 °C), the Elongator complex had similar behavior between each element relative to the percentage of cells with protein aggregates (Figure 3.19A), suggesting that the main role of the cm⁵U₃₄ modification occurs in the translation of mRNAs needed to facilitate cell survival during stress, as previously reported during oxidative stress (Fernández-Vázquez *et al.*, 2013).

Table 3.2. Summary of the Elongator complex protein aggregation data. The symbol + indicates the relative increase in protein aggregation. Arbitrary scale.

Strains	Protein aggregation phenotype
Elp1Δ	+++++
Elp2Δ	++
Elp3Δ	+++
Elp4Δ	++
Elp6Δ	++

The Elongator complex is conserved in eukaryotes and inactivation of its subunits is associated with multiple defects, namely developmental, cell proliferation, cell migration and neuron projection defects (Close *et al.*, 2006; Johansen *et al.*, 2008; Chen, Tuck and Byström, 2009; Creppe *et al.*, 2009). In humans, inactivation of each one of its subunits produces different diseases. For instance, mutations in human Elp1 (IKBKAP) have been associated with the hereditary neuropathy Familial Dysautonomia, a severe recessive

3. Genetic screen to identify RNAmods and their regulators

neurodevelopmental disease (Anderson *et al.*, 2001; Slaugenhaupt *et al.*, 2001; Karlsborn *et al.*, 2014), and male infertility (Lin *et al.*, 2013), while mutations in other Elongator subunits, namely the human homologous Elp3 and Elp4, have been related to the neurologic disorders Amyotrophic Lateral Sclerosis (ALS) (Simpson *et al.*, 2009) and Rolandic Epilepsy (Strug *et al.*, 2009), respectively. Moreover, absence of Elp1 in mouse leads to embryonic lethality and defects in vascular and neural development (Chen *et al.*, 2009).

3.3.1.2 Regulators of the Elongator complex

Elongator complex is regulated by Kti11-Kti14, Sit4 or Sap185/Sap190 (Fichtner *et al.*, 2002, 2003, Jablonowski *et al.*, 2004, 2009; Petrakis *et al.*, 2005; Bär *et al.*, 2008; Mehlgarten *et al.*, 2009; Abdel-Fattah *et al.*, 2015; Kolaj-Robin *et al.*, 2015). Those enzymes were also included in our genetic screen, but their deletion did not significantly increase protein aggregation levels, relative to WT, except in the case of Kti12 Δ (Kti12 Δ : 17.5-fold; Kti13 Δ : 2.3-fold; Kti14 Δ : 1.9-fold; Sap185 Δ : 2.1-fold; Sap190 Δ : 1.5-fold; Sit4 Δ : 0.8-fold change relative to WT; Figure 3.10A). Kti14 Δ and Sit4 Δ did not increase the levels of protein aggregation, but the strains used were heterozygous diploids since the respective genes are essential. Kti11 is an essential gene (without heterozygous diploid strain) and was not included in our screen. However, similar protein aggregation phenotypes were observed in the absence of these regulatory factors, particularly in Kti12, relative to the Elongator mutants (Petrakis *et al.*, 2005). Most of these regulatory factors are also involved in other cellular functions. For instance, Kti11 (Dph3) is involved in the biosynthesis of diphthamide, a post-transcriptional modified histidine residue in eEF2 (Fichtner *et al.*, 2003; Bär *et al.*, 2008). Kti13 (Ats1) was identified as a suppressor of class 2 α -tubulin, and the Kti11/Kti13 heterodimer has a double role in modifications of tRNA and eEF2 (Bär *et al.*, 2008; Glatt *et al.*, 2015).

3. Genetic screen to identify RNAmods and their regulators

Table 3.3. Summary of protein aggregation data of the regulators of the Elongator complex. The symbol + indicates the relative increase in protein aggregation. Arbitrary scale.

Strains	Protein aggregation phenotype
Kti12 Δ	+++++
Kti13 Δ	++
Kti14 Δ	++
Sit4 Δ	++
Sap185 Δ	+
Sap190 Δ	+

3.3.1.3 *Trm9 methyltransferase and its regulator*

We observed a significant increase in protein aggregation in Trm9 Δ (Trm9 Δ : 14.3-fold relative to WT; Figure 3.10A) relative to the enzymes that complete the synthesis of mcm⁵U₃₄. Since Trm112 mutants had a severe negative growth phenotype (Chen, Huang, Anderson, *et al.*, 2011), we used a heterozygous diploid strain in our studies that do not show increased protein aggregation (Trm112 Δ : 3.2-fold relative to WT; Figure 3.10A).

Previous studies show that Trm9 Δ strain grows slow in YEPD medium at both 30 °C and 37 °C (Chen, Huang, Anderson, *et al.*, 2011) and our data showed a similar fitness defect (Figure 3.18 and Figure 3.19B). Additionally, Trm9 has been associated with modulation of the toxicity of methylmethanesulfonate (MMS) and ionizing radiation (particularly, γ radiation) (Bennett *et al.*, 2001; Begley *et al.*, 2007; Chan *et al.*, 2010); Trm9-deficient yeast cells are sensitive to these DNA damaging agents. Cells deficient in Trm9 also displayed sensitivity to the translational error inducing antibiotic paromomycin at elevated temperatures (Kalhor and Clarke, 2003). Trm9 mammalian homologs are ALKBH8 and KIAA1456, also known as hTRM9L (human TRM9-like protein). The hTRM9L gene is located in the end of human chromosome 8, a region frequently lost or silenced in various types of cancer, including colorectal tumors, suggesting that hTRM9L is a tumor suppressor gene (Flanagan *et al.*, 2004; Begley *et al.*, 2013) and its deletion may lead to aberrant proteins synthesis in these tumors.

3. Genetic screen to identify RNAmods and their regulators

3.3.1.4 Wobble uridine thiolases and respective modifiers in mt-tRNAs

Regarding wobble uridine thiolases and mitochondrial wobble uridine modifying enzymes, most of the gene deletions did not result in increased protein aggregation, except Cia1 and the mitochondrial enzymes Mto1 and Slm3 (Cia1 Δ : 6.9-fold; Mto1 Δ : 9.4-fold; Slm3 Δ : 39.9-fold change relative to WT; Figure 3.10B, C and Table 3.4). However, deletion of the Cdf1, Nbp35, Nfs1 and Cia1 genes (heterozygous diploids) is lethal, but not necessarily due to the lack of the 2-thio group in tRNAs. Nfs1 is a phosphate-containing cysteine desulfurase that supplies sulfur to many cellular processes (Grosjean, 2005), besides the 2-thio modification of both mitochondrial (mt) and cytosolic (cy) tRNAs, particularly tRNA^{Lys}_{UUU} (Nakai *et al.*, 2004). Interestingly, those essential genes belong to the cytosolic iron-sulfur cluster assembly (CIA) machinery, composed by WD40 protein, Cia1, the iron-only hydrogenase-like protein, Nar1 (not available for this work) and two cytosolic P-loop nucleoside triphosphatases (NTPases), Cdf1 and Nbp35 (Lill and Uhlenhoff, 2006). Cdf1, Nbp35 and Cia1 are required for the 2-thio modification of cy-tRNAs (Figure 3.3) (Nakai *et al.*, 2007). Two scaffold proteins Isu1 and Isu2 also required for the 2-thio modification of cy-tRNAs and mt-tRNAs. Depletion of Nfs1 or Isu proteins induces a strong defect in the 2-thio modification of cy-tRNAs (Nakai *et al.*, 2007). Additionally, a cytosolic ubiquitin-like protein (UBL), Urm1, and its partner sulfurtransferase, Uba4, as well as the two cytosolic 2-thioridine synthetases, Ncs6 and Ncs2, are required for the formation of s²U₃₄ in cy-tRNAs (Huang, Lu and Byström, 2008; Schlieker *et al.*, 2008; Leidel *et al.*, 2009; Noma, Sakaguchi and Suzuki, 2009). The importance of Ncs6 for the 2-thiolation of tRNAs are demonstrated by the absence of mcm⁵s²U with concomitant increase in the levels of mcm⁵U in strains lacking Ncs6 gene (Björk *et al.*, 2007). Another enzyme whose gene disruption resulted in partial reduction of 2-thio modification in cy-tRNAs is Tum1, which functions as sulfur carrier to catalyze sulfur transfer reactions (Björk *et al.*, 2007; Noma, Shigi and Tsutomu, 2009; Nakai, Nakai and Yano, 2017).

Lack of s²U₃₄ in tRNA anticodon was reported to modulate the decoding activity of RAA (R representing C, G or U) codons, since s²U₃₄ modification is present in tRNAs for Glu, Gln and Lys, and may affect the global translation profile (Begley *et*

3. Genetic screen to identify RNAmods and their regulators

al., 2007; Björk *et al.*, 2007). Thiolation of mt-tRNA^{Lys}_{UUU}, mt-tRNA^{Glu}_{UUC} and mt-tRNA^{Gln}_{UUG} is not altered in the absence of Urm1 and Uba4 enzymes, but is absent in strains lacking the Slm3 enzyme (Umeda *et al.*, 2005; Leidel *et al.*, 2009). Slm3 (also known as Mtu1 or Mto2) is a mitochondrial tRNA-specific 2-thiouridylase that is required for the formation of cmnm⁵s²U and τ m⁵s²U in mitochondrial tRNAs in yeast and mammals, respectively. It synthesizes the 2-thio group by using ATP and sulfur provided by a mediator, likely Nfs1 (Umeda *et al.*, 2005). In our study, the absence of this enzyme resulted in higher percentage of cells with protein aggregates (39.9-fold change relative to WT; Figure 3.10C). We have also observed a decrease in mcm⁵s²U₃₄ with concomitant increase in mcm⁵U₃₄ (Figure 3.20), suggesting an additional effect in the thiolation of the cytosolic tRNAs. This supports the hypothesis that Slm3 affects the synthesis of mcm⁵s²U₃₄ in some cytoplasmic tRNAs, contrary of what was observed in cy-tRNA^{Lys}_{mcm5s2UUU} (Umeda *et al.*, 2005). Mss1 and Mto1 genes are responsible for the biosynthesis of the cmnm⁵ group of cmnm⁵s²U₃₄ in mt-tRNA^{Lys}, since Mss1 and Mto1 mutants lack cmnm⁵s²U modified nucleoside but have s²U₃₄ (Umeda *et al.*, 2005). These observations suggest that the modifications of positions 2 and 5 of U₃₄ in mt-tRNAs proceed independently, as observed in cy-tRNAs. Mto1 and Mss1 form a functional heterodimer complex (Colby, Wu and Tzagoloff, 1998) and Mss1 and Mto1 mutants cause mitochondrial dysfunction, but the effect is weaker than that observed in Slm3 Δ (Umeda *et al.*, 2005), similarly to what we have observed in our protein aggregation study (Mss1 Δ : 3.2-fold; Mto1 Δ : 9.4-fold change relative to WT; Figure 3.10C). These results suggest that the 2-thio modification of mt-tRNAs is important for mitochondrial translation, but our observation that mcm⁵s²U modified nucleoside was also decreased in Slm3 Δ (Figure 3.20) suggests an additional function of Slm3 in the 2-thiolation of cy-tRNAs. Thus, defects in both mitochondrial and cytosolic translational fidelity may explain the higher percentage of cells with protein aggregation observed in Slm3 Δ (Figure 3.10C).

3. Genetic screen to identify RNAmods and their regulators

Table 3.4. Summary of protein aggregation data of the U₃₄ thiolases and modifiers of mt-tRNAs. The symbol + indicates the relative increase in protein aggregation. Arbitrary scale.

Strains	Protein aggregation phenotype
Slm3Δ	+++++
Mto1Δ	+++++
Cia1Δ	+++++
Cfd1Δ	++
Nbp35Δ	+
Ncs2Δ	++
Ncs6Δ	++
Tum1Δ	+++
Urm1Δ	++
Uba4Δ	++
Isu1Δ	+++
Isu2Δ	++
Mss1Δ	+++
Nfs1Δ	+++

The absence of those modified nucleosides in only one mt-tRNA (mt-tRNA^{Lys}_{Tm5s2UUU}) is associated to the human MERRF disease (myoclonic epilepsy with ragged-red fibers) (Yasukawa *et al.*, 2001; Umeda *et al.*, 2005). Additionally, down-regulation of Mss1, Mto1 and Slm3 was observed in another mitochondrial disorder called MELAS (mitochondrial encephalomyopathy, lactic acidosis and stroke-like episodes) (Meseguer *et al.*, 2015). In other words, hypomodified mt-tRNAs in MELAS and MERFF are likely to alter the expression of nuclear-encoded mitochondrial proteins, resulting in serious mitochondrial dysfunctions (Meseguer *et al.*, 2015). Mutations in the Slm3 gene were also associated with acute infantile liver failure (Zeharia *et al.*, 2009; Wu *et al.*, 2016). The mechanism of these diseases is unknown but the steady-state levels of the hypomodified mt-tRNAs present in cells lacking Slm3 may decrease to critical levels compromising protein synthesis (Wang, Yan and Guan, 2007). In any case we did not observe differences in the levels of mt-tRNA^{Lys} relative to WT cells (Figure 3.23). The aminoacylation levels of

3. Genetic screen to identify rRNAmods and their regulators

unmodified mt-tRNAs were also reported to decrease, since unmodified mt-tRNAs are poor substrates for cognate aminoacyl-tRNA synthetases (Wang, Yan and Guan, 2009, 2010). Moreover, the loss of both $\text{cmnm}^5\text{U}_{34}$ and s^2U_{34} modifications has been related to significant failures in mitochondrial metabolism, complete loss of mitochondrial protein synthesis, instability of mitochondrial genome and a respiratory deficient phenotype (Wang, Yan and Guan, 2009, 2010). These phenotypes were not evaluated in our study, but it will be interesting to study them in future studies using our strains.

3.3.2 Deletion of rRNA-modifying enzymes causes protein aggregation

Regarding the strains harboring deletions in the 15 rRNAmods that we have analyzed (Figure 3.12), there was no statistical difference relative to the WT in the percentage of cells containing protein aggregates, but deletion of $\text{Shq1}\Delta$ and $\text{Spb1}\Delta$ resulted in increased levels of protein aggregates ($\text{Shq1}\Delta$: 14.2-fold; $\text{Spb1}\Delta$: 18.4-fold; $\text{Cbf5}\Delta$: 2.7-fold; $\text{Dim1}\Delta$: 7.4-fold; $\text{Mrm1}\Delta$: 1.7-fold; $\text{Mrm2}\Delta$: 3.7-fold; $\text{Naf1}\Delta$: 6.2-fold; $\text{Nhp2}\Delta$: 1.0-fold; $\text{Nop1}\Delta$: 0.6-fold; $\text{Nop10}\Delta$: 3.2-fold; $\text{Nop2}\Delta$: 1.0-fold; $\text{Nop56}\Delta$: 0.5-fold; $\text{Nop58}\Delta$: 1.8-fold; $\text{Snu13}\Delta$: 2.1-fold; Figure 3.12). These values of protein aggregation could be underestimated since we used heterozygous diploid strains in almost all cases.

Spb1 is a SAM-dependent methyltransferase, that is enriched in the nucleolus and is involved in the methylation of 1 of the 67 2'-O-ribose-methylated sites in cytoplasmic rRNA, Gm_{2922} (D Kressler *et al.*, 1999). This modification occurs at a late rRNA processing stage, before the conversion of 27S into 25S (Lapeyre and Purushothaman, 2004). Spb1 is also capable of catalyzing the formation of Um_{2921} , next to their target nucleoside, in some conditions, since in normal growth conditions snR52 acts on rRNA prior to Spb1 (Grosjean, 2005). Those two putative target positions of Spb1 are in the A-loop of the catalytic center of the ribosome, which is important for docking tRNAs (Grosjean, 2005; Baxter-Roshek, Petrov and Dinman, 2007). Some mutations in Spb1 result in a strong growth defect and severe deficit in 60S ribosomal subunits, with impaired production of 25S and 5.8S rRNAs due to accumulation of 27SB pre-rRNAs. In the same way, blocking the formation of Gm ,

3. Genetic screen to identify rRNAmods and their regulators

but not Um, strongly affected ribosome biogenesis and/or translation (D Kressler *et al.*, 1999; Lapeyre and Purushothaman, 2004). Our observation of high protein aggregation levels in a heterozygous diploid strain for Spb1 Δ (Spb1 haploinsufficiency) are in line with previous results.

The other rRNAmod selected in our genetic screen was Shq1, which is an essential gene that encodes an assembly factor required for the stability and accumulation of box H/ACA snoRNPs, which in turn is involved in the pseudouridylation of rRNA precursors during ribosome biogenesis (Yang *et al.*, 2002; Grozdanov, Roy, *et al.*, 2009). Shq1 binds to the RNA-binding surface of Cbf5, the catalytic subunit of the box H/ACA snoRNP, through its C-terminal domain, whereas its N-terminal CS domain (CHORD-containing proteins and Sglt1) is homologous to the Hsp90 chaperone, suggesting its participation in chaperone-assisted maintenance or assembly of the H/ACA snoRNP (Godin *et al.*, 2009; Grozdanov, Roy, *et al.*, 2009; Walbott *et al.*, 2011). Genetic depletion of Shq1 resulted in ribosomal RNA processing defects due to the loss of stable accumulation of box H/ACA snoRNAs (Yang *et al.*, 2002).

As mentioned before, Cbf5 is the catalytic subunit of the box H/ACA snoRNP possessing a pseudouridine synthase activity that catalyzes the isomerization of uridine in rRNAs. Mutations in the Cbf5 homolog dyskerin are associated with X-linked dyskeratosis congenita (X-DC), a rare bone marrow failure syndrome. Those mutations in dyskerin modulate affinity of dyskerin for Shq1, suggesting that disruption of Shq1 function in the maturation of H/ACA snoRNPs could be a consequence of X-DC mutations (Grozdanov, Fernandez-Fuentes, *et al.*, 2009; Li, Duan, Li, Ma, *et al.*, 2011). X-DC mutations have also been identified in Nhp2 and Nop10 proteins, with impairment of the pre-RNP assembly (Trahan, Martel and Dragon, 2010). Other mutations in Shq1 have been identified in leukemia and human prostate cancers, indicating that Shq1 acts as a tumor suppressor (Bullinger *et al.*, 2010; Taylor *et al.*, 2010).

3. Genetic screen to identify RNAmods and their regulators

3.3.3 Phenotypic characterization of the selected KO strains

Extensive analysis of each RNAmod and of its (putative) role in protein aggregation allowed us to identify the 6 RNAmods that are more relevant for protein folding: 2 rRNA-modifying enzymes involved in two different types of rRNA modification (Gm/Um and Ψ) and 4 tRNA wobble uridine modifying enzymes that function in the different reactions to form $mcm^5s^2U_{34}$ and its intermediates.

We have observed a slight increase (not statistically significant) of insoluble proteins in the 6 selected mutant strains relative to WT, which was not comparable with the increase in protein aggregation observed in the genetic screen. However, we observed that the SDS-PAGE protein profiles of the tRNAmod mutants were different relative to the WT, suggesting that the proteins that aggregate in the mutant strains are different from those that aggregate in the WT control. However, this analysis should be repeated with sorted cells since our genetic screen data showed that 50% or more of the cells of the RNAmod KO strains did not have protein aggregates and isolation of insoluble proteins was done using cell cultures containing both types of cells.

3.3.3.1 Degradation pathway of aggregated proteins

There are at least three different types of cytoplasmic protein aggregates, namely aggregates forming juxtannuclear inclusions (JUNQs), insoluble protein deposits (IPODs) and aggresomes. The JUNQs occur after severe stress conditions and contain misfolded ubiquitylated proteins that cannot be refolded or degraded by the UPS. These structures usually co-localize with proteasomes and with Hsp104 (Kaganovich, Kopito and Frydman, 2008). The IPODs are large perivacuolar inclusions located at the cell periphery and are formed by non-ubiquitylated proteins. These structures can be formed either in stressed and non-stressed cells and usually co-localize with the autophagosome marker Atg8 and with Hsp104 (Kaganovich, Kopito and Frydman, 2008). The aggresomes were first observed in mammalian cells, in which the ubiquitin proteasome system is overloaded (Johnston, Ward and Kopito, 1998), and correspond to insoluble perinuclear inclusions frequently targeted for degradation *via* autophagy that co-localize with the

3. Genetic screen to identify RNAmods and their regulators

microtubule organizing center (Kopito, 2000). Aggresomes were also observed in yeast, but do not co-localize with Hsp104 (Wang *et al.*, 2009).

The selected RNAmod KO strains analyzed by transmission electron microscopy showed the presence of protein aggregates as electron dense materials in their cytoplasm and, interestingly, we could also observe that Elp1 and Kti12 KO strains (cm⁵U₃₄ synthesis) had larger and dense vacuoles (Figure 3.15), suggesting that protein degradation *via* the autophagy pathway is activated in these strains. On the other hand, Slm3 and Spb1 KO strains showed more dense material dispersed over the entire cytoplasm, which was similar to dispersed protein granules (Figure 3.15), suggesting that these aberrant proteins may activate different mechanisms involved in the recovery of misfolded/unfolded proteins or their degradation, namely the molecular chaperones and the ubiquitin-proteasome system (UPS); autophagy being an auxiliary process in this case. The overexpression of Hsp104 and the binding of Hsp104 to the aggregated proteins was demonstrated by our GFP-Hsp104 reporter.

As mentioned before, Elp1 and Kti12 KO strains showed large vacuoles in their cytoplasm, suggesting that degradation of aggregated proteins was active *via* autophagy in these cells. To better understand whether protein degradation was also active in the other KO strains, we have quantified proteasome activity. In fact, Elp1 and Kti12 mutants (containing large vacuoles) seemed to use only the autophagy pathway to target proteins for degradation, since proteasome activity was at basal levels (Figure 3.17). Proteasome activity was slightly increased in the other mutants, particularly in Trm9 Δ and Slm3 Δ . Regarding rRNAmod mutants, proteasome activity was increased in Spb1 Δ , but not in Shq1 Δ , suggesting that aberrant proteins are targeted to the autophagy pathway or somehow escape degradation. Indeed, the proteasome is not the major degradation pathway of aggregated proteins, since they normally block its activity (Bence, Sampat and Kopito, 2001). Thus, it is likely that protein aggregates are mainly degraded by autophagy, as observed in Elp1 Δ and Kti12 Δ .

3. Genetic screen to identify RNAmods and their regulators

3.3.4 Characterization of the KO strains

Our mass-spectrometry analysis of the tRNA modifications showed that the level of ncm^5U and ncm^5Um drops to nearly undetectable levels in the ELP1 and Kti12 KO strains, while $\text{mcm}^5\text{s}^2\text{U}$ levels were highly decreased in Trm9, ELP1, Kti12 and Slm3 KO strains (Figure 3.24).

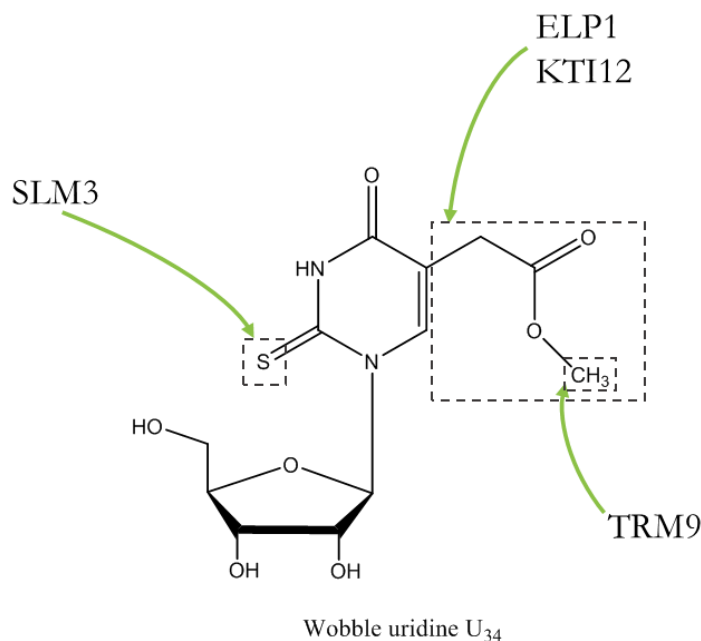


Figure 3.24. Synthesis of U₃₄ modification by the tRNAmods analyzed in this study.

Surprisingly, yW levels were decreased in strains with Trm9 and Kti12 deletions (0.13- and 0.36-fold) and were almost undetectable in the Slm3 mutant, suggesting that these enzymes influence critical pathways for yW formation, which was also observed in cells deficient in other tRNA modification enzymes (Chan *et al.*, 2010).

Interestingly, we have observed an increase in the modification levels of U₃₄ (I and mcm^5U ; 1.6 – 2.3-fold) in both Spb1 and Shq1 rRNA mutants, suggesting signature changes in tRNA modification to increase translation fidelity when ribosome biogenesis and function are impaired. Indeed, global pseudouridine defects in rRNA, as expected in the absence of Shq1, affect tRNA binding to the ribosome (Jack *et al.*, 2011).

3. Genetic screen to identify RNAmods and their regulators

The modifications of 25S and 18S rRNAs were almost undetectable or highly decreased in Spb1 and Shq1 mutants, with exception of the m⁴C modified nucleoside in the Spb1 mutant, which was slightly increased (Figure 3.21). Since deletion of Spb1 was previously associated with decrease in 60S subunit and pre-rRNA processing defects (D Kressler *et al.*, 1999; Lapeyre and Purushothaman, 2004), we expected that modifications in the 60S subunit would be absent. The increase of m⁴C suggests that its synthesis occurs prior to the action of both Spb1 and pseudouridylation H/ACA snoRNPs. In fact, Spb1 modification of the rRNA was reported to occur at a late processing stage (Lapeyre and Purushothaman, 2004). Interestingly, we could detect more modified nucleosides in rRNAs, particularly 5S and 5.8S, than the previously reported in bacteria and eukaryotes, namely hm⁵C, m¹acp³Ψ, m¹Ψ, m²₂G, m²G, m³U, m⁵C, and m⁶A (Cantara *et al.*, 2011; Machnicka *et al.*, 2013; Hia *et al.*, 2015). We isolated rRNAs by HPLC purification and used a highly sensitive chromatography-coupled mass spectrometry platform to identify modified ribonucleosides in RNA, which were confirmed with synthetic standards or CID fragmentation patterns. Again, we observed a specific pattern of modified nucleosides in the 5S and 5.8S rRNAs in the mutants lacking Shq1 and Spb1, probably to compensate the lack of modified nucleosides in 18S and 25S rRNAs.

The hypomodification of tRNAs results in decreased translational efficiency, increased translational errors and/or tRNA degradation. In fact, lack of tRNA modifications can induce specific RNA degradation pathways (Kadaba *et al.*, 2004; Alexandrov *et al.*, 2006; Kadaba, Wang and Anderson, 2006; Chernyakov *et al.*, 2008). For instance, loss of the m¹A₅₈ modification, due to mutation of Trm6 or Trm61, resulted in specific degradation of pre-tRNA^{Met}_i by the nuclear pre-tRNA surveillance pathway (Anderson *et al.*, 1998; Kadaba *et al.*, 2004). Contrary, the absence of m⁵C and m⁷G₄₆ modifications, due to deletion of Trm4 and Trm8 genes, resulted in rapid degradation and deacylation of mature tRNA^{Val}_{AAC} at elevated temperatures, by a mechanism distinct from the nuclear pre-tRNA surveillance pathway, the rapid tRNA degradation (RTD) pathway (Alexandrov *et al.*, 2006). Indeed, RTD pathway has been demonstrated to interact with the translation machinery and to act widely on hypomodified tRNAs (Dewe *et al.*, 2012). However, lack of a single modification or a combination of modifications only affects the levels

3. Genetic screen to identify RNAmods and their regulators

of one or two tRNA species, even when the modification occurs in various tRNAs. This was observed in 20 sequenced yeast tRNAs lacking m¹A₅₈ (Annex I.2), which is particularly associated with loss of pre-tRNA^{Met}_i (Anderson *et al.*, 1998). Also, the absence of m⁷G₄₆ and m⁵C₄₉ in 3 different tRNAs results in degradation of tRNA^{Val}_{AAC} only (Alexandrov *et al.*, 2006). Our results are in line with these published data since tRNA hypomodification in EIp1Δ and Kti12Δ strains only altered the levels of specific tRNAs: tRNA^{Ala}_{TGC} in EIp1Δ; tRNA^{Thr}_{TGT} and tRNA^{Arg}_{TCT} in both strains, and tRNA^{Gln}_{TTG} and tRNA^{Glu}_{TTC} in Kti12Δ (Figure 3.23). Hypomodification induced by Trm9 and Slm3 gene deletion did not reduce abundance of the affected tRNAs, as reported previously for Trm9Δ and the Tuc1Δ thiolase (Johansson *et al.*, 2008).

Our KO strains grew slightly slower than the WT control strain, possibly because protein refolding and degradation increased energetic requirements. Interestingly, we observed that growth phenotypes of mutant strains were more pronounced in solid media than in liquid culture (Figure 3.18B and D), particularly in the case of the rRNAmods mutants (Figure 3.18D).

Regarding cell viability, in the exponential phase and early stationary phase, all mutant strain cultures (excepting Shq1Δ) had slightly increased levels of death cells; 2-7-fold higher relative to WT cells (Annex IV.1), but the data were only statistically significant in middle stationary phase for Slm3, Trm9, Spb1 and Kti12 KO strains (Figure 3.18C). These differences decreased in stationary phase, suggesting that cell death occurred mainly during the initial stages of growth and that cells recover viability over time. For Shq1Δ, we did not observe significant differences in PI positive cells, relative to the control cells, suggesting that single copy expression of the RNAmod is sufficient to ensure cell viability and growth rate (Figure 3.18C).

Recent studies showed that translation elongation is dynamically regulated in presence of stress by the tRNA modification pattern (Gu, Begley and Dedon, 2014; Su *et al.*, 2014). We observed slightly higher levels of protein aggregation in the KO strains relative to WT (control) at 37 °C (120 min exposure), although without statistical significance (Figure 3.19A). Interestingly, all the Elongator KO strains had similar patterns of protein aggregation in this condition (Figure 3.19A), conversely to the observed during normal growth. This should be investigated in future studies.

3. Genetic screen to identify RNAmods and their regulators

3.4 CONCLUSION

The role of RNA modifications has been a subject of increasing study. Our study pointed out the relevance of modifications in the anticodon region of the tRNA for translation, being in line with previous studies (Laten, Gorman and Bock, 1978; Dihanich *et al.*, 1987; Lecointe *et al.*, 1998; Gerber and Keller, 1999; Björk *et al.*, 2001; Urbonavicius *et al.*, 2001; Pintard *et al.*, 2002; Kalhor and Clarke, 2003; Patil, Chan, *et al.*, 2012). We also observed an additional function of the thiolase SIm3, known as a mitochondrial enzyme, in the catalysis of cytoplasmic tRNAs and with high impact on protein synthesis fidelity.

**4. U₃₄ MODIFICATIONS OF tRNA
ANTICODONS MAINTAIN
PROTEOME INTEGRITY**

4. tRNA modifications at U₃₄ maintain proteome integrity avoiding mistranslation

4.1 INTRODUCTION

4.1.1 The role of modified nucleosides in translation

The role of tRNAs in translating the genome is critical for life. In yeast, the 42 different cytoplasmic tRNAs (1 initiator and 41 elongator tRNAs), encoded by 275 tRNA genes, are responsible for reading 61 sense codons, which code for the 20 universal amino acids (Percudani, Pavesi and Ottonello, 1997; Hani and Feldmann, 1998; Marck and Grosjean, 2002; <http://gtrnadb.ucsc.edu/genomes/eukaryota/Scere3/>). The same amino acid can have 2 or 3 synonymous triplets belonging to degenerated codon family boxes (Crick, 1968). There are 8 boxes in which all 4 codons belong to the same amino acid, known as unsplit boxes (Leu, Val, Gly, Arg, Ala, Thr, Pro and Ser); five boxes in which the two pyrimidine ending codons belong to one amino acid and the two purine ending codons belong to another, known as two-split boxes (Phe/Leu, His/Gln, Asn/Lys, Asp/Glu and Ser/Arg); and three special codon boxes (Ile/Met, Tyr/Stop and Cys/Stop/Trp) (Figure 4.1) (Crick, 1968).

		2 nd position of codon				
		U	C	A	G	
1 st position of codon	U	Phe	Ser	Tyr	Cys	U
		Leu		Stop	Stop	A
	C	Leu	Pro	His	Arg	U
				Gln		A
A	Ile	Thr	Asn	Ser	U	
	Met		Lys	Arg	A	
G	Val	Ala	Asp	Gly	U	
			Glu		A	
						G

Figure 4.1. The standard genetic code table. The standard genetic code covers 64 codons of which 61 encode 20 different amino acids and 3 encode stop codons. Unsplit boxes are shown in light grey; Stops codons are shown in dark grey.

4. tRNA modifications at U₃₄ maintain proteome integrity avoiding mistranslation

Decoding of the genetic code depends on the interaction between the three bases of the mRNA codon (numbered 1, 2 and 3) and the three bases of the cognate aminoacyl-tRNA anticodon (numbered 36, 35 and 34). Anticodon-codon pairing rules at the third codon position are flexible and allow one tRNA molecule to decode more than one codon triplet. In other words, the first base of the anticodon (position 34 or wobble nucleoside) may pair with more than one base in the third position of the codon (Crick, 1966); wobble rules. Additionally, nucleoside modification in tRNA anticodons guarantee that the decoding process is rigorous enough to differentiate between closely related codons, but also relaxed enough to allow decoding of more than one codon.

The first anticodon modifications to be associated with the recognition of specific codons by tRNA were at the wobble position 34, namely inosine, and at the conserved purine 37, 3' adjacent to the anticodon, namely N⁶-isopentenyladenosine (Crick, 1966; Gustilo, Vendeix and Agris, 2008). U at position 34 of the anticodon was initially considered to be able to recognize both A and G at the third position of the codon (Crick, 1966) and was later confirmed that modification of the uridine in the wobble position restrict and limit the recognition to only A and/or G in the third position of the codon. Unmodified U₃₄ can, in turn, recognize all four bases (Yokoyama *et al.*, 1985; Lim and Curran, 2001).

In two split codon-boxes, modifications function to better discriminate between the cognate pyrimidine-ending and noncognate purine-ending codons (Figure 4.2). For example, xnm⁵U in bacteria and xcm⁵U in eukaryotes (where x represents any of several different groups). Moreover, xm⁵s²U modification is responsible for decoding two codon sets that end in purine (R) (NNR codons). Since the conformation of xm⁵s²U is mostly fixed in C3'-endo form, conferring conformational rigidity, the xm⁵s²U modified nucleoside prefers to base pair with A and prevents misreading of NNY codons (Y for pyrimidine) (Agris, Soell and Seno, 1973; Yokoyama *et al.*, 1985). On the other hand, the presence of mcm⁵U₃₄ improves the ability of the tRNA to read G-ending codons (Johansson *et al.*, 2008).

In eukaryotes, all tri-pyrimidine anticodons (Lys – mcm⁵s²UUU, Arg – mcm⁵UCU, Glu – mcm⁵s²UUC, Gly – mcm⁵UCC) bear either mcm⁵U₃₄ or

4. tRNA modifications at U₃₄ maintain proteome integrity avoiding mistranslation

mcm⁵s²U₃₄. Additionally, the mcm⁵s² modification occurs only in the two tRNAs which contain U₃₅, while the mcm⁵U modification occurs for the two tRNAs which contain C₃₅. The other anticodon harboring mcm⁵s²U₃₄ (Gln – mcm⁵s²UUG) also contains a U₃₅. Thus, anticodon sequence context is central to understanding the function of tRNA modifications (Grosjean, 2009a).

Moreover, position 37 of the anticodon stem loop, also called the dangling base, is often modified to i⁶A₃₇, t⁶A₃₇, m¹I₃₇, m¹G₃₇ and yW₃₇. Usually, when position 36 is an A or U, position 37 is modified. Modifications at this position increase stacking, ordering the 3' side of the anticodon domain (Agris, 2008). During translation, the modified nucleoside at position 37 moves to a position above the third base of the anticodon and the first base of the codon to maintain the 3'-stack of the anticodon domain and stabilize the first base pair of the anticodon-codon interaction, facilitating codon binding (Agris, 1996, 2004). The diversity of modifications mostly stabilizes the first base pair of the codon-anticodon interaction, particularly A•U and U•A pairs and contributes to accurate decoding by reducing frameshifts (Agris, 1996, 2008; Urbonavicius *et al.*, 2001).

4. tRNA modifications at U₃₄ maintain proteome integrity avoiding mistranslation

Codon	Anticodon	Amino acid	Codon	Anticodon	Amino acid
UUU UUC	GmAA	Phe	UCU UCC	IGA	Ser
UUA UUG	ncm ⁵ UmAA m ⁵ CAA	Leu	UCA UCG	ncm ⁵ UGA CGA	
CUU CUC CUA CUG	GAG UAG	Leu	CCU CCC CCA CCG	AGG ncm ⁵ UGG	Pro
AUU AUC AUA	IAU ΨAΨ	Ile	ACU ACC ACA	IGU ncm ⁵ UGU	Thr
AUG	CAU	Met	ACG	CGU	
GUU GUC GUA GUG	IAC ncm ⁵ UAC CAC	Val	GCU GCC GCA GCG	IGC ncm ⁵ UGC	Ala
UAU UAC	GΨA	Tyr	UGU UGC	GCA	Cys
UAA UAG		Stop	UGA UGG		Stop Trp
CAU CAC	GUG	His	CGU CGC	ICG	Arg
CAA CAG	mcm ⁵ s ² UUG CUG	Gln	CGA CGG	CCG	
AAU AAC	GUU	Asn	AGU AGC	GCU	Ser
AAA AAG	mcm ⁵ s ² UUU CUU	Lys	AGA AGG	mcm ⁵ UCU CCU	Arg
GAU GAC	GUC	Asp	GGU GGC	GCC	Gly
GAA GAG	mcm ⁵ s ² UUC CUC	Glu	GGA GGG	mcm ⁵ UCC CCC	

Figure 4.2. Codon-anticodon pairing rules (yeast).

4.1.2 The role of modified nucleosides in translational accuracy

Ribosomal selection of a tRNA depends in part on the modification pattern of the tRNA and can be divided in two stages. First, the ribosome detects whether the mRNA-tRNA pairing is correct by checking the formation of Watson-Crick base pairs in the first two positions of the codon-anticodon minihelix. Non-cognate tRNAs are rejected, while near-cognate tRNAs are discriminated against with lower binding

4. tRNA modifications at U₃₄ maintain proteome integrity avoiding mistranslation

energy compared to cognate tRNAs. This energy of binding of the tRNA to the codon is a critical component of the second stage of the ribosomal selection. If the binding energy for a cognate tRNA to the codon is insufficient, the dissociation energy will increase and the tRNA has higher probability of being rejected (Rodnina and Wintermeyer, 2001). The RNA modifications are important for regulation of the energy of binding of the tRNA to a codon presented in the ribosomal A-site. This regulation can be achieved by influencing the structure of the anticodon stem loop prior to binding to the A-site and/or the energetics of base pairing at the wobble position (Yarian *et al.*, 2002; Grosjean, 2009a). In fact, hypomodification of the U₃₄ residue may lead to misreading in the third position of the codon and consequently the incorporation of the wrong amino acid into proteins. Although the decoding of the mRNA is faithful, errors occur at frequency of 10⁻³ to 10⁻⁴ per codon (Bouadloun, Donner and Kurland, 1983; Farabaugh and Björk, 1999). Most missense errors are not deleterious, since many amino acid substitutions are conservative and do not affect protein structure, but, in contrast, almost all frameshift errors are harmful due to the usual inactivation of the peptide caused by the shift in the reading frame (Farabaugh and Björk, 1999). Nucleoside hypomodification also influences frameshifting frequency (Qian *et al.*, 1998; Urbonavicius *et al.*, 2001).

4.1.3 Overview of this study

In this part of the thesis, we investigated the role of wobble uridine modifications, ncm⁵U₃₄, mcm⁵U₃₄ and mcm⁵s²U₃₄, on translational fidelity. Our main objective was to clarify if protein aggregation induced by tRNA hypomodification could be related to codon mistranslation. For this, we biochemically isolated aggregated proteins from yeast strains lacking Trm9, Elp1 or Slm3 tRNA-modifying enzymes, which modify the anticodons of 11 tRNAs in yeast (Kalhor and Clarke, 2003; Johansson and Byström, 2005; Björk *et al.*, 2007; Huang, Lu and Byström, 2008; Johansson *et al.*, 2008). Elp1, an element of the Elongator complex, uses uridine as substrate and catalyzes the formation of cm⁵U at the wobble position of tRNA^{Arg}_{AGA}, tRNA^{Gly}_{GGA}, tRNA^{Lys}_{AAA}, tRNA^{Gln}_{UUG}, tRNA^{Glu}_{UUC}, tRNA^{Leu}_{UUA}, tRNA^{Val}_{GUA}, tRNA^{Ser}_{UCA}, tRNA^{Pro}_{CCA}, tRNA^{Thr}_{ACA} and tRNA^{Ala}_{GCA}. In association with Trm112, Trm9 uses

4. *tRNA modifications at U₃₄ maintain proteome integrity avoiding mistranslation*

cm⁵U as substrate to catalyze the formation of mcm⁵U at the wobble position of tRNA^{Arg}_{AGA}, tRNA^{Gly}_{GGA}, tRNA^{Lys}_{AAA}, tRNA^{Gln}_{UUG} and tRNA^{Glu}_{UUC} (Kalhor and Clarke, 2003; Huang, Johansson and Byström, 2005; Huang, Lu and Byström, 2008; Mazauric *et al.*, 2010; Chen, Huang, Anderson, *et al.*, 2011). Slm3 is involved in the thiolation of the wobble uridine of tRNA^{Lys}_{AAA}, tRNA^{Gln}_{UUG} and tRNA^{Glu}_{UUC}, to yield mcm⁵s²U, as suggested previously. With the overall goal of assessing the effects of loss of ncm⁵U, mcm⁵U and mcm⁵s²U on global protein translation, we used yeast cells harboring deletions in the genes encoding the Trm9, Elp1 and Slm3 enzymes. As mentioned before, these strains lacked the ncm⁵U, mcm⁵U and mcm⁵s²U ribonucleosides (Figure 3.20), but the abundance of most of the hypomodified tRNAs was not significantly affected (Figure 3.23). By crosschecking codon bias and gene ontology (GO) term analysis data with amino acid misincorporation data we found that loss of ncm⁵U, mcm⁵U or mcm⁵s²U increased amino acid misincorporations specifically at codons that are decoded by the hypomodified tRNAs.

4.2 RESULTS

4.2.1 Identification of proteins that aggregated in yeast strains lacking U₃₄ modification

We observed up-regulation of the Hsp104 cytosolic chaperone in strains that lacked U₃₄ modifications, indicating perturbation of the conformational integrity of proteins (Figure 3.9 and Figure 3.10). Accordingly, loss of U₃₄ modifications resulted in increased protein aggregation (Figure 4.3). To identify the aggregated proteins, we collected exponentially growing yeast cells from WT and Trm9 Δ , Elp1 Δ and Slm3 Δ strains. Aggregated proteins were isolated using differential density centrifugation and were identified and quantified using label-free LC-MS/MS (see Methods 2.8 and Figure 4.4). A total of 1116, 970 and 1250 proteins were identified as being up-regulated relative to WT (fold-change > 1.2) in Trm9 Δ , Elp1 Δ and Slm3 Δ strains, respectively. Of these, 274 proteins were found to aggregate in all KO strains (Figure 4.5). 392, 288 and 450 aggregated proteins were unique to Trm9, Elp1 and Slm3 KO strains, respectively (Figure 4.5). 78% of the proteins present in the

4. tRNA modifications at U₃₄ maintain proteome integrity avoiding mistranslation

insoluble fraction of our strains are aggregation-prone proteins previously identified in the insoluble fraction of yeast cells (Ibstedt *et al.*, 2014). However, the up-regulated proteins in the insoluble fractions of Trm9 Δ , Elp1 Δ and Slm3 Δ strains only included 8%, 27% and 7% of the aggregation-prone proteins identified in that study, respectively. In other words, most of the up-regulated proteins in each KO strain aggregated due to the absence of U₃₄ tRNA modification.

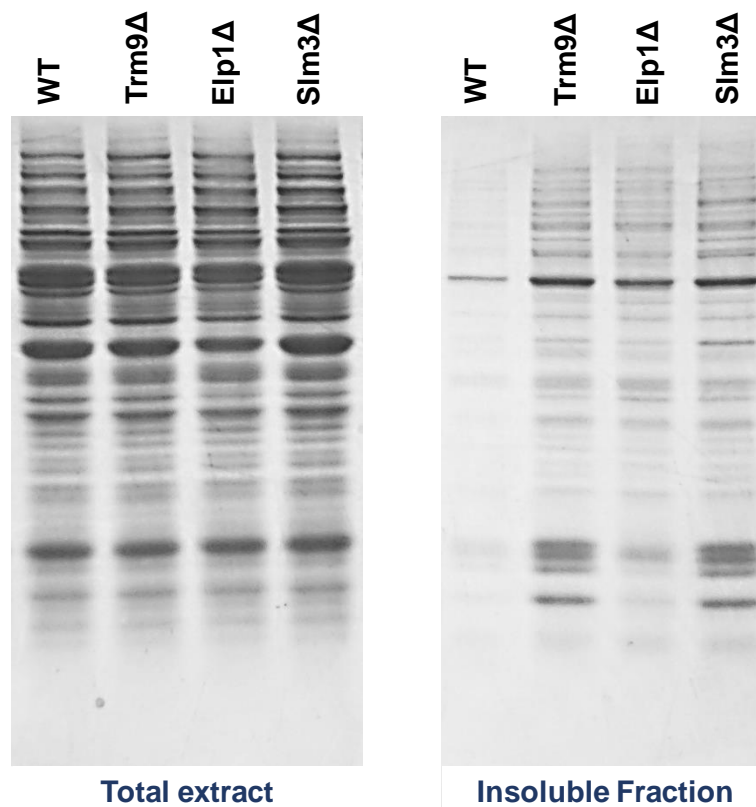


Figure 4.3. Absence of U₃₄ modifications leads to protein aggregation in yeast. Yeast growing cells of WT and KO strains were lysed with glass beads using a Precellys™ 24 disrupter. Insoluble protein fractions were then isolated by differential centrifugation. Total extracts and detergent insoluble protein aggregates isolated from WT and KO strains were visualized by SDS-PAGE (14%) and Coomassie staining.

4. tRNA modifications at U₃₄ maintain proteome integrity avoiding mistranslation

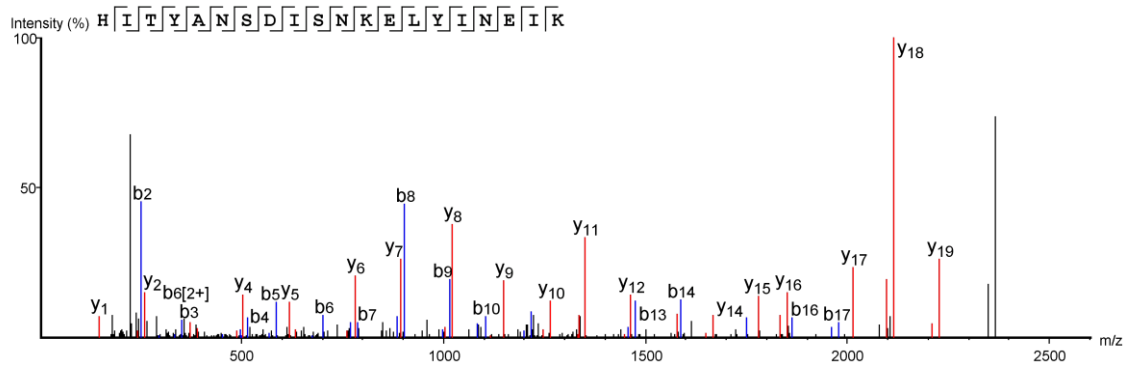
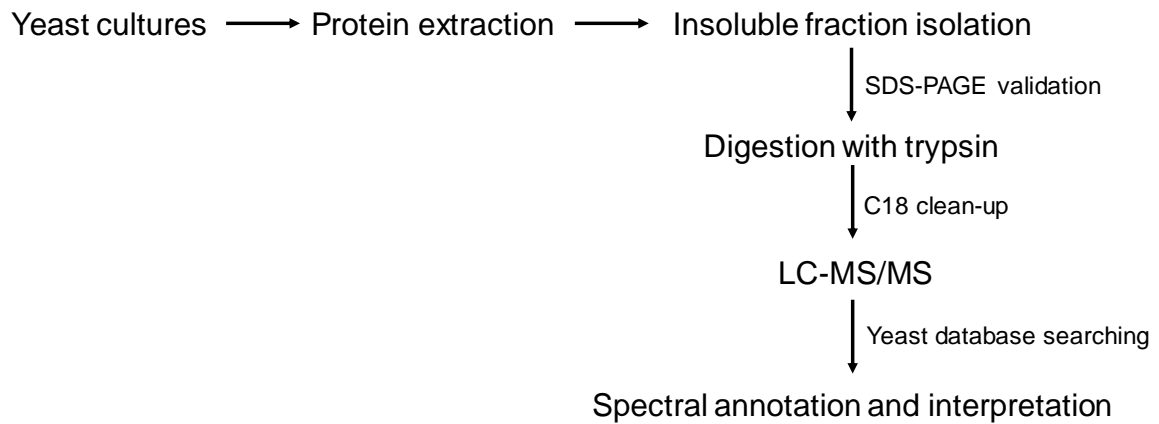


Figure 4.4. Workflow for proteome analysis of insoluble fractions by LC-MS/MS. Yeast cultures were lysed to isolate protein extracts and then insoluble proteins. Aggregated proteins were reduced, alkylated and tryptic digested into peptides in solution prior clean-up in a C18 column. Desalted peptides were separated by reversed-phase liquid chromatography and MS/MS spectra were acquired in an Orbitrap mass analyzer. Database search and interpretation of the search results were achieved using PEAKS Studio (v.8.0, Bioinformatics Solutions Inc.).

4. tRNA modifications at U₃₄ maintain proteome integrity avoiding mistranslation

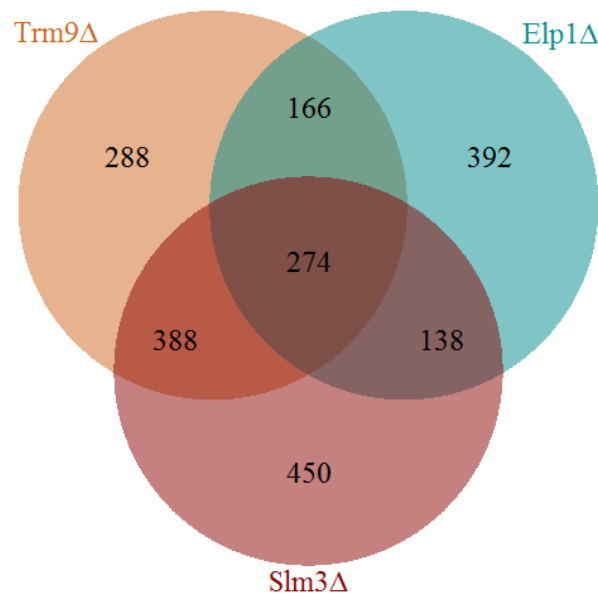


Figure 4.5. Label-free quantitative mass spectrometry identification of up-regulated proteins that aggregated in mutant strains, relative to WT. Venn diagram of the overlap between up-regulated aggregated proteins in each KO strain.

Aggregated proteins in Trm9 Δ and Slm3 Δ strains have higher molecular weight than the yeast proteome average (Figure 4.6D) and have a slight higher fraction of PEST sequences (Figure 4.6J), which are ubiquitination signals for protein degradation (Rogers, Wells and Rechsteiner, 1986). Aggregated proteins in Elp1 Δ have slightly larger size than the yeast proteome average (Figure 4.6D), but are clearly more abundant and highly expressed (indicated by high CAI) with higher translation rates and higher frequency in optimal codons than the yeast proteome/genome average (Figure 4.6A, B, E and F). Aggregated proteins in all KO strains have lower isoelectric point, hydrophobicity and aromaticity than the proteome average (Figure 4.6G, H and I).

4. tRNA modifications at U₃₄ maintain proteome integrity avoiding mistranslation

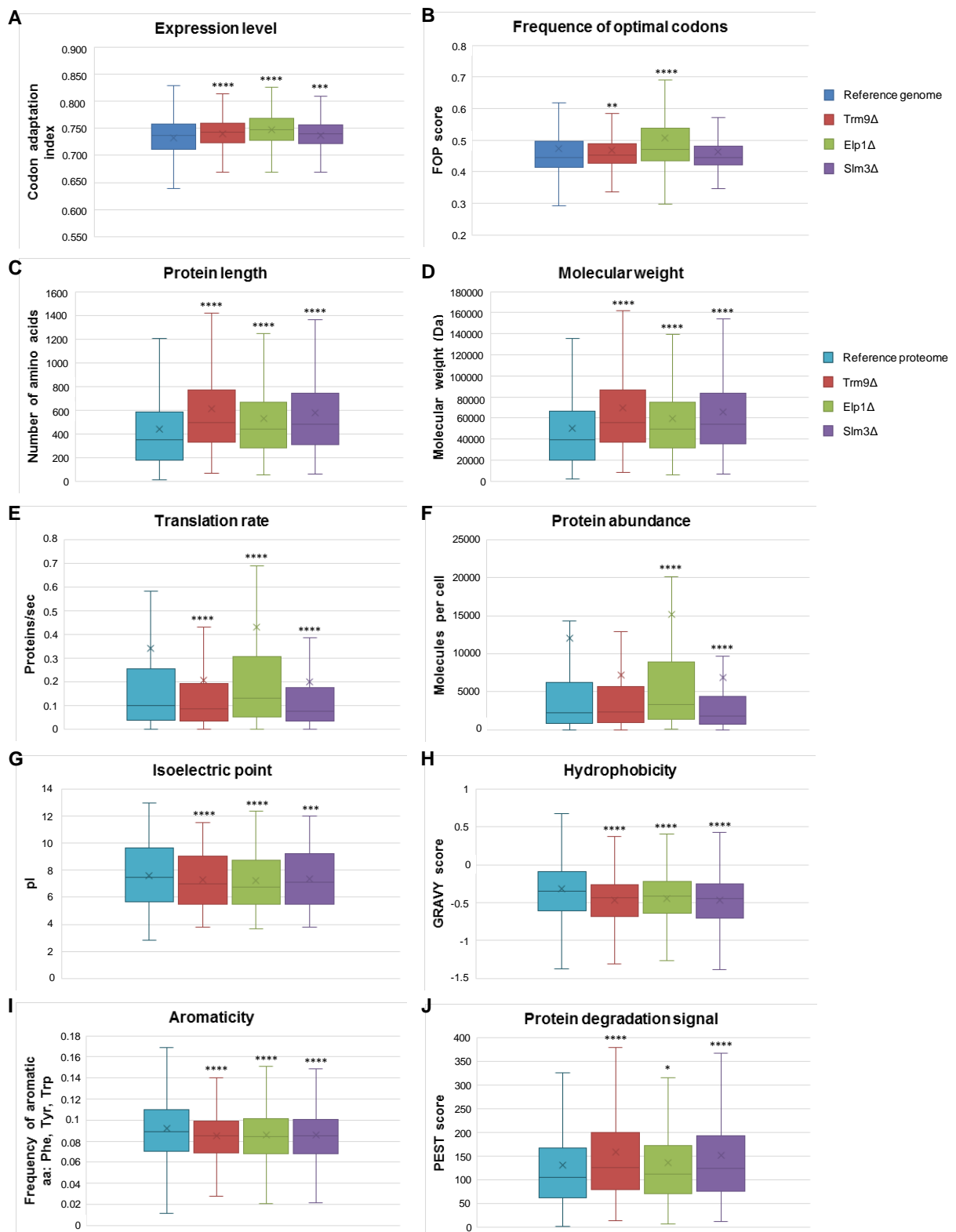


Figure 4.6. Biochemical characterization of up-regulated proteins that aggregated in the mutants lacking U₃₄ modifications. **A.** Predicted expression levels. The codon adaptation index (CAI) is an indication of gene expression level. **B.** Frequency of optimal codons in the aggregated proteins in each mutant strain relative to the reference genome.

4. *tRNA modifications at U₃₄ maintain proteome integrity avoiding mistranslation*

C. Protein length distribution in the aggregated proteins of the mutant strains relative to the reference proteome. **D.** Molecular weight distribution of the aggregated proteins of the mutant strains relative to the yeast proteome. **E.** Translation rates estimated per protein species in the insoluble fraction of the mutant strains relative to the average proteome. **F.** Protein abundance of the aggregated proteins in the KO strains relative to the proteome. **G.** Isoelectric point values for each dataset. **H.** Hydrophobicity of aggregated proteins in each dataset shown through the GRAVY scores. **I.** Frequency of the aromatic amino acids in the aggregated proteins of the KO strains relative to the proteome. **J.** Protein degradation signal of the aggregated proteins in each KO strains measured as the PEST score. (**** p < 0.0001, *** p < 0.001, ** p < 0.01, * p < 0.05 Mann Whitney test with CI 95% relative to Reference Genome/Proteome). x represents the mean of each set.

Gene ontology analysis indicated that aggregated proteins are enriched in certain functional categories. In the Trm9 Δ strain, functions related to DNA transcription, histone acetylation and chromatin silencing, RNA processing and ribosome biogenesis, tRNA wobble uridine modification, mRNA and tRNA catabolism, nuclear pore organization, microtubule-based movement and protein deacetylation were highly overrepresented (Figure 4.7). The Elp1 Δ strain was enriched in functions related to translation, regulation of chromatin silencing at telomeres, proteolysis involved in cellular protein catabolism, namely by proteasomal action, oxidation-reduction and various metabolic processes (Figure 4.8). Interestingly, Slm3 Δ , also proposed as mitochondrial tRNA-modifying enzyme, was enriched in functions related to mitochondrial translation, as well as nucleocytoplasmic transport (Figure 4.9). However, the percentage of mitochondrial proteins present in the insoluble protein fractions was similar in the three mutant strains (Trm9 Δ : 14.2%; Elp1 Δ : 15.7%; Slm3 Δ : 15.4%; 17.3% of mitochondrial proteins is shared).

As mentioned before, several aggregated proteins present in the insoluble protein fraction were shared by the 3 KO strains. These proteins are involved in DNA repair, replication, regulation of transcription, maturation of ribosomal subunits, protein polyubiquitination, signal transduction, cellular response to stress, cell cycle cytokinesis, among others (Figure 4.10 and Annex VIII.4). Glutathione metabolism and the sulfur relay system were enriched in all mutant strains (Annex VIII.4),

4. tRNA modifications at U₃₄ maintain proteome integrity avoiding mistranslation

whereas cell cycle, basal transcription factors and nucleotide excision repair pathways were enriched in Trm9Δ (Annex VIII.3A). Amino acids, purine and fatty acid metabolism, glycolysis/gluconeogenesis, amino acids and steroid biosynthesis, among other pathways were enriched in Eip1Δ (Annex VIII.3B).

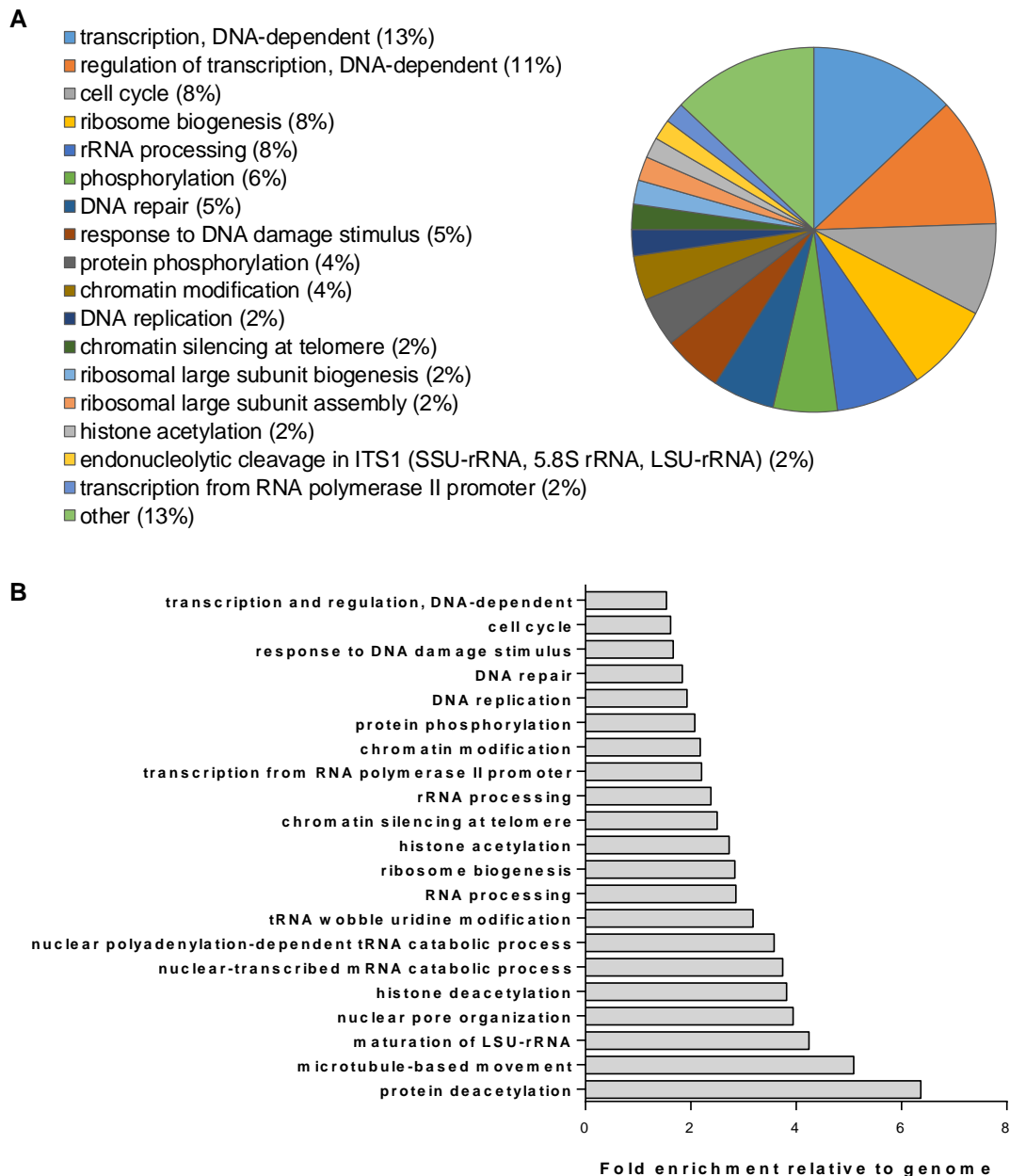


Figure 4.7. Functional enrichment in up-regulated proteins that aggregated in Trm9Δ. Biological processes that are significantly enriched in the insoluble fraction of Trm9Δ. **A.** Diagram indicates the distribution of aggregated proteins into functional categories. All shown categories were significant with 5% FDR. **B.** Bars indicate the fold-enrichment of

4. tRNA modifications at U₃₄ maintain proteome integrity avoiding mistranslation

functional categories compared to the genome using GO data from <http://genecodis.cnb.csic.es>.

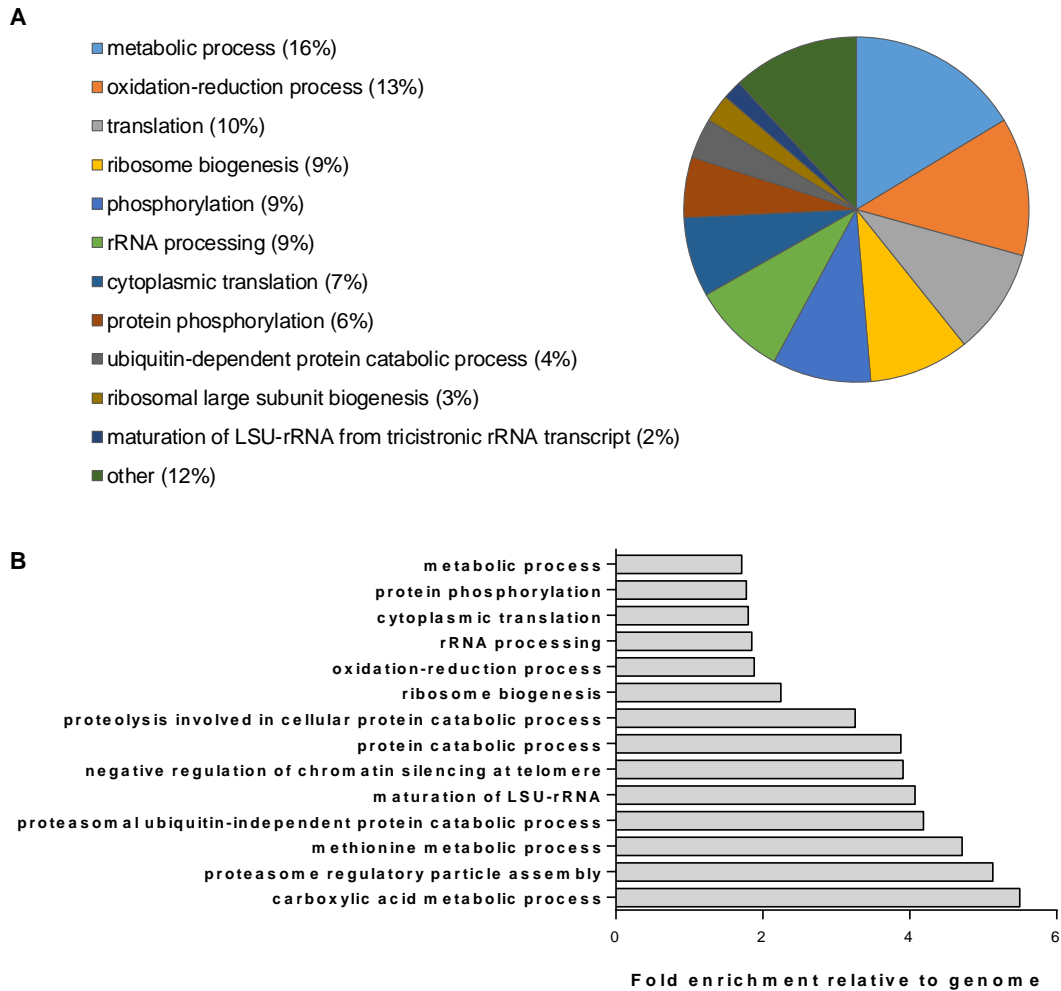


Figure 4.8. Functional enrichment in up-regulated proteins that aggregated in Elp1Δ. Biological processes that are significantly enriched in the insoluble fraction of Elp1Δ. **A.** Diagram indicates the distribution of aggregated proteins into functional categories. All shown categories were significant with 5% FDR. **B.** Bars indicate the fold-enrichment of functional categories compared to the genome using GO data from <http://genecodis.cnb.csic.es>.

4. tRNA modifications at U₃₄ maintain proteome integrity avoiding mistranslation

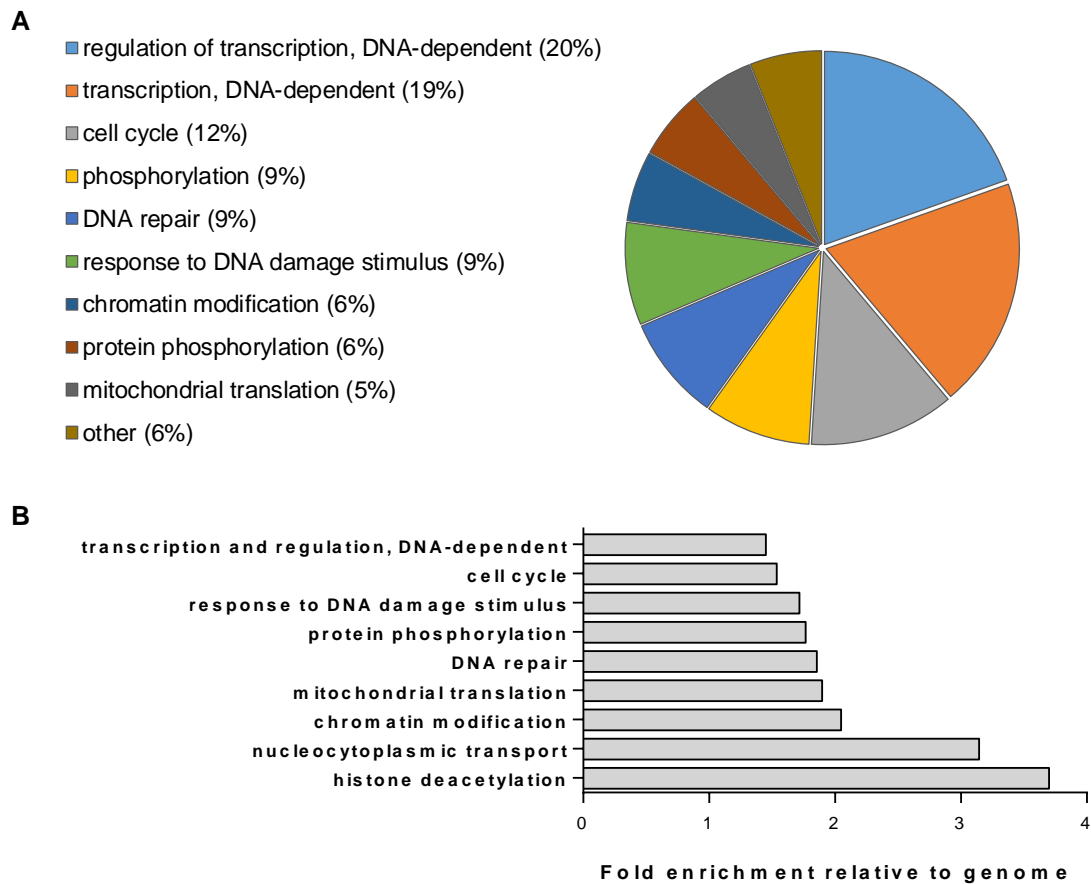


Figure 4.9. Functional enrichment in up-regulated proteins that aggregated in SIm3Δ. Biological processes that are significantly enriched in the insoluble fraction of SIm3Δ. **A.** Diagram indicates the distribution of aggregated proteins into functional categories. All shown categories were significant with 5% FDR. **B.** Bars indicate the fold-enrichment of functional categories compared to the genome using GO data from <http://genecodis.cnb.csic.es>.

4. tRNA modifications at U₃₄ maintain proteome integrity avoiding mistranslation

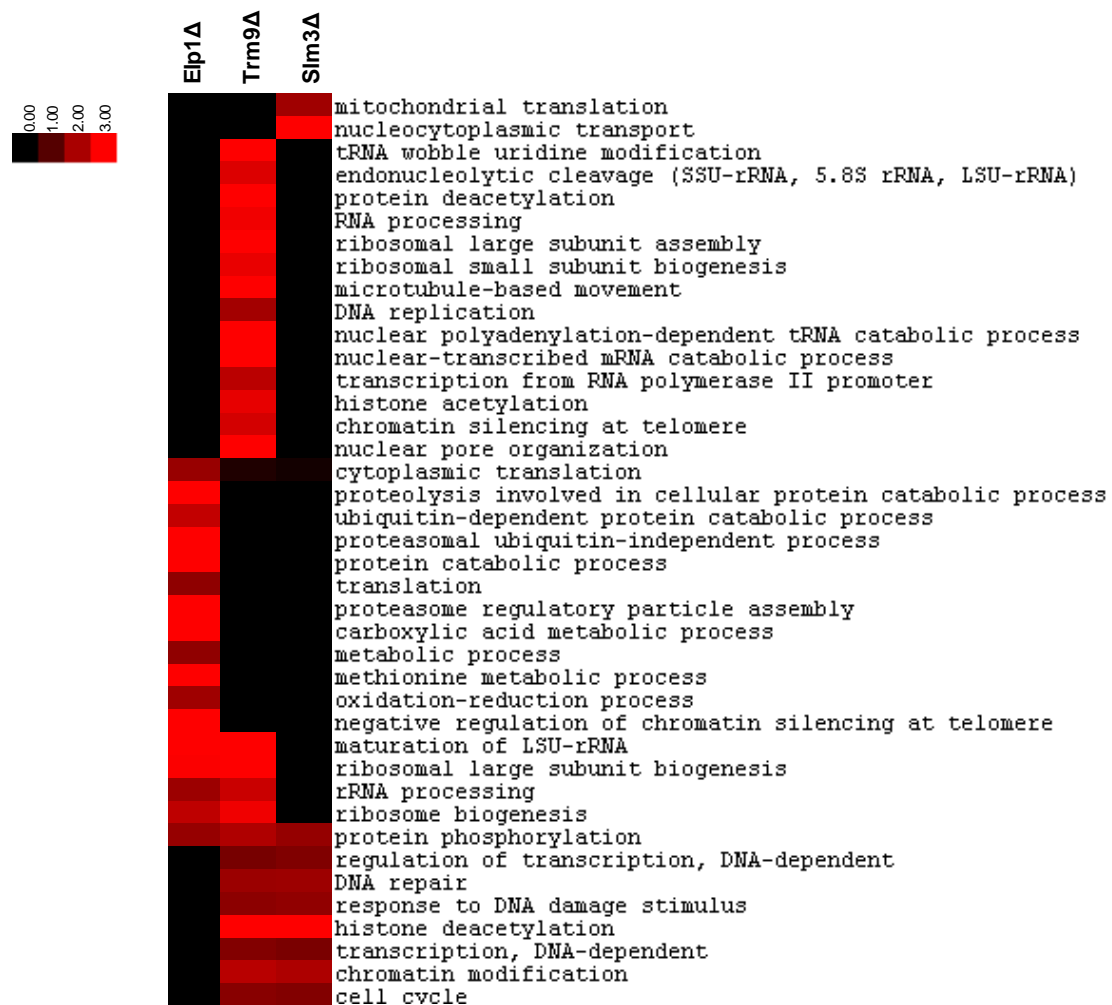


Figure 4.10. Heat-map of the functional enrichment in biological processes verified in the up-regulated proteins that aggregated in mutant strains. Biological processes that are significantly enriched in the insoluble fraction of each mutant strain compared to the genome using GO data from <http://genecodis.cnb.csic.es>. All shown categories were significant with 5% FDR.

4.2.2 Codon biases in the genes of the aggregated proteins

Some RNA-modifying enzymes have been associated to regulation of protein expression through modulation of translational speed of specific codons (Novoa and Ribas de Pouplana, 2012; Chevance, Le Guyon and Hughes, 2014). We hypothesized that genes encoding aggregated proteins should be enriched in codons whose translation is modulated by tRNA modifications catalyzed by Trm9, Eip1 and Slm3. In other words, we expected to identify proteins whose genes are

4. tRNA modifications at U₃₄ maintain proteome integrity avoiding mistranslation

enriched in codons decoded by the ncm⁵U₃₄ containing tRNAs, namely UUA, GUA, UCA, CCA, ACA and GCA in the Elp1Δ and AGA and GGA in the mcm⁵U₃₄ Elp1Δ and Trm9Δ insoluble fractions, as well as the mcm⁵s²U-dependent codons CAA, GAA and AAA in Elp1Δ, Trm9Δ and Slm3Δ insoluble fractions (Figure 4.11). Since the mcm⁵ side chain facilitates wobble decoding of A- and G-ending codons and ncm⁵ and s² side chains restrict wobble decoding to A (Lim and Curran, 2001; Johansson *et al.*, 2008; Grosjean and Westhof, 2016), proteins enriched in AGG and GGG may equally be affected by loss of U₃₄ modification (Figure 4.11).

Codon	Anticodon	Amino acid	Codon	Anticodon	Amino acid
UUU		Phe	UCU	IGA	Ser
UUC	GmAA		UCC		
UUA	ncm ⁵ UmAA	Leu	UCA	ncm ⁵ UGA	Ser
UUG	m ⁵ CAA		UCG	CGA	
CUU	GAG UAG	Leu	CCU	AGG	Pro
CUC			CCC	ncm ⁵ UGG	
CUA			CCA		
CUG			CCG		
AUU	IAU	Ile	ACU	IGU	Thr
AUC	ΨAΨ		ACC	ncm ⁵ UGU	
AUA			ACA		
AUG	CAU	Met	ACG	CGU	
GUU	IAC	Val	GCU	IGC	Ala
GUC	ncm ⁵ UAC		GCC	ncm ⁵ UGC	
GUA			GCA		
GUG			CAC		
UAU	GΨA	Tyr	UGU	GCA	Cys
UAC			UGC		
UAA		Stop	UGA		Stop
UAG			UGG	CmCA	Trp
CAU	GUG	His	CGU	ICG	Arg
CAC		Gln	CGC		
CAA			CGA		
CAG	CUG		CGG	CCG	
AAU		Asn	AGU	GCU	Ser
AAC	GUU		AGC		
AAA	mcm ⁵ s ² UUU	Lys	AGA	mcm ⁵ UCU	Arg
AAG	CUU		AGG	CCU	
GAU	GUC	Asp	GGU	GCC	Gly
GAC			GGC		
GAA	mcm ⁵ s ² UUC	Glu	GGA	mcm ⁵ UCC	Gly
GAG	CUC		GGG	CCC	

■ Elp1

■ Elp1 and Trm9

■ Elp1, Trm9 and Slm3

Figure 4.11. Codons hypothetically affected by U₃₄ hypomodification. Decoding of the 13 codons highlighted is affected by absence of Elp1. Trm9 absence affects the decoding

4. *tRNA modifications at U₃₄ maintain proteome integrity avoiding mistranslation*

of 7 codons highlighted in blue and green. Deletion of the gene encoding the Slm3 enzyme affects translation of the 3 codons highlighted in green.

The sequences of those proteins and their respective genes were analyzed to determine amino acid and codon composition of the aggregated proteins (Figure 4.12). Codons that paired with the anticodons of the hypomodified tRNAs were analyzed with special attention and a summary of data results are in Table 4.1. The Elp1 Δ aggregated proteins had statistically higher content of Ala, Glu, Gly, Lys and Val; the Trm9 Δ aggregated proteins had statistically higher content of Gln, Glu, Gly, Lys and the Slm3 Δ aggregated proteins had statistically higher content of the three expected amino acids (Gln, Glu and Lys), relative to the genome average (Figure 4.12A). Regarding codon usage patterns of the genes of the aggregated proteins the AAA, CAA and GAA codons that pair with tRNAs containing mcm⁵s²U₃₄ were overrepresented in all KO strains, with exception of the AAA codon in Elp1 Δ (Figure 4.12B). Since mcm⁵s²U₃₄ and ncm⁵U₃₄ modifications allow tRNAs to preferentially read A-ending codons and to less extent G-ending codons (Grosjean and Westhof, 2016), whereas mcm⁵U₃₄ modification allows tRNA to read both A- and G-ending codons, we analyzed the usage of both codons. The content of AGA, AGG and GGG codons that pair with mcm⁵U₃₄ containing tRNAs was statistically higher in Trm9 Δ , whereas only AGA codon content was statistically higher in Elp1 Δ , relative to genome average (Figure 4.12C). Content of CCA and UUG codons that pair with ncm⁵U₃₄ containing tRNAs was also statistically higher in Elp1 Δ , relative to the reference genome (Figure 4.12D).

4. tRNA modifications at U₃₄ maintain proteome integrity avoiding mistranslation

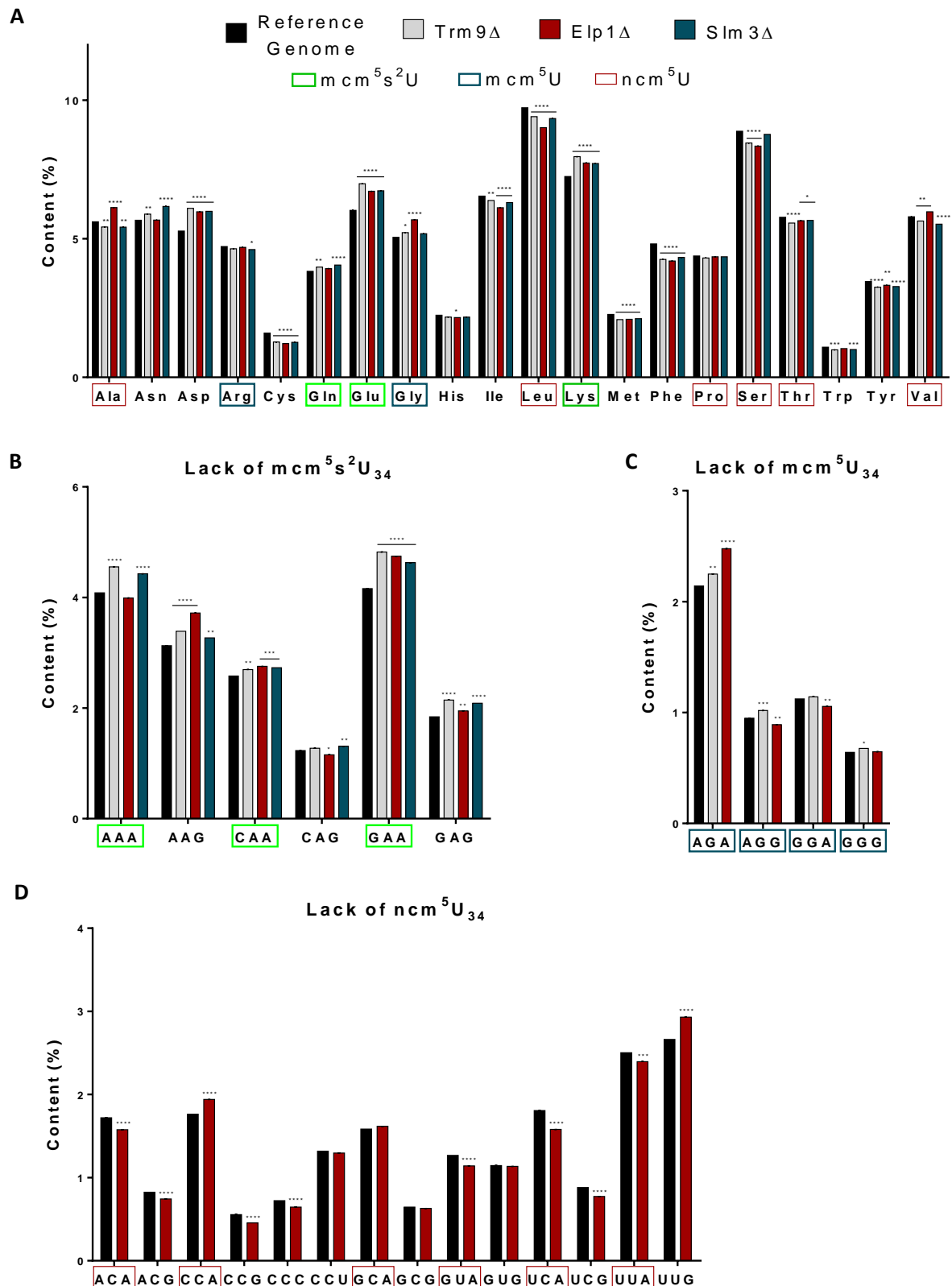


Figure 4.12. Amino acid and codon composition of aggregated proteins in the absence of wobble uridine modification. A. Relative amino acid composition of aggregated proteins in mutant cells compared to the yeast genome. **B, C, D.** Relative codon

4. *tRNA modifications at U₃₄ maintain proteome integrity avoiding mistranslation*

composition of corresponding genes of the aggregated proteins in mutant cells relative to the yeast genome average. **B.** Codons that pair with tRNAs modified with mcm⁵s²U. **C.** Codons that pair with tRNAs modified with mcm⁵U. **D.** Codons that pair with tRNAs modified with ncm⁵U. Relative content is shown for each mutant strain and reference genome. Data show mean ± SEM (**** p < 0.0001, *** p < 0.001, ** p < 0.01, * p < 0.05 heteroscedastic Student's *t*-test with CI 95% relative to Reference Genome).

Table 4.1. Summary of amino acid and codon composition data of the aggregated proteins in the absence of U₃₄ modification.

Strain	Codons with positive biases	Amino acid positive biases	Codons theoretically affected (aa)
Trm9Δ	AGA, AGG CAA -----> GAA, GAG -----> GGG -----> AAA, AAG -----> AAU -----> GAC, GAU ----->	Gln Glu Gly Lys Asn Asp	AGA, AGG (Arg) CAA, CAG (Gln) GAA, GAG (Glu) GGA, GGG (Gly) AAA, AAG (Lys) AAC, AAU (Asn) GAC, GAU (Asp) CAC, CAU (His) AGC, AGU (Ser)
Elp1Δ	AGA CAA GAA, GAG -----> UUG AAG -----> CCA AAC GAC, GAU ----->	Ala Glu Gly Lys Val Asp	GCA, GCG (Ala) AGA, AGG (Arg) CAA, CAG (Gln) GAA, GAG (Glu) GGA, GGG (Gly) UUA, UUG (Leu) AAA, AAG (Lys) CCA, CCG, CCC, CCU (Pro) GUA, GUG (Val) AAC, AAU (Asn) GAC, GAU (Asp) CAC, CAU (His) UUC, UUU (Phe) AGC, AGU (Ser)
Slm3Δ	CAA, CAG -----> GAA, GAG -----> AAA, AAG -----> AAC, AAU -----> GAC, GAU ----->	Gln Glu Lys Asn Asp	CAA, CAG (Gln) GAA, GAG (Glu) AAA, AAG (Lys) AAC, AAU (Asn) GAC, GAU (Asp) CAC, CAU (His)

4. *tRNA modifications at U₃₄ maintain proteome integrity avoiding mistranslation*

Additionally, gene-specific codon usage patterns of the 6705 genes of the yeast genome were analyzed to identify groups of proteins that are significantly enriched in each codon. We calculated a Z-score, using yeast BY4743 mRNA and tRNA abundance data, to identify over- or under-represented codons and the respective genes in the aggregated protein fraction relative to the genome average. Hierarchical clustering analysis of Z-scores of all genes showed clusters of codons with relatively similar patterns of usage across the genome. Regarding the up-regulated set of proteins, we observed that at least one codon of interest was enriched (Z-score > 0) relative to the genome average in the KO strains, with exception of *Slm3Δ* (99% of the up-regulated proteins had at least one codon of interest enriched) (Figure 4.13, Figure 4.14 and Figure 4.15). However, only 23.4%, 23.9% and 22.8% of that codon enrichment was statistically significant (p -value < 0.05) in *Trm9Δ*, *Elp1Δ* and *Slm3Δ*, respectively.

4. tRNA modifications at U_{34} maintain proteome integrity avoiding mistranslation

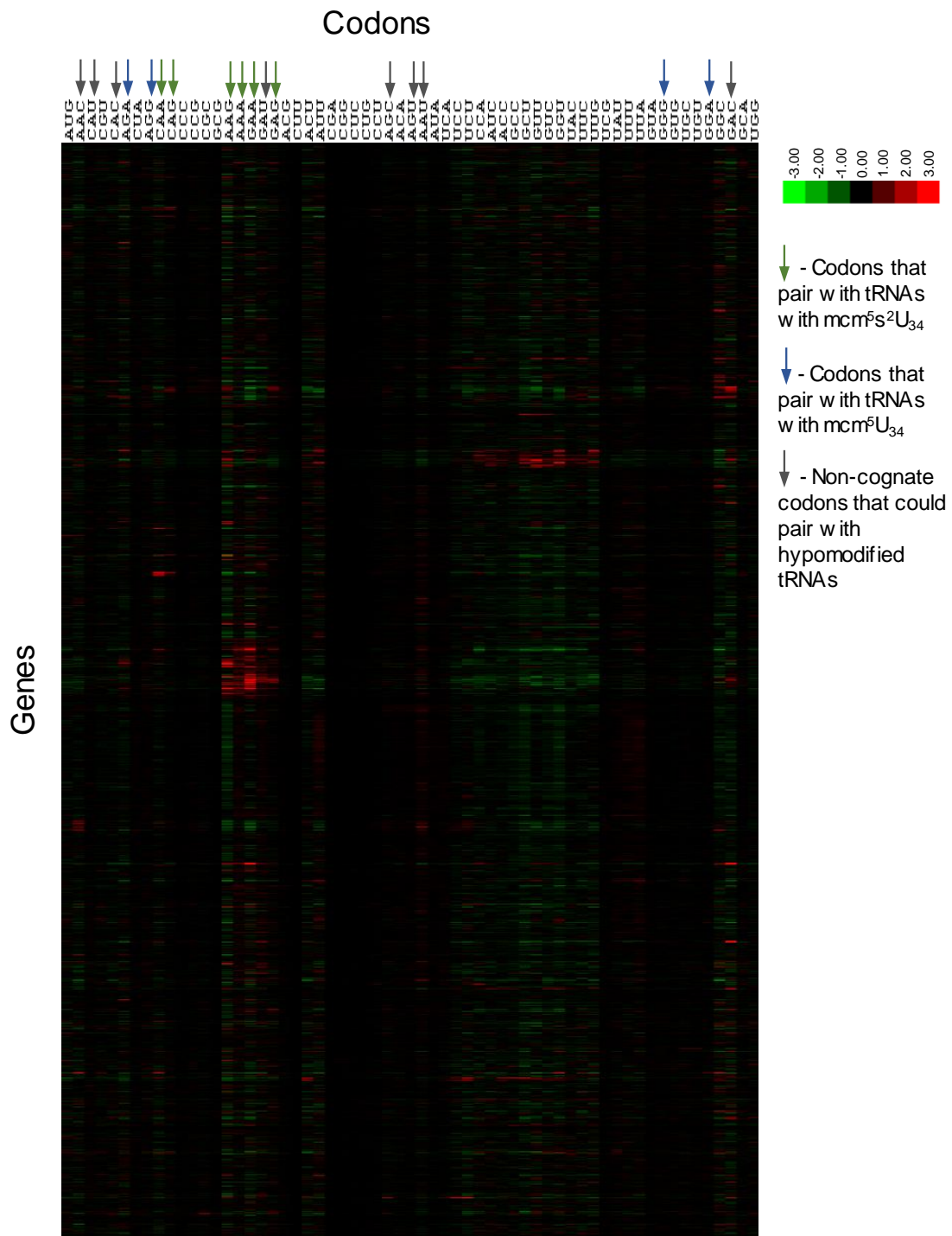


Figure 4.13. Hierarchical clustering analysis of gene-specific codon usage patterns (Z-scores) for genes corresponding to the aggregated proteins in *Trm9Δ*. Z-scores were calculated as the difference between the frequency of each codon used by each transcript and the genome average using BY4743 gene expression as a reference, divided by the standard deviation and weighted by yeast tRNA availability. The scores indicate whether a transcript is over- (red) or under-represented (green) with a specific codon

4. tRNA modifications at U₃₄ maintain proteome integrity avoiding mistranslation

relative to the genome average. Codons showing no difference from the genome average are displayed in black.

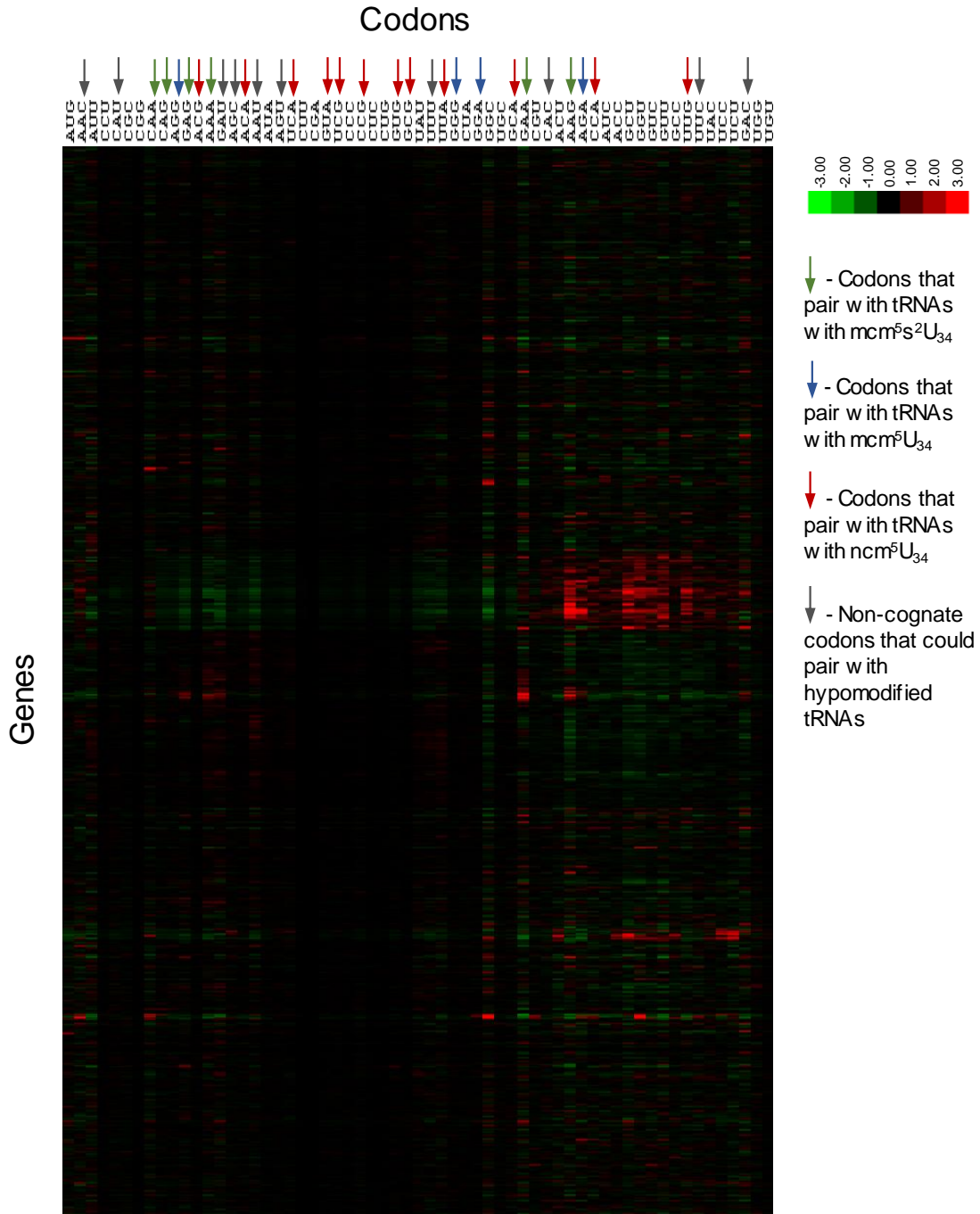


Figure 4.14. Hierarchical clustering analysis of gene-specific codon usage patterns (Z-scores) for genes corresponding to the aggregated proteins in Elp1Δ. Z-scores were calculated as the difference between the frequency of each codon used by each transcript and the genome average using BY4743 gene expression as a reference, divided by the standard deviation and weighted by yeast tRNA availability. The scores indicate

4. tRNA modifications at U₃₄ maintain proteome integrity avoiding mistranslation

whether a transcript is over- (red) or under-represented (green) with a specific codon relative to the genome average. Codons showing no difference from the genome average are displayed in black.

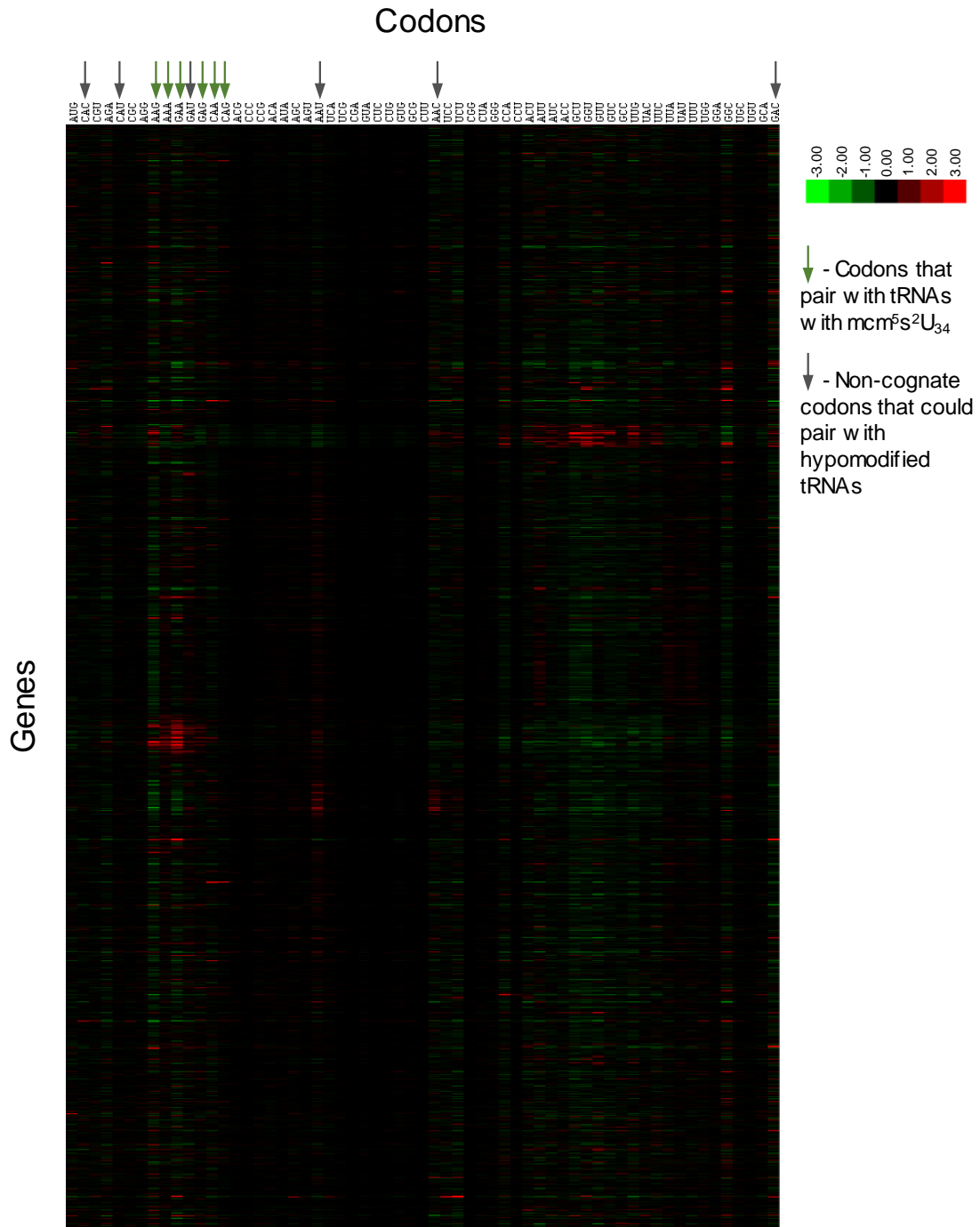


Figure 4.15. Hierarchical clustering analysis of gene-specific codon usage patterns (Z-scores) for genes corresponding to the aggregated proteins in *Slm3Δ*. Z-scores were calculated as the difference between the frequency of each codon used by each

4. tRNA modifications at U₃₄ maintain proteome integrity avoiding mistranslation

transcript and the genome average using BY4743 gene expression as a reference, divided by the standard deviation and weighted by yeast tRNA availability. The scores indicate whether a transcript is over- (red) or under-represented (green) with a specific codon relative to the genome average. Codons showing no difference from the genome average are displayed in black.

As mentioned previously, hypomodified tRNAs in Slm3Δ are still mcm⁵U₃₄ modified (Figure 3.20), thus those tRNAs should read AAA, CAA and GAA, but also G-ending codons AAG, CAG and GAG. Indeed, the content of these codons was also statistically higher in Slm3Δ (Figure 4.12B). Since the hypomodified tRNAs in Trm9Δ strain should have cm⁵U₃₄ or even cm⁵s²U₃₄ (not confirmed by MS data), pairing with AAA, CAA, GAA, AGA and GGA codons should not be significantly affected because tRNAs with ncm⁵U modification reads preferentially A-ending codons and also G-ending codons to a less extent. On the other hand, U₃₄ is unmodified in the Elp1Δ strain (Figure 3.20), the exception being s²U₃₄ which could be present in Gln, Glu and Lys U₃₄ tRNAs. In these cases, the affected tRNAs containing unmodified U₃₄ could read all 4 nucleotides in the third codon position and base pair with non-cognate codons; when those codons belong to split codon boxes. If so, an incorrect amino acid could be inserted in the nascent polypeptide, inducing protein instability and even aggregation. We observed positive usage biases of AAC, GAC and GAU non-cognate codons that may pair with the hypomodified tRNAs present in Elp1Δ (Figure 4.16), as well as a higher content of Asp (Figure 4.12A and Table 4.1). Trm9Δ aggregated proteins had positive usage biases of AAU, GAC and GAU non-cognate codons, accompanied by higher content of the respective amino acids, Asn and Asp (Figure 4.16, Figure 4.12A and Table 4.1). Aggregated proteins in Slm3Δ presented a positive usage biases in AAC, AAU, GAC and GAU non-cognate codons, correlated with higher content of the respective amino acids (Figure 4.16, Figure 4.12A and Table 4.1).

4. tRNA modifications at U₃₄ maintain proteome integrity avoiding mistranslation

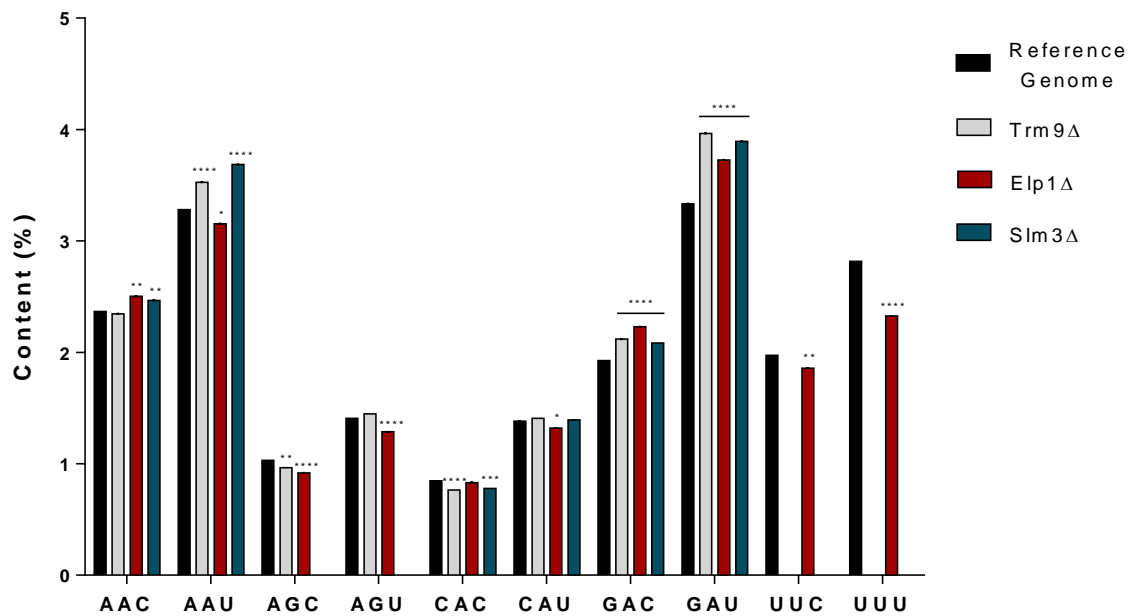


Figure 4.16. Codon composition of the proteins that aggregated in the absence of wobble uridine modification. Relative codon composition of the genes of the aggregated proteins in mutant cells, relative to the average yeast genome. Represented codons are expected to pair with hypomodified tRNAs in mutant cells. Relative content is shown for Trm9Δ, Elp1Δ, Slm3Δ and reference genome. Data show mean ± SEM (**** p < 0.0001, *** p < 0.001, ** p < 0.01, * p < 0.05 heteroscedastic Student's *t*-test with CI 95% relative to Reference Genome).

4.2.3 U₃₄ modifications fine tune translational accuracy

In vitro studies have shown that wobble base tRNA modifications play a role in translation fidelity (Yarian *et al.*, 2002). Molecular modeling, nuclear magnetic resonance and X-ray data show that these modifications can alter the geometry of the ribosome-decoding center and promote the binding of anticodons to their cognate codons (Agris, 2004; Durant *et al.*, 2005). As mentioned before, ncm⁵U and mcm⁵s²U modifications improve reading of A-ending codons, whereas mcm⁵U modification improves reading of A- and G-ending codons (Lim and Curran, 2001; Björk *et al.*, 2007; Johansson *et al.*, 2008; Grosjean and Westhof, 2016). Additionally, tRNA wobble base modifications found in two-split codon boxes can prevent binding to U and C-ending codons (Agris, 2004; Durant *et al.*, 2005). Thus,

4. *tRNA modifications at U₃₄ maintain proteome integrity avoiding mistranslation*

it is possible that mutants lacking modifications at the wobble position incorporate *in vivo* incorrect amino acids at a significant rate by failing to prevent anticodon binding to U- and C-ending codons.

The mcm⁵s²U₃₄ modification catalyzed by Trm9, Elp1 and Slm3, the mcm⁵U₃₄ modification catalyzed by Trm9 and Elp1 and the ncm⁵U₃₄ modification catalyzed by Elp1 promote discrimination of cognate from near-cognate codons in mRNA, for example, AAA and AAG from AAU and AAC. Thus, in the absence of ncm⁵U₃₄, mcm⁵U₃₄ and mcm⁵s²U₃₄ modifications, amino acid misincorporations should occur during translation of codons belonging to Arg, Glu, Gln, Lys and Leu mixed codon boxes (Figure 4.17). In this sense, we hypothesized that serine-to-arginine, aspartic-to-glutamic acid, asparagine-to-lysine, histidine-to-glutamine and phenylalanine-to-leucine misincorporations could occur in the KO strains. Indeed, we identified amino acid misincorporations in the insoluble fraction of KO and WT strains using the SPIDER algorithm integrated in the PEAKS studio software platform (Figure 4.18). We observed higher frequency of predicted amino acid misincorporations in the up-regulated aggregated proteins in the KO strains, except for Asp-to-Glu in Trm9Δ and Ser-to-Arg and Phe-to-Leu in all mutant cells (Figure 4.19A). Regarding the distribution of amino acid misincorporations in near-cognate codon sites, we observed that Asp-to-Glu misincorporation at GAU codons was higher in Elp1Δ and Slm3Δ, while misincorporation at GAC codons was higher in Slm3Δ; His-to-Gln misincorporation at CAC codons occurred in Trm9Δ and Slm3Δ and at CAU codons in the Elp1Δ and Slm3Δ strains. Asn-to-Lys misincorporation at AAU codons was increased in all KO strains and AAC codon was mistranslated more frequently in Elp1Δ and Slm3Δ (Figure 4.19C).

4. tRNA modifications at U₃₄ maintain proteome integrity avoiding mistranslation

Codon	Anticodon	Amino acid	Codon	Anticodon	Amino acid
UUU	GmAA	Phe	UCU	IGA	Ser
UUC			UCC		
UUA			UCA		
UUG	m ⁵ CAA	Leu	UCG	ncm ⁵ UGA	Arg
CAU	GUG		CGU	ICG	
CAC			CGC		
CAA		mcm ⁵ s ² UUG	CGA		
CAG	CUG	Gln	CGG	CCG	
AAU	GUU		AGU	GCU	Ser
AAC			AGC		
AAA		mcm ⁵ s ² UUU	AGA		
AAG	CUU	Lys	AGG	mcm ⁵ UCU	Arg
GAU	GUC		GGU	GCC	
GAC			GGC		
GAA		mcm ⁵ s ² UUC	GGA		
GAG	CUC	Asp	GGG	mcm ⁵ UCC	Gly
				CCC	

■ Elp1 ■ Elp1 and Trm9 ■ Elp1, Trm9 and Slm3

Figure 4.17. Mini-genetic code table with two-split codon boxes. U₃₄ modifications in tRNAs in the two-split codon boxes promote discrimination of cognate from near-cognate codons in mRNA, suggesting that tRNAs lacking such U₃₄ modifications may mistranslate the indicated near-cognate codons.

4. tRNA modifications at U₃₄ maintain proteome integrity avoiding mistranslation

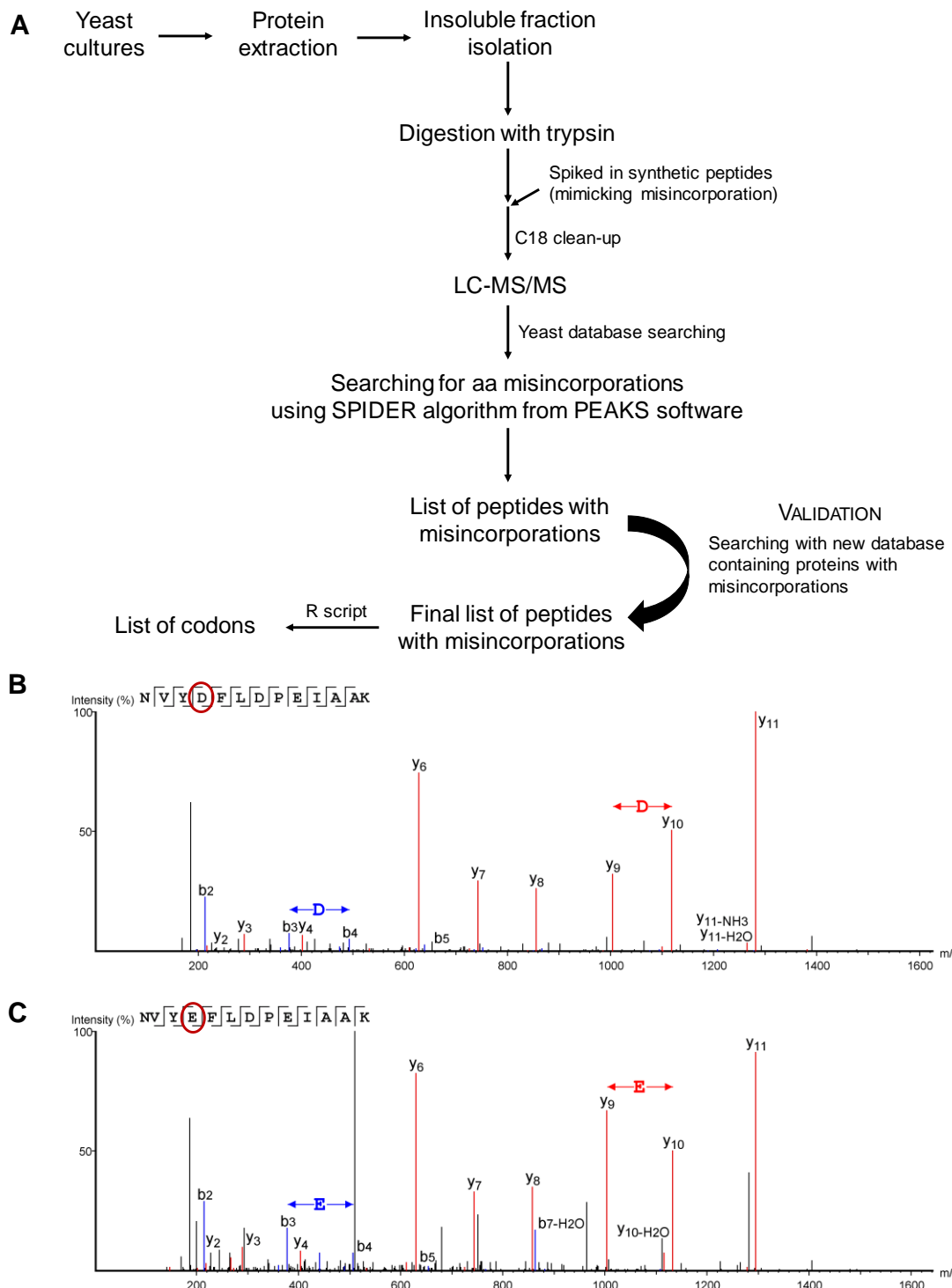


Figure 4.18. Detection of amino acid misincorporation. **A.** Diagram of the various steps used in the detection of amino acid misincorporations. Samples preparation involved lysis of yeast cells, extraction of protein total extracts, isolation of insoluble fraction and tryptic digestion. We added synthetic peptides to the digested peptides prior clean-up and LC-MS/MS analysis, to use in data analysis. MS/MS data was searched against yeast proteome and amino acid misincorporations were identified using SPIDER algorithm from PEAKS

4. tRNA modifications at U₃₄ maintain proteome integrity avoiding mistranslation

software. To remove false-negatives, MS/MS data was searched against yeast proteome plus new proteins with the misincorporations detected. An R script was used to find codons where misincorporations occurred. **B.** Spectrum of the WT synthetic peptide. **C.** Spectrum of a peptide with misincorporation of Glu at Asp site.

4. tRNA modifications at U₃₄ maintain proteome integrity avoiding mistranslation

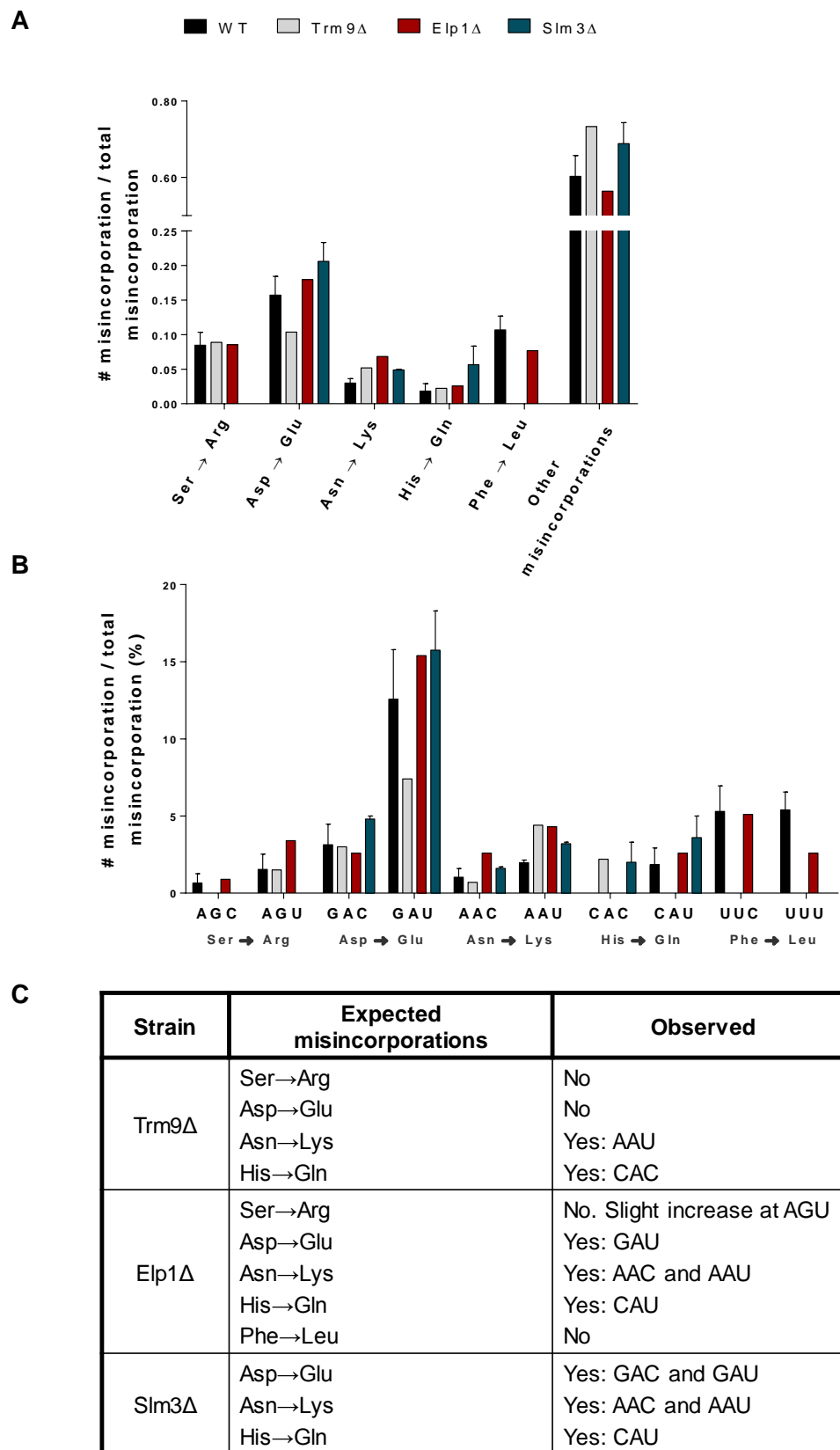


Figure 4.19. Amino acid misincorporations observed in up-regulated aggregated proteins in KO strains. A. Relative frequency of predicted amino acid misincorporations

4. *tRNA modifications at U₃₄ maintain proteome integrity avoiding mistranslation*

and other misincorporations in the mutant and WT strains. **B.** Relative frequency of predicted amino acid misincorporations distributed by the specific codons in the mutant and WT strains. Distribution of amino acid misincorporations is relative to total number of amino acid misincorporations in each sample. **C.** Summary table with expected and observed misincorporations.

We also collected data of the relative abundance of peptides containing amino acid misincorporations. In other words, we analyzed the frequency of peptides with amino acid misincorporations at a specific codon site relative to the total number of peptides for that specific codon site and plotted it displaying also the relative frequencies of each misincorporation type (Annex IX.4). The frequency of peptides with higher level of amino acid misincorporations relative to WT peptides was higher in KO relative to the WT strain, except for Phe-to-Leu misincorporation in *Elp1Δ* and His-to-Gln in *Trm9Δ* (Annex IX.4). In other words, amino acid misincorporations occurred in both KO and WT strains, but the frequency of peptides containing those amino acid misincorporations was higher in the KO strains than in the WT strain.

The absence of U₃₄ modifications may also decrease decoding speed of a subset of codons enriched in the aggregated proteins. This could also lead to protein misfolding and degradation. We have analyzed the distribution of codons in the mutated sites (Figure 4.20A, Annex IX.3 and Annex IX.5-Annex IX.7) and in the specific codons that pair with hypomodified tRNAs in the KO strains (Figure 4.20B, C and D). These codons corresponded to sites for amino acid misincorporation, particularly codons AAA and GAA in *Trm9Δ* and *Slm3Δ*, AGG in *Trm9Δ* and CAA, AGA, CCC, GCG and UUA in *Elp1Δ* (Figure 4.20B, C and D).

4. tRNA modifications at U₃₄ maintain proteome integrity avoiding mistranslation

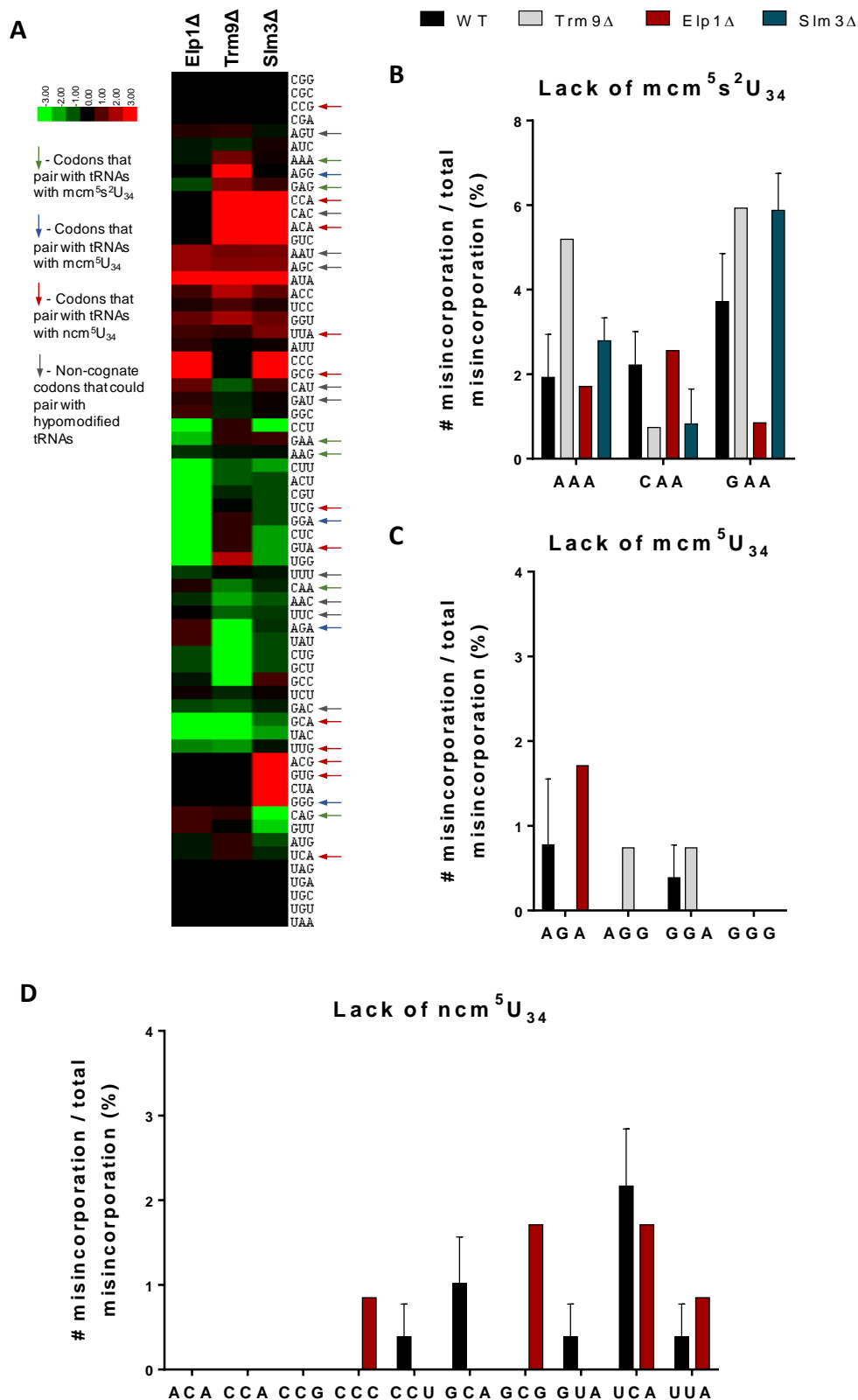


Figure 4.20. Amino acid misincorporations occurred in specific codon sites. **A.** Distribution of amino acid misincorporations among codons in KO relative to WT strains. **B,**

4. *tRNA modifications at U₃₄ maintain proteome integrity avoiding mistranslation*

C, D. Relative frequency of amino acid misincorporations in the codons indicated in the x-axis. **B.** Codons that pair with tRNAs modified with mcm⁵s²U₃₄. **C.** Codons that pair with tRNAs modified with mcm⁵U₃₄. **D.** Codons that pair with tRNAs modified with ncm⁵U₃₄. Distribution of amino acid misincorporations among specific codons is relative to total number of amino acid misincorporations in each sample.

4.2.4 Aggregated proteins have homologues in humans

Protein misfolding and aggregation occur in various neurodegenerative and age-related disorders, namely Alzheimer's disease (AD), Parkinson's disease (PD) and familial amyotrophic lateral sclerosis (ALS). These disorders are primarily characterized by acquisition of non-native conformations and aggregation of specific proteins. However, aberrant interactions between disease-associated and other cellular proteins might result in extensive co-aggregation and loss of function of non-disease proteins (Stefani and Dobson, 2003; Hartl, Bracher and Hayer-Hartl, 2011). We searched our protein aggregation data set to identify possible human orthologues. For this, we used human or mouse proteins that are implicated in protein folding disorders and/or co-aggregate with specific folding disorder-associated proteins in AD (Liao *et al.*, 2004; Wang *et al.*, 2005), PD (Xia *et al.*, 2009) and/or familial ALS (Basso *et al.*, 2009). Interestingly, yeast orthologues of disease-associated proteins are statistically overrepresented among the aggregated proteins present in Elp1 Δ only. Considering that up-regulated protein aggregates identified in Elp1 Δ constitute 14% of the total yeast genome, it is notable that this protein set contains 36% more orthologous proteins that co-aggregate with α -synuclein in PD ($p = 0.047$) than the genome average and 35% more orthologous proteins that aggregate in a familial ALS mouse model ($p = 0.036$) than the genome average. These findings suggest that the basic mechanisms that govern protein aggregation associated with translational errors in yeast may be valid in human disease processes. In particular, the enzyme SOD1, which is associated with familial ALS pathogenesis (Basso *et al.*, 2009), is also aggregated in Elp1 Δ mutant (Table 4.2 and Annex X.1).

4. tRNA modifications at U₃₄ maintain proteome integrity avoiding mistranslation

Table 4.2. List of human orthologues associated to disease found in the aggregated proteins in the E1p1Δ strain.

Disorder	Uniprot ID	Description	Yeast orthologues in aggregated proteins E1p1Δ
α-synuclein associated	P06744	Glucose phosphate isomerase	PGI1
	P04406	Glyceraldehyde-3-phosphate dehydrogenase	TDH3
	P09471	Guanine nucleotide binding protein α	GPA2
	P08238	Heat shock protein 90kda	HSC82
	P31939	Imp cyclohydrolase	ADE16
	P30044	Peroxiredoxin 53	AHP1
	Q96QK1	Vacuolar protein sorting 35	VPS35
Familial ALS associated	P07901	Heat shock protein HSP 90 α	HSC82
	Q99K10	Aconitase	ACO1
	P26443	Glutamate dehydrogenase 1	GDH3, GDH1
	P17182	α-enolase	ENO1, ENO2
	P05201	Aspartate aminotransferase	AAT2
	P17742	Peptidyl-prolyl cis-trans isomerase A (CypA)	CPR1
	P00441	SOD1	SOD1

4.3 DISCUSSION

For most amino acids, there is more than one codon (codon redundancy), but these codons are not used at the same frequency in genes and influence gene expression in ways that are not yet fully understood. This mechanism of codon usage bias, as well as the tRNA modification patterns, are important to coordinate the expression of groups of genes involved in specific cellular pathways (Bauer *et al.*, 2012). Recent evidences suggest that tRNA activity is highly coordinated with mRNA codon demand (Maraia and Iben, 2014). This study showed that loss of tRNA anticodon modification increases protein aggregation. Our amino acid misincorporation data also show that proteins may aggregate as a direct consequence of loss of translational accuracy.

4. *tRNA modifications at U₃₄ maintain proteome integrity avoiding mistranslation*

4.3.1 **U₃₄ modification is important to maintain proteome homeostasis**

In the Elp1 Δ strain, where mcm⁵s²U, mcm⁵U and ncm⁵U are absent in 11 different tRNAs, 970 enriched proteins were identified in the insoluble fraction (fold change > 1.2 relative to WT). These proteins are mainly involved in translation and ribosome biogenesis, proteolysis and proteasomal ubiquitin-dependent protein catabolism, phosphorylation, regulation of chromatin silencing, among other metabolic processes (Figure 4.8). The enrichment of proteins involved in proteasomal and ubiquitin-dependent mechanisms (Annex VIII.2B) suggest that U₃₄ modification defects increase proteotoxic stress in yeast. Interestingly, Elp1 Δ cells contained up-regulated aggregated proteins involved in the regulation of chromatin silencing at the telomeres. The Elongator complex is apparently required for efficient translation of factors regulating chromatin silencing at centromeres and chromatin remodeling in yeast (Esberg *et al.*, 2006; Bauer *et al.*, 2012), supporting our data. One of those candidate genes is Sir4 (a known regulator of telomere maintenance), whose efficient mRNA translation is impaired in Elongator mutants (Chen, Huang, Eliasson, *et al.*, 2011). We also observed up-regulation of Sir4 in the insoluble fraction of Elp1 Δ and Slm3 Δ (fold-change of 2.6 and 12.0, respectively), suggesting that Sir4 protein is mistranslated in these strains. In higher eukaryotes, the Elongator complex is also associated to tubulin acetylation in the context of neuron migration and differentiation (Creppe *et al.*, 2009).

The Trm9 Δ strain had 1116 up-regulated proteins in the insoluble fraction, where mcm⁵U and mcm⁵s²U absence affected 5 different tRNAs. A gene ontology analysis also revealed a significant enrichment of RNA processing and ribosome biogenesis, histone metabolism and chromatin modification, tRNA and mRNA catabolism genes, among others (Figure 4.7). Trm9 activity was previously linked with enhanced translation of 425 transcripts, whose proteins are involved in stress response, protein biosynthesis and other biological processes (Begley *et al.*, 2007). However, we only found 39 of those 425 proteins in the insoluble fraction of Trm9 Δ . The enrichment of proteins involved in the cell cycle (Figure 4.7) confirmed previous observations that Trm9-dependent translation regulates cell cycle progression (Patil, Dyavaiah, *et al.*, 2012; Deng *et al.*, 2015).

4. *tRNA modifications at U₃₄ maintain proteome integrity avoiding mistranslation*

In the *Slm3Δ* strain, where *mcm*⁵*s*²*U* is absent in 3 tRNAs, the 1250 up-regulated proteins found in the aggregated fraction (fold change > 1.2 relative to WT) are involved in transcription and its regulation, cell cycle, protein phosphorylation, histone deacylation and chromatin modification and mitochondrial translation (Figure 4.9). Mitochondrial translation defects and deficient expression of mitochondrial genes were previously described in *Slm3Δ* cells (Wang, Yan and Guan, 2010). We observed the presence of 193 mitochondrial proteins in the insoluble fraction of *Slm3Δ*, including *Cox12*, *Ai1m* and *Atp23* (fold-change 4.1, 2.2, and 12.6, respectively).

The up-regulated proteins that were shared among the KO strains are enriched in functional groups of protein polyubiquitination and free ubiquitin chain polymerization and cellular response to amino acid starvation (Annex VIII.4B). Proteins involved in the regulation of RNA polymerase II transcription were enriched in the set of proteins that aggregated in all mutant strains. Previous studies have shown that Elongator mutants, having hypomodified tRNAs lacking *mcm*⁵*s*²*U*₃₄, have RNA polymerase II dependent phenotypes (Esberg *et al.*, 2006). tRNAs containing *mcm*⁵*s*²*U* are also important for efficient expression of gene products required for DNA damage response. And loss of *Trm9* was suggested to recapitulate the stress response associated with exposure to protein- and nucleic acid-damaging agents (Begley *et al.*, 2007; Chen, Huang, Eliasson, *et al.*, 2011), which is consistent with our data on the enrichment of proteins involved in DNA repair, regulation of DNA damage checkpoint and DNA double-strand break processing (Annex VIII.4B). Additionally, 5'-3' exonuclease activity is enriched in the shared proteins between mutant strains (Annex VIII.4A), suggesting increased hydrolysis of nucleic acids ester bonds; likely in tRNAs due to their hypomodification.

4.3.2 Loss of U₃₄ modifications affects the translation of genes enriched in specific codons

It was proposed that specific transcripts, named MoTTs (modification tunable transcripts), may have over-representation of specific codons, particularly of split codon boxes to fine tune their translation (Begley *et al.*, 2007; Dedon and Begley,

4. tRNA modifications at U₃₄ maintain proteome integrity avoiding mistranslation

2013). From the list of 425 MoTTs identified in *S. cerevisiae*, we detected 39, 90 and 48 proteins encoding transcripts in the insoluble protein fraction of the Trm9 Δ , Elp1 Δ and Slm3 Δ strains, respectively. Those protein transcripts contain statistically significant deviations in the usage of 29 codons relative to the genome average (Begley *et al.*, 2007).

We found that the genes encoding the aggregated proteins present in the insoluble protein fraction of mcm⁵s²U mutant cells had statistically higher content of GAA, GAG and AAG codons, and to a lesser extent CAA, whereas the content of AAA codons was statistically higher in aggregated proteins of the Trm9 Δ and Slm3 Δ strains, while CAG codon content was statistically higher in Slm3 Δ , relative to the genome average (Figure 4.12B and summary at Table 4.1). Regarding mcm⁵U mutant cells, only the AGA codon content was statistically higher in up-regulated aggregated proteins of the Elp1 Δ and Trm9 Δ strains (Figure 4.12C). The CCA codon content was statistically higher in aggregated proteins found in ncm⁵U mutant cells (Figure 4.12D and summary at Table 4.1). Since mcm⁵U₃₄ modification allows tRNAs to read both A- and G-ending codons (Johansson *et al.*, 2008), we also analyzed codon content of G-ending near-cognate codons. The content of the AGG and GGG codons that base pair with tRNA anticodons containing mcm⁵U₃₄ was statistically higher in Trm9 Δ relative to genome average (Figure 4.12C and summary at Table 4.1). Although, ncm⁵U modification preferentially read A-ending codons, it can also read G-ending codons less efficiently. Exceptions were previously observed in Pro and Ala tRNAs with ncm⁵U modification that can read A-, G-, C- or U- and A- or G-ending codons, respectively (Grosjean and Westhof, 2016). Our data only showed positively biased usage of the UUG codon in the Elp1 Δ strain relative to genome average (Figure 4.12D and summary at Table 4.1).

Global proteome data support the hypothesis that Trm9-catalyzed tRNA anticodon modifications enhance decoding of AGA, GAA and CAA codons of arginine, glutamic acid and glutamine mixed codon boxes, respectively (Begley *et al.*, 2007; Deng *et al.*, 2015). This is consistent with our results, because the absence of Trm9-catalyzed tRNA anticodon modifications should affect tRNA selection if the AGA, GAA, CAA and AAA codons are present in the ribosome A-site, increasing translational errors (Figure 4.12B, C). Analysis of codon bias of

4. tRNA modifications at U₃₄ maintain proteome integrity avoiding mistranslation

fission yeast Elongator mutants showed overrepresentation of A-ending codons, particularly AAA and GAA in proteins expressed at low level (Bauer *et al.*, 2012), whereas codon bias analysis of our Elongator mutant (Elp1 Δ) showed that the aggregated protein genes are enriched in GAA and CAA codons (Figure 4.12B).

To identify/exclude confounding factors, namely gene expression and tRNA availability, we calculated Z-scores, which indicate whether a certain codon is over- or under-represented in each gene, relative to the genome average. We observed that in each mutant strain, at least one codon of interest was enriched (Z-score > 0) relative to genome average of the KO strains (Figure 4.13, Figure 4.14 and Figure 4.15). However, that enrichment of the codons of interest was statistically significant (p -value < 0.05) only in 23.4%, 23.9% and 22.8% of the cases in Trm9 Δ , Elp1 Δ and Slm3 Δ , respectively. The higher content of expected codons in our samples is also in line with ribosome footprinting data showing that U₃₄ non-modified tRNAs bind poorly to the ribosome, reducing translation rate at specific codons. Loss of mcm⁵ modification (Elp3 Δ) was associated with increased ribosome density at CAA and GAA codons located at the ribosomal A-site and to less extent in GAG codons (Zinshteyn and Gilbert, 2013), which is consistent with the enrichment of aggregated proteins in CAA, GAA and GAG codons observed in Elp1 Δ (Figure 4.12B). On the other hand, loss of s² modification increased CAA and AAA codons enrichment at ribosomal A-sites (Ncs6 Δ and Uba4 Δ mutants) and to less extent the GAA and GAG codons (Uba4 Δ) (Zinshteyn and Gilbert, 2013), which is again consistent with the enrichment of aggregated proteins in AAA, CAA, GAA and GAG codons that we observed in Slm3 Δ (Figure 4.12B). Recent works showed that loss of mcm⁵U and mcm⁵s²U reduced the translation of genes enriched in AGA and GAA codons due to ribosomal pausing (Deng *et al.*, 2015). These data did not clarify the slight increase in the occupancy of ribosomes by codons that pair with mcm⁵U or mcm⁵s²U modified tRNA anticodons. Since we observed increased aggregation of proteins whose genes are enriched in codons affected by the hypomodification of tRNAs, we assume that a slight increase in pausing of the ribosomes at those codon sites could lead to amino acid misincorporation or misfolding of the respective protein products.

4. tRNA modifications at U₃₄ maintain proteome integrity avoiding mistranslation

4.3.3 Loss of U₃₄ modifications elevates codon mistranslation rate

As mentioned above, the mcm⁵U₃₄ and mcm⁵s²U₃₄ modifications have been implicated in differentiating between cognate and near cognate codons in split codon boxes and optimizing codon-anticodon interactions (Kalhor and Clarke, 2003; Patil, Chan, *et al.*, 2012). U₃₄ hypomodification of glutamine, glutamic acid and lysine tRNAs reduced the speed of translation in a codon-dependent context (Ashraf *et al.*, 1999; Begley *et al.*, 2007), a phenotype that was reversed by overexpression of the hypomodified tRNAs (Esberg *et al.*, 2006; Bauer *et al.*, 2012). Two hypotheses can be extrapolated from these observations. First, mcm⁵s²U₃₄, mcm⁵U₃₄ and ncm⁵U₃₄ modifications enhance ribosomal binding of anticodons to cognate codons, increasing speed of translation in a codon-dependent context. Second, the primary role of the mcm⁵s²U or mcm⁵U modifications is not to reduce misreading of non-cognate codons ending with U or C in the split codon boxes, but to improve the efficiency of reading cognate codons ending with A. Since U₃₄ modification defects lead to codon-specific translational pausing (Zinshteyn and Gilbert, 2013; Nedialkova and Leidel, 2015), we propose that pausing affects co-translational protein folding and amino acid misincorporation rate.

Indeed, we observed that up-regulated aggregated proteins in Trm9Δ cells were not only enriched in AAA, AAG, CAA, GAA, GAG, AGA, AGG and GGG codons that pair with hypomodified tRNAs (Figure 4.12B, C), but also had higher frequency of amino acid misincorporations at AAA, GAA, GAG, AGG and GGA codons relative to WT (Figure 4.20A, B, C and Annex IX.3A). Similarly, the genes of the up-regulated aggregated proteins in Slm3Δ cells were enriched in the codons that pair with mcm⁵s²U modified tRNAs (AAA, GAA and GAG, and to a less extent CAA, AAG and CAG, Figure 4.12B) and amino acid misincorporations were also detected at higher frequency in AAA and GAA codons, relative to WT (Figure 4.20A, B and Annex IX.3A). Interestingly, the genes encoding the up-regulated aggregated proteins in the Elp1Δ strain showed different patterns of codon enrichment and amino acid misincorporation at the same codon sites, however we could also observe aggregated proteins enriched in CAA and AGA codons and higher level of amino acid misincorporations at these codon sites relative to WT (Figure 4.20).

4. tRNA modifications at U₃₄ maintain proteome integrity avoiding mistranslation

tRNAs in Elp1Δ lacking U₃₄ modification should read 4 codons by base pairing with all 4 nucleotides at the third position of codons; they may even pair with near-cognate codons that belong to split codon boxes. Ribosome occupancy data showed increased occupancy of only CAC and CAU codons in Elongator mutants (Nedialkova and Leidel, 2015), whereas we observed that the content of AAC, GAC and GAU near-cognate codons that may pair with the hypomodified tRNAs of Elp1Δ was higher relative to the genome average (Figure 4.16 and Table 4.3). This suggests that amino acid misincorporation at those codon sites may be a major contributor to protein aggregation. In fact, we observed higher frequency of Asn-to-Lys misincorporation at AAC and AAU codons and a slight increase in the frequency of Asp-to-Glu misincorporation at GAU codons in the Elp1Δ compared to WT strain (Figure 4.19 and Table 4.3). Amino acid misincorporations also occurred more frequently in split codon boxes in the other mutant strains, namely Asn-to-Lys and His-to-Gln misincorporations at AAU and CAC codons, respectively, in Trm9Δ and Asp-to-Glu, His-to-Gln and Asn-to-Lys misincorporations at GAC/GAU, CAU and AAC/AAU codons, respectively, in the Slm3Δ strain (Figure 4.19 and Table 4.3). Comparing these results with the codon content observed in the aggregated proteins of these strains, we observed an increase in the content of those codons, namely AAU, GAC and GAU in Trm9Δ and AAC, AAU, GAC and GAU in Slm3Δ (Figure 4.16 and Table 4.3).

Table 4.3. Summary of codon usage and amino acid misincorporation observed in KO strains.

Strain	Codons with positive biases	Codons with aa misincorporations	Type of aa misincorporation
Trm9Δ	AAU -----> GAC, GAU	AAU -----> CAC ----->	Asn→Lys His→Gln
Elp1Δ	AAC -----> GAC, GAU ----->	AAC, AAU -----> GAU -----> AGU -----> CAU ----->	Asn→Lys Asp→Glu Ser→Arg His→Gln
Slm3Δ	AAC, AAU -----> GAC, GAU ----->	AAC, AAU -----> GAC, GAU -----> CAU ----->	Asn→Lys Asp→Glu His→Gln

4. *tRNA modifications at U₃₄ maintain proteome integrity avoiding mistranslation*

Other studies reported that hypomodified tRNA^{Lys_{AAA}} (mcm⁵s²U₃₄) cause significant +1 frameshifting at AAG codons and to less extent at the AAA cognate codon sites (Urbonavicius *et al.*, 2001; Agris, 2004). Those frameshift errors could not be detected using our methodology, but are likely to occur in mutant cells considering the higher content of AAG codons in the up-regulated aggregated proteins (Figure 4.12B).

4.4 CONCLUSION

Our study confirmed the role of tRNA modification, in particular at position U₃₄ of the anticodon, in the efficiency and accuracy of translation of specific codons. The global protein aggregation patterns that accompanied loss of U₃₄ tRNA modifications was likely caused by perturbed codon-anticodon interactions at the ribosome level, resulting in slower decoding of near- and cognate codons and mistranslation. Loss of U₃₄ tRNA modifications has been associated with neurodegeneration (Chen, Tuck and Byström, 2009) and other protein misfolding diseases, in which protein aggregation is a hallmark. Remarkably, several orthologues of our Elp1Δ aggregated proteins are associated with PD and familial ALS, suggesting that tRNA modification may play a role in these diseases.

5. GENERAL DISCUSSION

5. General discussion

Protein biosynthesis is a highly regulated and energetically demanding biological process. In normal laboratory conditions, exponentially growing yeast cells produce 13 000 proteins per second (Haar, 2008). Inherent protein synthesis errors usually occur at low level, but drugs, nutritional stress, oxidative stress and other physiological perturbations can increase those errors, disrupting protein structure and contributing to proteotoxic stress. Those errors are produced by mischarging of tRNAs (error rate $> 10^{-4}$) or tRNA-mRNA mispairing in the ribosome (error rate *in vitro* of 10^{-4}) (Ibba and Soll, 2000), but do not occur at similar levels in different codons or at the same level for all amino acids. tRNA-mRNA pairing and mRNA decoding efficiency have been linked to the presence of tRNA anticodon modifications. The modification of ribonucleosides is a key step of RNA maturation and is performed by a wide variety of RNA-modifying enzymes, with direct or indirect action on the ribonucleosides. We focused our study on the role of RNA modifications in the fidelity of protein synthesis by analyzing proteome homeostasis in yeast strains lacking specific RNAmods.

5.1 rRNA MODIFICATIONS AND PROTEOSTASIS

Despite the advances in identifying rRNAmods, the functions of rRNA modifications in translation remain mostly unknown. However, their conservation, their presence at functional sites and the elaborated pathways used to synthesize them, suggest that they are important for regulating ribosome function and optimizing translation. In fact, rRNA modifications have been associated with mRNA decoding accuracy by stabilizing the codon-anticodon mini-helix formed in the decoding center of the SSU of the ribosome (Polikanov *et al.*, 2015). We observed increased protein aggregation in yeast strains lacking rRNAmods, even in diploid strains where one copy of the gene was still intact, reinforcing the fundamental role of rRNA modifications on translational accuracy.

5.2 tRNA MODIFICATIONS AND PROTEOSTASIS

Biochemical and molecular studies showed that some tRNA modifications affect tRNA stability, processing, interaction with proteins and gene expression, and that tRNAs are the most modified of all RNAs. However, the majority of the tRNA modifications are nonessential and deletion of many genes encoding tRNAmods causes only mild phenotypes (Grosjean, 2009a; Phizicky and Hopper, 2010), raising the question of how tRNA modifications contribute to translational fidelity and gene expression? In the present study, we used KO strains of the known tRNA-modifying enzymes to understand the impact of the different modifications (Figure 5.1) in the efficiency of tRNA selection by the ribosome and codon-anticodon interaction accuracy. We demonstrated that tRNA modifications that occur in the anticodon-loop, in particular at the first anticodon base, have a strong impact in proteostasis. On the other hand, lack of modifications in the body of the tRNAs did not significantly disturb proteostasis, reinforcing their role in fine tuning tRNA folding, stability and aminoacylation. Indeed, defects in aminoacylation and rapid degradation of hypomodified tRNAs were observed in cells lacking modifications in the body of tRNAs (Alexandrov *et al.*, 2006; Chernyakov *et al.*, 2008; Whipple *et al.*, 2011).

Our data contribute to clarify the role of tRNA modifications in codon decoding efficiency, accuracy and translational regulation of gene expression in a type and site-dependent manner. In yeast, Trm9 dependent tRNA modification (mcm⁵U) permits Arg-tRNAs to decode Arg-AGA codons and lack of this enzyme slowed translation of AGA-rich transcripts (Begley *et al.*, 2007). Deletion of Trm7 down regulates the expression of specific Phe-codon rich genes due to its role in the synthesis of Cm₃₂ and Gm₃₄ in tRNA^{Phe}. These modifications influence codon-anticodon recognition and affect interaction of the Phe-tRNA isoacceptors with PheRS (Guy *et al.*, 2012). Deletion of the Pus3 gene, which is responsible for the synthesis of pseudouridine at position 39 in tRNA^{Trp}_{CmCA}, tRNA^{Tyr}_{GψA} and tRNA^{Lys}_{CUU}, decreases readthrough efficiency of stop codons in yeast (Grosjean, 2005) and Sua5 mediated modification of A₃₇ to t⁶A₃₇ in the anticodon-loop of various tRNAs, including the initiator tRNA^{Met}, stabilizes codon-anticodon interactions for efficient translation initiation and reading frame maintenance (Lin, Ellis and True, 2010). In other words, lack of tRNA modifications is likely to slow

5. General discussion

down codon decoding or even stall ribosomes at specific codon sites, increasing the level of missense, nonsense and frameshifting events and protein aggregation.

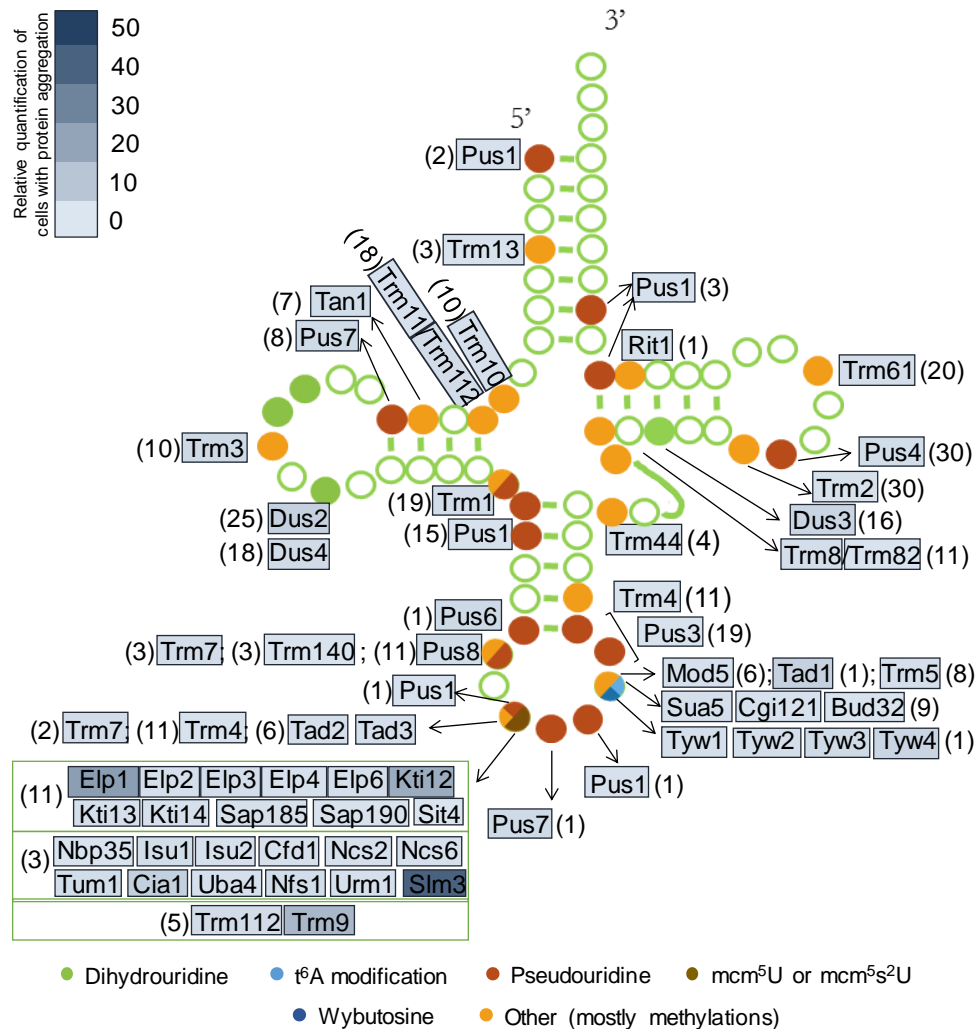


Figure 5.1. Positions of the modifications catalyzed by the tRNAmods analyzed in this study. Each tRNAmod studied is highlighted accordingly to the relative percentage of cells with protein aggregates. The number of tRNAs modified by each tRNAmod is shown between parenthesis.

5.2.1 tRNAmods that modify the body of tRNAs have little impact on proteostasis

We observed only few cases in which deletion of enzymes that modify the body of tRNAs increased the percentage of cells with protein aggregates. In the case of the dihydrouridine synthases, deletion of Dus2 showed significant effect on protein

aggregation (6.65-fold change relative WT; Figure 3.11D). Dihydrouridine synthases reduce the C5-C6 bond in uridine to form dihydrouridine, whose non-planar base is incapable of forming stacking interactions with bases of other nucleosides, increasing flexibility (Dalluge *et al.*, 1996). Additionally, dihydrouridine has been associated to translational fidelity by promoting cognate interactions with correct aminoacyl-tRNA synthetases (D₂₀) (Hendrickson, 2001). As observed in our genetic screen, synthesis of D nucleoside at position 20 of the tRNAs by Dus2 is important for translation fidelity. Interestingly, lung cancer cells overexpress the Dus2 enzyme to increase survival and tumor growth (Kato *et al.*, 2005).

Regarding pseudouridine synthases, nine genes encoding putative RNA pseudouridine synthases were identified in yeast. Our genetic screen showed that deletion of Pus6 increases protein aggregation with statistical significance by 4-fold relative to WT; which is similar to the other pseudouridine synthases (Figure 3.11E and Figure 3.12). Disruption of pseudouridine synthase genes were reported to have no marked effect on cell viability and growth, even in cases of double disruptions, with exception of the Pus3 gene KO, as mentioned above (Agostoni Carbone *et al.*, 1991; Lecointe *et al.*, 2002; Behm-Ansmant, Branlant and Motorin, 2007). Homozygous mutation of the human Pus3 gene is correlated with intellectual disability (Shaheen *et al.*, 2016) and a mutation in the human Pus1 gene is associated with Mitochondrial Myopathy and Sideroblastic Anemia (MLASA) (Bykhovskaya *et al.*, 2004; Patton *et al.*, 2005).

The 2'-O-ribosyl-phosphate transferase Rit1 modifies adenosine at position 64 in tRNA^{Met}_i, tagging it for translation initiation (Aström and Byström, 1994). In this way, 2'-O-ribosyl-phosphate modification at position 64 of the initiator tRNA^{Met}_i has a role as an initiator/elongator tRNA discriminatory element. Although discrimination between the initiation and the elongation processes of protein biosynthesis is imperative for translation regulation, the absence of the Rit1 enzyme and the respective modification in tRNA^{Met}_i has no effect on yeast growth (Aström and Byström, 1994; Astrom *et al.*, 1999) and our results show that it has little effect on protein aggregation (Figure 3.11G).

N4-acetylcytidine (ac⁴C) modification at position 12 of serine and leucine tRNAs is synthesized by Tan1 and deletion of its gene affects the stability of tRNA^{Ser}

5. General discussion

(Johansson and Byström, 2004). We did not observe a significant difference in the percentage of cells with protein aggregates in our Tan1 KO strain (Figure 3.11G), suggesting that Tan1 may not play a significant role in proteome homeostasis.

Regarding the group of tRNA methyltransferases (Trm) that modify site-specific or multisite-specific nucleosides within the tRNA (Figure 3.11G), we did not observe a significant difference in the levels of protein aggregates in the strains lacking Trm enzymes relative to the WT control strain, with exception of Trm3 Δ (Figure 3.11G). Most of the modifications catalyzed by the tRNA methyltransferases may affect tRNA folding and structure and stabilize correctly folded anticodon stems (Steinberg and Cedergren, 1995; Purushothaman *et al.*, 2005). These modifications are critical for tRNA maturation and stability (Anderson *et al.*, 1998; Anderson, Phan and Hinnebusch, 2000). A mutation in the human homolog of Trm4, NSun2, was identified in Autosomal-Recessive Intellectual Disability and mutations in the Trmt1 (homolog of Trm1 in yeast), FtsJ1 (homolog of yeast Trm7), and Wdr4 (homolog of yeast Trm82) genes are associated with Intellectual Disability (Michaud *et al.*, 2000; Najmabadi *et al.*, 2011; Abbasi-Moheb *et al.*, 2012; Ahmad Khan *et al.*, 2012). Additionally, a splice mutation in NSun2 was identified as the first causal gene in Dubowitz syndrome spectrum phenotype, characterized by mild microcephaly, growth and mental retardation, eczema and peculiar facies (Martinez *et al.*, 2012); and mutations in Trm82 homolog Wdr4 were associated to microcephalic primordial dwarfism, characterized by extreme pre-natal and post-natal growth deficiency (Shaheen *et al.*, 2015). Moreover, NSun2 and Trm6/61 are overexpressed in tumor cells, suggesting that these RNA methyltransferases induce cell-proliferation and growth, being involved in cancer progression and aggressiveness (Frye and Watt, 2006; Macari *et al.*, 2015). These data suggest that RNA methyltransferases are relevant in the context of neurocognitive development and cancer.

5.2.2 tRNAmods that modify the tRNA anticodon loop affect proteostasis

5.2.2.1 Modifications of position 37 of the tRNA anticodon loop

Our data show that deletion of some of the enzymes that modify anticodon loop position 37 increases the levels of protein aggregation. For instance, Tad1 Δ mutant

strains have a mild increase in protein aggregation; less than 10% (Figure 3.11A). This adenosine deaminase converts A₃₇ to I₃₇ in yeast tRNA^{Ala}_{IGC}, which then is methylated to m¹I₃₇ by Trm5 methyltransferase (Gerber *et al.*, 1998; Björk *et al.*, 2001). In cells lacking Tad1 or Trm5, the levels of m¹I₃₇ dropped to nearly undetectable levels, but growth rate was similar to the WT (Gerber *et al.*, 1998; Björk *et al.*, 2001). Trm5 is also involved in the m¹G₃₇ and, subsequent, yW₃₇ modifications in a subset of tRNAs, namely tRNA^{Ala}_{IGC}, tRNA^{Leu}, tRNA^{Asp}_{GUC}, tRNA^{His}_{GUG}, tRNA^{Pro}_{ncm5UGG}, and tRNA^{Phe}_{GmAA} (Björk *et al.*, 2001; Sprinzl and Vassilenko, 2005; Czerwoniec *et al.*, 2009).

Another group of tRNAmods involved in the modification of position 37 is responsible for the synthesis of t⁶A in almost all ANN (N representing one of the four canonical nucleotides) decoding tRNAs. t⁶A is synthesized in a two-step reaction: first, the threonyl-carbamoyl-AMP (TC-AMP) intermediate is produced by Tcs1 (YrdC) or Tcs2 (Sua5), using threonine and CO₂/HCO₃⁻ as substrates; second, TC-AMP is placed on tRNA by the threonyl-carbamoyl transferase complex (TCTC, KEOPS or EKC complex), consisting of Tcs3 (Kae1), Tcs5 (Bud32), Tcs6 (Pcc1), and Tcs7 (Cgi121). Fungi have an extra enzyme called Tcs8 (Gon7) (El Yacoubi *et al.*, 2009, 2011; Perrochia *et al.*, 2013; Thiaville, Iwata-Reuyl and de Crécy-Lagard, 2014). The involvement of the KEOPS complex in the formation of t⁶A was demonstrated *in vitro*, with Kae1 comprising the catalytic subunit that condensates TC-AMP with tRNA (Perrochia *et al.*, 2013). Bud32 is an ATPase in the presence of Kae1 that undergoes autophosphorylation when it is in a complex with Cgi121 (Perrochia *et al.*, 2013). Sua5 is also involved in the formation of t⁶A in mt-tRNAs, together with Tcs4 (Qri7). It was reported that mutating Bud32 and Gon7 in yeast abolishes t⁶A, but this did not occur when Pcc1, Kae1 and Cgi121 were mutated. In these cases, the mutant strains had t⁶A reduction to 30%, 25% and 60% of WT levels, respectively (Daugeron *et al.*, 2011; Thiaville, Iwata-Reuyl and de Crécy-Lagard, 2014). Similarly, deletion of the Sua5 gene erases the t⁶A modification, slowing growth and increasing +1 frameshift events (El Yacoubi *et al.*, 2009). In our study, Bud32 and Cgi121 KO diploid heterozygous strains produced similar levels of cells with protein aggregates, but only the levels observed in the Sua5Δ strain were statistically significant (Figure 3.11B). In fact, the t⁶A₃₇ modified nucleoside

5. General discussion

produces a planar hydrophobic structure that stacks above the third base of the anticodon and the first base of the codon, stabilizing the weaker A·U base pair, and increasing ribosome binding (Weissenbach and Grosjean, 1981; Agris, Vendeix and Graham, 2007; Agris, 2008).

Mod5 is a tRNA isopentenyltransferase that catalyzes the addition of an isopentenyl group to adenosine, forming i^6A , at position 37 of mitochondrial and cytoplasmic tRNAs (tRNA^{Cys}_{GCA}, tRNA^{Ser}, and tRNA^{Tyr}_{GψA}), using dimethylallyl pyrophosphate (DMAPP) as substrate (Dihanich *et al.*, 1987; Gillman *et al.*, 1991; Benko *et al.*, 2000). Mutation in the Mod5 gene reduced both the levels of i^6A and the decoding efficiency of a tRNA^{Tyr} UAA suppressor due to destabilization of the codon-anticodon interaction (Laten, Gorman and Bock, 1978). However, lack of i^6A does not affect growth rate (Laten, Gorman and Bock, 1978) and our screen did not show significant differences in protein aggregation levels between Mod5Δ and WT control strains (1.9-fold change relative to WT; Figure 3.11G).

Wybutosine (yW) is other modification that occurs at position 37 of tRNA^{Phe}_{GAA} in Archaea and Eukarya that enhances base-stacking interactions with adjacent adenosines (A₃₆ and A₃₈), to reduce the flexibility of the anticodon (Stuart *et al.*, 2003). Deletion of one of the Tyw1-to-Tyw4 genes erases yW, but the mutant strains do not show significant differences in growth rate (Noma *et al.*, 2006; Rodriguez *et al.*, 2012). Similarly, in our study the Tyw1-to-Tyw4 KO strains had similar percentage of cells with protein aggregates and only Tyw4Δ strain showed statistically significant protein aggregation levels, relative to WT controls (Figure 3.11C). tRNA^{Phe} lacking yW can be found in rat, mouse and in Ehrlich ascites tumors and neuroblastoma mice cells, suggesting a role of yW in translation fidelity (Mushinski and Marini, 1979; Kuchino *et al.*, 1982). Overexpression of Tyw2 was also observed in breast cancer cells (Rodriguez *et al.*, 2007).

5.2.2.2 Modifications of position 34 of tRNA anticodon

The formation of I₃₄ requires an adenosine deaminase, consisting of two subunits Tad2 and Tad3, with Tad2 being the catalytic subunit of the heterodimer (Gerber and Keller, 1999). These two genes are essential for cell viability (Gerber and Keller, 1999). We used heterozygous diploid KO strains for Tad2 and Tad3 in our genetic

screen and there was no increase of protein aggregation in these strains relative to WT controls (Figure 3.11A). I₃₄ containing tRNA is predicted to read U, C and A ending codons while unmodified A₃₄ read codons ending with U and rather poorly A-ending codons (Grosjean, 2005). I₃₄ in tRNA^{Ile}_{IAU} is also a positive identity determinant for isoleucyl-tRNA synthase (Senger *et al.*, 1997) and a single mutation in human Tad3 (Adat3) is the likely cause of intellectual disability and strabismus (Alazami *et al.*, 2013).

The synthesis of the yeast wobble nucleoside mcm⁵U requires at least 14 gene products of which 7 actively modify uridine (Elongator complex and Trm9), while the others regulate the former (namely, Kti12, Sap185, Sit4, etc.) (Figure 3.3) (Kalhor and Clarke, 2003; Huang, Lu and Byström, 2008). Similarly, tRNA wobble uridine thiolation requires the cytosolic iron-sulfur cluster assembly machinery (CIA), composed by Cfd1, Nbp35 and Cia1, two mitochondrial scaffold proteins (Isu1 and Isu2) and other regulators (e.g. Urm1 and Uba4) (Huang, Lu and Byström, 2008). In our genetic screen, the absence of Elp1, Kti12, Trm9 and Slm3 tRNAmods significantly increased the level of cells containing protein aggregates. We have also identified another protein involved in thiolation of cytosolic tRNAs, Slm3, which was previously identified as an exclusive mitochondrial thiolase (Umeda *et al.*, 2005). The pattern of tRNA modification observed in the Slm3Δ strain was similar to that of the Urm1Δ strain: those tRNAs contained mcm⁵U₃₄ (increased) and lacked the s²U₃₄ modification (Huang, Lu and Byström, 2008; Schlieker *et al.*, 2008).

5.3 WOBBLE URIDINE MODIFICATION

We demonstrated that absence of n/mcm⁵U₃₄ modification and defects in tRNA thiolation in the Trm9Δ, Elp1Δ and Slm3Δ strains lead to codon specific translational defects (Figure 5.2). Our data are consistent with yeast genetic evidences indicating that the reading of A-ending codons is enhanced by the mcm⁵s²U₃₄ modification (Johansson *et al.*, 2008; Rezgui *et al.*, 2013). Recent studies indicated that transcripts enriched in AAA, GAA and CAA codons are poorly translated in those mutant cells and that the respective proteins are involved in specific biological processes such as translation, rRNA processing and ribosomal subunit biogenesis

5. General discussion

(Laxman *et al.*, 2013; Rezgui *et al.*, 2013). Similarly, our data showed that transcripts enriched in codons that base pair with wobble uridine modified tRNAs (Figure 5.2) encode proteins that aggregate at higher level.

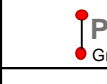




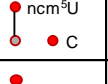


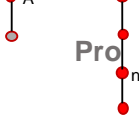



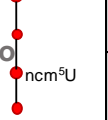


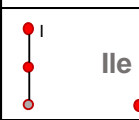
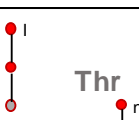





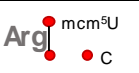
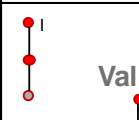
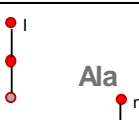
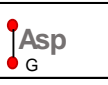
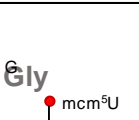
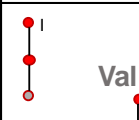
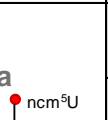


		2 nd position of codon				
		U	C	A	G	
1 st position of codon	U	 Phe Gm	 Ser ncm ⁵ U	 Tyr Gm	 Cys G	U
		 Leu ncm ⁵ Um m ⁵ C	 Ser ncm ⁵ U	Stop	 Trp Cm	A
	C	 Leu G U	 Pro A ncm ⁵ U	 His G	 Arg I C	U
		 Leu G U	 Pro ncm ⁵ U	 Gln mcm ⁵ s ² U C	 Arg C	A
A	 Ile I ψ	 Thr I ncm ⁵ U	 Asn G	 Ser G	U	
	 Met C	 Thr ncm ⁵ U	 Lys mcm ⁵ s ² U C	 Arg mcm ⁵ U C	A	
G	 Val I ncm ⁵ U	 Ala I ncm ⁵ U	 Asp G	 Gly G mcm ⁵ U	U	
	 Val I ncm ⁵ U	 Ala ncm ⁵ U	 Glu mcm ⁵ s ² U C	 Gly mcm ⁵ U C	A	
					G	

Figure 5.2. The genetic code and tRNA wobble modifications. The coding capacities of tRNAs modified in the wobble position is shown. A circle corresponds to a codon read by a tRNA with the position 34 described. A line connecting two or more circles indicates that the same tRNA is able to read those codons. A red circle indicates the capability of that tRNA to base pair with a particular codon, either by Watson-Crick or by wobble rules, whereas a grey filled circle indicates a restricted base pairing (Grosjean and Westhof, 2016). Adapted from Björk *et al.*, 2007.

Our results are also in line with previous studies showing impairment of mitochondrial protein synthesis due to deletion of wobble uridine tRNA_{mods} (Tigano *et al.*, 2015). Aggregated mitochondrial proteins are observed in the absence of wobble uridine modification in the cytosolic tRNAs, re-enforcing evidences that nuclear-encoded tRNAs are imported into mitochondria (Kamenski *et al.*, 2007; Schneider, 2011), namely mcm⁵s²U modified tRNAs.

Deletion of Trm9 and Slm3 affected the yW modification and the enzymes involved in yW modification aggregated in those strains (Tyw1-Tyw3 in Trm9Δ and

Tyw1-Tyw4 in Slm3 Δ). TAN1 was slightly up-regulated in the aggregated protein fraction of Trm9 Δ , Elp1 Δ and Slm3 Δ , and ac⁴C levels were slightly lower in the mutant cells, particularly in Elp1 Δ and Trm9 Δ . Surprisingly, Ncs2 and Ncs6 enzymes, which are involved in the thiolation of the wobble uridine, were enriched in the insoluble fractions of Trm9 Δ and Slm3 Δ , whereas Ncs6 was enriched in Elp1 Δ strain. Thus, the absence of s²U modification in cells lacking Trm9 and Elp1 enzymes was due to the presence of non-functional enzymes of the thiolation pathway.

5.3.1 Absence of U₃₄ modifications increases mistranslation

Our data highlight a critical role of tRNA modifications in preventing translational errors (mistranslation), which is fundamental for proteome stability and function. Thus, preventing mistranslation is an important role of the modified ribonucleosides. The level of amino acid misincorporations into proteins is usually very low (below 0.001%) and the identification of such misincorporations in complex protein mixtures is a significant technical challenge. We used insoluble proteins (instead of total extracts) to enrich our proteins in misincorporated amino acids to increase the probability of detecting mutant peptides. Synthetic peptides containing specific amino acid mutations were also added to our samples at different concentrations to validate our bioinformatics pipeline. To reduce the percentage of false positives, the peptides containing misincorporations were matched to the respective WT proteins, creating a secondary database of yeast proteins. Re-searching LC-MS/MS raw data against this new database with mutant proteins was used to validate the amino acid misincorporations. In this way, we were able to match amino acid misincorporations with codons in a large data set, using R scripts.

Our data showed a clear increase in amino acid misincorporations in our yeast KO strains, harboring tRNA hypomodifications. Previous works showed that mistranslation induced protein aggregation saturates the proteostasis network, activates the UPR and down-regulates protein synthesis rate (Paredes *et al.*, 2012). We were able to identify the proteins and the cellular pathways whose activity is regulated by RNA modifications. The amino acid misincorporations detected

5. General discussion

occurred mostly in abundant proteins, suggesting that amino acid misincorporation detection should be optimized to detect misincorporations in low abundant proteins, namely in those that aggregate in the KO strains.

5.3.2 Protein synthesis errors and human disease

Protein conformational diseases are a group of heterogeneous diseases with high impact in society. Most of the neurodegenerative and some metabolic and liver diseases are associated with protein aggregation (Gregersen *et al.*, 2006). The molecular and structural basis of these diseases are under intense analysis, but studies focus on the mechanisms of protein folding, degradation and on the proteostasis network. Apparently there is down regulation of molecular chaperones during aging which may explain the perturbation of the proteome homeostasis across the lifespan (Soti and Csermely, 2003; Hartl, Bracher and Hayer-Hartl, 2011). Additionally, protein aggregation itself impairs the function of the UPS, resulting in accumulation of protein ubiquitin conjugates (Bence, Sampat and Kopito, 2001), increased protein aggregation and saturation of the proteostasis network. This mechanism of positive-feedback might explain the cell death phenotype and the loss of neuronal function, which are characteristic of various neurodegenerative diseases.

These proteostasis network mechanisms play critical roles in human health, but recent genome wide association studies and other genetic studies have identified multiple single nucleotide polymorphisms (SNPs) in genes encoding tRNAmods and rRNAmods associated with cancer, neurodegenerative diseases, diabetes, hearing loss and several metabolic syndromes (T. Yasukawa *et al.*, 2000; Gonzales *et al.*, 2005; Montanaro *et al.*, 2006; Chen, Tuck and Byström, 2009; Torres, Batlle and Ribas de Pouplana, 2014), suggesting that they also play a role in protein misfolding diseases. For example, mutations in the FTSJ1 methyltransferase, which modifies positions 32 and 34 of tRNA^{Phe} were found in patients with non-syndromic X-linked mental retardation (Guy *et al.*, 2015), while the MELAS and MERRF syndromes are associated with hypomodification of mitochondrial tRNAs (T. Yasukawa *et al.*, 2000; Takehiro Yasukawa *et al.*, 2000).

Also, mutations in tRNA methyltransferases are associated with type 2 diabetes (Igoillo-Esteve *et al.*, 2013) and lack of mcm⁵ and ncm⁵ side chains of tRNA wobble uridines cause neurological and developmental defects in *C. elegans* (Chen, Tuck and Byström, 2009). Indeed, Elongator complex activity is impaired in patients with familial dysautonomia (Nguyen *et al.*, 2010) and evidences suggest that the Elongator complex may be disrupted in other neurological diseases, such as sporadic ALS (Simpson *et al.*, 2009) and rolandic epilepsy (Strug *et al.*, 2009). We identified several proteins in the Elp1Δ strain that are orthologous to human proteins involved in PD and familial ALS, suggesting that perturbation of RNA modifications by mutations in RNAmods, environmental factors and metabolic deregulation might induce protein aggregation, proteotoxic stress, saturation of the proteostasis network, cell death and/or loss of fitness. This suggests that yeast could be a good model organism to study the role of tRNA- and rRNA-modifying enzymes and tRNA hypomodification in human diseases.

5.4 CONCLUSION AND FUTURE WORK

Our study identified RNA-modifying enzymes that are fundamental to maintain the folding state of the proteome and proteome homeostasis. The data showed that modifications in the tRNA anticodon loop are essential for protein synthesis fidelity and highlighted in diverse phenotypes that have also been described by other groups (Frohloff *et al.*, 2001; Esberg *et al.*, 2006; Grosjean, 2009a; Wang, Yan and Guan, 2010). Aggregated proteins identified in the tRNAmod KO strains are encoded by genes enriched in codons that base pair with the tRNAs modified by such enzymes. Some of these codons are decoded with elevated level of error. Translation accuracy of near-cognate codons is also degraded further highlighting the role of RNAmods in proteome stability.

Our proteomics study was carried out with a low number of biological and technical replicates of each mutant strain: 1 biological replicate for Elp1Δ and Trm9Δ and 2 biological replicates for Slm3Δ, one of these datasets (Slm3Δ clone 2) has 4 technical replicates. Therefore, it is necessary to increase the number of replicates to validate the conclusions described in this thesis. It would also be interesting to

5. General discussion

analyze soluble protein fractions of each mutant strain to evaluate if the pattern of amino acid misincorporations is different from that of the insoluble fraction.

Since RNA modifications have impact on protein synthesis accuracy, we postulate that tRNA hypomodification activates the unfolded protein response (UPR), repressing protein synthesis rate through phosphorylation of the translation initiation factor eIF2 α . This hypothesis should be validated in future studies. It would also be interesting to evaluate protein synthesis rate in the mutant cells to clarify if decreased fitness induced by mistranslation is associated to repression of protein synthesis rate (Paredes *et al.*, 2012).

Remarkably, stress-induced regulation of tRNA modification allows ribosomes to efficiently translate yeast stress genes (Chan *et al.*, 2012), while mRNA mistranslation produces both genetic and phenotypic diversity of high adaptation potential (Pan, 2013). In other words, tRNA modifications may, at least in yeast, play important roles in stress adaptation and evolution of adaptive phenotypic traits. The role of RNA modifications in phenotypic variability and inheritance of stress tolerance traits should also be investigated.

Unfortunately, we did not have time to clarify the role of rRNA modifications in protein synthesis fidelity. Thus, the level of rRNA modification in the heterozygous diploid strains and the stability of the hypomodified rRNA should be clarified in future studies.

Ribosome pausing sites were identified by others using similar strains that we have used in our study (Zinshteyn and Gilbert, 2013; Nedialkova and Leidel, 2015). It will be interesting to map ribosome pausing sites in our strains using ribosome profiling analysis and compare these data with mistranslation data to clarify if amino acid misincorporation events occur at codon pausing sites. Additionally, RNAseq analysis will be important to evaluate the transcriptome of each strain and better understand functional codon usage. The study of codon context associated with amino acid misincorporations and the study of codon usage of RNAmo genes should also be investigated.

6. REFERENCES

6. References

- Abbasi-Moheb, L. *et al.* (2012) Mutations in NSUN2 Cause Autosomal-Recessive Intellectual Disability, *The American Journal of Human Genetics*, 90, pp. 847–855. doi: 10.1016/j.ajhg.2012.03.021.
- Abdel-Fattah, W. *et al.* (2015) Phosphorylation of Elp1 by Hrr25 Is Required for Elongator-Dependent tRNA Modification in Yeast, *PLoS genetics*, 11(1). doi: 10.1371/journal.pgen.1004931.
- Abelson, J., Trotta, C. R. and Li, H. (1998) tRNA splicing, *Journal of Biological Chemistry*, 273(21), pp. 12685–12688. doi: 10.1074/jbc.273.21.12685.
- Acker, J., Conesa, C. and Lefebvre, O. (2013) Yeast RNA polymerase III transcription factors and effectors, *Biochimica et biophysica acta*. Elsevier B.V., 1829(3–4), pp. 283–95. doi: 10.1016/j.bbagr.2012.10.002.
- Adeli, K. (2011) Translational control mechanisms in metabolic regulation: critical role of RNA binding proteins, microRNAs, and cytoplasmic RNA granules, *Am J Physiol Endocrinol Metab*, 301. doi: 10.1152/ajpendo.00399.2011.
- Aebi, M. *et al.* (1990) Isolation of a temperature-sensitive mutant with an altered tRNA nucleotidyltransferase and cloning of the gene encoding tRNA nucleotidyltransferase in the yeast *Saccharomyces cerevisiae*, *Journal of Biological Chemistry*, 265(27), pp. 16216–16220.
- Agostoni Carbone, M. L. *et al.* (1991) A gene tightly linked to CEN6 is important for growth of *Saccharomyces cerevisiae*, *Current Genetics*, 19, pp. 1–8. doi: 10.1007/BF00362080.
- Agris, P. F. (1996) The Importance of Being Modified: Roles of Modified Nucleosides and Mg²⁺ in RNA Structure and Function, *Progress in Nucleic Acid Research and Molecular Biology*, 53, pp. 79–129. doi: 10.1016/S0079-6603(08)60143-9.
- Agris, P. F. (2004) Decoding the genome: a modified view, *Nucleic acids research*, 32(1), pp. 223–38. doi: 10.1093/nar/gkh185.
- Agris, P. F. (2008) Bringing order to translation: the contributions of transfer RNA anticodon-domain modifications, *EMBO reports*, 9(7), pp. 629–35. doi: 10.1038/embor.2008.104.
- Agris, P. F., Soell, D. and Seno, T. (1973) Biological function of 2-thiouridine in *Escherichia coli* glutamic acid transfer ribonucleic acid, *Biochemistry*, 12(22), pp. 4331–4337. doi: 10.1021/bi00746a005.
- Agris, P. F., Vendeix, F. a P. and Graham, W. D. (2007) tRNA's wobble decoding of the genome: 40 years of modification, *Journal of molecular biology*, 366(1), pp. 1–13. doi: 10.1016/j.jmb.2006.11.046.
- Ahmad Khan, M. *et al.* (2012) Mutation in NSUN2, which Encodes an RNA Methyltransferase, Causes Autosomal-Recessive Intellectual Disability, *The*

American Journal of Human Genetics, 90, pp. 856–863. doi: 10.1016/j.ajhg.2012.03.023.

Alazami, A. M. *et al.* (2013) Mutation in ADAT3, encoding adenosine deaminase acting on transfer RNA, causes intellectual disability and strabismus, *Journal of medical genetics*, 50, pp. 425–30. doi: 10.1136/jmedgenet-2012-101378.

Alexandrov, A. *et al.* (2006) Rapid tRNA decay can result from lack of nonessential modifications, *Molecular cell*, 21(1), pp. 87–96. doi: 10.1016/j.molcel.2005.10.036.

Alexandrov, A., Martzen, M. R. and Phizicky, E. M. (2002) Two proteins that form a complex are required for 7-methylguanosine modification of yeast tRNA, *RNA*, 8(10), pp. 1253–66.

Allan Drummond, D. and Wilke, C. O. (2009) The evolutionary consequences of erroneous protein synthesis, *Nature Reviews Genetics*. Nature Publishing Group, 10(10), pp. 715–724. doi: 10.1038/nrg2662.

Allmang, C. *et al.* (2000) Degradation of ribosomal RNA precursors by the exosome, *Nucleic Acids Research*, 28(8), pp. 1684–1691.

Anderson, J. *et al.* (1998) The essential Gcd10p–Gcd14p nuclear complex is required for 1-methyladenosine modification and maturation of initiator methionyl-tRNA, *Genes & Development*, 12, pp. 3650–3662.

Anderson, J., Phan, L. and Hinnebusch, A. G. (2000) The Gcd10p/Gcd14p complex is the essential two-subunit tRNA(1-methyladenosine) methyltransferase of *Saccharomyces cerevisiae*, *PNAS*, 97(10), pp. 5173–5178.

Anderson, S. L. *et al.* (2001) Familial Dysautonomia Is Caused by Mutations of the IKAP Gene, *Am. J. Hum. Genet*, 68, pp. 753–758.

Anfinsen, C. (1973) Principles that Govern the Folding of Protein Chains, *Science*, 181(4096), pp. 223–230.

Ansmant, I. *et al.* (2000) Identification of the *Saccharomyces cerevisiae* RNA:pseudouridine synthase responsible for formation of Ψ 2819 in 21S mitochondrial ribosomal RNA, *Nucleic Acids Research*, 28(9), pp. 1941–1946.

Ansmant, I. *et al.* (2001) Identification and Characterization of the tRNA:Y31 - Synthase (Pus6p) of *Saccharomyces cerevisiae*, *The Journal of Biological Chemistry*, 276(37), pp. 34934–34940. doi: 10.1074/jbc.M103131200.

Arava, Y. *et al.* (2003) Genome-wide analysis of mRNA translation profiles in *Saccharomyces cerevisiae*, *PNAS*. National Academy of Sciences, 100(7), pp. 3889–94. doi: 10.1073/pnas.0635171100.

Ares, M., Grate, L. and Pauling, M. H. (1999) A handful of intron-containing genes produces the lion's share of yeast mRNA, *RNA*, 5, pp. 1138–1139. doi:

6. References

10.1017/S1355838299991379.

Armache, J.-P. *et al.* (2010) Localization of eukaryote-specific ribosomal proteins in a 5.5-Å cryo-EM map of the 80S eukaryotic ribosome, *PNAS*, 107(46), pp. 19754–19759. doi: 10.1073/pnas.1010005107.

Armistead, J. and Triggs-Raine, B. (2014) Diverse diseases from a ubiquitous process: the ribosomopathy paradox, *FEBS letters*, 588(9), pp. 1491–500. doi: 10.1016/j.febslet.2014.03.024.

Ashraf, S. S. *et al.* (1999) Single atom modification (O → S) of tRNA confers ribosome binding, *RNA*, 5, pp. 188–194.

Astrom, S. U. *et al.* (1999) Genetic interactions between a null allele of the RIT1 gene encoding an initiator tRNA-specific modification enzyme and genes encoding translation factors in *Saccharomyces cerevisiae*, *Mol Gen Genet*, 261, pp. 967–976.

Aström, S. U. and Byström, S. (1994) Rit1, a tRNA backbone-modifying enzyme that mediates initiator and elongator tRNA discrimination, *Cell*, 79(3), pp. 535–46.

Auxilien, S. *et al.* (1996) Mechanism, specificity and general properties of the yeast enzyme catalysing the formation of inosine 34 in the anticodon of transfer RNA, *Journal of molecular biology*, 262, pp. 437–58. doi: 10.1006/jmbi.1996.0527.

Balchin, D., Hayer-Hartl, M. and Hartl, F. U. (2016) In vivo aspects of protein folding and quality control, *Science*, 353, p. aac4354-aac4354. doi: 10.1126/science.aac4354.

Bär, C. *et al.* (2008) A versatile partner of eukaryotic protein complexes that is involved in multiple biological processes: Kti11/Dph3, *Molecular Microbiology*, 69(July), pp. 1221–1233. doi: 10.1111/j.1365-2958.2008.06350.x.

Barral, J. M. *et al.* (2004) Roles of molecular chaperones in protein misfolding diseases, *Seminars in cell & developmental biology*, 15(1), pp. 17–29. doi: 10.1016/j.semcd.2003.12.010.

Bartlett, J. M. *et al.* (2010) Mammostrat® as a tool to stratify breast cancer patients at risk of recurrence during endocrine therapy, *Breast Cancer Research*, 12. doi: 10.1186/bcr2604.

Basso, M. *et al.* (2009) Characterization of Detergent-Insoluble Proteins in ALS Indicates a Causal Link between Nitritative Stress and Aggregation in Pathogenesis, *PLoS ONE*. Edited by L. Petrucelli. Public Library of Science, 4(12). doi: 10.1371/journal.pone.0008130.

Bauer, F. *et al.* (2012) Translational control of cell division by Elongator, *Cell reports*. The Authors, 1(5), pp. 424–33. doi: 10.1016/j.celrep.2012.04.001.

Baxter-Roshek, J. L., Petrov, A. N. and Dinman, J. D. (2007) Optimization of ribosome structure and function by rRNA base modification, *PloS one*. Public Library of Science, (1). doi: 10.1371/journal.pone.0000174.

Becker, H. F. *et al.* (1997) The yeast gene YNL292w encodes a pseudouridine synthase (Pus4) catalyzing the formation of Ψ 55 in both mitochondrial and cytoplasmic tRNAs, *Nucleic Acids Research*, 25(22), pp. 4493–4499.

Begley, U. *et al.* (2007) Trm9-catalyzed tRNA modifications link translation to the DNA damage response, *Molecular cell*, 28(5), pp. 860–70. doi: 10.1016/j.molcel.2007.09.021.

Begley, U. *et al.* (2013) A human tRNA methyltransferase 9-like protein prevents tumour growth by regulating LIN9 and HIF1- α , *EMBO molecular medicine*, 5(3), pp. 366–83. doi: 10.1002/emmm.201201161.

Behm-Ansmant, I. *et al.* (2006) A previously unidentified activity of yeast and mouse RNA:pseudouridine synthases 1 (Pus1p) on tRNAs, *RNA*, 12, pp. 1583–1593. doi: 10.1261/rna.100806.

Behm-Ansmant, I. *et al.* (2003) The *Saccharomyces cerevisiae* U2 snRNA:pseudouridine-synthase Pus7p is a novel multisite–multisubstrate RNA:Y-synthase also acting on tRNAs, *RNA*, 9(11), pp. 1371–1382. doi: 10.1261/rna.5520403.

Behm-Ansmant, I. *et al.* (2004) Pseudouridylation at Position 32 of Mitochondrial and Cytoplasmic tRNAs Requires Two Distinct Enzymes in *Saccharomyces cerevisiae*, *The Journal of Biological Chemistry*, 279(51), pp. 52998–53006. doi: 10.1074/jbc.M409581200.

Behm-Ansmant, I., Branlant, C. and Motorin, Y. (2007) The *Saccharomyces cerevisiae* Pus2 protein encoded by YGL063w ORF is a mitochondrial tRNA: Ψ 27/28-synthase, *RNA*, 13, pp. 1641–1647. doi: 10.1261/rna.605607.on.

Beltramel, M. and Tollervey, D. (1995) Base pairing between U3 and the pre-ribosomal RNA is required for 18S rRNA synthesis, *The EMBO Journal*, 14(17), pp. 4350–4356.

Bence, N. F., Sampat, R. M. and Kopito, R. R. (2001) Impairment of the Ubiquitin-Proteasome System by Protein Aggregation, *Science*, 292(5521), pp. 1552–1555. doi: 10.1126/science.292.5521.1552.

Benko, A. L. *et al.* (2000) Competition between a sterol biosynthetic enzyme and tRNA modification in addition to changes in the protein synthesis machinery causes altered nonsense suppression, *PNAS*, 97(1), pp. 61–66.

Bennett, C. B. *et al.* (2001) Genes required for ionizing radiation resistance in yeast, *Nature genetics*, 29, pp. 426–434. doi: 10.1038/ng778.

Berg, B. van den, Ellis, R. J. and Dobson, C. (1999) Effects of macromolecular

6. References

crowding on protein folding and aggregation, *The EMBO Journal*, 18(24), pp. 6927–6933. doi: 10.1371/journal.pcbi.1000833.

Berg, M. *et al.* (2010) Distinct high resolution genome profiles of early onset and late onset colorectal cancer integrated with gene expression data identify candidate susceptibility loci, *Molecular Cancer*, 9(100). doi: 10.1186/1476-4598-9-100.

Berke, S. J. S. and Paulson, H. L. (2003) Protein aggregation and the ubiquitin proteasome pathway: gaining the UPPer hand on neurodegeneration, *Current Opinion in Genetics & Development*, 13, pp. 253–261. doi: 10.1016/S0959-437X(03)00053-4.

Bertram, G. *et al.* (2001) Endless possibilities: Translation termination and stop codon recognition, *Microbiology*, 147(2), pp. 255–269.

Björk, G. R. *et al.* (1999) Transfer RNA modification: influence on translational frameshifting and metabolism, *FEBS Letters*, 452, pp. 47–51. doi: 10.1016/S0014-5793(99)00528-1.

Björk, G. R. *et al.* (2001) A primordial tRNA modification required for the evolution of life?, *The EMBO journal*, 20(1 & 2), pp. 231–239.

Björk, G. R. *et al.* (2007) A conserved modified wobble nucleoside (mcm5s2U) in lysyl-tRNA is required for viability in yeast, *RNA*, 13, pp. 1245–1255. doi: 10.1261/rna.558707.position.

Björk, G. R., Wikström, P. M. and Byström, A. S. (1989) Prevention of translational frameshifting by the modified nucleoside 1-methylguanosine, *Science*, 244, pp. 986–9. doi: 10.1126/science.2471265.

Bonnefond, L. *et al.* (2007) Crystal Structure of Human Mitochondrial Tyrosyl-tRNA Synthetase Reveals Common and Idiosyncratic Features, *Structure*, 15, pp. 1505–1516. doi: 10.1016/j.str.2007.09.018.

Bouadloun, F., Donner, D. and Kurland, C. G. (1983) Codon-specific missense errors in vivo, *The EMBO Journal*, 2(8), pp. 1351–1356.

Brohée, S. and Van Helden, J. (2006) Evaluation of clustering algorithms for protein-protein interaction networks, *BMC Bioinformatics*, 7(488). doi: 10.1186/1471-2105-7-488.

Buchberger, A., Bukau, B. and Sommer, T. (2010) Protein quality control in the cytosol and the endoplasmic reticulum: brothers in arms, *Molecular cell*. Elsevier Inc., 40(2), pp. 238–52. doi: 10.1016/j.molcel.2010.10.001.

Bullinger, L. *et al.* (2010) Identification of acquired copy number alterations and uniparental disomies in cytogenetically normal acute myeloid leukemia using high-resolution single-nucleotide polymorphism analysis, *Leukemia*, 24, pp. 438–449. doi: 10.1038/leu.2009.263.

Bykhovskaya, Y. *et al.* (2004) Report Missense Mutation in Pseudouridine Synthase 1 (PUS1) Causes Mitochondrial Myopathy and Sideroblastic Anemia (MLASA), *Am J Hum Genet*, 74, pp. 1303–1308.

Cantara, W. a. *et al.* (2011) The RNA modification database, RNAMDB: 2011 update, *Nucleic Acids Research*, 39, pp. 195–201. doi: 10.1093/nar/gkq1028.

Carlile, T. M. *et al.* (2014) Pseudouridine profiling reveals regulated mRNA pseudouridylation in yeast and human cells, *Nature*. Nature Publishing Group, 515, pp. 143–6. doi: 10.1038/nature13802.

Carmona-Saez, P. *et al.* (2007) GENECODIS: a web-based tool for finding significant concurrent annotations in gene lists, *Genome Biology*, 8(1). doi: 10.1186/gb-2007-8-1-r3.

Chan, C. T. Y. *et al.* (2010) A quantitative systems approach reveals dynamic control of tRNA modifications during cellular stress, *PLoS genetics*, 6(12), p. e1001247. doi: 10.1371/journal.pgen.1001247.

Chan, C. T. Y. *et al.* (2012) Reprogramming of tRNA modifications controls the oxidative stress response by codon-biased translation of proteins, *Nat Commun*, 3(937). doi: 10.1038/ncomms1938.Reprogramming.

Charette, M. and Gray, M. W. (2000) Pseudouridine in RNA: what, where, how, and why, *IUBMB life*, 49(March), pp. 341–351. doi: 10.1080/152165400410182.

Chen, C., Huang, B., Eliasson, M., *et al.* (2011) Elongator complex influences telomeric gene silencing and DNA damage response by its role in wobble uridine tRNA modification, *PLoS genetics*, 7(9). doi: 10.1371/journal.pgen.1002258.

Chen, C., Huang, B., Anderson, J. T., *et al.* (2011) Unexpected accumulation of ncm5U and ncm5S2U in a trm9 mutant suggests an additional step in the synthesis of mcm5U and mcm5S2U, *PloS one*, 6(6). doi: 10.1371/journal.pone.0020783.

Chen, C., Tuck, S. and Byström, A. S. (2009) Defects in tRNA modification associated with neurological and developmental dysfunctions in *Caenorhabditis elegans* elongator mutants, *PLoS genetics*, 5(7). doi: 10.1371/journal.pgen.1000561.

Chen, Y.-T. *et al.* (2009) Loss of Mouse Ikbkap, a Subunit of Elongator, Leads to Transcriptional Deficits and Embryonic Lethality That Can Be Rescued by Human IKBKAP, *Molecular and Cellular Biology*, 29(3), pp. 736–744. doi: 10.1128/MCB.01313-08.

Chernyakov, I. *et al.* (2008) Identification and analysis of tRNAs that are degraded in *Saccharomyces cerevisiae* due to lack of modifications, *Methods in Enzymology*, 449, pp. 221–237. doi: 10.1016/S0076-6879(08)02411-7.

Cherry, J. M. *et al.* (1998) SGD: *Saccharomyces Genome Database*, *Nucleic*

6. References

Acids Research, 26(1).

Chevance, F. F. V, Le Guyon, S. and Hughes, K. T. (2014) The effects of codon context on in vivo translation speed, *PLoS genetics*, 10(6), p. e1004392. doi: 10.1371/journal.pgen.1004392.

Choesmel, V. *et al.* (2007) Impaired ribosome biogenesis in Diamond-Blackfan anemia, *Blood*. American Society of Hematology, 109(3), pp. 1275–83. doi: 10.1182/blood-2006-07-038372.

Close, P. *et al.* (2006) Transcription Impairment and Cell Migration Defects in Elongator-Depleted Cells: Implication for Familial Dysautonomia, *Molecular Cell*. Elsevier Inc, 22, pp. 521–531. doi: 10.1016/j.molcel.2006.04.017.

Cochella, L. and Green, R. (2005) Fidelity in protein synthesis, *Current Biology*, 15(14), pp. R536-40. doi: 10.1016/j.cub.2005.07.018.

Colby, G., Wu, M. and Tzagoloff, A. (1998) MTO1 Codes for a Mitochondrial Protein Required for Respiration in Paromomycin-resistant Mutants of *Saccharomyces cerevisiae*, *J Biol Chem*, 273(43), pp. 27945–27952.

Collart, M. A. and Oliviero, S. (2001) Preparation of yeast RNA, in *Current protocols in molecular biology*. Harvard Medical School, Boston, Massachusetts, p. 13.12.1-13.12.5. doi: 10.1002/0471142727.mb1301s23.

Copela, L. a *et al.* (2008) Competition between the Rex1 exonuclease and the La protein affects both Trf4p-mediated RNA quality control and pre-tRNA maturation., *RNA*, 14(6), pp. 1214–1227. doi: 10.1261/rna.1050408.

Creppe, C. *et al.* (2009) Elongator Controls the Migration and Differentiation of Cortical Neurons through Acetylation of α -Tubulin, *Cell*, 136, pp. 551–564. doi: 10.1016/j.cell.2008.11.043.

Crick, F. (1958) On protein synthesis, *Symposia of the Society for Experimental Biology*, 12, pp. 138–163.

Crick, F. H. C. (1966) Codon—anticodon pairing: The wobble hypothesis, *Journal of Molecular Biology*, 19, pp. 548–555. doi: 10.1016/S0022-2836(66)80022-0.

Crick, F. H. C. (1968) The origin of the genetic code, *Journal of Molecular Biology*, 38(3), pp. 367–379. doi: 10.1016/0022-2836(68)90392-6.

Czerwoniec, A. *et al.* (2009) MODOMICS: a database of RNA modification pathways. 2008 update, *Nucleic Acids Res*, 37, pp. D118–D121. doi: 10.1093/nar/gkj084.

Dalluge, J. J. *et al.* (1996) Conformational flexibility in RNA: the role of dihydrouridine, *Nucleic Acids Research*, 24(6), pp. 1073–1079.

Dauden, M. I. *et al.* (2017) Architecture of the yeast Elongator complex, *EMBO Reports*, 18(2), pp. 264–279. doi: 10.15252/embr.

Daugeron, M.-C. *et al.* (2011) Gcn4 misregulation reveals a direct role for the evolutionary conserved EKC/KEOPS in the t6A modification of tRNAs, *Nucleic acids research*, 39(14), pp. 6148–60. doi: 10.1093/nar/gkr178.

Decatur, W. A. and Fournier, M. J. (2003) RNA-guided nucleotide modification of ribosomal and other, *The Journal of Biological Chemistry*, 278(17), pp. 695–698. doi: 10.1074/jbc.R200023200.

Decatur, W. A. and Schnare, M. N. (2008) Different Mechanisms for Pseudouridine Formation in Yeast 5S and 5.8S rRNAs, *Molecular and Cellular Biology*, 28(10), pp. 3089–3100. doi: 10.1128/MCB.01574-07.

Decatur, W. a and Fournier, M. J. (2002) rRNA modifications and ribosome function, *Trends in biochemical sciences*, 27(7), pp. 344–51.

Dedon, P. C. and Begley, T. J. (2013) A System of RNA Modifications and Biased Codon Use Controls Cellular Stress Response at the Level of Translation, *American Chemical Society*.

Demasi, M., Silva, G. M. and Netto, L. E. S. (2003) 20 S proteasome from *Saccharomyces cerevisiae* is responsive to redox modifications and is S-glutathionylated, *Journal of Biological Chemistry*, 278, pp. 679–685. doi: 10.1074/jbc.M209282200.

Deng, W. *et al.* (2015) Trm9-Catalyzed tRNA Modifications Regulate Global Protein Expression by Codon-Biased Translation, *PLoS Genetics*, 11(12), pp. 1–23. doi: 10.1371/journal.pgen.1005706.

Dever, T. E. (1999) Translation initiation: adept at adapting, *Trends in biochemical sciences*, 24(10), pp. 398–403.

Dever, T. E. (2002) Gene-specific regulation by general translation factors, *Cell*, 108(4), pp. 545–56.

Dever, T. E. and Hinnebusch, A. G. (2005) GCN2 Whets the Appetite for Amino Acids, *Molecular Cell*, 18, pp. 141–148. doi: 10.1016/j.molcel.2005.03.023.

Dever, T. E., Kinzy, T. G. and Pavitt, G. D. (2016) Mechanism and Regulation of Protein Synthesis in *Saccharomyces cerevisiae*, *Genetics*, 203, pp. 65–107. doi: 10.1534/genetics.115.186221.

Dewe, J. M. *et al.* (2012) The yeast rapid tRNA decay pathway competes with elongation factor 1A for substrate tRNAs and acts on tRNAs lacking one or more of several modifications, *RNA*, 18(10), pp. 1886–96. doi: 10.1261/rna.033654.112.

Dez, C. *et al.* (2002) Naf1p, an Essential Nucleoplasmic Factor Specifically Required for Accumulation of Box H/ACA Small Nucleolar RNPs, *Molecular and*

6. References

Cellular Biology, 22(20), pp. 7053–7065. doi: 10.1128/MCB.22.20.7053–7065.2002.

Dez, C., Houseley, J. and Tollervey, D. (2006) Surveillance of nuclear-restricted pre-ribosomes within a subnucleolar region of *Saccharomyces cerevisiae*, *The EMBO Journal*, 25, pp. 1534–1546. doi: 10.1038/.

Dihanich, M. E. *et al.* (1987) Isolation and characterization of MOD5, a gene required for isopentenylation of cytoplasmic and mitochondrial tRNAs of *Saccharomyces cerevisiae*, *Molecular and cellular biology*, 7(1), pp. 177–184.

Dobson, C. M. (2001) The structural basis of protein folding and its links with human disease, *Philosophical transactions of the Royal Society of London. Series B, Biological sciences*, 356(1406), pp. 133–45. doi: 10.1098/rstb.2000.0758.

Dobson, C. M. (2004) Principles of protein folding, misfolding and aggregation, *Seminars in cell & developmental biology*, 15(1), pp. 3–16. doi: 10.1016/j.semcd.2003.12.008.

Doyle, S. M., Genest, O. and Wickner, S. (2013) Protein rescue from aggregates by powerful molecular chaperone machines, *Nature Reviews Molecular Cell Biology*. Nature Publishing Group, 14(10), pp. 617–629. doi: 10.1038/nrm3660.

Durant, P. C. *et al.* (2005) Structural Effects of Hypermodified Nucleosides in the *Escherichia coli* and Human tRNA, *Biochemistry*, 44, pp. 8078–8089. doi: 10.1021/bi050343f.

Eldred, E. W. and Schimmel, P. R. (1972) Rapid Deacylation by Isoleucyl Transfer Ribonucleic Acid Synthetase of Isoleucine-specific Transfer Ribonucleic Acid Aminoacylated with Valine, *The Journal of biological chemistry*, 274(9).

Emilsson, V., Näslund, A. K. and Kurland, C. G. (1992) Thiolation of transfer RNA in *Escherichia coli* varies with growth rate, *Nucleic acids research*. Oxford University Press, 20(17), pp. 4499–505.

Eriani, G. *et al.* (1990) Partition of tRNA synthetases into two classes based on mutually exclusive sets of sequence motifs, *Nature*, 347, pp. 203–206. doi: 10.1038/347203a0.

Erjavec, N. *et al.* (2007) Accelerated aging and failure to segregate damaged proteins in Sir2 mutants can be suppressed by overproducing the protein aggregation-remodeling factor Hsp104p, *Genes & development*, 21(19), pp. 2410–21. doi: 10.1101/gad.439307.

Esberg, A. *et al.* (2006) Elevated Levels of Two tRNA Species Bypass the Requirement for Elongator Complex in Transcription and Exocytosis, *Molecular Cell*, 24, pp. 139–148. doi: 10.1016/j.molcel.2006.07.031.

Esberg, B. *et al.* (1997) Three modified nucleosides present in the anticodon stem and loop influence the in vivo aa-tRNA selection in a tRNA-dependent manner, *Journal of Molecular Biology*, 271, pp. 209–21. doi: 10.1006/jmbi.1997.1176.

- Fahiminiya, S. *et al.* (2014) Whole exome sequencing unravels disease-causing genes in consanguineous families in Qatar, *Clinical Genetics*, 86, pp. 134–141. doi: 10.1111/cge.12280.
- Farabaugh, P. J. and Björk, G. R. (1999) How translational accuracy influences reading frame maintenance, *The EMBO Journal*, 18(6), pp. 1427–1434. doi: 10.1093/emboj/18.6.1427.
- Fatica, A., Dlakic, M. and Tollervey, D. (2002) Naf1p is a box H/ACA snoRNP assembly factor, *RNA*, 8, pp. 1502–1514.
- Feng, W. and Hopper, A. K. (2002) A Los1p-independent pathway for nuclear export of intronless tRNAs in *Saccharomyces cerevisiae*, *PNAS*, 99(8), pp. 5412–5417.
- Fernández-Vázquez, J. *et al.* (2013) Modification of tRNA(Lys) UUU by elongator is essential for efficient translation of stress mRNAs, *PLoS genetics*, 9(7), p. e1003647. doi: 10.1371/journal.pgen.1003647.
- Fichtner, L. *et al.* (2002) Molecular analysis of KTI12/TOT4, a *Saccharomyces cerevisiae* gene required for *Kluyveromyces lactis* zymocin action, *Molecular Microbiology*, 43, pp. 783–791. doi: 10.1046/j.1365-2958.2002.02794.x.
- Fichtner, L. *et al.* (2003) Elongator's toxin-target (TOT) function is nuclear localization sequence dependent and suppressed by post-translational modification, *Molecular Microbiology*, 49, pp. 1297–1307. doi: 10.1046/j.1365-2958.2003.03632.x.
- Fink, A. L. (1998) Protein aggregation: folding aggregates, inclusion bodies and amyloid, *Folding & Design*, 3(1), pp. 9–23.
- Flanagan, J. M. *et al.* (2004) Mapping of a candidate colorectal cancer tumor-suppressor gene to a 900-kilobase region on the short arm of chromosome 8, *Genes Chromosomes and Cancer*, 40(May), pp. 247–260. doi: 10.1002/gcc.20039.
- Fleissner, E. and Borek, E. (1962) A new enzyme of RNA synthesis: RNA methylase, *PNAS. National Academy of Sciences*, 48(7), pp. 1199–203.
- Forster, C., Chakraborty, K. and Sprinzl, M. (1993) Discrimination between initiation and elongation of protein biosynthesis in yeast: identity assured by a nucleotide modification in the initiator tRNA, *Nucleic Acids Research*, 21(24), pp. 5679–5683.
- Freude, K. *et al.* (2004) Report Mutations in the FTSJ1 Gene Coding for a Novel S-Adenosylmethionine-Binding Protein Cause Nonsyndromic X-Linked Mental Retardation, *Am J Hum Genet*, 75, pp. 305–309.
- Frohloff, F. *et al.* (2001) *Saccharomyces cerevisiae* Elongator mutations confer resistance to the *Kluyveromyces lactis* zymocin, *The EMBO Journal*, 20(8), pp. 1993–2003.

6. References

- Frye, M. and Watt, F. M. (2006) The RNA Methyltransferase Misu (NSun2) Mediates Myc-Induced Proliferation and Is Upregulated in Tumors, *Current Biology*, 16, pp. 971–981. doi: 10.1016/j.cub.2006.04.027.
- Fujita, K. *et al.* (1998) Hsp104 Responds to Heat and Oxidative Stress with Different Intracellular Localization in *Saccharomyces cerevisiae*, *Biochemical and Biophysical Research Communications*, 248(3), pp. 542–547. doi: 10.1006/bbrc.1998.9008.
- Furukawa, K. *et al.* (2000) A protein Conjugation System in Yeast with Homology to Biosynthetic Enzyme Reaction of Prokaryotes, *The Journal of biological chemistry*, 275(11), pp. 7462–7465.
- Gagnon, K. T., Qu, G. and Maxwell, E. S. (2009) Multicomponent 2'-O-Ribose Methylation Machines: Evolving Box C/D RNP Structure and Function, in *DNA and RNA Modification Enzymes: Structure, Mechanism, Function and Evolution*. Austin, Texas, USA: Landes Bioscience, pp. 436–449.
- Gartmann, M. *et al.* (2010) Mechanism of eIF6-mediated Inhibition of Ribosomal Subunit Joining, *The Journal of Biological Chemistry*, 285(20), pp. 14848–14851. doi: 10.1074/jbc.C109.096057.
- Gebauer, F. and Hentze, M. W. (2004) Molecular mechanisms of translational control, *Nature Reviews Molecular Cell Biology*, 5(October), pp. 827–835. doi: 10.1038/nrm1488.
- Gerber, A. *et al.* (1998) Tad1p, a yeast tRNA-specific adenosine deaminase, is related to the mammalian pre-mRNA editing enzymes ADAR1 and ADAR2, *The EMBO Journal*, 17(16), pp. 4780–4789.
- Gerber, A. P. and Keller, W. (1999) An Adenosine Deaminase that Generates Inosine at the Wobble Position of tRNAs, *Science*, 286(November), pp. 1146–1150. doi: 10.1126/science.1245938.
- Gething, M. J. and Sambrook, J. (1992) Protein Folding in the Cell, *Nature*, 355, pp. 33–45.
- Ghaemmaghami, S. *et al.* (2003) Global analysis of protein expression in yeast, *Nature*, 425(1997), pp. 737–41. doi: 10.1038/nature02046.
- Giaever, G. *et al.* (2002) Functional profiling of the *Saccharomyces cerevisiae* genome, *Nature*, 418(6896), pp. 387–91. doi: 10.1038/nature00935.
- Gietz, R. D. and Woods, R. A. (2006) Yeast Transformation by the LiAc/SS Carrier DNA/PEG Method, in Xiao, W. (ed.) *Yeast Protocols*. Second. New Jersey: Humana Press, pp. 107–120. doi: 10.1385/1592599583.
- Gillman, E. C. *et al.* (1991) MOD5 Translation Initiation Sites Determine N6-Isopentenyladenosine Modification of Mitochondrial and Cytoplasmic tRNA, *Molecular and Cellular Biology*, 11(5), pp. 2382–2390.

- Glatt, S. *et al.* (2012) The Elongator subcomplex Elp456 is a hexameric RecA-like ATPase, *Nature Structural & Molecular Biology*, 19(3), pp. 314–320. doi: 10.1038/nsmb.2234.
- Glatt, S. *et al.* (2015) Structure of the Kti11/Kti13 Heterodimer and Its Double Role in Modifications of tRNA and Eukaryotic Elongation Factor 2, *Structure*, 23, pp. 149–160. doi: 10.1016/j.str.2014.11.008.
- Gnrirke, A. *et al.* (1989) The Allosteric Three-site Model for the Ribosomal Elongation Cycle, *The Journal of Biological Chemistry*, 264(May 5), pp. 7291–7301.
- Godin, K. S. *et al.* (2009) The Box H/ACA snoRNP assembly factor Shq1p is a chaperone protein homologous to Hsp90 co-chaperones that binds to the Cbf5p enzyme, *J Mol Biol*, 390(2), pp. 231–244. doi: 10.1016/j.jmb.2009.04.076.
- Goldman, E. (2008) Transfer RNA, *Encyclopedia of Life Sciences*. doi: 10.1002/9780470015902.a0000878.pub2.
- Goll, M. G. *et al.* (2006) Methylation of tRNA^{Asp} by the DNA Methyltransferase Homolog Dnmt2, *Science*, 311, pp. 395–398. doi: 10.1126/science.1120976.
- Gomes, A. C. *et al.* (2007) A genetic code alteration generates a proteome of high diversity in the human pathogen *Candida albicans*, *Genome Biology*, 8(10). doi: 10.1186/gb-2007-8-10-r206.
- Gonzales, B. *et al.* (2005) The Treacher Collins syndrome (TCOF1) gene product is involved in pre-rRNA methylation, *Human molecular genetics*, 14(14), pp. 2035–43. doi: 10.1093/hmg/ddi208.
- Goodenbour, J. M. and Pan, T. (2006) Diversity of tRNA genes in eukaryotes, *Nucleic Acids Research*, 34(21), pp. 6137–6146. doi: 10.1093/nar/gkl725.
- Grandi, P. *et al.* (2002) 90S Pre-Ribosomes Include the 35S Pre-rRNA, the U3 snoRNP, and 40S Subunit Processing Factors but Predominantly Lack 60S Synthesis Factors, *Molecular Cell*, 10, pp. 105–115.
- Gregersen, N. *et al.* (2006) Protein misfolding and human disease, *Annual review of genomics and human genetics*, 7, pp. 103–24. doi: 10.1146/annurev.genom.7.080505.115737.
- Grosjean, H. (1998) *Modification And Editing Of Rna*. Edited by H. Grosjean and R. Benne. Washington, D. C.: Asm Press.
- Grosjean, H. (2005) *Fine-Tuning of RNA Functions by Modifications and Editing*, *Topics in Current Genetics*. Edited by H. Grosjean. Springer-Verlag Berlin Heidelberg. doi: 10.1007/b106848.
- Grosjean, H. (2009a) *DNA and RNA Modification Enzymes: Structure, Mechanism, Function and Evolution*. Austin, Texas, USA: Molecular Biology Intelligence Unit, Landes Bioscience.

6. References

Grosjean, H. (2009b) Nucleic Acids Are Not Boring Long Polymers of Only Four Types of Nucleotides: A Guided Tour, in *DNA and RNA Modification Enzymes: Structure, Mechanism, Function and Evolution*. Austin, Texas, USA: Landes Bioscience, pp. 1–18.

Grosjean, H. and Westhof, E. (2016) An integrated, structure- and energy-based view of the genetic code, *Nucleic Acids Research*, 44(17), pp. 8020–8040. doi: 10.1093/nar/gkw608.

Grosshans, H., Hurt, E. and Simos, G. (2000) An aminoacylation-dependent nuclear tRNA export pathway in yeast, *Genes and Development*, 14(0), pp. 830–840. doi: 10.1101/gad.14.7.830.

Grozdanov, P. N., Fernandez-Fuentes, N., *et al.* (2009) Pathogenic NAP57 mutations decrease ribonucleoprotein assembly in dyskeratosis congenita, *Human Molecular Genetics*, 18(23), pp. 4546–4551. doi: 10.1093/hmg/ddp416.

Grozdanov, P. N., Roy, S., *et al.* (2009) SHQ1 is required prior to NAF1 for assembly of H/ACA small nucleolar and telomerase RNPs, *RNA*, 15, pp. 1188–1197. doi: 10.1261/rna.1532109.1.

Grune, T. *et al.* (1998) Peroxynitrite increases the degradation of aconitase and other cellular proteins by proteasome, *Journal of Biological Chemistry*, 273, pp. 10857–10862. doi: 10.1074/jbc.273.18.10857.

Gu, C., Begley, T. J. and Dedon, P. C. (2014) tRNA modifications regulate translation during cellular stress, *FEBS letters*. NIH Public Access, 588(23), pp. 4287–96. doi: 10.1016/j.febslet.2014.09.038.

Guan, M.-X. *et al.* (2006) Mutation in TRMU Related to Transfer RNA Modification Modulates the Phenotypic Expression of the Deafness-Associated Mitochondrial 12S Ribosomal RNA Mutations, *The American Journal of Human Genetics*, 79, pp. 291–302.

Gustilo, E. M., Vendeix, F. A. and Agris, P. F. (2008) tRNA's modifications bring order to gene expression, *Current opinion in microbiology*, 11(2), pp. 134–40. doi: 10.1016/j.mib.2008.02.003.

Guy, M. P. *et al.* (2012) Yeast Trm7 interacts with distinct proteins for critical modifications of the tRNAPhe anticodon loop, *RNA*, 18(10), pp. 1921–33. doi: 10.1261/rna.035287.112.

Guy, M. P. *et al.* (2015) Defects in tRNA anticodon loop 2'-O-methylation are implicated in non-syndromic X-linked intellectual disability due to mutations in FTSJ1, *Hum Mutat*, 36(12), pp. 1176–1187. doi: 10.1002/humu.22897.

Haar, T. von der (2008) A quantitative estimation of the global translational activity in logarithmically growing yeast cells, *BMC Systems Biology*, 2(87).

Hamma, T. *et al.* (2005) The Cbf5–Nop10 complex is a molecular bracket that

organizes box H/ACA RNPs, *Nature Structural & Molecular Biology*, 12(12), pp. 1101–1107. doi: 10.1038/nsmb1036.

Hani, J. and Feldmann, H. (1998) tRNA genes and retroelements in the yeast genome, *Nucleic Acids Research*, 26(3), pp. 689–696. doi: 10.1093/nar/26.3.689.

Hartl, F. U., Bracher, A. and Hayer-Hartl, M. (2011) Molecular chaperones in protein folding and proteostasis, *Nature*, 475, pp. 324–332. doi: 10.1016/S0959-440X(96)80093-5.

Haslbeck, M. *et al.* (2005) Disassembling protein aggregates in the yeast cytosol. The cooperation of Hsp26 with Ssa1 and Hsp104., *The Journal of biological chemistry*, 280(25), pp. 23861–8. doi: 10.1074/jbc.M502697200.

Heiss, M., Reichle, V. F. and Kellner, S. (2017) Observing the fate of tRNA and its modifications by nucleic acid isotope labeling mass spectrometry: NAIL-MS, *RNA Biology*. Taylor & Francis, pp. 1–9. doi: 10.1080/15476286.2017.1325063.

Helm, M. (2006) Post-transcriptional nucleotide modification and alternative folding of RNA, *Nucleic acids research*. Oxford University Press, 34(2), pp. 721–33. doi: 10.1093/nar/gkj471.

Hendrickson, T. L. (2001) Recognizing the D-loop of transfer RNAs, *PNAS*, 98(24), pp. 13473–13475.

Henras, A. K. *et al.* (2004) Cbf5p, the putative pseudouridine synthase of H/ACA-type snoRNPs, can form a complex with Gar1p and Nop10p in absence of Nhp2p and box H/ACA snoRNAs, *RNA*, 10, pp. 1704–1712. doi: 10.1261/rna.7770604.Tycowski.

Hershko, A. and Ciechanover, A. (1998) The Ubiquitin System, *Annual Review of Biochemistry*, 67, pp. 425–479. doi: 10.1146/annurev.biochem.67.1.425.

Hessling, M., Richter, K. and Buchner, J. (2009) Dissection of the ATP-induced conformational cycle of the molecular chaperone Hsp90, *Nature Structural & Molecular Biology*, 16(3), pp. 287–293. doi: 10.1038/nsmb.1565.

Hia, F. *et al.* (2015) Mycobacterial RNA isolation optimized for non-coding RNA: high fidelity isolation of 5S rRNA from *Mycobacterium bovis* BCG reveals novel post-transcriptional processing and a complete spectrum of modified ribonucleosides, *Nucleic Acids Research*, 43(5). doi: 10.1093/nar/gku1317.

Honda, S. *et al.* (2015) Four-leaf clover qRT-PCR: A convenient method for selective quantification of mature tRNA, *RNA biology*, 12(5), pp. 501–8. doi: 10.1080/15476286.2015.1031951.

Hopper, A. K. (2013) Transfer RNA post-transcriptional processing, turnover, and subcellular dynamics in the yeast *Saccharomyces cerevisiae*, *Genetics*, 194(1), pp. 43–67. doi: 10.1534/genetics.112.147470.

6. References

Hopper, A. K., Pai, D. A. and Engelke, D. R. (2010) Cellular dynamics of tRNAs and their genes, *FEBS Letters*, 584(2). doi: 10.1016/j.febslet.2009.11.053.

Hopper, A. K. and Phizicky, E. M. (2003) tRNA transfers to the limelight., *Genes & development*, 17(2), pp. 162–80. doi: 10.1101/gad.1049103.

Houry, W. A. *et al.* (2015) Cooperation of Hsp70 and Hsp100 chaperone machines in protein disaggregation, *Frontiers in Molecular Biosciences*, 2. doi: 10.3389/fmolb.2015.00022.

Houseley, J., LaCava, J. and Tollervey, D. (2006) RNA-quality control by the exosome, *Nature Reviews Molecular Cell Biology*, 7(July), pp. 529–539. doi: 10.1038/nrm1964.

Huang, B., Lu, J. and Byström, A. S. (2008) A genome-wide screen identifies genes required for formation of the wobble nucleoside 5-methoxycarbonylmethyl-2-thiouridine in *Saccharomyces cerevisiae*, *RNA*, 14(10), pp. 2183–94. doi: 10.1261/rna.1184108.

Huang, B. O., Johansson, M. J. O. and Byström, A. S. (2005) An early step in wobble uridine tRNA modification requires the Elongator complex, pp. 424–436. doi: 10.1261/rna.7247705.complex.

Huang, W. and Klionsky, D. J. (2002) Autophagy in Yeast: A Review of the Molecular Machinery, *Cell Structure and Function*, 27, pp. 409–420.

Hughes, J. M. X. and Ares, M. (1991) Depletion of U3 small nucleolar RNA inhibits cleavage in the 5' external transcribed spacer of yeast pre-ribosomal RNA and impairs formation of 18S ribosomal RNA, *The EMBO Journal*, 10(13), pp. 4231–4239.

Huh, W.-K. *et al.* (2003) Global analysis of protein localization in budding yeast, *Nature*, 425(6959), pp. 686–91. doi: 10.1038/nature02026.

Ibba, M. and Soll, D. (2000) Aminoacyl-tRNA synthesis, *Annu Rev Biochem*, 69, pp. 617–50.

Ibstedt, S. *et al.* (2014) Global analysis of protein aggregation in yeast during physiological conditions and arsenite stress, *Biology open*, 3(10), pp. 913–23. doi: 10.1242/bio.20148938.

Igoillo-Esteve, M. *et al.* (2013) tRNA Methyltransferase Homolog Gene TRMT10A Mutation in Young Onset Diabetes and Primary Microcephaly in Humans, *PLoS genetics*, 9(10), p. e1003888. doi: 10.1371/journal.pgen.1003888.

Ikemura, T. (1985) Codon usage and tRNA content in unicellular and multicellular organisms, *Molecular Biology and Evolution*, 2, pp. 13–34. doi: 10.1093/oxfordjournals.molbev.a040335.

Inge-Vechtormov, S., Zhouravleva, G. and Philippe, M. (2003) Eukaryotic

release factors (eRFs) history, *Biology of the Cell*, 95(3–4), pp. 195–209. doi: 10.1016/S0248-4900(03)00035-2.

Ishiguro, A. *et al.* (2002) Essential Roles of Bdp1 , a Subunit of RNA Polymerase III Initiation Factor TFIIIB , in Transcription and tRNA Processing Essential Roles of Bdp1 , a Subunit of RNA Polymerase III Initiation Factor TFIIIB , in Transcription and tRNA Processing, *Molecular and Cellular Biology*, 22(10), pp. 3264–3275. doi: 10.1128/MCB.22.10.3264.

Ishitani, R., Yokoyama, S. and Nureki, O. (2008) Structure, dynamics, and function of RNA modification enzymes, *Current opinion in structural biology*, 18(3), pp. 330–9. doi: 10.1016/j.sbi.2008.05.003.

Jablonowski, D. *et al.* (2004) The Yeast Elongator Histone Acetylase Requires Sit4- dependent Dephosphorylation for Toxin-Target Capacity, *Molecular Biology of the Cell*, 15, pp. 1459–1469. doi: 10.1091/mbc.E03–10.

Jablonowski, D. *et al.* (2009) Distinct Subsets of Sit4 Holophosphatases Are Required for Inhibition of *Saccharomyces cerevisiae* Growth by Rapamycin and Zymocin, *Eukaryotic Cell*, 8(11), pp. 1637–1647. doi: 10.1128/EC.00205-09.

Jack, K. *et al.* (2011) rRNA Pseudouridylation Defects Affect Ribosomal Ligand Binding and Translational Fidelity from Yeast to Human Cells, *Mol Cell*, 44(4), pp. 660–666. doi: 10.1016/j.molcel.2011.09.017.

Jackson, R. J., Hellen, C. U. T. and Pestova, T. V (2010) The mechanism of eukaryotic translation initiation and principles of its regulation, *Nature reviews. Molecular cell biology*. Nature Publishing Group, 11(2), pp. 113–127. doi: 10.1038/nrm2838.

Jakubowski, H. (2012) Quality control in tRNA charging., *Wiley interdisciplinary reviews. RNA*, 3(3), pp. 295–310. doi: 10.1002/wrna.122.

Jang, H. H. *et al.* (2004) Two Enzymes in One: Two Yeast Peroxiredoxins Display Oxidative Stress-Dependent Switching from a Peroxidase to a Molecular Chaperone Function, *Cell*, 117, pp. 625–635.

Jansen, M. *et al.* (1995) Translational control of gene expression, *Pediatric research*, 37(6), pp. 681–6. doi: 10.1203/00006450-199506000-00001.

Jarosz, D. F. and Lindquist, S. (2010) Hsp90 and environmental stress transform the adaptive value of natural genetic variation, *Science*, 330(6012), pp. 1820–4. doi: 10.1126/science.1195487.

Jenner, L. *et al.* (2012) Crystal structure of the 80S yeast ribosome, *Current Opinion in Structural Biology*. Elsevier Ltd, 22(6), pp. 759–767. doi: 10.1016/j.sbi.2012.07.013.

Jenner, L. B. *et al.* (2010) Structural aspects of messenger RNA reading frame maintenance by the ribosome, *Nature Structural & Molecular Biology*. Nature

6. References

Publishing Group, 17(5), pp. 555–560. doi: 10.1038/nsmb.1790.

Johansen, L. D. *et al.* (2008) IKAP localizes to membrane ruffles with filamin A and regulates actin cytoskeleton organization and cell migration, *Journal of Cell Science*, 121(6), pp. 854–864. doi: 10.1242/jcs.013722.

Johansson, M. J. O. *et al.* (2008) Eukaryotic wobble uridine modifications promote a functionally redundant decoding system., *Molecular and cellular biology*, 28(10), pp. 3301–12. doi: 10.1128/MCB.01542-07.

Johansson, M. J. O. and Byström, A. S. (2004) The *Saccharomyces cerevisiae* TAN1 gene is required for N⁴-acetylcytidine formation in tRNA, *RNA*, 10, pp. 712–719. doi: 10.1261/rna.5198204.early.

Johansson, M. J. O. and Byström, A. S. (2005) Transfer RNA modifications and modifying enzymes in *Saccharomyces cerevisiae*, 12(January). doi: 10.1007/b105814.

Johnson, P. F. and Abelson, J. (1983) The yeast tRNA^{Tyr} gene intron is essential for correct modification of its tRNA product, *Nature*, 302(5910), pp. 681–687. doi: 10.1038/302681a0.

Johnston, J. A., Ward, C. L. and Kopito, R. R. (1998) Aggresomes: A Cellular Response to Misfolded Proteins, *The Journal of Cell Biology*, 143(7), pp. 1883–1898.

Jørgensen, F. and Kurland, C. G. (1990) Processivity errors of gene expression in *Escherichia coli*, *Journal of molecular biology*, 215, pp. 511–21. doi: 10.1016/S0022-2836(05)80164-0.

Jühling, F. *et al.* (2009) tRNAdb 2009: Compilation of tRNA sequences and tRNA genes, *Nucleic Acids Research*, 37(SUPPL. 1), pp. 159–162. doi: 10.1093/nar/gkn772.

Kadaba, S. *et al.* (2004) Nuclear surveillance and degradation of hypomodified initiator tRNA Met in *S. cerevisiae*, *Genes and Development*, 18(11), pp. 1227–1240. doi: 10.1101/gad.1183804.

Kadaba, S., Wang, X. and Anderson, J. T. (2006) Nuclear RNA surveillance in *Saccharomyces cerevisiae*: Trf4p-dependent polyadenylation of nascent hypomethylated tRNA and an aberrant form of 5S rRNA, *RNA*, 12(3), pp. 508–521. doi: 10.1261/rna.2305406.

Kaganovich, D., Kopito, R. and Frydman, J. (2008) Misfolded proteins partition between two distinct quality control compartments, *Nature*, 454(7208), pp. 1088–1095. doi: 10.1038/nature07195.

Kaiser, C. M. *et al.* (2011) The Ribosome Modulates Nascent Protein Folding, *Science*, 334(6063), pp. 1723–1727. doi: 10.1126/science.1209740.

Kalhor, H. R. and Clarke, S. (2003) Novel methyltransferase for modified uridine residues at the wobble position of tRNA, *Molecular and cellular biology*, 23(24), pp. 9283–9292. doi: 10.1128/MCB.23.24.9283-9292.2003.

Kamenski, P. *et al.* (2007) Evidence for an Adaptation Mechanism of Mitochondrial Translation via tRNA Import from the Cytosol, *Molecular Cell*, 26, pp. 625–637. doi: 10.1016/j.molcel.2007.04.019.

Kapp, L. D. and Lorsch, J. R. (2004) The molecular mechanics of eukaryotic translation, *Annual review of biochemistry*, 73, pp. 657–704. doi: 10.1146/annurev.biochem.73.030403.080419.

Karaca, E. *et al.* (2014) Human CLP1 mutations alter tRNA biogenesis affecting both peripheral and central nervous system function, *Cell*, 157(3), pp. 636–650. doi: 10.1016/j.cell.2014.02.058.

Karlsborn, T. *et al.* (2014) *Familial dysautonomia (FD) patients have reduced levels of the modified wobble nucleoside mcm5s2U in tRNA*, *Biochemical and Biophysical Research Communications*. doi: 10.1016/j.bbrc.2014.10.116.

Kato, T. *et al.* (2005) A Novel Human tRNA-Dihydrouridine Synthase Involved in Pulmonary Carcinogenesis, *Cancer Res*, 65(13), pp. 5638–46.

Kim, S. (2014) *Aminoacyl-tRNA Synthetases in Biology and Medicine*. Springer. doi: 10.1007/978-94-017-8701-7.

Kim, S. H. *et al.* (1972) The Three-Dimensional Structure of Yeast Phenylalanine Transfer RNA: Shape of the Molecule at 5.5-Å Resolution, *PNAS*, 69(12), pp. 3746–3750.

Kim, S. J. *et al.* (2015) Translational tuning optimizes nascent protein folding in cells, *Science*, 348(6233), pp. 444–448. doi: 10.1126/science.aaa3974.

Kirchner, S. and Ignatova, Z. (2014) Emerging roles of tRNA in adaptive translation, signalling dynamics and disease, *Nature Reviews Genetics*. Nature Publishing Group. doi: 10.1038/nrg3861.

Kirillov, S. V, Makarov, E. M. and Semenov YuP (1983) Quantitative study of interaction of deacylated tRNA with Escherichia coli ribosomes. Role of 50 S subunits in formation of the E site, *FEBS letters*, 157(1), pp. 91–94.

Kirino, Y. *et al.* (2005) Specific correlation between the wobble modification deficiency in mutant tRNAs and the clinical features of a human mitochondrial disease, *PNAS*, 102(20), pp. 7127–32. doi: 10.1073/pnas.0500563102.

Kirino, Y. and Suzuki, T. (2005) Human mitochondrial diseases associated with tRNA wobble modification deficiency, *RNA biology*, 2(2), pp. 41–44. doi: 10.4161/rna.2.2.1610.

Kirkin, V. *et al.* (2009) A Role for Ubiquitin in Selective Autophagy, *Molecular*

6. References

Cell, 34, pp. 259–269.

Klinge, S. *et al.* (2011) Crystal Structure of the Eukaryotic 60S Ribosomal Subunit in Complex with Initiation Factor 6, *Science*, 334(6058), pp. 941–948. doi: 10.1126/science.1211204.

Klinge, S. *et al.* (2012) Atomic structures of the eukaryotic ribosome, *Trends in Biochemical Sciences*. Elsevier Ltd, 37(5), pp. 189–198. doi: 10.1016/j.tibs.2012.02.007.

Koegl, M. *et al.* (1999) A Novel Ubiquitination Factor, E4, Is Involved in Multiubiquitin Chain Assembly, *Cell*, 96, pp. 635–644.

Kolaj-Robin, O. *et al.* (2015) Structure of the Elongator cofactor complex Kti11/Kti13 provides insight into the role of Kti13 in Elongator-dependent tRNA modification, *FEBS Journal*, 282, pp. 819–833. doi: 10.1111/febs.13199.

Koo, B.-K. *et al.* (2011) Structure of H/ACA RNP protein Nhp2p reveals cis/trans isomerization of a conserved proline at the RNA and Nop10 binding interface, *J Mol Biol*, 411(5), pp. 927–942. doi: 10.1016/j.jmb.2011.06.022.

Kopito, R. R. (2000) Aggresomes, inclusion bodies and protein aggregation, *TRENDS in Cell Biology*, 10(2000), pp. 524–530.

Koplin, A. *et al.* (2010) A dual function for chaperones SSB-RAC and the NAC nascent polypeptide-associated complex on ribosomes, *Journal of Cell Biology*, 189(1), pp. 57–68. doi: 10.1083/jcb.200910074.

Kosolapov, A. and Deutsch, C. (2009) Tertiary Interactions within the Ribosomal Exit Tunnel, *Nat Struct Mol Biol*, 16(4), pp. 405–411. doi: 10.1038/nsmb.1571.

Kozak, M. (1991) Structural Features in Eukaryotic mRNAs That Modulate the Initiation of Translation, *The Journal of Biological Chemistry*, 266(30), pp. 19867–19870.

Kramer, E. B. and Farabaugh, P. J. (2007) The frequency of translational misreading errors in *E. coli* is largely determined by tRNA competition, *RNA*, 13, pp. 87–96. doi: 10.1261/rna.294907.

Kramer, E. B. and Hopper, A. K. (2013) Retrograde transfer RNA nuclear import provides a new level of tRNA quality control in *Saccharomyces cerevisiae*, *PNAS*, 110(52), pp. 21042–21047. doi: 10.1073/pnas.1316579110/-DCSupplemental.www.pnas.org/cgi/doi/10.1073/pnas.1316579110.

Kressler, D. *et al.* (1999) Protein trans-Acting Factors Involved in Ribosome Biogenesis in *Saccharomyces cerevisiae*, *Molecular and Cellular Biology*, 19(12), pp. 7897–7912.

Kressler, D. *et al.* (1999) Spb1p is a putative methyltransferase required for

60S ribosomal subunit biogenesis in *Saccharomyces cerevisiae*, *Nucleic acids research*, 27(23), pp. 4598–608.

Krogan, N. J. and Greenblatt, J. F. (2001) Characterization of a Six-Subunit Holo-Elongator Complex Required for the Regulated Expression of a Group of Genes in *Saccharomyces cerevisiae*, *Molecular and Cellular Biology*, 21(23), pp. 8203–8212. doi: 10.1128/MCB.21.23.8203–8212.2001.

Kruiswijk, T., Planta, R. J. and Krop, J. M. (1978) The course of the assembly of ribosomal subunits in yeast, *BBA Section Nucleic Acids And Protein Synthesis*, 517, pp. 378–389. doi: 10.1016/0005-2787(78)90204-6.

Kuchino, Y. *et al.* (1982) Changes of post-transcriptional modification of wye base in tumor-specific tRNAPhe, *Nucleic Acids Research*, 10(20).

Kutter, C. *et al.* (2011) Pol III binding in six mammals shows conservation among amino acid isotypes despite divergence among tRNA genes, *Nature Genetics*, 43(10). doi: 10.1038/ng.906.

Lacava, J. *et al.* (2005) RNA Degradation by the Exosome Is Promoted by a Nuclear Polyadenylation Complex, *Cell*, 121, pp. 713–724. doi: 10.1016/j.cell.2005.04.029.

Lafontaine, D. L. J. and Tollervey, D. (2001) The function and synthesis of ribosomes, *Nature Reviews Molecular Cell Biology*, 2, pp. 514–520.

Lafontaine, D. and Tollervey, D. (1995) Trans-acting factors in yeast pre-rRNA and pre-snoRNA processing, *Biochem Cell Biol*, 73, pp. 803–812.

Lapeyre, B. and Purushothaman, S. K. (2004) Spb1p-directed formation of Gm2922 in the ribosome catalytic center occurs at a late processing stage, *Molecular cell*, 16(4), pp. 663–9. doi: 10.1016/j.molcel.2004.10.022.

Laten, H., Gorman, J. and Bock, R. M. (1978) Isopentenyladenosine deficient tRNA from an antisuppressor mutant of *saccharomyces cerevisiae*, *Nucleic Acids Research*, 5(1), pp. 4329–4342. doi: 10.1093/nar/5.11.4329.

Latour, P. *et al.* (2010) A Major Determinant for Binding and Aminoacylation of tRNA Ala in Cytoplasmic Alanyl-tRNA Synthetase Is Mutated in Dominant Axonal Charcot-Marie-Tooth Disease, *The American Journal of Human Genetics*, 86, pp. 77–82. doi: 10.1016/j.ajhg.2009.12.005.

Laxman, S. *et al.* (2013) Sulfur amino acids regulate translational capacity and metabolic homeostasis through modulation of tRNA thiolation, *Cell*, 154(2), pp. 416–429. doi: 10.1016/j.cell.2013.06.043.

Lecoite, F. *et al.* (1998) Characterization of Yeast Protein Deg1 as Pseudouridine Synthase (Pus3) Catalyzing the Formation of Y38 and Y39 in tRNA Anticodon Loop, *The Journal of Biological Chemistry*, 273(3), pp. 1316–1323.

6. References

- Lecoite, F. *et al.* (2002) Lack of Pseudouridine 38/39 in the Anticodon Arm of Yeast Cytoplasmic tRNA Decreases *In Vivo* Recoding Efficiency, *The Journal of Biological Chemistry*, 277(34), pp. 30445–30453. doi: 10.1074/jbc.M203456200.
- Lee, J. W. *et al.* (2006) Editing-defective tRNA synthetase causes protein misfolding and neurodegeneration, *Nature*, 443(September), pp. 50–55. doi: 10.1038/nature05096.
- Lee, Y. and Nazar, R. N. (2003) Terminal structure mediates 5 S rRNA stability and integration during ribosome biogenesis, *Journal of Biological Chemistry*, 278(9), pp. 6635–6641. doi: 10.1074/jbc.M212220200.
- Leidel, S. *et al.* (2009) Ubiquitin-related modifier Urm1 acts as a sulphur carrier in thiolation of eukaryotic transfer RNA, *Nature*, 458, pp. 228–32. doi: 10.1038/nature07643.
- Lemay, V. *et al.* (2011) Identification of novel proteins associated with yeast snR30 small nucleolar RNA, *Nucleic Acids Research*, 39(22), pp. 9659–9670.
- Leulliot, N. *et al.* (2007) The Box H/ACA RNP Assembly Factor Naf1p Contains a Domain Homologous to Gar1p Mediating its Interaction with Cbf5p, *Journal of Molecular Biology*, 371, pp. 1338–1353. doi: 10.1016/j.jmb.2007.06.031.
- Li, S., Duan, J., Li, D., Yang, B., *et al.* (2011) Reconstitution and structural analysis of the yeast box H/ACA RNA-guided pseudouridine synthase, *Genes and Development*, 25, pp. 2409–2421. doi: 10.1101/gad.175299.111.
- Li, S., Duan, J., Li, D., Ma, S., *et al.* (2011) Structure of the Shq1–Cbf5–Nop10–Gar1 complex and implications for H/ACA RNP biogenesis and dyskeratosis congenita, *The EMBO Journal*, 30, pp. 5010–5020. doi: 10.1038/emboj.2011.427.
- Liang, W. Q. and Fournier, M. J. (1995) U14 base-pairs with 18S rRNA: A novel snoRNA interaction required for rRNA processing, *Genes and Development*, 9, pp. 2433–2443. doi: 10.1101/gad.9.19.2433.
- Liao, L. *et al.* (2004) Proteomic Characterization of Postmortem Amyloid Plaques Isolated by Laser Capture Microdissection, *The Journal of Biological Chemistry*. in Press, 279(35), pp. 37061–37068. doi: 10.1074/jbc.M403672200.
- Lilienbaum, A. (2013) Relationship between the proteasomal system and autophagy, *Int J Biochem Mol Biol*, 4(1), pp. 1–26.
- Lill, R. and Uhlenhoff, U. (2006) Iron-Sulfur Protein Biogenesis in Eukaryotes: Components and Mechanisms, *Annu Rev Cell Dev Biol*, 22, pp. 457–86. doi: 10.1146/annurev.cellbio.22.010305.104538.
- Lim, V. I. and Curran, J. F. (2001) Analysis of codon: anticodon interactions within the ribosome provides new insights into codon reading and the genetic code structure, *RNA*, 7, pp. 942–957.

- Lin, C. A., Ellis, S. R. and True, H. L. (2010) The Sua5 protein is essential for normal translational regulation in yeast, *Molecular and cellular biology*, 30(1), pp. 354–63. doi: 10.1128/MCB.00754-09.
- Lin, F. J. *et al.* (2013) Ikbkap/Elp1 Deficiency Causes Male Infertility by Disrupting Meiotic Progression, *PLoS Genetics*, 9(5), pp. 1–16. doi: 10.1371/journal.pgen.1003516.
- Lin, K.-F. *et al.* (2012) Cotranslational Protein Folding within the Ribosome Tunnel Influences Trigger-Factor Recruitment, *Biophysical Journal*, 102(12), pp. 2818–2827. doi: 10.1016/j.bpj.2012.04.048.
- Lindner, A. B. and Demarez, A. (2009) Protein aggregation as a paradigm of aging, *Biochimica et Biophysica Acta*. Elsevier B.V., 1790(10), pp. 980–996. doi: 10.1016/j.bbagen.2009.06.005.
- Ling, J., Reynolds, N. and Ibba, M. (2009) Aminoacyl-tRNA synthesis and translational quality control, *Annual review of microbiology*, 63, pp. 61–78. doi: 10.1146/annurev.micro.091208.073210.
- Lipowsky, G. *et al.* (1999) Coordination of tRNA nuclear export with processing of tRNA, *RNA*, 5, pp. 539–549. doi: 10.1017/S1355838299982134.
- Lodish, H. F. (1976) Translational control of protein synthesis, *Annual review of biochemistry*, 45, pp. 39–72. doi: 10.1146/annurev.bi.45.070176.000351.
- Lu, P. *et al.* (2007) Absolute protein expression profiling estimates the relative contributions of transcriptional and translational regulation, *Nature Biotechnology*, 25(1), pp. 117–124. doi: 10.1038/nbt1270.
- Lynch-Day, M. A. and Klionsky, D. J. (2010) The Cvt pathway as a model for selective autophagy, *FEBS Lett*, 584(7), pp. 1359–1366. doi: 10.1016/j.febslet.2010.02.013.
- Ma, X., Zhao, X. and Yu, Y.-T. (2003) Pseudouridylation (Y) of U2 snRNA in *S.cerevisiae* is catalyzed by an RNA-independent mechanism, *The EMBO Journal*, 22(8), pp. 1889–1897.
- Macari, F. *et al.* (2015) TRM6/61 connects PKC α with translational control through tRNA^{iMet} stabilization: impact on tumorigenesis, *Oncogene*, (October 2014), pp. 1–12. doi: 10.1038/onc.2015.244.
- Machnicka, M. A. *et al.* (2013) MODOMICS: a database of RNA modification pathways-2013 update, *Nucleic Acids Research*. Oxford University Press, 41, pp. D262–D267. doi: 10.1093/nar/gks1007.
- Macintosh, G. C. *et al.* (2001) Characterization of Rny1, the *Saccharomyces cerevisiae* member of the T2 RNase family of RNases: Unexpected functions for ancient enzymes?, *PNAS*, 98(3), pp. 1018–1023.

6. References

- Madison, J. T. and Holley, R. W. (1965) The presence of 5,6-dihydrouridylic acid in yeast “soluble” ribonucleic acid, *Biochemical and Biophysical Research Communications*, 18(2), pp. 153–157.
- Mahoney, S. J., Dempsey, J. M. and Blenis, J. (2009) Cell signaling in protein synthesis ribosome biogenesis and translation initiation and elongation, *Progress in molecular biology and translational science*. Elsevier Inc., 90, pp. 53–107. doi: 10.1016/S1877-1173(09)90002-3.
- Maraia, R. J. and Iben, J. R. (2014) Different types of secondary information in the genetic code, *RNA*, 20, pp. 977–984. doi: 10.1261/rna.044115.113.
- Marck, C. *et al.* (2006) The RNA polymerase III-dependent family of genes in hemiascomycetes: comparative RNomics, decoding strategies, transcription and evolutionary implications, *Nucleic acids research*. Oxford University Press, 34(6), pp. 1816–35. doi: 10.1093/nar/gkl085.
- Marck, C. and Grosjean, H. (2002) tRNomics: Analysis of tRNA genes from 50 genomes of Eukarya, Archaea, and Bacteria reveals anticodon-sparing strategies and domain-specific features, *RNA*, 8, pp. 1189–1232.
- Marquez, S. M. *et al.* (2005) Structural implications of novel diversity in eucaryal RNase P RNA, *RNA*, 11(5), pp. 739–751. doi: 10.1261/rna.7211705.
- Martinez, F. *et al.* (2012) Whole Exome Sequencing identifies a splicing mutation in NSUN2 as a cause of a Dubowitz-like syndrome, *J Med Genet*, 49(6), pp. 380–385. doi: 10.1136/jmedgenet-2011-100686.
- Mashaghi, A. *et al.* (2013) Reshaping of the conformational search of a protein by the chaperone trigger factor, *Nature*, 500, pp. 98–101. doi: 10.1038/nature12293.
- Mazauric, M.-H. *et al.* (2010) Trm112p is a 15-kDa zinc finger protein essential for the activity of two tRNA and one protein methyltransferases in yeast, *The Journal of biological chemistry*, 285(24), pp. 18505–15. doi: 10.1074/jbc.M110.113100.
- Mehlgarten, C. *et al.* (2009) Elongator function depends on antagonistic regulation by casein kinase Hrr25 and protein phosphatase Sit4, *Molecular Microbiology*, 73(August), pp. 869–881. doi: 10.1111/j.1365-2958.2009.06811.x.
- Mei, Y. *et al.* (2010) tRNA binds to cytochrome c and inhibits caspase activation, *Mol Cell*, 37(5), pp. 668–678. doi: 10.1016/j.molcel.2010.01.023.
- Mélèse, T. and Xue, Z. (1995) The nucleolus: an organelle formed by the act of building a ribosome, *Current Opinion in Cell Biology*, 7, pp. 319–324. doi: 10.1016/0955-0674(95)80085-9.
- Melnikov, S. *et al.* (2012) One core, two shells: bacterial and eukaryotic ribosomes, *Nature Structural & Molecular Biology*, 19(6), pp. 560–567. doi: 10.1038/nsmb.2313.

Menninger, J. R. (1977) Ribosome editing and the error catastrophe hypothesis of cellular aging, *Mechanisms of Ageing and Development*, 6, pp. 131–142. doi: 10.1016/0047-6374(77)90014-8.

Meseguer, S. *et al.* (2015) The ROS-sensitive microRNA-9/9 * controls the expression of mitochondrial tRNA-modifying enzymes and is involved in the molecular mechanism of MELAS syndrome, *Human Molecular Genetics*, 24(1), pp. 167–184. doi: 10.1093/hmg/ddu427.

Michaud, J. *et al.* (2000) Isolation and Characterization of a Human Chromosome 21q22.3 Gene (WDR4) and Its Mouse Homologue That Code for a WD-Repeat Protein, *Genomics*, 68, pp. 71–79. doi: 10.1006/geno.2000.6258.

Mogk, A., Schmidt, R. and Bukau, B. (2007) The N-end rule pathway for regulated proteolysis: prokaryotic and eukaryotic strategies, *Trends in Cell Biology*, 17(4), pp. 165–172. doi: 10.1016/j.tcb.2007.02.001.

Montanaro, L. *et al.* (2006) Dyskerin expression influences the level of ribosomal RNA pseudo-uridylation and telomerase RNA component in human breast cancer, (July), pp. 10–18. doi: 10.1002/path.

Morimoto, R. I. (2008) Proteotoxic stress and inducible chaperone networks in neurodegenerative disease and aging, *Genes & Development*, 22, pp. 1427–1438. doi: 10.1101/gad.1657108.

Morrissey, J. P. and Tollervey, D. (1993) Yeast snR30 Is a Small Nucleolar RNA Required for 18S rRNA Synthesis, *Molecular and Cellular Biology*, 13(4), pp. 2469–2477.

Moschopoulos, C. N. *et al.* (2011) Which clustering algorithm is better for predicting protein complexes?, *BMC Research Notes*, 4(549). doi: 10.1186/1756-0500-4-549.

Motorin, Y. *et al.* (1998) The yeast tRNA:pseudouridine synthase Pus1p displays a multisite substrate specificity, *RNA*, 4, pp. 856–869.

Motorin, Y. and Grosjean, H. (2005) Transfer RNA Modification, *Encyclopedia of Life Sciences*, pp. 1–10. doi: 10.1038/npg.els.0003866.

Moura, G. *et al.* (2005) Comparative context analysis of codon pairs on an ORFeome scale, *Genome Biology*, 6(3).

Moura, G. R., Paredes, J. A. and Santos, M. A. S. (2010) Development of the genetic code: Insights from a fungal codon reassignment, *FEBS Letters*. Federation of European Biochemical Societies, 584, pp. 334–341. doi: 10.1016/j.febslet.2009.11.066.

Mueller, E. G. and Ferré-D'Amaré, A. R. (2009) Pseudouridine Formation, the Most Common Transglycosylation in RNA, in *DNA and RNA Modification Enzymes: Structure, Mechanism, Function and Evolution*. Austin, Texas, USA: Landes

6. References

Bioscience, pp. 363–376.

Murthi, A. *et al.* (2010) Regulation of tRNA Bidirectional Nuclear-Cytoplasmic Trafficking in *Saccharomyces cerevisiae*, *Molecular Biology of the Cell*, 21, pp. 639–649. doi: 10.1091/mbc.E09.

Mushinski, J. F. and Marini, M. (1979) Tumor-associated Phenylalanyl Transfer RNA Found in a Wide Spectrum of Rat and Mouse Tumors but Absent in Normal Adult, Fetal, and Regenerating Tissues, *Cancer Research*, 39(April), pp. 1253–1258.

Najmabadi, H. *et al.* (2011) Deep sequencing reveals 50 novel genes for recessive cognitive disorders, *Nature*, 478, pp. 57–63. doi: 10.1038/nature10423.

Nakai, Y. *et al.* (2004) Yeast Nfs1p Is Involved in Thio-modification of Both Mitochondrial and Cytoplasmic tRNAs, *The Journal of Biological Chemistry*, 279(13), pp. 12363–12368.

Nakai, Y. *et al.* (2007) Thio modification of yeast cytosolic tRNA is an iron-sulfur protein-dependent pathway, *Molecular and cellular biology*, 27(8), pp. 2841–7. doi: 10.1128/MCB.01321-06.

Nakai, Y., Nakai, M. and Yano, T. (2017) Sulfur Modifications of the Wobble U 34 in tRNAs and their Intracellular Localization in Eukaryotic Cells, *Biomolecules*, 7(17). doi: 10.3390/biom7010017.

Näsvall, S. J., Chen, P. and Björk, G. R. (2007) The wobble hypothesis revisited : Uridine-5-oxyacetic acid is critical for reading of G-ending codons, *RNA*, 13, pp. 2151–2164. doi: 10.1261/rna.731007.1.

Nazar, R. N. (2004) Ribosomal RNA processing and ribosome biogenesis in eukaryotes, *IUBMB life*, 56(8), pp. 457–465. doi: 10.1080/15216540400010867.

Nedialkova, D. D. and Leidel, S. A. (2015) Optimization of Codon Translation Rates via tRNA Modifications Maintains Proteome Integrity, *Cell*. The Authors, 161, pp. 1–13. doi: 10.1016/j.cell.2015.05.022.

Neznanov, N. *et al.* (2011) Proteotoxic stress targeted therapy (PSTT): induction of protein misfolding enhances the antitumor effect of the proteasome inhibitor bortezomib, *Oncotarget*, 2(3), pp. 209–221.

Nguyen, L. *et al.* (2010) Elongator - an emerging role in neurological disorders, *Trends in molecular medicine*, 16(1), pp. 1–6. doi: 10.1016/j.molmed.2009.11.002.

Nissan, T. A. *et al.* (2002) 60S pre-ribosome formation viewed from assembly in the nucleolus until export to the cytoplasm, *The EMBO Journal*, 21(20), pp. 5539–5547.

Nogales-Cadenas, R. *et al.* (2009) GeneCodis: interpreting gene lists through enrichment analysis and integration of diverse biological information, *Nucleic Acids*

Research Web Server, 37, pp. 317–322. doi: 10.1093/nar/gkp416.

Noma, A. *et al.* (2006) Biosynthesis of wybutosine, a hyper-modified nucleoside in eukaryotic phenylalanine tRNA, *The EMBO journal*, 25(10), pp. 2142–54. doi: 10.1038/sj.emboj.7601105.

Noma, A., Sakaguchi, Y. and Suzuki, T. (2009) Mechanistic characterization of the sulfur-relay system for eukaryotic 2-thiouridine biogenesis at tRNA wobble positions, *Nucleic Acids Research*, 37(4), pp. 1335–1352. doi: 10.1093/nar/gkn1023.

Noma, A., Shigi, N. and Tsutomu, S. (2009) Biogenesis and Functions of Thio-Compounds in Transfer RNA: Comparison of Bacterial and Eukaryotic Thiolation Machineries, in *DNA and RNA Modification Enzymes: Structure, Mechanism, Function and Evolution*. Austin, Texas, USA: Landes Bioscience, pp. 392–405.

Normand, C. *et al.* (2006) Analysis of the binding of the N-terminal conserved domain of yeast Cbf5p to a box H/ACA snoRNA, *RNA*, 12, pp. 1868–1882. doi: 10.1261/rna.141206.uridylation.

Novoa, E. M. and Ribas de Pouplana, L. (2012) Speeding with control: codon usage, tRNAs, and ribosomes., *Trends in genetics: TIG*, 28(11), pp. 574–81. doi: 10.1016/j.tig.2012.07.006.

Ogle, J. M. and Ramakrishnan, V. (2005) Structural insights into translational fidelity, *Annu Rev Biochem*, 74, pp. 129–77. doi: 10.1146/annurev.biochem.74.061903.155440.

Outeiro, T. F. O. (2004) *Yeast as a Model Organism to Study Diseases of Protein Misfolding*. Universidade do Porto.

Pan, T. (2013) Adaptative translation as a mechanism of stress response and adaptation, *Annual review of genetics*, 47, pp. 121–137. doi: 10.1016/j.biotechadv.2011.08.021.Secreted.

Paraskevopoulou, C. *et al.* (2006) The Elongator subunit Elp3 contains a Fe4S4 cluster and binds S-adenosylmethionine, *Molecular Microbiology*, 59, pp. 795–806. doi: 10.1111/j.1365-2958.2005.04989.x.

Paredes, J. A. *et al.* (2012) Low level genome mistranslations deregulate the transcriptome and translome and generate proteotoxic stress in yeast, *BMC biology*. BioMed Central Ltd, 10(55). doi: 10.1186/1741-7007-10-55.

Parker, J. (1989) Errors and alternatives in reading the universal genetic code, *Microbiological Reviews*, 53(3), pp. 273–298.

Passmore, L. a. *et al.* (2007) The Eukaryotic Translation Initiation Factors eIF1 and eIF1A Induce an Open Conformation of the 40S Ribosome, *Molecular Cell*, 26(1), pp. 41–50. doi: 10.1016/j.molcel.2007.03.018.

6. References

Patil, A., Dyavaiah, M., *et al.* (2012) Increased tRNA modification and gene-specific codon usage regulate cell cycle progression during the DNA damage response, *Cell cycle*, 11(19), pp. 3656–65. doi: 10.4161/cc.21919.

Patil, A., Chan, C. T. Y., *et al.* (2012) Translational infidelity-induced protein stress results from a deficiency in Trm9-catalyzed tRNA modifications, *RNA biology*, 9(7), pp. 990–1001. doi: 10.4161/rna.20531.

Patton, J. R. *et al.* (2005) Mitochondrial Myopathy and Sideroblastic Anemia (MLASA): missense mutation in the pseudouridine synthase 1 (*pus1*) gene is associated with the loss of trna pseudouridylation, *The Journal of Biological Chemistry*, 280(20), pp. 19823–19828. doi: 10.1074/jbc.M500216200.

Pavon-Eternod, M. *et al.* (2009) tRNA over-expression in breast cancer and functional consequences, *Nucleic Acids Research*, 37(21), pp. 7268–7280. doi: 10.1093/nar/gkp787.

Peebles, C. L., Gegenheimer, P. and Abelson, J. (1983) Precise excision of intervening sequences from precursor tRNAs by a membrane-associated yeast endonuclease, *Cell*, 32(2), pp. 525–536. doi: 10.1016/0092-8674(83)90472-5.

Perche-Letuvée, P. *et al.* (2014) Wybutosine biosynthesis: Structural and mechanistic overview, *RNA Biology*, 11(12), pp. 1508–1518. doi: 10.4161/15476286.2014.992271.

Percudani, R., Pavesi, A. and Ottonello, S. (1997) Transfer RNA Gene Redundancy and Translational Selection in *Saccharomyces cerevisiae*, *J Mol Biol*, 268, pp. 322–330.

Perona, J. J. and Hadd, A. (2012) Structural diversity and protein engineering of the aminoacyl-tRNA synthetases, *Biochemistry*, 51, pp. 8705–8729. doi: 10.1021/bi301180x.

Perrochia, L. *et al.* (2013) In vitro biosynthesis of a universal t6A tRNA modification in Archaea and Eukarya, *Nucleic acids research*, 41(3), pp. 1953–64. doi: 10.1093/nar/gks1287.

Petrakis, T. G. *et al.* (2005) Physical and Functional Interaction between Elongator and the Chromatin-associated Kti12 Protein, *The Journal of Biological Chemistry*, 280(20), pp. 19454–19460. doi: 10.1074/jbc.M413373200.

Pfaffl, M. W., Horgan, G. w and Dempfle, L. (2002) Relative expression software tool (REST©) for group-wise comparison and statistical analysis of relative expression results in real-time PCR, *Nucleic Acids Research*, 30(9). doi: <https://doi.org/10.1093/nar/30.9.e36>.

Phizicky, E. M. *et al.* (1992) Yeast tRNA ligase mutants are nonviable and accumulate tRNA splicing intermediates, *Journal of Biological Chemistry*, 267(7), pp. 4577–4582.

- Phizicky, E. M. and Hopper, A. K. (2010) tRNA biology charges to the front, *Genes & development*, 24(17), pp. 1832–60. doi: 10.1101/gad.1956510.
- Pintard, L. *et al.* (2002) Trm7p catalyses the formation of two 2'-O-methylriboses in yeast tRNA anticodon loop, *The EMBO Journal*, 21(7), pp. 1811–1820.
- Planta, R. J. and Raué, H. A. (1988) Control of ribosome biogenesis in yeast, *Trends in genetics: TIG*, 4(3), pp. 64–68. doi: 10.1016/0168-9525(88)90042-X.
- Polikanov, Y. S. *et al.* (2015) Structural insights into the role of rRNA modifications in protein synthesis and ribosome assembly, *Nature Structural & Molecular Biology*, pp. 17–20. doi: 10.1038/nsmb.2992.
- Pouplana, L. R. De and Schimmel, P. (2001) Aminoacyl-tRNA synthetases: potential markers of genetic code development, *TRENDS in Biochemical Sciences*, 26(10), pp. 591–596.
- Purushothaman, S. K. *et al.* (2005) Trm11p and Trm112p Are both Required for the Formation of 2-Methylguanosine at Position 10 in Yeast tRNA, *Molecular and Cellular Biology*, 25(11), pp. 4359–4370. doi: 10.1128/MCB.25.11.4359–4370.2005.
- Qian, Q. *et al.* (1998) A New Model for Phenotypic Suppression of Frameshift Mutations by Mutant tRNAs, *Molecular Cell*, 1, pp. 471–482.
- Ramaswamy, P. and Woodson, S. A. (2009) Global stabilization of rRNA structure by ribosomal proteins S4, S17 and S20, *J Mol Biol*, 392(3), pp. 666–677. doi: 10.1016/j.jmb.2009.07.032.
- Ramser, J. *et al.* (2004) A splice site mutation in the methyltransferase gene FTSJ1 in Xp11.23 is associated with non-syndromic mental retardation in a large Belgian family (MRX9), *J Med Genet*, 41, pp. 679–683. doi: 10.1136/jmg.2004.019000.
- Rand, J. D. and Grant, C. M. (2006) The Thioredoxin System Protects Ribosomes against Stress-induced Aggregation, *Molecular Biology of the Cell*, 17(January), pp. 387–401. doi: 10.1091/mbc.E05.
- Ranjan, N. and Rodnina, M. V (2016) tRNA wobble modifications and protein homeostasis, *Translation*. Taylor & Francis, 4(1). doi: 10.1080/21690731.2016.1143076.
- Reichow, S. L. *et al.* (2007) The structure and function of small nucleolar ribonucleoproteins, *Nucleic acids research*. Oxford University Press, 35(5), pp. 1452–64. doi: 10.1093/nar/gkl1172.
- Rezgui, V. A. N. *et al.* (2013) tRNA tKUUU, tQUUG, and tEUUC wobble position modifications fine-tune protein translation by promoting ribosome A-site binding, *PNAS*, 110(30), pp. 12289–94. doi: 10.1073/pnas.1300781110.

6. References

Rich, A. and Schimmel, P. R. (1977) Structural organization of complexes of transfer RNAs with aminoacyl transfer RNA synthetases, *Nucleic acids research*, 4(5), pp. 1649–1665. doi: 10.1093/nar/gkq840.

Rodnina, M. V, Beringer, M. and Wintermeyer, W. (2006) Mechanism of peptide bond formation on the ribosome., *Quarterly reviews of biophysics*, 39(3), pp. 203–25. doi: 10.1017/S003358350600429X.

Rodnina, M. V and Wintermeyer, W. (2001) Fidelity of aminoacyl-tRNA selection on the ribosome: Kinetic and Structural Mechanisms, *Annu Rev Biochem*, 70, pp. 415–35.

Rodriguez, V. *et al.* (2007) Chromosome 8 BAC Array Comparative Genomic Hybridization and Expression Analysis Identify Amplification and Overexpression of TRMT12 in Breast Cancer, *Genes, chromosomes & cancer*, 46, pp. 694–707. doi: 10.1002/gcc.

Rodriguez, V. *et al.* (2012) Structure-Function Analysis of Human TYW2 Enzyme Required for the Biosynthesis of a Highly Modified Wybutosine (yW) Base in Phenylalanine-tRNA, *PLoS ONE*, 7(6). doi: 10.1371/journal.pone.0039297.

Rogers, S., Wells, R. and Rechsteiner, M. (1986) Amino Acid Sequences Common to Rapidly Degraded Proteins: The PEST Hypothesis, *Science*, 234(4774), pp. 364–368.

Ruggero, D. *et al.* (2003) Dyskeratosis Congenita and Ribosomal RNA Modification, *Science*, 299, pp. 259–262.

Salomons, F. A. *et al.* (2009) Selective Accumulation of Aggregation-Prone Proteasome Substrates in Response to Proteotoxic Stress, *Molecular and cellular Biology*, 29(7), pp. 1774–1785. doi: 10.1128/MCB.01485-08.

Sander, I. M., Chaney, J. L. and Clark, P. L. (2014) Expanding Anfinsen's Principle: Contributions of Synonymous Codon Selection to Rational Protein Design, *J Am Chem Soc*, 136, pp. 858–861.

Sandmeier, J. J. *et al.* (2002) RPD3 is required for the inactivation of yeast ribosomal DNA genes in stationary phase, *EMBO Journal*, 21(18), pp. 4959–4968. doi: 10.1093/emboj/cdf498.

Santo, R. Di, Bandau, S. and Stark, M. J. R. (2014) A conserved and essential basic region mediates tRNA binding to the Elp1 subunit of the *Saccharomyces cerevisiae* Elongator complex, *Molecular Microbiology*, 92(6), pp. 1227–1242. doi: 10.1111/mmi.12624.

Santos, M. A. S. *et al.* (1999) Selective advantages created by codon ambiguity allowed for the evolution of an alternative genetic code in *Candida* spp, *Molecular Microbiology*, 31(3), pp. 937–947.

Santos, M. A. S., Perreau, V. M. and Tuite, M. F. (1996) Transfer RNA

structural change is a key element in the reassignment of the CUG codon in *Candida albicans*, *The EMBO Journal*, 15(18), pp. 5060–5068.

Sarkar, S., Azad, A. K. and Hopper, A. K. (1999) Nuclear tRNA aminoacylation and its role in nuclear export of endogenous tRNAs in *Saccharomyces cerevisiae*, *PNAS*, 96(25), pp. 14366–14371.

Schafer, T. *et al.* (2003) The path from nucleolar 90S to cytoplasmic 40S pre-ribosomes, *The EMBO Journal*, 22(6), pp. 1370–1380.

Schaffer, A. E. *et al.* (2014) CLP1 Founder Mutation Links tRNA Splicing and Maturation to Cerebellar Development and Neurodegeneration, *Cell*, 157(3), pp. 651–663. doi: 10.1016/j.cell.2014.03.049.

Scheper, G. C. *et al.* (2007) Mitochondrial aspartyl-tRNA synthetase deficiency causes leukoencephalopathy with brain stem and spinal cord involvement and lactate elevation, *Nature Genetics*, 39(4), pp. 534–539. doi: 10.1038/ng2013.

Schiffer, S., Rösch, S. and Marchfelder, A. (2002) Assigning a function to a conserved group of proteins: The tRNA 3'-processing enzymes, *EMBO Journal*, 21(11), pp. 2769–2777. doi: 10.1093/emboj/21.11.2769.

Schimmel, P. (2008a) An editing activity that prevents mistranslation and connection to disease, *The Journal of biological chemistry*, 283(43), pp. 28777–82. doi: 10.1074/jbc.X800007200.

Schimmel, P. (2008b) Development of tRNA synthetases and connection to genetic code and disease, *Protein Science*, 17, pp. 1643–1652. doi: 10.1110/ps.037242.108.tree.

Schimmel, P. R. (1979) Aminoacyl-tRNA Synthetases: General Features and Recognition of Transfer RNAs, *Annual review of biochemistry*, 48, pp. 601–648.

Schlieker, C. D. *et al.* (2008) A functional proteomics approach links the ubiquitin-related modifier Urm1 to a tRNA modification pathway, *PNAS*, 105(47), pp. 18255–18260.

Schneider, A. (2011) Mitochondrial tRNA Import and Its Consequences for Mitochondrial Translation, *Annual Review of Biochemistry*, 80, pp. 1033–1053. doi: 10.1146/annurev-biochem-060109-092838.

Senger, B. *et al.* (1997) The modified wobble base inosine in yeast tRNA(Ile) is a positive determinant for aminoacylation by isoleucyl-tRNA synthetase, *Biochemistry*, 36(97), pp. 8269–8275. doi: 10.1021/bi970206l.

Shah, P. and Gilchrist, M. A. (2010) Effect of Correlated tRNA Abundances on Translation Errors and Evolution of Codon Usage Bias, *PLoS Genet*, 6(9). doi: 10.1371/journal.pgen.1001128.

Shaheen, R. *et al.* (2015) Mutation in WDR4 impairs tRNA m7G46 methylation

6. References

and causes a distinct form of microcephalic primordial dwarfism, *Genome Biology*, 16(210). doi: 10.1186/s13059-015-0779-x.

Shaheen, R. *et al.* (2016) A homozygous truncating mutation in PUS3 expands the role of tRNA modification in normal cognition, *Hum Genet*, 135(7), pp. 707–713. doi: 10.1007/s00439-016-1665-7.

Shimada, K. *et al.* (2009) A novel human AlkB homologue, ALKBH8, contributes to human bladder cancer progression, *Cancer Research*, 69(7), pp. 3157–3164. doi: 10.1158/0008-5472.CAN-08-3530.

Shin, B.-S. *et al.* (2012) Initiation Factor eIF2 γ Promotes eIF2–GTP–Met-tRNA i Met Ternary Complex Binding to the 40S Ribosome, *Nat Struct Mol Biol*, 18(11), pp. 1227–1234. doi: 10.1038/nsmb.2133.

Shoemaker, C. J. and Green, R. (2011) Kinetic analysis reveals the ordered coupling of translation termination and ribosome recycling in yeast, *PNAS*, 108(51), pp. E1392–E1398. doi: 10.1073/pnas.1113956108.

Silva, R. M. *et al.* (2007) Critical roles for a genetic code alteration in the evolution of the genus *Candida*, *The EMBO Journal*, pp. 1–11. doi: 10.1038/sj.emboj.7601876.

Simpson, C. L. *et al.* (2009) Variants of the elongator protein 3 (ELP3) gene are associated with motor neuron degeneration, *Human molecular genetics*, 18(3), pp. 472–81. doi: 10.1093/hmg/ddn375.

Slaugenhaupt, S. A. *et al.* (2001) Tissue-Specific Expression of a Splicing Mutation in the IKBKAP Gene Causes Familial Dysautonomia, *Am J Hum Genet*, 68, pp. 598–605.

Sleigh, J. N. *et al.* (2014) Neuromuscular junction maturation defects precede impaired lower motor neuron connectivity in Charcot–Marie– Tooth type 2D mice, *Human Molecular Genetics*, 23(10), pp. 2639–2650. doi: 10.1093/hmg/ddt659.

Sloan, K. E. *et al.* (2016) Tuning the ribosome: The influence of rRNA modification on eukaryotic ribosome biogenesis and function, *RNA Biology*, 0(0), pp. 1–16. doi: 10.1080/15476286.2016.1259781.

Snel, B. *et al.* (2000) STRING: a web-server to retrieve and display the repeatedly occurring neighbourhood of a gene, *Nucleic acids research*. Oxford University Press, 28(18), pp. 3442–4.

Song, X. and Nazar, R. N. (2002) Modification of rRNA as a “quality control mechanism” in ribosome biogenesis, *FEBS Letters*, 523, pp. 182–186.

Sontag, E. M., Vonk, W. I. M. and Frydman, J. (2014) Sorting out the trash: the spatial nature of eukaryotic protein quality control, *Curr Opin Cell Biol*, 26, pp. 139–146. doi: 10.1016/j.ceb.2013.12.006.

Soti, C. and Csermely, P. (2003) Aging and molecular chaperones, *Experimental Gerontology*, 38, pp. 1037–1040. doi: 10.1016/S0531-5565(03)00185-2.

Spahn, C. M. T. *et al.* (2001) Structure of the 80S ribosome from *Saccharomyces cerevisiae* - tRNA-ribosome and subunit-subunit interactions, *Cell*, 107(3), pp. 373–386. doi: 10.1016/S0092-8674(01)00539-6.

Spenkuch, F., Motorin, Y. and Helm, M. (2015) Pseudouridine: Still mysterious, but never a fake (uridine)!, *RNA Biology*, 11(December), pp. 1540–1554. doi: 10.4161/15476286.2014.992278.

Sprinzl, M. and Vassilenko, K. S. (2005) Compilation of tRNA sequences and sequences of tRNA genes, *Nucleic Acids Research*, 33(1), pp. D139–D140. doi: 10.1093/nar/gki012.

Starr, J. L. (1963) The incorporation of methyl groups into amino acid transfer ribonucleic acid, *Biochemical and biophysical research communications*, 10, pp. 175–80.

Stefani, M. (2004) Protein misfolding and aggregation: new examples in medicine and biology of the dark side of the protein world, *Biochimica et Biophysica Acta*, 1739, pp. 5–25. doi: 10.1016/j.bbadis.2004.08.004.

Stefani, M. and Dobson, C. M. (2003) Protein aggregation and aggregate toxicity: New insights into protein folding, misfolding diseases and biological evolution, *Journal of Molecular Medicine*, 81, pp. 678–699. doi: 10.1007/s00109-003-0464-5.

Stefano, J. E. (1984) Purified lupus antigen La recognizes an oligouridylate stretch common to the 3' termini of RNA polymerase III transcripts, *Cell*, 36(1), pp. 145–154. doi: 10.1016/0092-8674(84)90083-7.

Steinberg, S. and Cedergren, R. (1995) A correlation between N2-dimethylguanosine presence and alternate tRNA conformers, *RNA*, 1, pp. 886–891.

Steinthorsdottir, V. *et al.* (2007) A variant in CDKAL1 influences insulin response and risk of type 2 diabetes, *Nature Genetics*, 39(6), pp. 770–775. doi: 10.1038/ng2043.

Strug, L. J. *et al.* (2009) Centrottemporal sharp wave EEG trait in rolandic epilepsy maps to Elongator Protein Complex 4 (ELP4), *European Journal of Human Genetics*. Nature Publishing Group, 17, pp. 1171–81. doi: 10.1038/ejhg.2008.267.

Strunk, B. S. *et al.* (2011) Ribosome Assembly Factors Prevent Premature Translation Initiation by 40S Assembly Intermediates, *Science*, 333(6048), pp. 1449–1453. doi: 10.1126/science.1208245.

Strunk, B. S. *et al.* (2012) Joining of 60S subunits and a translation-like cycle in 40S ribosome maturation, *Cell*, 150(1), pp. 111–121.

6. References

- Stuart, J. W. *et al.* (2003) Naturally-occurring Modification Restricts the Anticodon Domain Conformational Space of tRNA^{Phe}, *Journal of Molecular Biology*, 334, pp. 901–918. doi: 10.1016/j.jmb.2003.09.058.
- Su, D. *et al.* (2014) Quantitative analysis of ribonucleoside modifications in tRNA by HPLC-coupled mass spectrometry, *Nature protocols*, 9(4), pp. 828–41. doi: 10.1038/nprot.2014.047.
- Suzuki, Y. *et al.* (2009) Structural basis of tRNA modification with CO₂ fixation and methylation by wybutosine synthesizing enzyme TYW4, *Nucleic Acids Research*, 37(9), pp. 2910–2925. doi: 10.1093/nar/gkp158.
- Svensson, I. *et al.* (1963) Studies on microbial RNA, *Journal of molecular biology*, 7, pp. 254–71.
- Szklarczyk, D. *et al.* (2015) STRING v10: protein-protein interaction networks, integrated over the tree of life, *Nucleic acids research*. Oxford University Press, 43, pp. D447-52. doi: 10.1093/nar/gku1003.
- Szklarczyk, D. *et al.* (2017) The STRING database in 2017: quality-controlled protein-protein association networks, made broadly accessible, *Nucleic acids research*. Oxford University Press, 45, pp. D362–D368. doi: 10.1093/nar/gkw937.
- Tabas-Madrid, D., Nogales-Cadenas, R. and Pascual-Montano, A. (2012) GeneCodis3: a non-redundant and modular enrichment analysis tool for functional genomics, *Nucleic Acids Research*, 40, pp. W478–W483. doi: 10.1093/nar/gks402.
- Takeoka, S. *et al.* (2001) Amino-acid substitutions in the IKAP gene product significantly increase risk for bronchial asthma in children, *J Hum Genet*, 46, pp. 57–63.
- Taylor, B. S. *et al.* (2010) Integrative genomic profiling of human prostate cancer, *Cancer Cell*, 18(1), pp. 11–22. doi: 10.1016/j.ccr.2010.05.026.
- Thiaville, P. C., Iwata-Reuyl, D. and de Crécy-Lagard, V. (2014) Diversity of the biosynthesis pathway for threonylcarbamoyladenosine (t⁶A), a universal modification of tRNA, *RNA biology*. Taylor & Francis, 11(12), pp. 1529–39. doi: 10.4161/15476286.2014.992277.
- Thompson, D. M. and Parker, R. (2009) Stressing out over tRNA cleavage, *Cell*. Elsevier, 138(2), pp. 215–9. doi: 10.1016/j.cell.2009.07.001.
- Thompson, M. *et al.* (2003) Nucleolar clustering of dispersed tRNA genes, *Science*, 302(5649), pp. 1399–1401. doi: 10.1126/science.1089814.
- Tigano, M. *et al.* (2015) Elongator-dependent modification of cytoplasmic tRNA^{Lys}UUU is required for mitochondrial function under stress conditions, *Nucleic acids research*. Oxford University Press, 43(17), pp. 8368–80. doi: 10.1093/nar/gkv765.

Tollervey, D. (1996) Trans-Acting Factors in Ribosome Synthesis, *Experimental Cell Research*, 229(229), pp. 226–232. doi: 10.1006/excr.1996.0364.

Tomoyasu, T. *et al.* (2001) Genetic dissection of the roles of chaperones and proteases in protein folding and degradation in the Escherichia coli cytosol, *Molecular microbiology*, 40(2), pp. 397–413.

Torres, A. G., Batlle, E. and Ribas de Pouplana, L. (2014) Role of tRNA modifications in human diseases, *Trends in Molecular Medicine*. Elsevier Ltd, 934, pp. 1–9. doi: 10.1016/j.molmed.2014.01.008.

Trahan, C., Martel, C. and Dragon, F. O. (2010) Effects of dyskeratosis congenita mutations in dyskerin, NHP2 and NOP10 on assembly of H/ACA pre-RNPs, *Human Molecular Genetics*, 19(5), pp. 825–836. doi: 10.1093/hmg/ddp551.

Umeda, N. *et al.* (2005) Mitochondria-specific RNA-modifying enzymes responsible for the biosynthesis of the wobble base in mitochondrial tRNAs: Implications for the molecular pathogenesis of human mitochondrial diseases, *The Journal of biological chemistry*, 280(2), pp. 1613–24. doi: 10.1074/jbc.M409306200.

Urbonavicius, J. *et al.* (2001) Improvement of reading frame maintenance is a common function for several tRNA modifications, *The EMBO journal*. European Molecular Biology Organization, 20(17), pp. 4863–73. doi: 10.1093/emboj/20.17.4863.

Valdez, B. C. *et al.* (2004) The Treacher Collins syndrome (TCOF1) gene product is involved in ribosomal DNA gene transcription by interacting with upstream binding factor, *PNAS*, 101(29), pp. 10709–10714.

Vanrobays, E. *et al.* (2001) Processing of 20S pre-rRNA to 18S ribosomal RNA in yeast requires Rrp10p, an essential non-ribosomal cytoplasmic protein, *The EMBO Journal*, 20(15), pp. 4204–4213.

Varshavsky, A. (1997) The N-end rule pathway of protein degradation, *Genes to cells*, 2, pp. 13–28. doi: 10.1016/0309-1651(90)90142-L.

Venema, J. and Tollervey, D. (1995) Processing of pre-ribosomal RNA in *Saccharomyces cerevisiae*, *Yeast*, 11(16), pp. 1629–1650. doi: 10.1002/yea.320111607.

Venema, J. and Tollervey, D. (1999) Ribosome synthesis in *Saccharomyces cerevisiae*, *Annual review of genetics*, 33, pp. 261–311.

Verine Massenet, S. *et al.* (1999) Pseudouridine Mapping in the *Saccharomyces cerevisiae* Spliceosomal U Small Nuclear RNAs (snRNAs) Reveals that Pseudouridine Synthase Pus1p Exhibits a Dual Substrate Specificity for U2 snRNA and tRNA, *Molecular and Cellular Biology*, 19(3), pp. 2142–2154.

Vermulst, M. *et al.* (2015) Transcription errors induce proteotoxic stress and shorten cellular lifespan, *Nature Communications*. Nature Publishing Group, 6, p.

6. References

8065. doi: 10.1038/ncomms9065.

Voisine, C., Pedersen, J. S. and Morimoto, R. I. (2010) Chaperone networks: Tipping the balance in protein folding diseases, *Neurobiology of Disease*. Elsevier Inc., 40(1), pp. 12–20. doi: 10.1016/j.nbd.2010.05.007.

Walbott, H. *et al.* (2011) The H/ACA RNP assembly factor SHQ1 functions as an RNA mimic, *Genes & development*, 25(22), pp. 2398–408. doi: 10.1101/gad.176834.111.

Waldron, C. and Lacroute, F. (1975) Effect of growth rate on the amounts of ribosomal and transfer ribonucleic acids in yeast, *Journal of Bacteriology*, 122(3), pp. 855–865.

Walker, S. C. and Engelke, D. R. (2006) Ribonuclease P: The Evolution of an Ancient RNA Enzyme, *Crit Rev Biochem Mol Biol*, 41(2), pp. 77–102. doi: 10.1080/10409230600602634.Ribonuclease.

Walter, S. and Buchner, J. (2002) Molecular Chaperones – Cellular Machines for Protein Folding, *Angewandte Chemie Int. Ed.*, 41, pp. 1098–1113.

Wang, P. *et al.* (2015) Accurate placement of substrate RNA by Gar1 in H/ACA RNA-guided pseudouridylation, *Nucleic Acids Research*, 43(10), pp. 7207–7216. doi: 10.1093/nar/gkv757.

Wang, Q. *et al.* (2005) Proteomic analysis of neurofibrillary tangles in Alzheimer disease identifies GAPDH as a detergent-insoluble paired helical filament tau binding protein, *The FASEB Journal*, 19(7), pp. 869–871. doi: 10.1096/fj.04-3210fje.

Wang, X., Yan, Q. and Guan, M.-X. (2009) Mutation in MTO1 involved in tRNA modification impairs mitochondrial RNA metabolism in the yeast *Saccharomyces cerevisiae*, *Mitochondrion*, 9(3), pp. 180–185. doi: 10.1021/nl061786n.Core-Shell.

Wang, X., Yan, Q. and Guan, M.-X. (2010) Combination of the loss of cmnm5U34 with the lack of s2U34 modifications of tRNA^{Lys}, tRNA^{Glu}, and tRNA^{Gln} altered mitochondrial biogenesis and respiration, *Journal of molecular biology*. NIH Public Access, 395(5), pp. 1038–48. doi: 10.1016/j.jmb.2009.12.002.

Wang, X., Yan, Q. and Guan, M. X. (2007) Deletion of the MTO2 gene related to tRNA modification causes a failure in mitochondrial RNA metabolism in the yeast *Saccharomyces cerevisiae*, *FEBS Letters*, 581, pp. 4228–4234. doi: 10.1016/j.febslet.2007.07.067.

Wang, Y. *et al.* (2009) Abnormal proteins can form aggresome in yeast: aggresome-targeting signals and components of the machinery, *The FASEB Journal*, 23, pp. 451–463. doi: 10.1096/fj.08-117614.

Warner, J. R. (1999) The economics of ribosome biosynthesis in yeast, *Trends in Biochemical Sciences*, 24(11), pp. 437–440. doi: 10.1016/S0968-0004(99)01460-

7.

Watkins, N. J. *et al.* (2000) A Common Core RNP Structure Shared between the Small Nuclear Box C/D RNPs and the Spliceosomal U4 snRNP, *Cell*, 103, pp. 457–466.

Watkins, N. J. and Bohnsack, M. T. (2012) The box C/D and H/ACA snoRNPs: Key players in the modification, processing and the dynamic folding of ribosomal RNA, *Wiley Interdisciplinary Reviews: RNA*, 3(June), pp. 397–414. doi: 10.1002/wrna.117.

Wedekind, J. E. and Beal, P. A. (2009) Mechanism of Action and Structural Aspects of ADARS (A-to-I) and APOBEC-Related (C-to-U) Deaminases, in Grosjean, H. (ed.) *DNA and RNA Modification Enzymes: Structure, Mechanism, Function and Evolution*. Austin, Texas, USA: Landes Bioscience, pp. 203–223.

Wei, F.-Y. *et al.* (2011) Deficit of tRNA^{Lys} modification by Cdkal1 causes the development of type 2 diabetes in mice, *The Journal of Clinical Investigation*, 121(9), pp. 3598–3608.

Weissenbach, J. and Grosjean, H. (1981) Effect of threonylcarbamoyl modification (t6A) in yeast tRNA Arg III on codon-anticodon and anticodon-anticodon interactions. A thermodynamic and kinetic evaluation, *European journal of biochemistry*, 116(1), pp. 207–13.

Weisser, M. *et al.* (2013) The crystal structure of the eukaryotic 40S ribosomal subunit in complex with eIF1 and eIF1A, *Nature structural & molecular biology*. Nature Publishing Group, 20(8), pp. 1015–7. doi: 10.1038/nsmb.2622.

Wek, S. A., Zhu, S. and Wek, R. C. (1995) The Histidyl-tRNA Synthetase-Related Sequence in the eIF-2a Protein Kinase GCN2 Interacts with tRNA and Is Required for Activation in Response to Starvation for Different Amino Acids, *Molecular and Cellular Biology*, 15(8), pp. 4497–4506.

Wery, M. *et al.* (2009) The nuclear poly(A) polymerase and Exosome cofactor Trf5 is recruited cotranscriptionally to nucleolar surveillance, *RNA*, 15, pp. 406–419. doi: 10.1261/rna.1402709.

Whipple, J. M. *et al.* (2011) The yeast rapid tRNA decay pathway primarily monitors the structural integrity of the acceptor and T-stems of mature tRNA, *Genes & Development*, 25, pp. 1173–1184. doi: 10.1101/gad.2050711.tion.

Willmund, F. *et al.* (2013) The cotranslational function of ribosome-associated Hsp70 in eukaryotic protein homeostasis, *Cell*, 152(1–2), pp. 196–209. doi: 10.1016/j.cell.2012.12.001.

Wilson, D. N. and Nierhaus, K. H. (2006) The E-site story: the importance of maintaining two tRNAs on the ribosome during protein synthesis, *Cellular and molecular life sciences: CMLS*, 63(23), pp. 2725–37. doi: 10.1007/s00018-006-6125-4.

6. References

Wilusz, J. E. (2015) Controlling translation via modulation of tRNA levels, *Wiley interdisciplinary reviews RNA*. NIH Public Access, 6(4), pp. 453–70. doi: 10.1002/wrna.1287.

Winkler, G. S. *et al.* (2001) RNA Polymerase II Elongator Holoenzyme Is Composed of Two Discrete Subcomplexes, *The Journal of Biological Chemistry*, 276(35), pp. 32743–32749. doi: 10.1074/jbc.M105303200.

Wittschieben, B. Ø. *et al.* (1999) A Novel Histone Acetyltransferase Is an Integral Subunit of Elongating RNA Polymerase II Holoenzyme, *Molecular Cell*, 4, pp. 123–128.

Woese, C. R. *et al.* (2000) Aminoacyl-tRNA Synthetases, the Genetic Code, and the Evolutionary Process, *Microbiology and Molecular Biology Reviews*, 64(1). doi: 10.1128/MMBR.64.1.202-236.2000.Updated.

Wolfe, C. L., Hopper, A. K. and Martin, N. C. (1996) Mechanisms leading to and the consequences of altering the normal distribution of ATP(CTP):tRNA nucleotidyltransferase in yeast, *Journal of Biological Chemistry*, 271(9), pp. 4679–4686. doi: 10.1074/jbc.271.9.4679.

Woodson, S. A. (2011) Pathways of RNA folding and ribosome assembly from time-resolved footprinting, *Acc Chem Res*, 44(12), pp. 1312–1319. doi: 10.1021/ar2000474.

Woolford, J. L. and Baserga, S. J. (2013) Ribosome biogenesis in the yeast *Saccharomyces cerevisiae*, *Genetics*, 195(3), pp. 643–81. doi: 10.1534/genetics.113.153197.

Wright, R. (2000) Transmission electron microscopy of yeast, *Microscopy research and technique*, 51(July), pp. 496–510. doi: 10.1002/1097-0029(20001215)51:6<496::AID-JEMT2>3.0.CO;2-9.

Wu, P. *et al.* (1998) Nop5p Is a Small Nucleolar Ribonucleoprotein Component Required for Pre-18 S rRNA Processing in Yeast, *J Biol Chem*, 273(26), pp. 16453–16463.

Wu, Y. *et al.* (2016) Mtu1-Mediated Thiouridine Formation of Mitochondrial tRNAs Is Required for Mitochondrial Translation and Is Involved in Reversible Infantile Liver Injury, *PLoS genetics*. Public Library of Science, 12(9). doi: 10.1371/journal.pgen.1006355.

Xia, Q. *et al.* (2009) Proteomic identification of novel proteins associated with Lewy bodies, *Front Biosci*, 13, pp. 3850–3856.

Xing, F. *et al.* (2004) The specificities of four yeast dihydrouridine synthases for cytoplasmic tRNAs, *The Journal of biological chemistry*, 279(17), pp. 17850–60. doi: 10.1074/jbc.M401221200.

Xing, F., Martzen, M. R. and Phizicky, E. M. (2002) A conserved family of

Saccharomyces cerevisiae synthases effects dihydrouridine modification of tRNA., *RNA*, 8(3), pp. 370–81.

El Yacoubi, B. *et al.* (2009) The universal YrdC/Sua5 family is required for the formation of threonylcarbamoyladenine in tRNA, *Nucleic acids research*, 37(9), pp. 2894–909. doi: 10.1093/nar/gkp152.

El Yacoubi, B. *et al.* (2011) A role for the universal Kae1/Qri7/YgjD (COG0533) family in tRNA modification, *The EMBO journal*, 30(5), pp. 882–93. doi: 10.1038/emboj.2010.363.

El Yacoubi, B., Bailly, M. and de Crécy-Lagard, V. (2012) Biosynthesis and function of posttranscriptional modifications of transfer RNAs, *Annual review of genetics*, 46, pp. 69–95. doi: 10.1146/annurev-genet-110711-155641.

Yadavalli, S. S. and Ibba, M. (2012) Quality control in aminoacyl-tRNA synthesis its role in translational fidelity., in *Advances in protein chemistry and structural biology*, pp. 1–43. doi: 10.1016/B978-0-12-386497-0.00001-3.

Yang, P. K. *et al.* (2002) The Shq1p Naf1p Complex Is Required for Box H/ACA Small Nucleolar Ribonucleoprotein Particle Biogenesis, *The Journal of Biological Chemistry*, 277(47), pp. 45235–45242.

Yang, P. K. *et al.* (2005) Cotranscriptional Recruitment of the Pseudouridylsynthetase Cbf5p and of the RNA Binding Protein Naf1p during H/ACA snoRNP Assembly, *Molecular and Cellular Biology*, 25(8), pp. 3295–3304. doi: 10.1128/MCB.25.8.3295–3304.2005.

Yang, X. *et al.* (2012) Kinetic and thermodynamic characterization of the reaction pathway of box H/ACA RNA-guided pseudouridine formation, *Nucleic Acids Research*, 40(21), pp. 10925–10936. doi: 10.1093/nar/gks882.

Yao, P. and Fox, P. L. (2013) Aminoacyl-tRNA synthetases in medicine and disease, *EMBO Mol Med*, 5, pp. 332–343. doi: 10.1002/emmm.201100626.

Yarian, C. *et al.* (2002) Accurate Translation of the Genetic Code Depends on tRNA Modified Nucleosides, *The Journal of Biological Chemistry*, 277(19), pp. 16391–16395. doi: 10.1074/jbc.M200253200.

Yarus, M. (1972) Phenylalanyl-tRNA Synthetase and Isoleucyl-tRNAPhe: A Possible Verification Mechanism for Aminoacyl-tRNA, *PNAS*, 69(7), pp. 1915–1919.

Yasukawa, T. *et al.* (2000) Defect in modification at the anticodon wobble nucleotide of mitochondrial tRNA^{Lys} with the MERRF encephalomyopathy pathogenic mutation, *FEBS Letters*, 467, pp. 175–178. doi: 10.1016/S0014-5793(00)01145-5.

Yasukawa, T. *et al.* (2000) Modification Defect at Anticodon Wobble Nucleotide of Mitochondrial tRNAs^{LeuUUR} with Pathogenic Mutations of Mitochondrial Myopathy, Encephalopathy, Lactic Acidosis, and Stroke-like

6. References

Episodes, *Journal of Biological Chemistry*, 275(6), pp. 4251–4257. doi: 10.1074/jbc.275.6.4251.

Yasukawa, T. *et al.* (2001) Wobble modification defect in tRNA disturbs codon-anticodon interaction in a mitochondrial disease, *The EMBO*, 20(17), pp. 4794–4802.

Yokoyama, S. *et al.* (1985) Molecular mechanism of codon recognition by tRNA species with modified uridine in the first position of the anticodon, *Biochemistry*, 82, pp. 4905–4909.

Yoo, C. J. and Wolin, S. L. (1997) The yeast La protein is required for the 3' endonucleolytic cleavage that matures tRNA precursors, *Cell*, 89(3), pp. 393–402. doi: 10.1016/S0092-8674(00)80220-2.

Yoshihisa, T. *et al.* (2003) Possibility of Cytoplasmic pre-tRNA Splicing: the Yeast tRNA Splicing Endonuclease Mainly Localizes on the Mitochondria, *Molecular biology of the cell*, 14, pp. 3266–3279. doi: 10.1091/mbc.E02-11-0757.

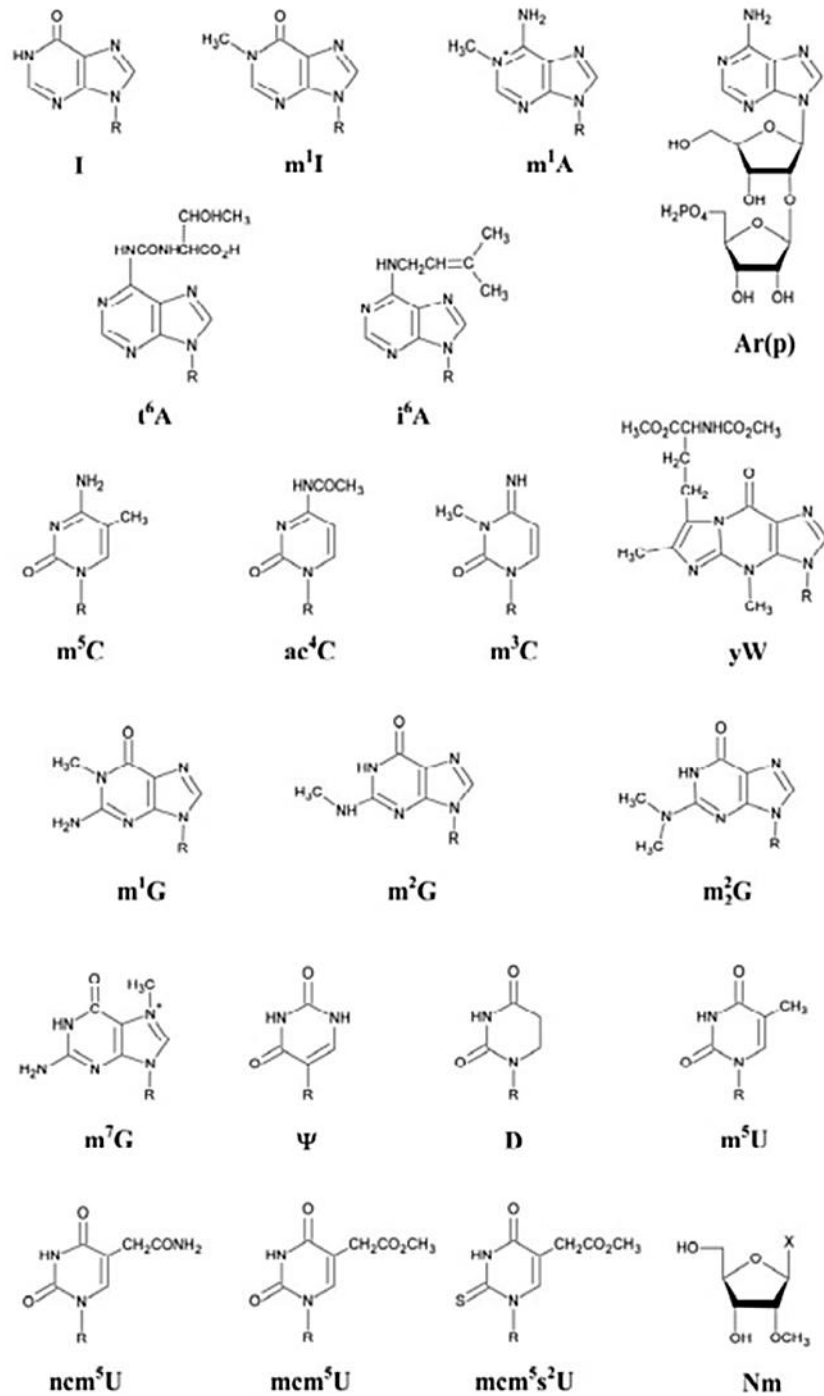
Zeharia, A. *et al.* (2009) Acute infantile liver failure due to mutations in the TRMU gene, *The American Journal of Human Genetics*. Elsevier, 85, pp. 401–7. doi: 10.1016/j.ajhg.2009.08.004.

Zhang, G., Hubalewska, M. and Ignatova, Z. (2009) Transient ribosomal attenuation coordinates protein synthesis and co-translational folding, *Nature Structural & Molecular Biology*, 16(3), pp. 274–280. doi: 10.1038/nsmb.1554.

Zinshteyn, B. and Gilbert, W. V. (2013) Loss of a Conserved tRNA Anticodon Modification Perturbs Cellular Signaling, *PLoS Genetics*, 9(8), p. e1003675. doi: 10.1371/journal.pgen.1003675.

7. ANNEXES

Annex I. *S. cerevisiae* tRNAs and modified nucleosides



Annex I.1. Structures of modified nucleosides found in *S. cerevisiae* cytoplasmic tRNAs. R: ribose; X: any base; Nm: 2'-O-methylated nucleosides. Adapted from Grosjean, 2005.

Annex I.2. Distribution of modified nucleosides in cytoplasmic tRNAs in *S. cerevisiae*. In *S. cerevisiae*, 275 nucleus-encoded tRNA genes code for the 42 different cytoplasmic tRNA species (1 initiator and 41 elongator tRNAs) that pair with the 61 sense codons (Percudani *et al.*, 1997; Hani and Feldmann, 1998; <http://gtrnadb.ucsc.edu/genomes/eukaryota/Scere3/>). Of the 42 tRNA species, 31 RNA sequences are known and could be consulted at <http://modomics.genesilico.pl/sequences/list/tRNA/>. For the remaining eleven tRNA species, the RNA sequence is not known. Indicated within parenthesis is the number of genes for each specie. The position of each modified nucleoside in the tRNA is indicated and positions that are not observed in all subspecies are indicated within parenthesis.

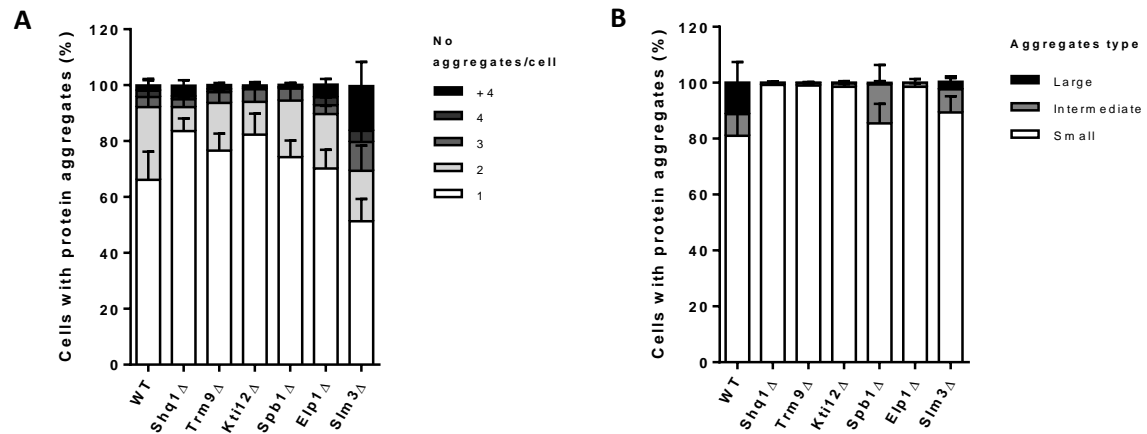
tRNA species (Number of genes)	Modified nucleoside / position in tRNA																									
	I	m ¹ I	m ¹ A	t ⁶ A	i ⁶ A	Ar(p)	Am	m ⁵ C	ac ⁴ C	m ³ C	Cm	m ¹ G	m ² G	m ² G	Gm	m ⁷ G	yW	Ψ	D	m ⁵ U	Um	mcm ⁵ U	mcm ⁵ s ² U	ncm ⁵ U	ncm ⁵ Um	
tRNA ^{Ala} _{IGC} (11)	34	37										9		26					38, 55	16, 20, 47	54					
tRNA ^{Arg} _{ICG} (6)	34		58					49				9	10	26					1, 27, 55	16, 20, 47	54					
tRNA ^{Arg} _{mcm5UCU} (11)			58	37								9	10	26					27, 39, 55	16, 47	54		34			
tRNA ^{Asn} _{GUU} (10)			58	37				48					10	26					39, 55	16, 17, 20, 20A, 47	54					
tRNA ^{Asp} _{GUC} (16)								49				37							13, 32, 55	16, 20	54					
tRNA ^{Cys} _{GCA} (4)			58		37			48									46		32, 39, 55	16, 20, 47	54					
tRNA ^{Glu} _{mcm5s2UUC} (14)								49											13, 27, 55	20A	54		34			
tRNA ^{Gly} _{GCC} (16)								49			4	9							13, 32, 38, 55	16, 20	54					
tRNA ^{Gly} _{mcm5UCC} (3)																			13,55	16, 20, 20A	54		34			
tRNA ^{His} _{GUG} (7)							4	49				37			18				13, 32, (39), 55	16, 20, 20A	54					
tRNA ^{Ile} _{IAU} (13)	34		58	37				48				9	10						55	16, 17, 20, 20A, 47	54					
tRNA ^{Ile} _{ΨAW} (2)			58	37				48					10				46		27, 34, 36, 55, 67	16, 20, 20A, 47	54					
tRNA ^{Leu} _{mSCAA} (10)								34, 48	12			37	10	26	18				32, 39, 55	20, 20B	54					
tRNA ^{Leu} _{ncm5UAAA} (7)			58					48	12		32	37	10	26	18				39, 55	16, 20, 20B	54					34
tRNA ^{Leu} _{UAG} (3)			58					48	12			37	10	26	18				27, 32, 39, 55	16, 20, 20A, 20B	54					
tRNA ^{Lys} _{CUU} (14)			58	37								9	10	26			46		27, 39, 55	16, 20	54					
tRNA ^{Lys} _{mcm5s2UUU} (7)			58	37				48					10	26			46		1, 27, 28, 55, 67	16, 17, 20, 47	54		34			
tRNA ^{Met} _i (5)			58	37		64		48, 49				9	10	26			46			16, 47						
tRNA ^{Met} _m (5)			58	37				48					10	26			46		27, 31, 39, 55	16, 47	54					
tRNA ^{Phe} _{GmAA} (10)			58					40, 49			32		10	26	34	46	37		39, 55	16, 17	54					
tRNA ^{Pro} _{ncm5UGG} (10)			58								4	9, 37					46		13, 32, 38, 55	16, 20	54				34	
tRNA ^{Ser} _{CGA} (1)					37			48	12	32				26	18				39, 55	16, 20, 20A	54	44				
tRNA ^{Ser} _{GCU} (4)					37			48	12					26	18				55	16, 20, 20A	54	44				
tRNA ^{Ser} _{GGA} (11)	34				37			48	12					26	18				32, 39, 55	16, 20, 20A	54	44				
tRNA ^{Ser} _{ncm5UGA} (3)					37			48	12	32				26	18				39, 55	16, 20, 20A	54	44			34	
tRNA ^{Thr} _{IGU} (11)	34		58	37				48		32			10	26					39, 55	16, 17, 20, 47	54					
tRNA ^{Trp} _{CmCA} (6)			58								32, 34	9	10		18	46			26, 27, 28, 39, 55, 65	16, 20, 47	54					
tRNA ^{Tyr} _{GWA} (8)			58		37			48					10	26	18				35, 39, 55	16, 17, 20, 20A, 20B, 47	54					
tRNA ^{Val} _{CAC} (2)			58					49					10, 26				46		13, 27, 28, 32, 55	20A, 47	54					
tRNA ^{Val} _{IAC} (14)	34		58					49				9					46		13, 27, 32, 55	16, 20, 20A, 47	54					
tRNA ^{Val} _{ncm5UAC} (2)			58					49					10	26					27, 32, 55	16, 20, 20A, 47	54				34	

7. Annexes

Annex I.3. Distribution of modified nucleosides in mitochondrial tRNAs in *S. cerevisiae*. 16 RNA sequences of mitochondrial tRNAs are known and could be consulted at <http://modomics.genesilico.pl/sequences/list/tRNA/>. The position of each modified nucleoside in the tRNA is indicated and positions that are not observed in all subspecies are indicated within parenthesis.

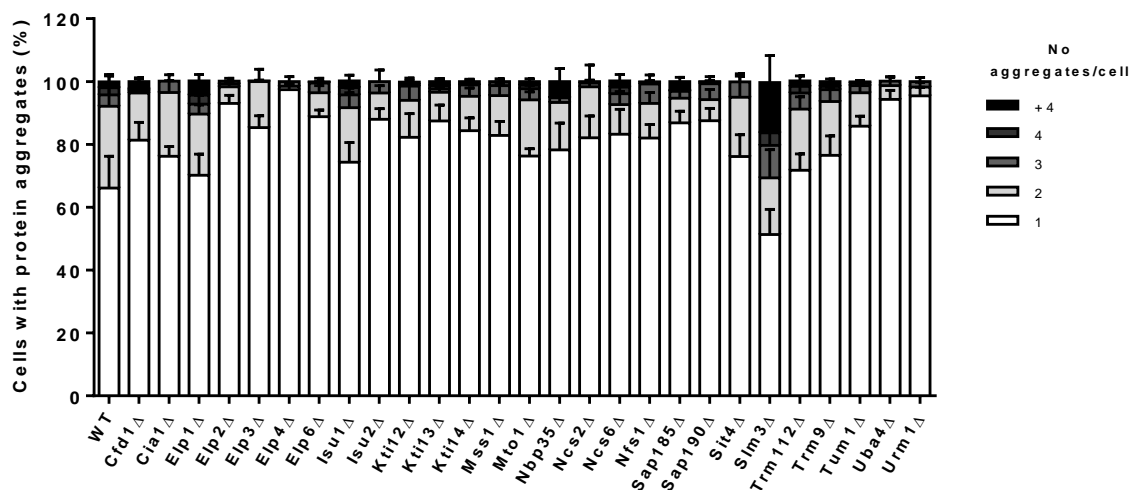
tRNA species	Modified nucleoside / position in tRNA										
	t ⁶ A	i ⁶ A	m ¹ G	m ² G	m ² ₂ G	Ψ	D	m ⁵ U	cmnm ⁵ U	cmnm ⁵ s ² U	Unknown
tRNA ^{Arg} _{ACG}						27, 39, 55	16, 20	54			
tRNA ^{Arg} _{UCU}	37					27, 39, 55	16, 20	54			U ₃₄
tRNA ^{Gly} _{UCC}		37			26	31, 55	16, 20	54			U ₃₄
tRNA ^{His} _{GUG}			37			27, 38, 55	16, 20	54			
tRNA ^{Ile} _{GAU}	37					31, 55	16, 17, 20	54			
tRNA ^{Leu} _{cmnm5UAA}			37		26	31, 39, 55	16, 20	54	34		
tRNA ^{Lys} _{cmnm5s2UUU}	37					28, 31, 55	16, 20	54		34	
tRNA ^{Met} _i			37			55, 72	16, 20	54			
tRNA ^{Met} _m	37					31, 55	16, 17, 20	54			
tRNA ^{Phe} _{GAA}			37		26	39, 55	16, 20				
tRNA ^{Pro} _{UGG}			37	26		55	20	54			
tRNA ^{Ser} _{GCU}						31, 55	16, 20	54			
tRNA ^{Ser} _{UGA}			37	26		(27), 39, 55	16, 20	54			
tRNA ^{Thr} _{UAG}			37	26		27, 31, 38, 55	16, 20	54			
tRNA ^{Trp} _{cmnm5UCA}						39, 55	16,20	54	34		A37
tRNA ^{Tyr} _{GUA}		37		26		27, 55	16, 20	54			

Annex II. Characterization of protein aggregates from genetic screen



Annex II.1. Number and type of protein aggregates per cell in selected KO strains.

Yeast cells containing localized Hsp104-GFP fluorescence foci were counted and differentiated according to the number (**A**) and the size (**B**) of localized Hsp104-GFP fluorescence foci per cell. Results are expressed as the percentage of positive cells (with Hsp104-GFP foci) relative the total number of cells with protein aggregates. Data represent the mean \pm SEM of triplicates of three independent clones.

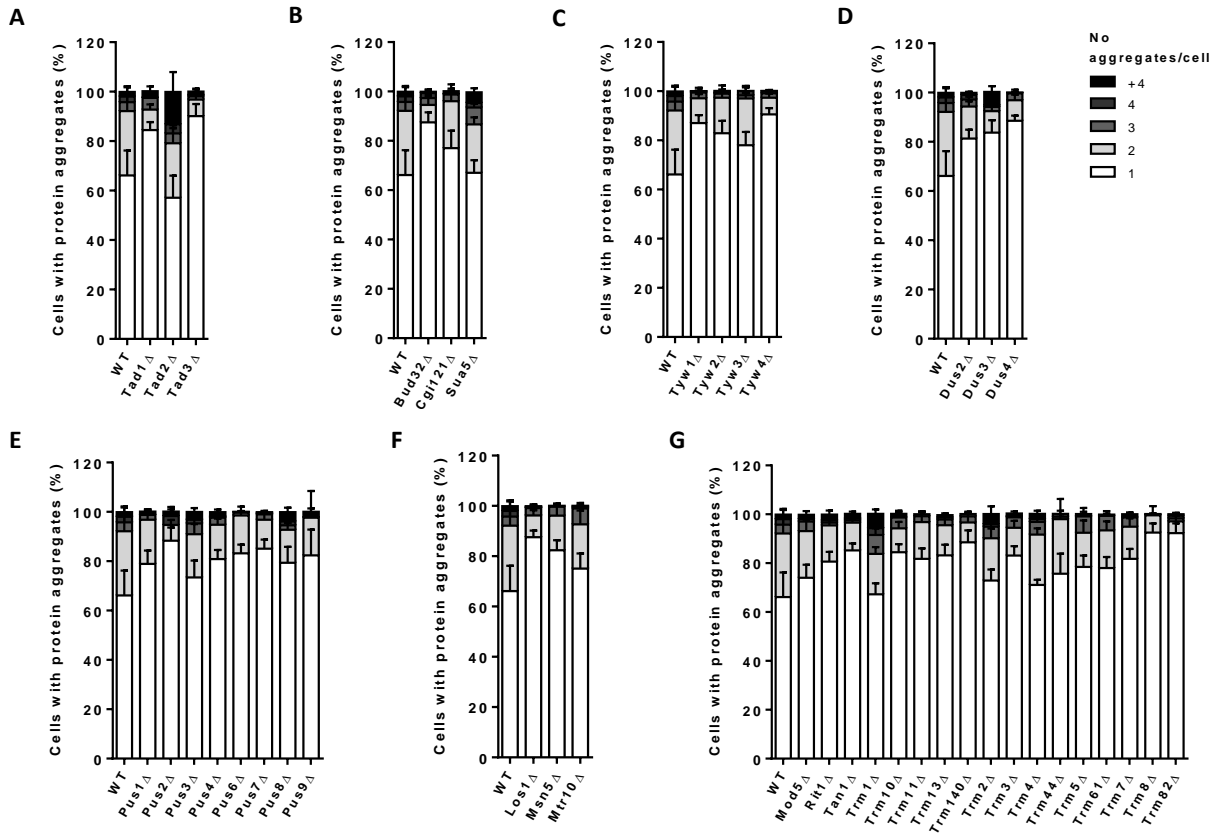


Annex II.2. Number of protein aggregates per cell in wobble uridine modifying enzyme KO strains.

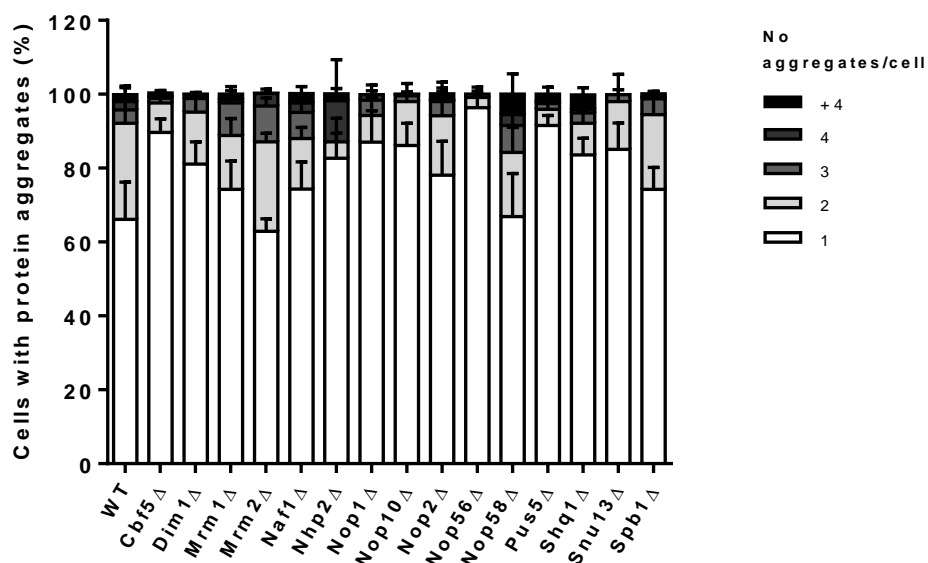
Yeast cells containing localized Hsp104-GFP fluorescence foci were counted and differentiated according to the number of localized Hsp104-GFP fluorescence foci per cell. Results are expressed as the percentage of positive cells (with Hsp104-GFP

7. Annexes

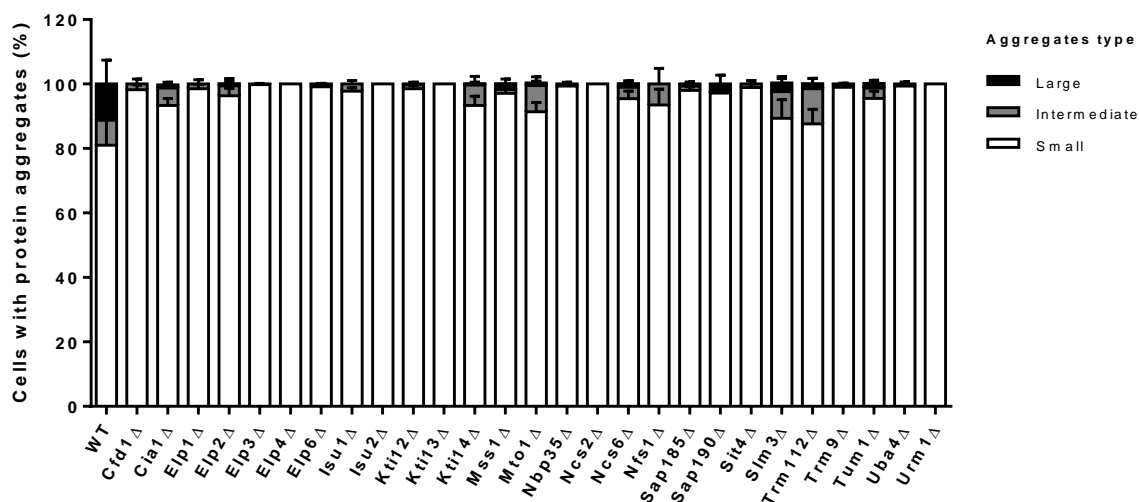
foci) relative the total number of cells with protein aggregates. Data represent the mean \pm SEM of triplicates of three independent clones.



Annex II.3. Number of protein aggregates per cell in tRNAmod KO strains. Yeast cells containing localized Hsp104-GFP fluorescence foci were counted and differentiated according to the number of localized Hsp104-GFP fluorescence foci per cell. Results are expressed as the percentage of positive cells (with Hsp104-GFP foci) relative the total number of cells with protein aggregates. Data represent the mean \pm SEM of triplicates of three independent clones.



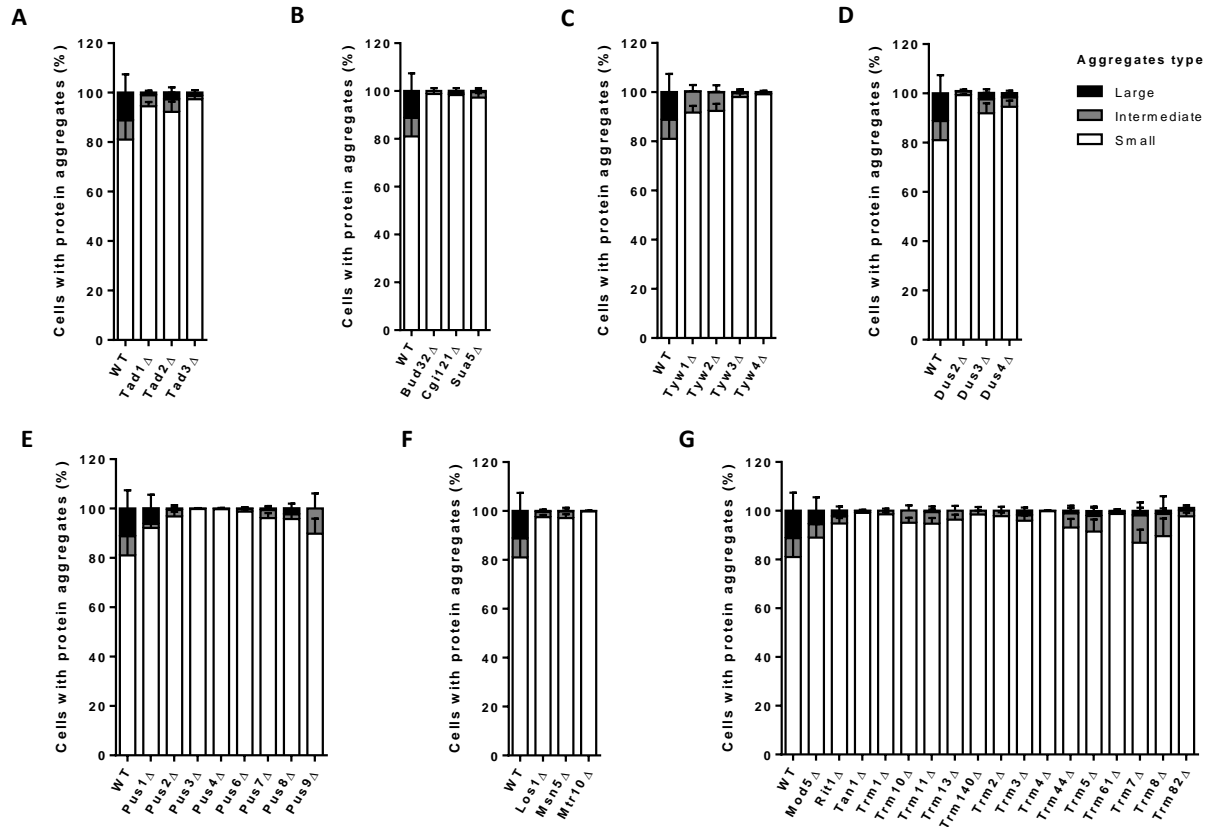
Annex II.4. Number of protein aggregates per cell in rRNAmoD KO strains. Yeast cells containing localized Hsp104-GFP fluorescence foci were counted and differentiated according to the number of localized Hsp104-GFP fluorescence foci per cell. Results are expressed as the percentage of positive cells (with Hsp104-GFP foci) relative the total number of cells with protein aggregates. Data represent the mean \pm SEM of triplicates of three independent clones.



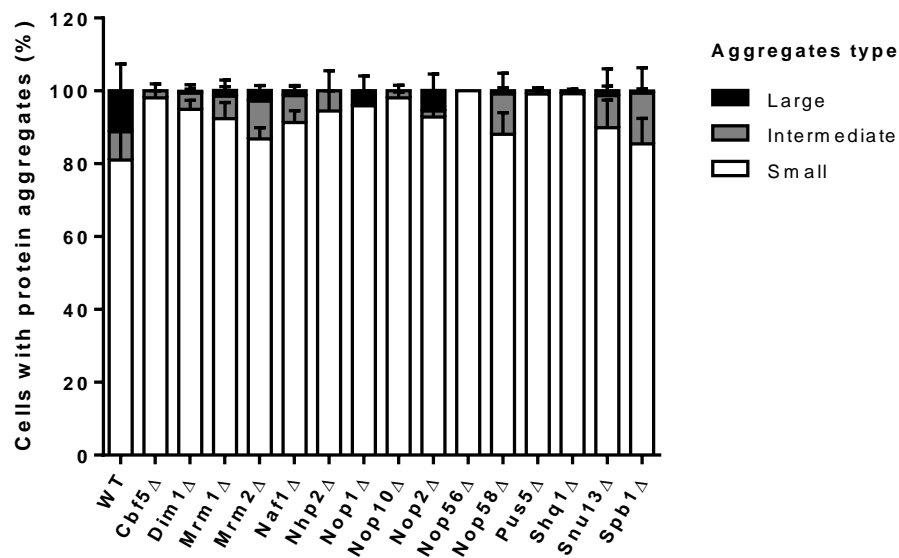
Annex II.5. Type of protein aggregates per cell in wobble uridine modifying enzyme KO strains. Yeast cells containing localized Hsp104-GFP fluorescence foci were counted and differentiated according to the size of localized Hsp104-GFP fluorescence foci per cell. Results are expressed as the percentage of positive cells (with Hsp104-GFP foci) relative

7. Annexes

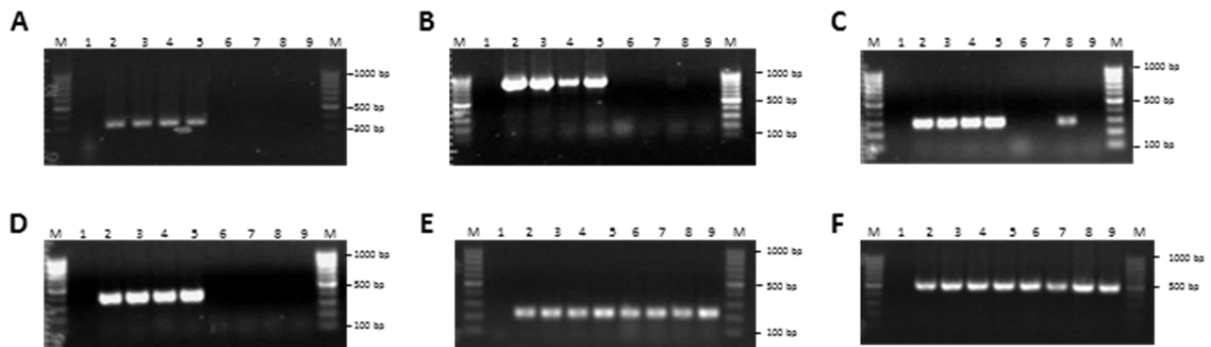
the total number of cells with protein aggregates. Data represent the mean \pm SEM of triplicates of three independent clones.



Annex II.6. Type of protein aggregates per cell in tRNAmod KO strains. Yeast cells containing localized Hsp104-GFP fluorescence foci were counted and differentiated according to the size of localized Hsp104-GFP fluorescence foci per cell. Results are expressed as the percentage of positive cells (with Hsp104-GFP foci) relative the total number of cells with protein aggregates. Data represent the mean \pm SEM of triplicates of three independent clones.

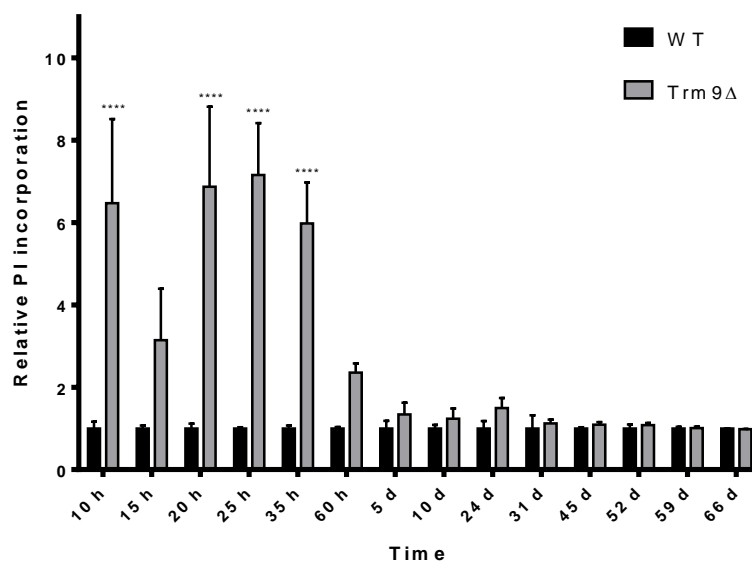


Annex II.7. Type of protein aggregates per cell in rRNAmoD KO strains. Yeast cells containing localized Hsp104-GFP fluorescence foci were counted and differentiated according to the size of localized Hsp104-GFP fluorescence foci per cell. Results are expressed as the percentage of positive cells (with Hsp104-GFP foci) relative the total number of cells with protein aggregates. Data represent the mean \pm SEM of triplicates of three independent clones.

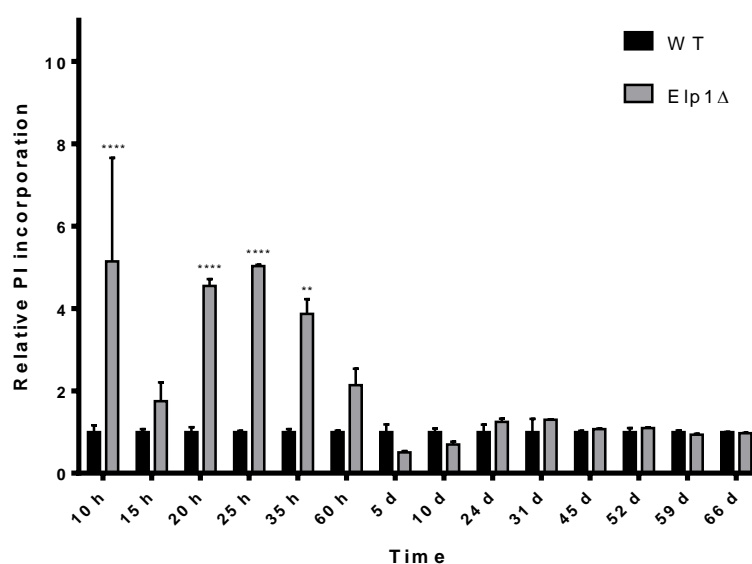
Annex III. Validation of gene deletion in the selected KO strains

Annex III.1. Validation of gene deletion in the selected KO strains by PCR. Agarose gels from PCR validation of gene deletion. **A.** Lane 1: negative control; Lane 2: BY4743; Lanes 3, 4 and 5: BY4743 clone 1, clone 2, and clone 3, respectively; Lane 6: *Trm9 Δ* (original from EUROSCARF); Lanes 7, 8 and 9: *Trm9 Δ* clone 1, clone 2, and clone 3, respectively. **B.** Lane 1: negative control; Lane 2: BY4743; Lanes 3, 4 and 5: BY4743 clone 1, clone 2, and clone 3, respectively; Lane 6: *Elp1 Δ* (original from EUROSCARF); Lanes 7, 8 and 9: *Elp1 Δ* clone 1, clone 2, and clone 3, respectively. **C.** Lane 1: negative control; Lane 2: BY4743; Lanes 3, 4 and 5: BY4743 clone 1, clone 2, and clone 3, respectively; Lane 6: *Kti12 Δ* (original from EUROSCARF); Lanes 7, 8 and 9: *Kti12 Δ* clone 1, clone 2, and clone 3, respectively. **D.** Lane 1: negative control; Lane 2: BY4743; Lanes 3, 4 and 5: BY4743 clone 1, clone 2, and clone 3, respectively; Lane 6: *Slm3 Δ* (original from EUROSCARF); Lanes 7, 8 and 9: *Slm3 Δ* clone 1, clone 2, and clone 3, respectively. **E.** Lane 1: negative control; Lane 2: BY4743; Lanes 3, 4 and 5: BY4743 clone 1, clone 2, and clone 3, respectively; Lane 6: *Spb1 Δ* (original from EUROSCARF); Lanes 7, 8 and 9: *Spb1 Δ* clone 1, clone 2, and clone 3, respectively. **F.** Lane 1: negative control; Lane 2: BY4743; Lanes 3, 4 and 5: BY4743 clone 1, clone 2, and clone 3, respectively; Lane 6: *Shq1 Δ* (original from EUROSCARF); Lanes 7, 8 and 9: *Shq1 Δ* clone 1, clone 2, and clone 3, respectively. M: GeneRuler™ 100 bp DNA Ladder.

Annex IV. Viability of selected RNAmods



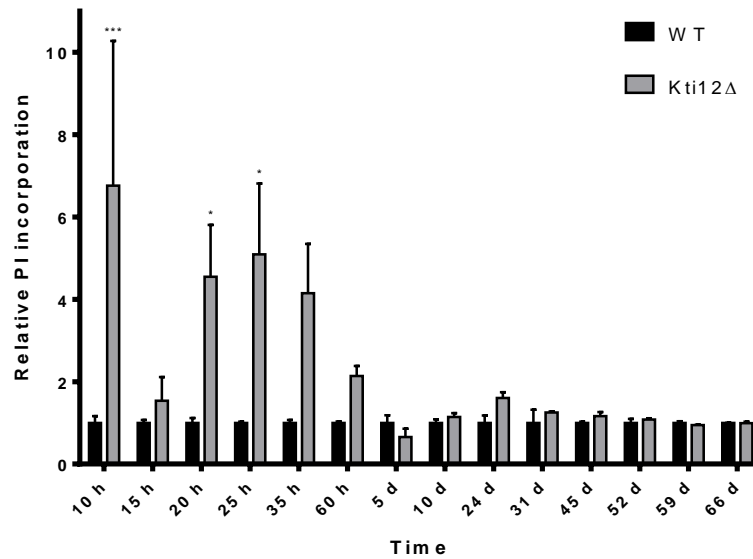
Annex IV.1. Viability of *S. cerevisiae* cells lacking Trm9 and WT cells, from 10 hours to 66 days. Cells were labeled with PI and analyzed by flow cytometry at different time points. Increased PI incorporation correlates with lower viability of cells. Data represent the mean \pm SEM of 3 independent clones (**** $p < 0.0001$, two-way Anova post Sidak's multiple comparison test with CI 95% relative to WT).



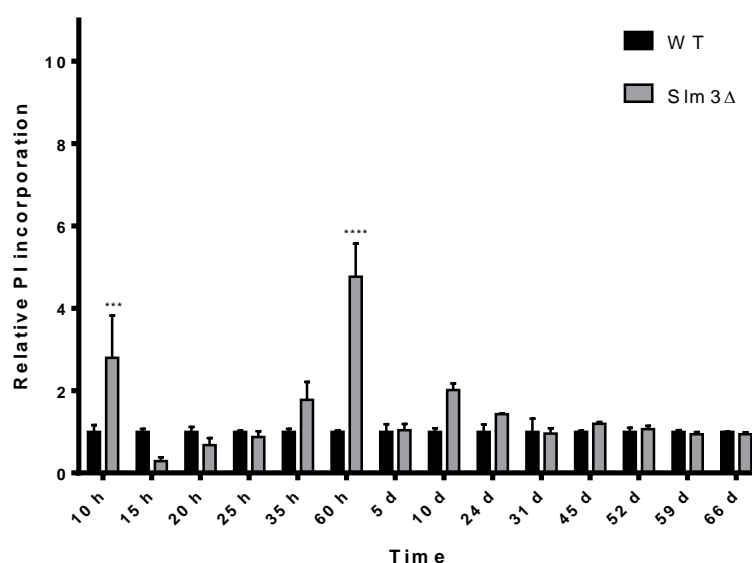
Annex IV.2. Viability of *S. cerevisiae* cells lacking Eip1 and WT cells, from 10 hours to 66 days. Cells were labeled with PI and analyzed by flow cytometry at different time

7. Annexes

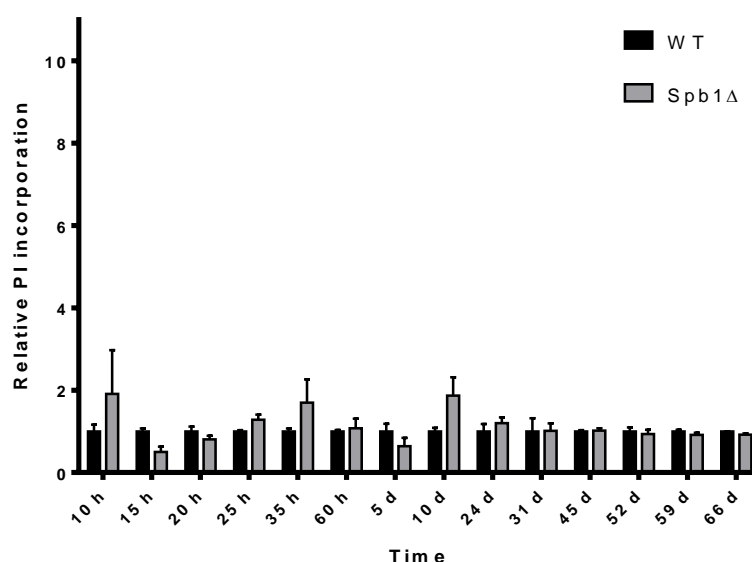
points. Increased PI incorporation correlates with lower viability of cells. Data represent the mean \pm SEM of 3 independent clones (**** $p < 0.0001$, ** $p < 0.01$, two-way Anova post Sidak's multiple comparison test with CI 95% relative to WT).



Annex IV.3. Viability of *S. cerevisiae* cells lacking Kti12 and WT cells, from 10 hours to 66 days. Cells were labeled with PI and analyzed by flow cytometry at different time points. Increased PI incorporation correlates with lower viability of cells. Data represent the mean \pm SEM of 3 independent clones (*** $p < 0.001$, * $p < 0.05$, two-way Anova post Sidak's multiple comparison test with CI 95% relative to WT).

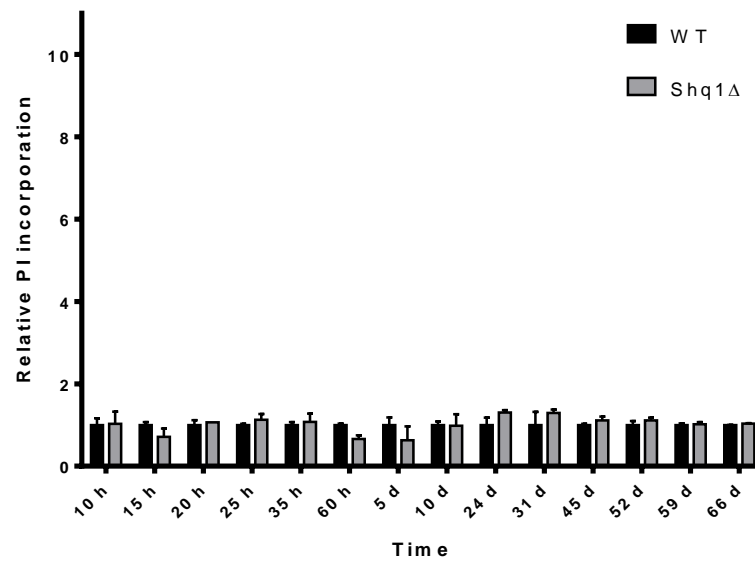


Annex IV.4. Viability of *S. cerevisiae* cells lacking SIm3 and WT cells, from 10 hours to 66 days. Cells were labeled with PI and analyzed by flow cytometry at different time points. Increased PI incorporation correlates with lower viability of cells. Data represent the mean \pm SEM of 3 independent clones (**** $p < 0.0001$, *** $p < 0.001$, two-way Anova post Sidak's multiple comparison test with CI 95% relative to WT).



Annex IV.5. Viability of *S. cerevisiae* cells lacking Spb1 and WT cells, from 10 hours to 66 days. Cells were labeled with PI and analyzed by flow cytometry at different time points. Increased PI incorporation correlates with lower viability of cells. Data represent the mean \pm SEM of 3 independent clones (two-way Anova post Sidak's multiple comparison test with CI 95% relative to WT).

7. Annexes



Annex IV.6. Viability of *S. cerevisiae* cells lacking Shq1 and WT cells, from 10 hours to 66 days. Cells were labeled with PI and analyzed by flow cytometry at different time points. Increased PI incorporation correlates with lower viability of cells. Data represent the mean \pm SEM of 3 independent clones (two-way Anova post Sidak's multiple comparison test with CI 95% relative to WT).

Annex V. Biochemical characterization of RNAs

Annex V.1. Normalized mass spectrometer signal intensities for tRNA modifications in *S. cerevisiae* KOs. Data represent mean \pm SD of triplicates of three independent clones, with Student's *t*-test relative to WT. Significant values (p -value < 0.05) are highlighted in gray.

Mod	WT		Trm9 Δ			Elp1 Δ			Kti12 Δ			Sim3 Δ			Spb1 Δ			Shq1 Δ		
	Average	SD	Average	SD	<i>t</i> -test	Average	SD	<i>t</i> -test	Average	SD	<i>t</i> -test	Average	SD	<i>t</i> -test	Average	SD	<i>t</i> -test	Average	SD	<i>t</i> -test
ac ⁴ C	23889	21660	15716	12388	0,601	9293	4225	0,316	15710	7599	0,571	25890	15704	0,903	30190	10805	0,675	36464	2949	0,375
Am	24697	4027	23117	1723	0,566	25132	754	0,863	24267	583	0,864	22942	986	0,504	25996	1099	0,619	25015	394	0,899
Cm	118435	35416	77032	10706	0,125	97356	10959	0,380	93889	5329	0,301	80375	13653	0,157	76851	9911	0,122	61724	2369	0,050
D	24899	3686	29211	3369	0,209	26724	3628	0,574	27257	1651	0,369	27958	3019	0,329	27355	1413	0,342	30104	1327	0,083
Gm	73843	25471	56720	8216	0,330	57606	5426	0,341	63759	6446	0,543	62808	9478	0,521	69606	3086	0,789	67145	2117	0,673
I	7212	3332	10184	4375	0,402	5924	1793	0,587	9076	1185	0,413	9762	4404	0,469	14091	2015	0,038	16875	2674	0,017
i ⁶ A	41678	2717	35695	7320	0,255	45217	2658	0,182	47623	3700	0,088	31650	1875	0,006	50738	2179	0,011	45831	2644	0,131
m ¹ A	432318	114816	302270	16877	0,124	321851	34899	0,186	373422	75281	0,499	355266	122769	0,472	428120	91018	0,963	521926	121269	0,405
m ¹ G	376179	203818	273230	24157	0,434	263472	19886	0,394	270447	5048	0,420	268086	9697	0,411	281691	21616	0,469	277591	12130	0,450
m ¹ I	72072	24532	55394	1845	0,305	56738	2815	0,343	56147	1967	0,325	55110	3046	0,300	59031	5793	0,421	55880	1374	0,317
m ² ₂ G	455779	176405	346880	27244	0,350	348048	32000	0,357	366641	22269	0,434	360658	25143	0,407	392989	21116	0,574	375334	8043	0,474
m ² G	287876	78923	232710	17620	0,303	244787	13003	0,404	243928	6967	0,391	207323	30328	0,174	234786	29265	0,336	200580	15882	0,134
m ³ C	120827	7655	120525	14569	0,976	113059	4849	0,212	134898	25541	0,412	108754	7963	0,131	113638	7144	0,300	88510	47469	0,309
m ⁵ C	212366	57489	174035	15486	0,327	165388	41038	0,313	193851	15976	0,619	188074	29468	0,550	205062	16405	0,843	189325	9301	0,531
m ⁵ U	23769	1457	28349	149	0,006	26884	1967	0,092	27097	1708	0,062	23278	1584	0,713	26131	561	0,059	25909	282	0,067
m ⁶ A	93290	38013	119137	65089	0,585	127265	17616	0,233	130103	52971	0,383	84680	42041	0,805	118995	104715	0,710	48520	17193	0,137
m ⁷ G	233709	56924	141249	47520	0,097	167160	30658	0,149	183423	58476	0,346	201483	74323	0,583	216591	83759	0,784	279226	23420	0,269
mcm ⁵ s ² U	1202	625	6	4	0,030	3	1	0,029	25	5	0,031	123	34	0,041	978	1236	0,794	804	956	0,579
mcm ⁵ U	3089	951	123	100	0,006	26	8	0,005	177	69	0,006	8169	1008	0,003	5080	1375	0,108	6220	1862	0,060
ncm ⁵ U	841	399	848	615	0,988	0	1	0,022	6	10	0,022	759	199	0,766	731	178	0,684	693	12	0,554
ncm ⁵ Um	456	448	309	336	0,673	0	0	0,153	5	6	0,156	450	210	0,983	659	249	0,532	547	68	0,747
t ⁶ A	18308	2323	23231	9486	0,432	17876	2606	0,841	21542	7130	0,497	21889	5205	0,338	23767	9006	0,367	19709	514	0,365
Um	316	219	408	228	0,640	335	77	0,892	606	209	0,172	451	233	0,504	565	27	0,123	569	22	0,118
ψ	9589	1570	11476	985	0,153	10336	1358	0,567	10620	656	0,353	10849	1265	0,340	10568	632	0,373	11692	572	0,095
yW	2829	1023	377	587	0,023	2891	236	0,924	1029	262	0,042	32	31	0,009	1277	1278	0,176	1278	1667	0,242

Annex V.2. Ratios of the levels of tRNA modifications in selected KO strains relative to WT. Underlined: mutant was determined to be significantly different from WT by Student's t-test with p -value < 0.05; Yellow: ratios < 0.02 (values of 0.001 indicate undetectable ribonucleosides in the mutant strains); Green: ratios < 0.6; Red: ratios > 1.5.

Mod	Trm9Δ	Elp1Δ	Kti12Δ	Slm3Δ	Spb1Δ	Shq1Δ
ac ⁴ C	0.658	0.389	0.658	1.084	1.264	1.526
Am	0.936	1.018	0.983	0.929	1.053	1.013
Cm	0.650	0.822	0.793	0.679	0.649	0.521
D	1.173	1.073	1.095	1.123	1.099	1.209
Gm	0.768	0.780	0.863	0.851	0.943	0.909
I	1.412	0.821	1.258	1.354	1.954	2.340
i ⁶ A	0.856	1.085	1.143	<u>0.759</u>	<u>1.217</u>	1.100
m ¹ A	0.699	0.744	0.864	0.822	0.990	1.207
m ¹ G	0.726	0.700	0.719	0.713	0.749	0.738
m ¹ I	0.769	0.787	0.779	0.765	0.819	0.775
m ² ₂ G	0.761	0.764	0.804	0.791	0.862	0.824
m ² G	0.808	0.850	0.847	0.720	0.816	0.697
m ³ C	0.998	0.936	1.116	0.900	0.941	0.733
m ⁵ C	0.820	0.779	0.913	0.886	0.966	0.892
m ⁵ U	<u>1.193</u>	1.131	1.140	0.979	1.099	1.090
m ⁶ A	1.277	1.364	1.395	0.908	1.276	0.520
m ⁷ G	0.604	0.715	0.785	0.862	0.927	1.195
mcm ⁵ s ² U	<u>0.005</u>	<u>0.002</u>	<u>0.021</u>	0.103	0.814	0.669
mcm ⁵ U	0.040	<u>0.008</u>	<u>0.057</u>	2.645	1.645	2.014
ncm ⁵ U	1.008	<u>0.001</u>	<u>0.007</u>	0.903	0.869	0.823
ncm ⁵ Um	0.678	<u>0.001</u>	<u>0.011</u>	0.986	1.443	1.198
t ⁶ A	1.269	0.976	1.177	1.196	1.298	1.077
Um	1.292	1.062	1.919	1.429	1.788	1.800
Ψ	1.197	1.078	1.107	1.131	1.102	1.219
yW	0.133	1.022	0.364	<u>0.011</u>	0.451	0.452

Annex V.3. Normalized mass spectrometer signal intensities for 25S and 18S rRNA modifications in *S. cerevisiae* KOs. Data represent mean \pm SD of triplicates of three independent clones, with Student's *t*-test relative to WT.

Mod	WT		Spb1 Δ			Shq1 Δ		
	Average	SD	Average	SD	<i>t</i> -test	Average	SD	<i>t</i> -test
ac ⁴ C	4002254	6914302	2	3	0.373	1142	1017	0.373
Am	14127112	24284714	108029	7860	0.374	127851	16311	0.375
Cm	3220799	5465476	38031	3951	0.370	59138	25689	0.373
Gm	6429842	10974156	88429	7593	0.374	111091	17919	0.375
I	3545379	6140397	488	180	0.374	303	297	0.374
m ¹ A	6465752	11198995	0	0	0.374	0	0	0.374
m ¹ acp ³ Ψ	4099567	7099670	195	17	0.374	210	33	0.374
m ¹ G	3378944	5811814	40035	16883	0.376	43127	12397	0.376
m ² ₂ G	4693105	8062596	58333	19784	0.376	60829	12982	0.376
m ² G	2893988	4994033	21303	8619	0.375	21023	8699	0.375
m ⁴ C	3383	1139	6077	2140	0.127	3487	3212	0.961
m ⁵ C	2887790	4949841	34897	9962	0.375	38913	2773	0.375
m ⁶ ₂ A	398375	689905	24	2	0.374	28	3	0.374
m ⁶ A	106470	178417	21825	4330	0.458	25004	4311	0.473
m ⁷ G	14531231	25095740	4513	824	0.373	6298	5955	0.373
Um	98149	167559	1422	138	0.374	1380	45	0.374
Ψ	1760	783	1466	74	0.552	1500	160	0.603

7. Annexes

Annex V.4. Ratios of the levels of 25S and 18S rRNA modifications in selected KO strains relative to WT. Underlined: mutant was determined to be significantly different from WT by Student's t-test with p -value < 0.05; Yellow: ratios < 0.02 (values of 0.000000 indicate undetectable ribonucleosides in the mutant strains); Green: ratios < 0.6; Red: ratios > 1.5.

Mod	Spb1Δ	Shq1Δ
ac ⁴ C	0.000000	0.000285
Am	0.007647	0.009050
Cm	0.011808	0.018361
Gm	0.013753	0.017277
I	0.000138	0.000086
m ¹ A	0.000000	0.000000
m ¹ acp ³ Ψ	0.000048	0.000051
m ¹ G	0.011848	0.012763
m ² ₂ G	0.012429	0.012961
m ² G	0.007361	0.007264
m ⁴ C	1.796319	1.030544
m ⁵ C	0.012084	0.013475
m ⁶ ₂ A	0.000061	0.000071
m ⁶ A	0.204990	0.234845
m ⁷ G	0.000311	0.000433
Um	0.014487	0.014058
Ψ	0.832743	0.852208

Annex V.5. Normalized mass spectrometer signal intensities for 5.8S rRNA modifications in *S. cerevisiae* KOs. Data represent mean \pm SD of triplicates of three independent clones, with Student's *t*-test relative to WT.

Mod	WT		Spb1 Δ			Shq1 Δ		
	Average	SD	Average	SD	<i>t</i> -test	Average	SD	<i>t</i> -test
ac ⁴ C	11209	12337	2597	2171	0.300	20859	25705	0.589
Am	33294	13059	18631	5008	0.144	15802	6132	0.104
Cm	9720	3722	4550	1299	0.086	3525	2710	0.080
Gm	28211	11027	18008	6534	0.240	11912	8079	0.108
I	305	86	246	16	0.305	233	121	0.446
m ¹ A	8757	15146	8	10	0.374	28878	39596	0.457
m ¹ acp ³ Ψ	585	619	206	46	0.350	362	204	0.584
m ¹ G	29472	23068	29747	18033	0.988	16647	10404	0.430
m ² ₂ G	112824	29365	116227	23868	0.884	105828	53642	0.853
m ² G	16528	11739	15103	7189	0.866	11491	4963	0.531
m ⁴ C	33979	31943	49755	10870	0.463	16810	29115	0.529
m ⁵ C	42900	13976	37928	11517	0.659	36363	21590	0.683
m ⁶ A	15147	13911	24322	5896	0.352	10128	16936	0.712
m ⁷ G	12008	14922	1535	450	0.291	17483	21548	0.736
Um	708	271	581	131	0.507	402	233	0.212
Ψ	1571	281	1215	262	0.184	876	457	0.088

Annex V.6. Ratios of the levels of 5.8S rRNA modifications in selected KO strains relative to WT. Underlined: mutant was determined to be significantly different from WT by Student's *t*-test with *p*-value < 0.05; Yellow: ratios < 0.02 (values of 0.000000 indicate undetectable ribonucleosides in the mutant strains); Green: ratios < 0.6; Red: ratios > 1.5.

Mod	Spb1 Δ	Shq1 Δ
ac ⁴ C	0.231662	1.860968
Am	0.559600	0.474632
Cm	0.468091	0.362659
Gm	0.638318	0.422224
I	0.805620	0.762870
m ¹ A	0.000863	3.297670
m ¹ acp ³ Ψ	0.352337	0.618312
m ¹ G	1.009334	0.564859
m ² ₂ G	1.030163	0.937993
m ² G	0.913735	0.695219
m ⁴ C	1.464294	0.494707
m ⁵ C	0.884101	0.847624
m ⁶ A	1.605668	0.668626
m ⁷ G	0.127818	1.455982
Um	0.821097	0.567371
Ψ	0.773455	0.557386

7. Annexes

Annex V.7. Normalized mass spectrometer signal intensities for 5S rRNA modifications in *S. cerevisiae* KOs. Data represent mean \pm SD of triplicates of three independent clones, with Student's t-test relative to WT.

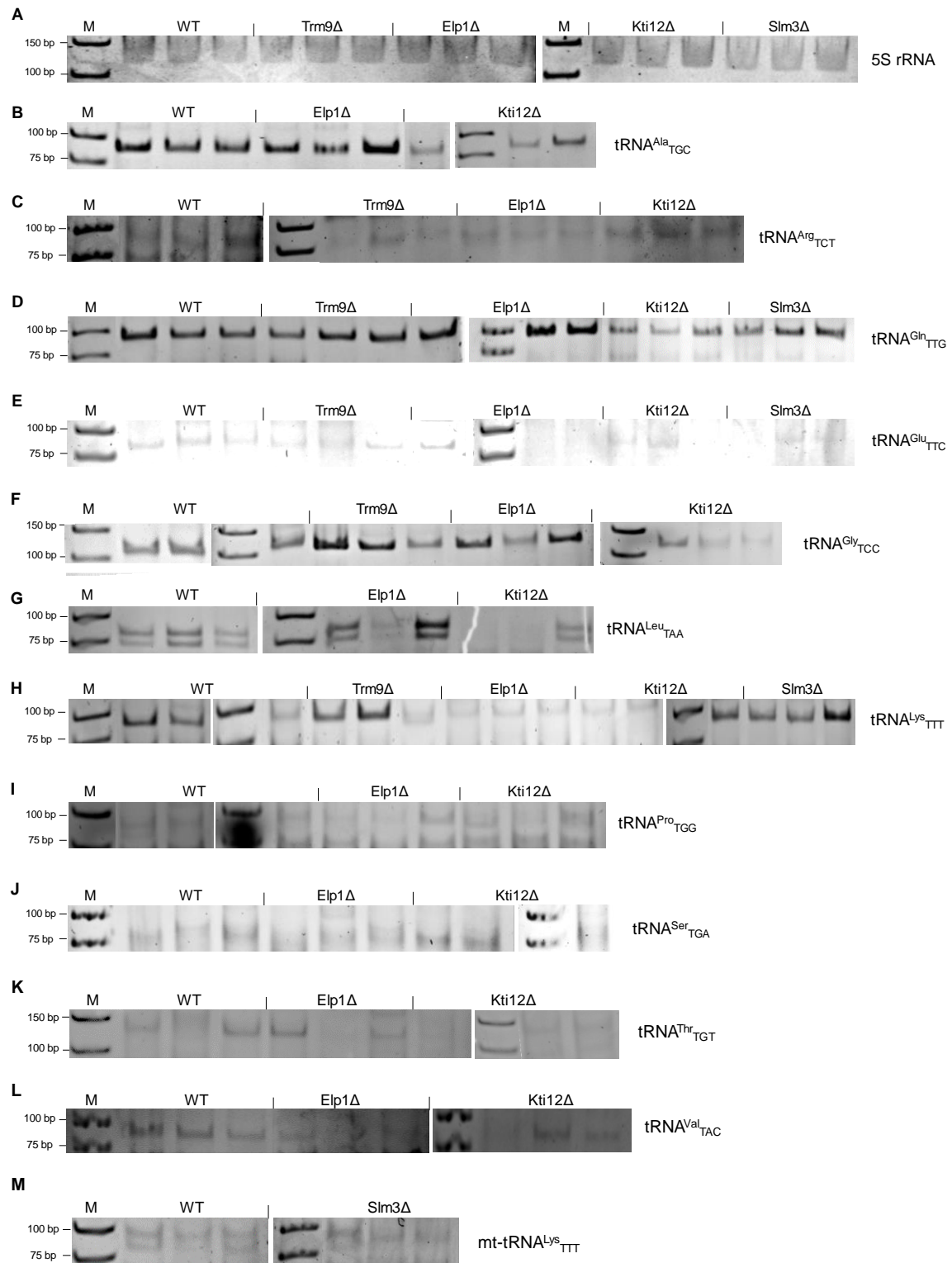
Mod	WT		Spb1 Δ			Shq1 Δ		
	Average	SD	Average	SD	t-test	Average	SD	t-test
ac ⁴ C	12211	8907	11226	10114	0.905	14965	10553	0.747
Am	17798	8910	8880	2401	0.169	6322	902	0.091
Cm	7169	3474	3074	1198	0.126	2100	1999	0.094
Gm	20785	7395	15413	4327	0.339	8392	6917	0.101
hm ⁵ C	4	6	3	5	0.888	0	0	0.369
I	797	184	466	181	0.091	507	275	0.204
m ¹ A	18632	17281	5	5	0.135	16275	15306	0.868
m ¹ acp ³ Ψ	716	457	355	181	0.273	604	789	0.843
m ¹ G	53030	12065	43935	13933	0.441	28996	22210	0.175
m ¹ Y	965	741	968	425	0.994	375	369	0.285
m ² ₂ G	91986	13024	84468	19068	0.603	55911	37241	0.188
m ² G	27560	6292	24739	8730	0.673	17552	10239	0.223
m ³ U	35	32	16	23	0.451	1	1	0.138
m ⁴ C	6733	11662	7765	12970	0.923	0	0	0.374
m ⁵ C	37655	11529	35609	8600	0.818	28158	20746	0.526
m ⁶ ₂ A	68	41	34	13	0.237	63	70	0.921
m ⁶ A	5763	9910	5947	9492	0.983	100	94	0.378
m ⁷ G	24662	15860	25976	21150	0.936	27200	18405	0.865
Ψ	1364	722	1609	205	0.601	904	590	0.441

Annex V.8. Ratios of the levels of 5S rRNA modifications in selected KO strains relative to WT. Underlined: mutant was determined to be significantly different from WT by Student's *t*-test with *p*-value < 0.05; Yellow: ratios < 0.02 (values of 0.000000 indicate undetectable ribonucleosides in the mutant strains); Green: ratios < 0.6; Red: ratios > 1.5.

Mod	Spb1Δ	Shq1Δ
ac ⁴ C	0.919362	1.225600
Am	0.498922	0.355221
Cm	0.428813	0.292932
Gm	0.741525	0.403769
hm ⁵ C	0.824662	0.080893
I	0.584347	0.635779
m ¹ A	0.000293	0.873520
m ¹ acp ³ Ψ	0.496376	0.844193
m ¹ G	0.828489	0.546780
m ¹ Y	1.003901	0.388835
m ² ₂ G	0.918267	0.607821
m ² G	0.897656	0.636876
m ³ U	0.455216	0.027708
m ⁴ C	1.153220	0.000045
m ⁵ C	0.945665	0.747772
m ⁶ ₂ A	0.496387	0.927791
m ⁶ A	1.031778	0.017424
m ⁷ G	1.053272	1.102905
Ψ	1.180084	0.662685

7. Annexes

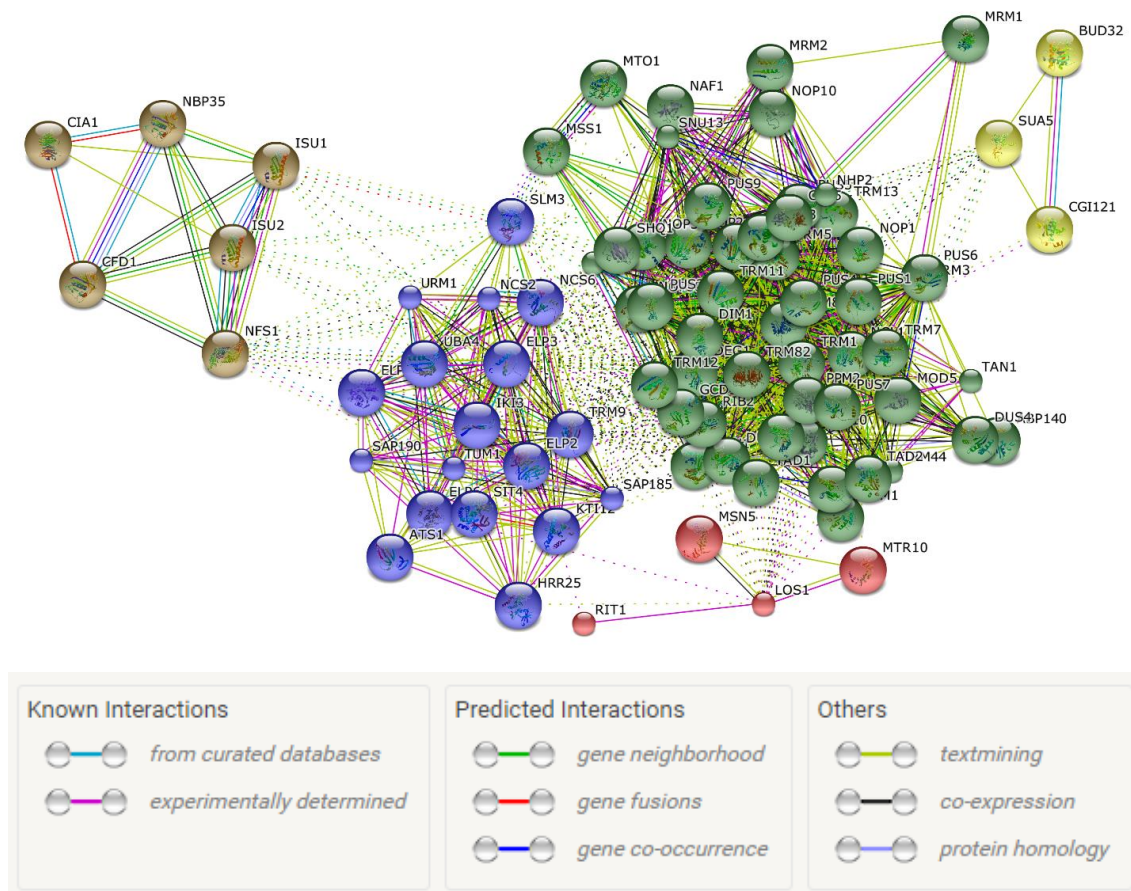
Annex VI. Wobble uridine modified tRNAs quantification



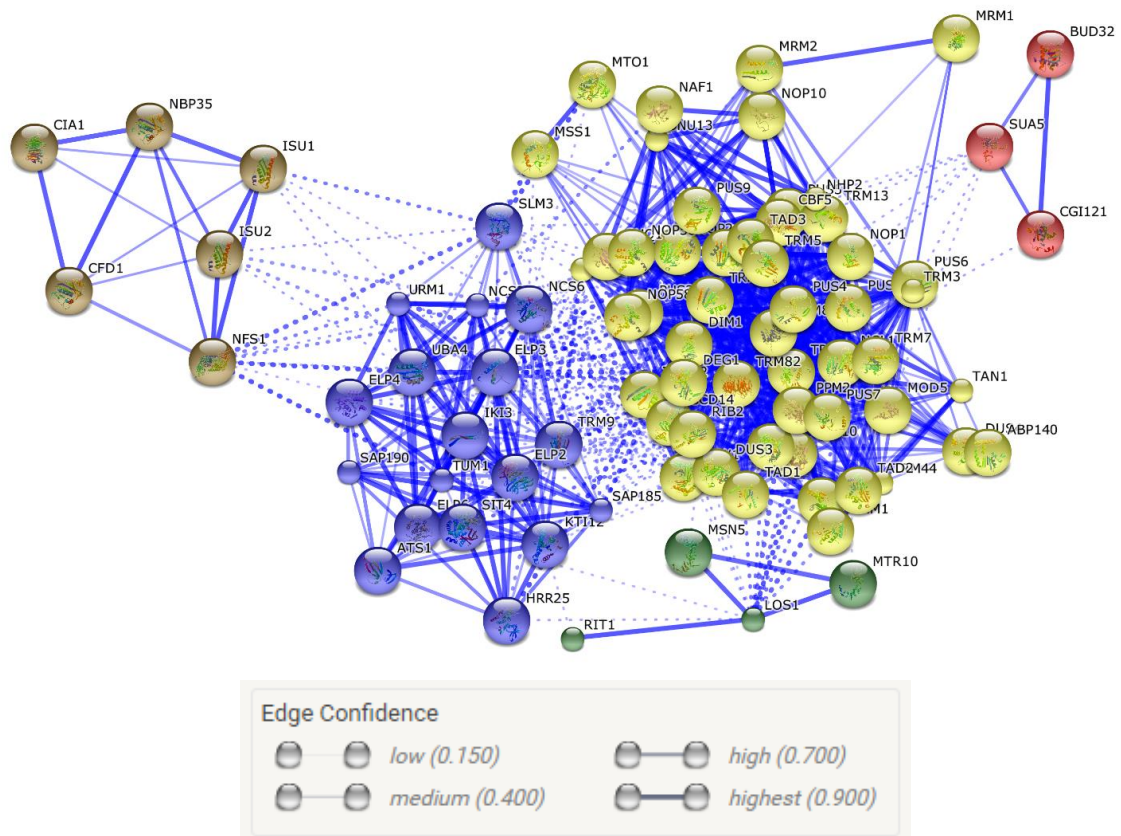
Annex VI.1. Native PAGE of cDNA amplified by FL-PCR. Wobble uridine modified tRNAs were quantified by FL-PCR and generated specific bands of amplified cDNAs developed by

native PAGE. Each lane represents an independent clone of the strain mentioned above each lane and contains cDNA from three technical replicates (NOTE: Due to the low amount of some tRNAs in specific KO strains, bands could be very light – but detected in an Applied Biosystems 7500 Real-Time PCR System with confidence). **A.** Amplified cDNA for 5S rRNA in WT, Trm9 Δ , Elp1 Δ , Kti12 Δ and Slm3 Δ strains (expected band size: 113 bp). **B.** Amplified cDNA for tRNA^{Ala}_{TGC} in WT, Elp1 Δ and Kti12 Δ strains (expected band size: 86 bp). **C.** Amplified cDNA for tRNA^{Arg}_{TCT} in WT, Trm9 Δ , Elp1 Δ and Kti12 Δ strains (expected band size: 90 bp). **D.** Amplified cDNA for tRNA^{Gln}_{TTG} in WT, Trm9 Δ , Elp1 Δ , Kti12 Δ and Slm3 Δ strains (expected band size: 93 bp). **E.** Amplified cDNA for tRNA^{Glu}_{TTC} in WT, Trm9 Δ , Elp1 Δ , Kti12 Δ and Slm3 Δ strains (expected band size: 83 bp). **F.** Amplified cDNA for tRNA^{Gly}_{TCC} in WT, Trm9 Δ , Elp1 Δ and Kti12 Δ strains (expected band size: 81 bp). **G.** Amplified cDNA for tRNA^{Leu}_{TAA} in WT, Elp1 Δ and Kti12 Δ strains (expected band size: 81 bp). **H.** Amplified cDNA for tRNA^{Lys}_{TTT} in WT, Trm9 Δ , Elp1 Δ , Kti12 Δ and Slm3 Δ strains (expected band size: 94 bp). **I.** Amplified cDNA for tRNA^{Pro}_{TGG} in WT, Elp1 Δ and Kti12 Δ strains (expected band size: 92 bp). **J.** Amplified cDNA for tRNA^{Ser}_{TGA} in WT, Elp1 Δ and Kti12 Δ strains (expected band size: 79 bp). **K.** Amplified cDNA for tRNA^{Thr}_{TGT} in WT, Elp1 Δ and Kti12 Δ strains (expected band size: 89 bp). **L.** Amplified cDNA for tRNA^{Val}_{TAC} in WT, Elp1 Δ and Kti12 Δ strains (expected band size: 84 bp). **M.** Amplified cDNA for mt-tRNA^{Lys}_{TTT} in WT and Slm3 Δ strains (expected band size: 86 bp). M: GeneRuler™ Ultra Low Range DNA Ladder.

Annex VII. Network analysis of the 83 studied RNAmods



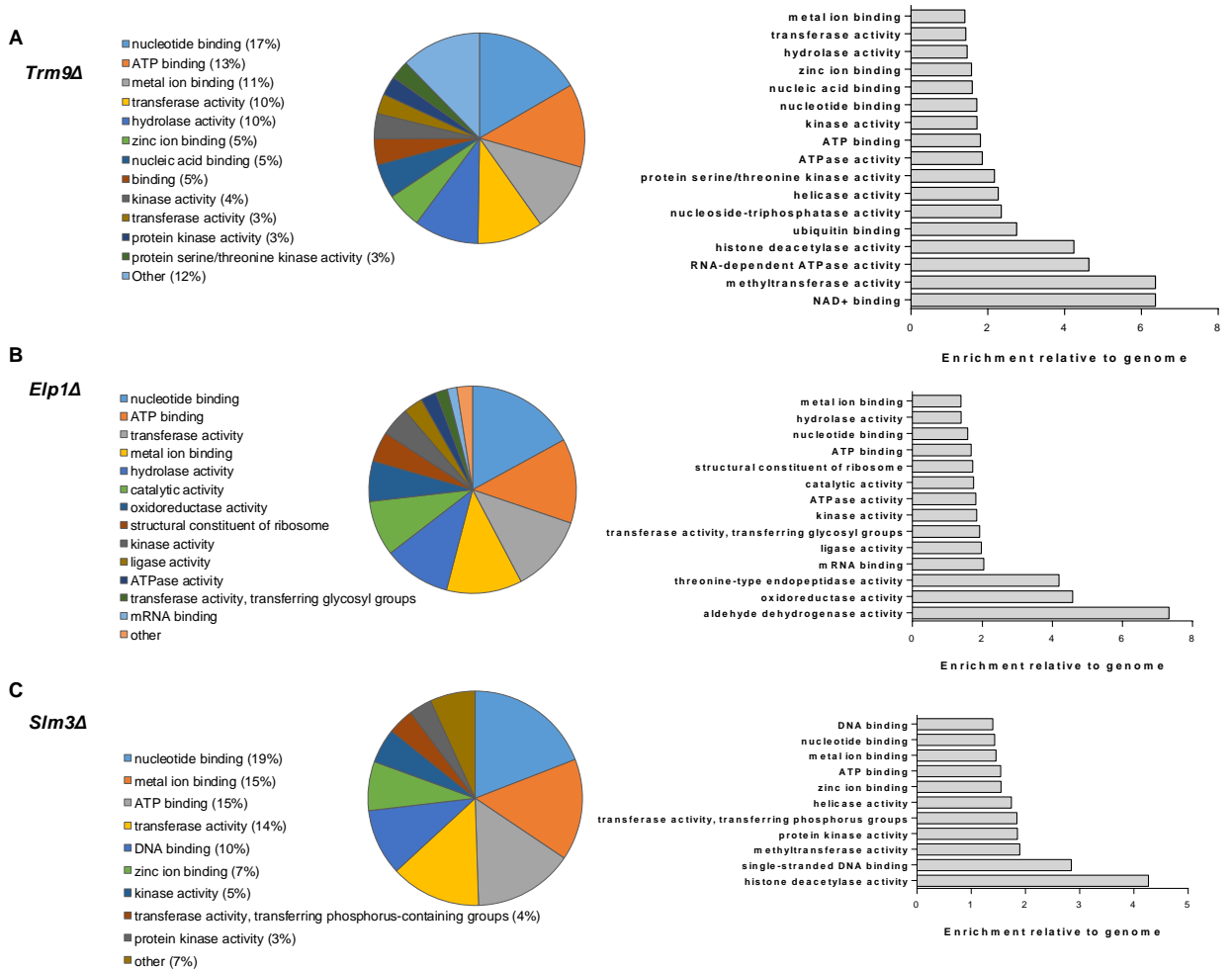
Annex VII.1. Network analysis of RNAmods. Interactome was predicted using STRING database (version 10.0). Clustering was performed using MCL algorithm with inflation parameter = 2. Colored lines between the proteins indicate the various types of interaction evidence. Small nodes represent proteins of unknown 3D structure; Large nodes represent some known or predicted 3D structure. Dashed lines represent inter-cluster edges.



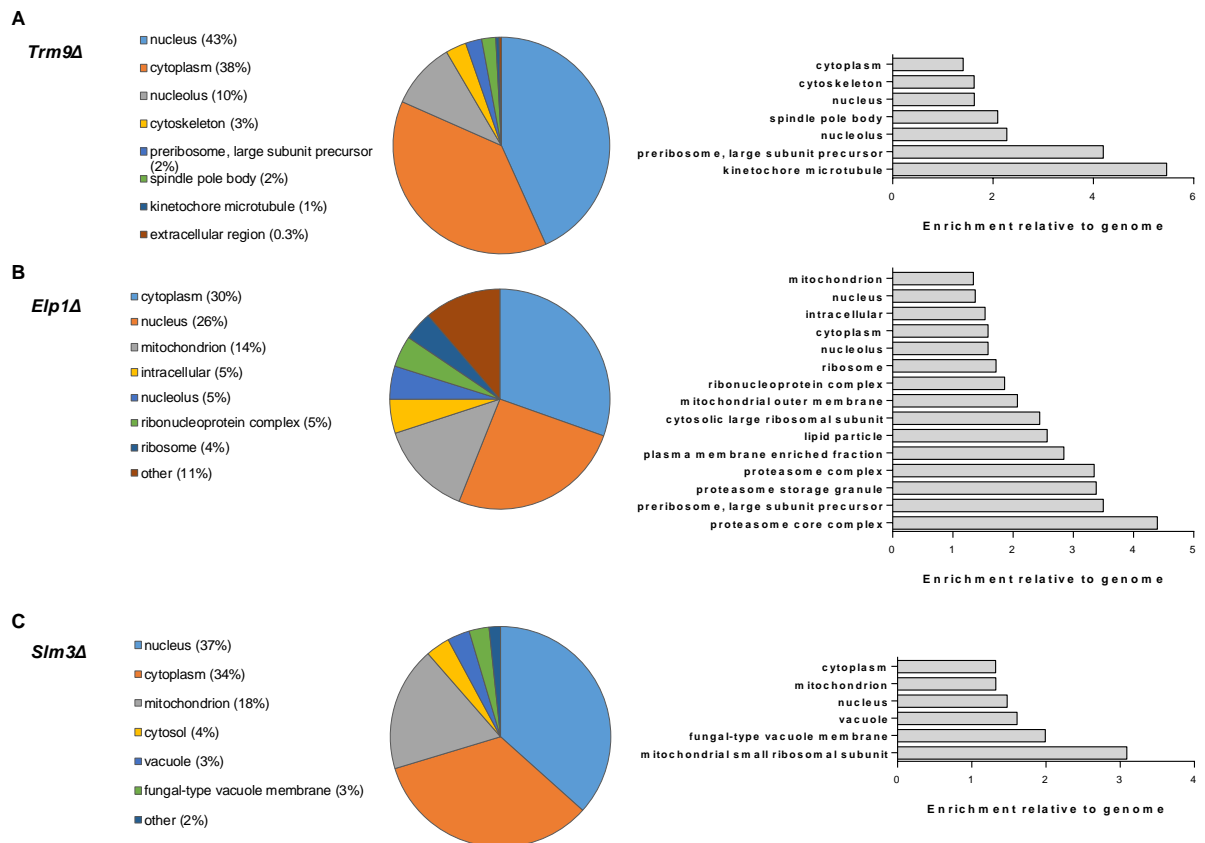
Annex VII.2. Network analysis of RNAmods. Interactome was predicted using STRING database (version 10.0). Clustering was performed using MCL algorithm with inflation parameter = 2. Blue lines between the proteins indicate the various types of interaction confidence. Small nodes represent proteins of unknown 3D structure; Large nodes represent some known or predicted 3D structure. Dashed lines represent inter-cluster edges.

7. Annexes

Annex VIII. Functional enrichment of up-regulated proteins that aggregated in the absence of U₃₄ modification



Annex VIII.1. Functional enrichment in up-regulated proteins that aggregated in mutant strains lacking U₃₄ modification. Molecular functions that are significantly enriched in the insoluble fraction of *Trm9Δ* (A), *Elp1Δ* (B) and *Slm3Δ* (C) cells compared to the *S. cerevisiae* genome. Circle diagrams indicate the distribution of aggregated proteins into functional categories. Bar diagrams indicate the fold-enrichment of functional categories compared to the genome using GO data from <http://genecodis.cnb.csic.es>. All shown categories were significant with 5% FDR.

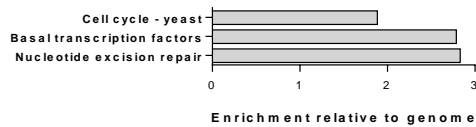


Annex VIII.2. Functional enrichment in up-regulated proteins that aggregated in mutant strains lacking U_{34} modification. Cellular components that are significantly enriched in the insoluble fraction of *Trm9Δ* (A), *Elp1Δ* (B) and *Slm3Δ* (C) cells compared to the *S. cerevisiae* genome. Circle diagrams indicate the distribution of aggregated proteins into functional categories. Bar diagrams indicate the fold-enrichment of functional categories compared to the genome using GO data from <http://genecodis.cnb.csic.es>. All shown categories were significant with 5% FDR.

7. Annexes

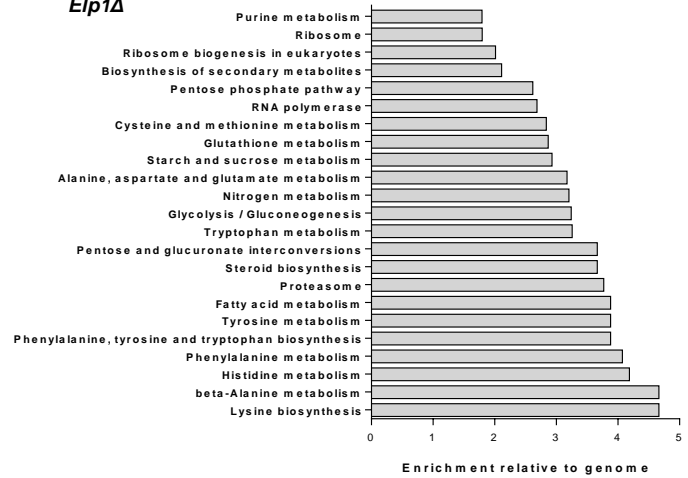
A

Trm9Δ

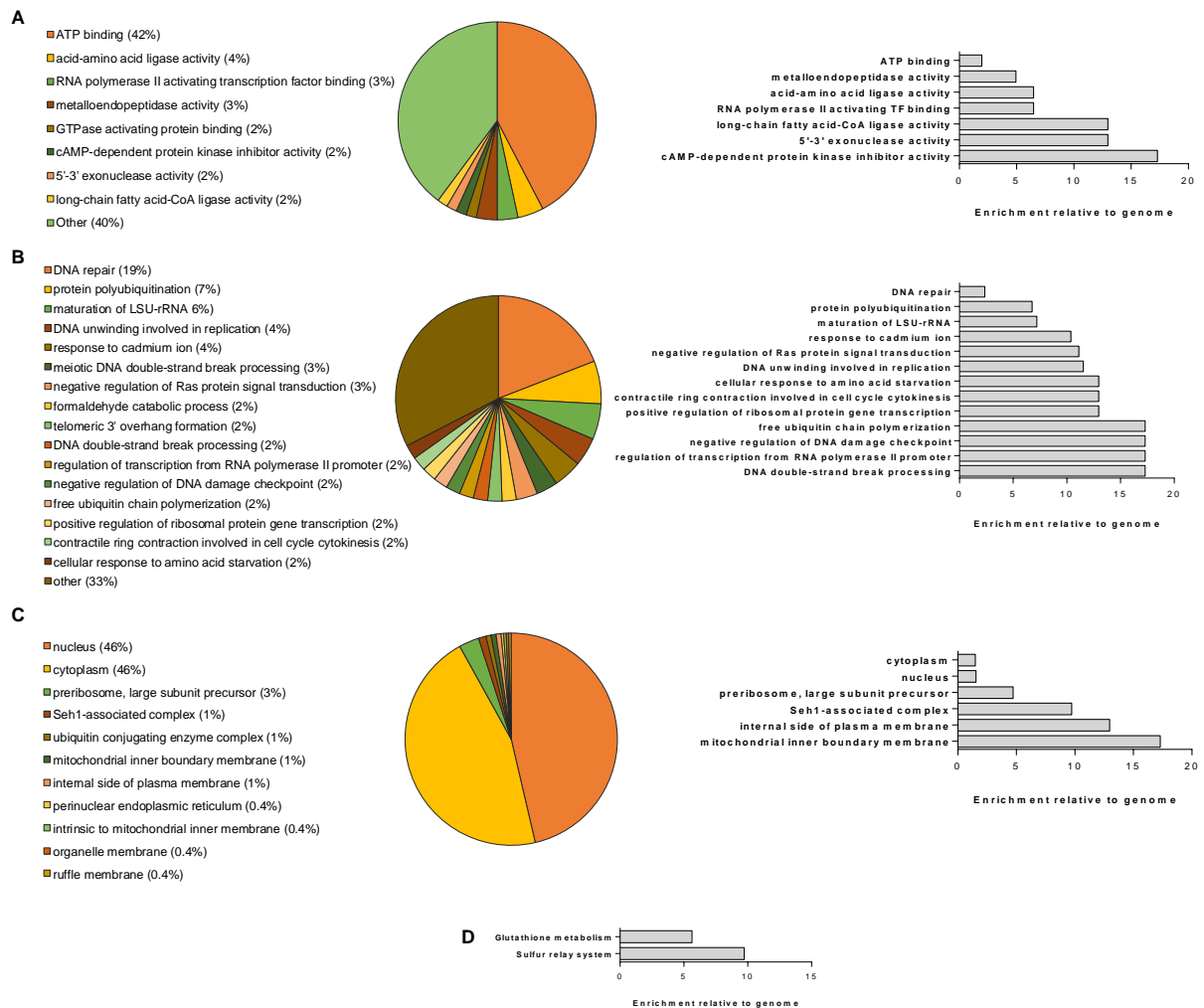


B

Elp1Δ



Annex VIII.3. Functional enrichment in up-regulated proteins that aggregated in mutant strains lacking U_{34} modification. KEGG pathways that are significantly enriched in the insoluble fraction of *Trm9Δ* (**A**) and *Elp1Δ* (**B**) cells compared to the *S. cerevisiae* genome. Diagrams indicate the fold-enrichment of KEGG pathways compared to the genome using GO data from <http://genecodis.cnb.csic.es>. All shown categories were significant with 5% FDR.



Annex VIII.4. Functional enrichment in common up-regulated proteins that aggregated in Trm9 Δ , Elp1 Δ and Slm3 Δ mutant strains lacking U₃₄ modification. Molecular functions (A), biological processes (B), cellular components (C) and KEGG pathways (D) that are significantly enriched in common proteins that aggregated in Trm9 Δ , Elp1 Δ and Slm3 Δ cells compared to the *S. cerevisiae* genome. Circle diagrams indicate the distribution of aggregated proteins into functional categories. Bar diagrams indicate the fold-enrichment of functional categories compared to the genome using GO data from <http://genecodis.cnb.csic.es>. All shown categories were significant with 1% FDR.

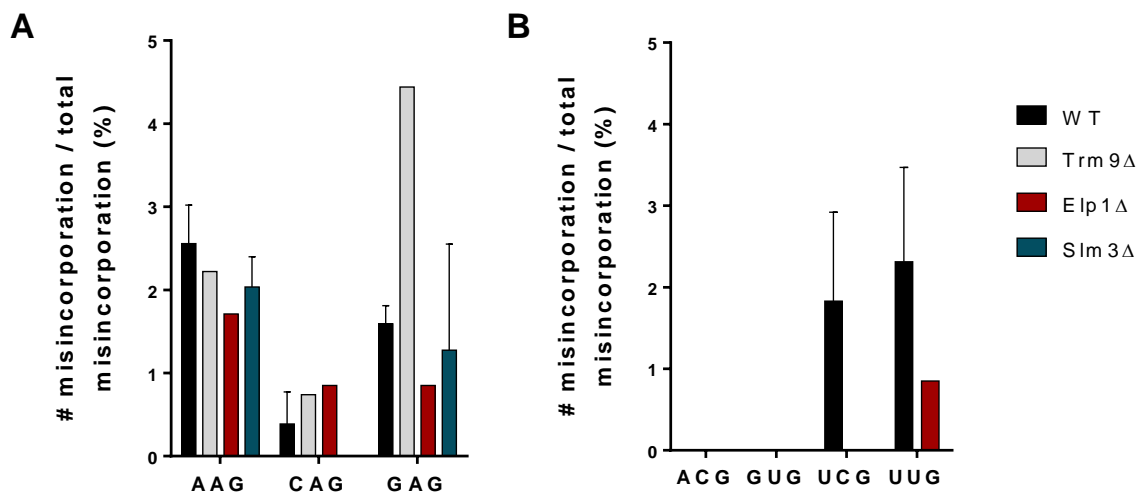
Annex IX. Amino acid misincorporations pattern in cells lacking U_{34} modification

Annex IX.1. Summary of the amino acid misincorporations found in up-regulated proteins that aggregated in mutant cells and WT. Highlighted in grey are amino acid misincorporations not expected to occur by the hypomodification observed in that strain.

Sample	# aa	S→R	D→E	N→K	H→Q	F→L	Other aa misincorporations	Total aa misincorporations
WTc1	530262	5	13	3	0	6	59	86
WTc2	413777	4	6	2	2	6	33	53
WTc3	435846	7	12	1	1	8	29	58
Trm9Δ c3	487269	12	14	7	3		99	135
Elp1Δ c1	448507	10	21	8	3	9	66	117
Slm3Δ c1	337702		14	3	5		38	60
Slm3Δ c2	979201		119	32	20		496	667

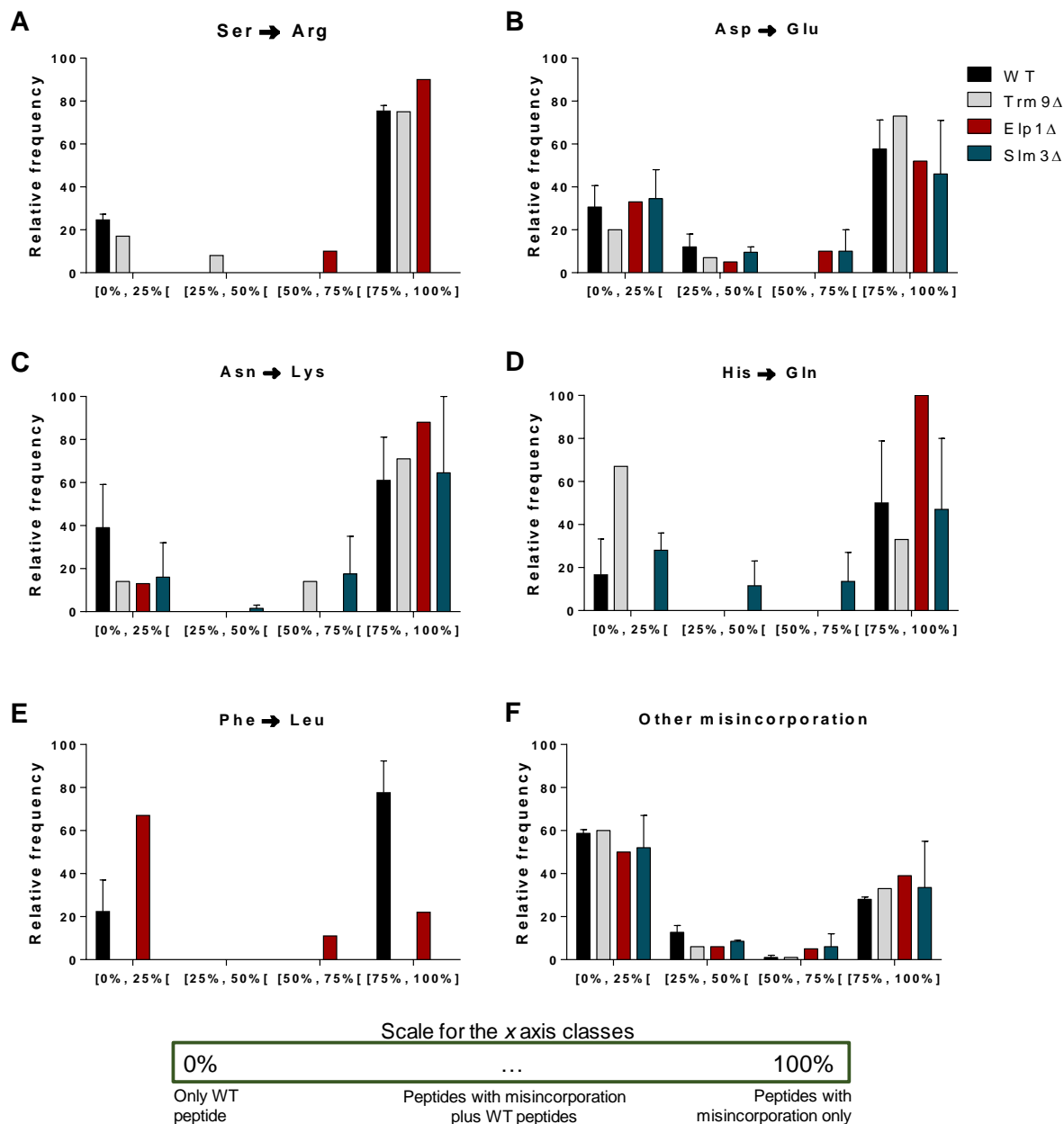
Annex IX.2. Percentage of amino acid misincorporations shared between samples.

Shared	WT	Trm9Δ	Elp1Δ	Slm3Δ
WT	100.0%	8.8%	15.5%	5.3%
Trm9Δ	7.0%	100.0%	7.2%	3.2%
Elp1Δ	10.5%	6.2%	100.0%	4.4%
Slm3Δ	21.0%	15.9%	25.8%	100.0%



Annex IX.3. Amino acid misincorporations occurred in specific codon sites. Relative frequency of amino acid misincorporations in the codons indicated in the x-axis, in the mutant strains and WT. **A.** Codons that pair with tRNAs modified with $mcm^5s^2U_{34}$. **B.** Codons that pair with tRNAs modified with ncm^5U_{34} . Distribution of amino acid

misincorporations among specific codons is relative to total number of amino acid misincorporations in each sample.



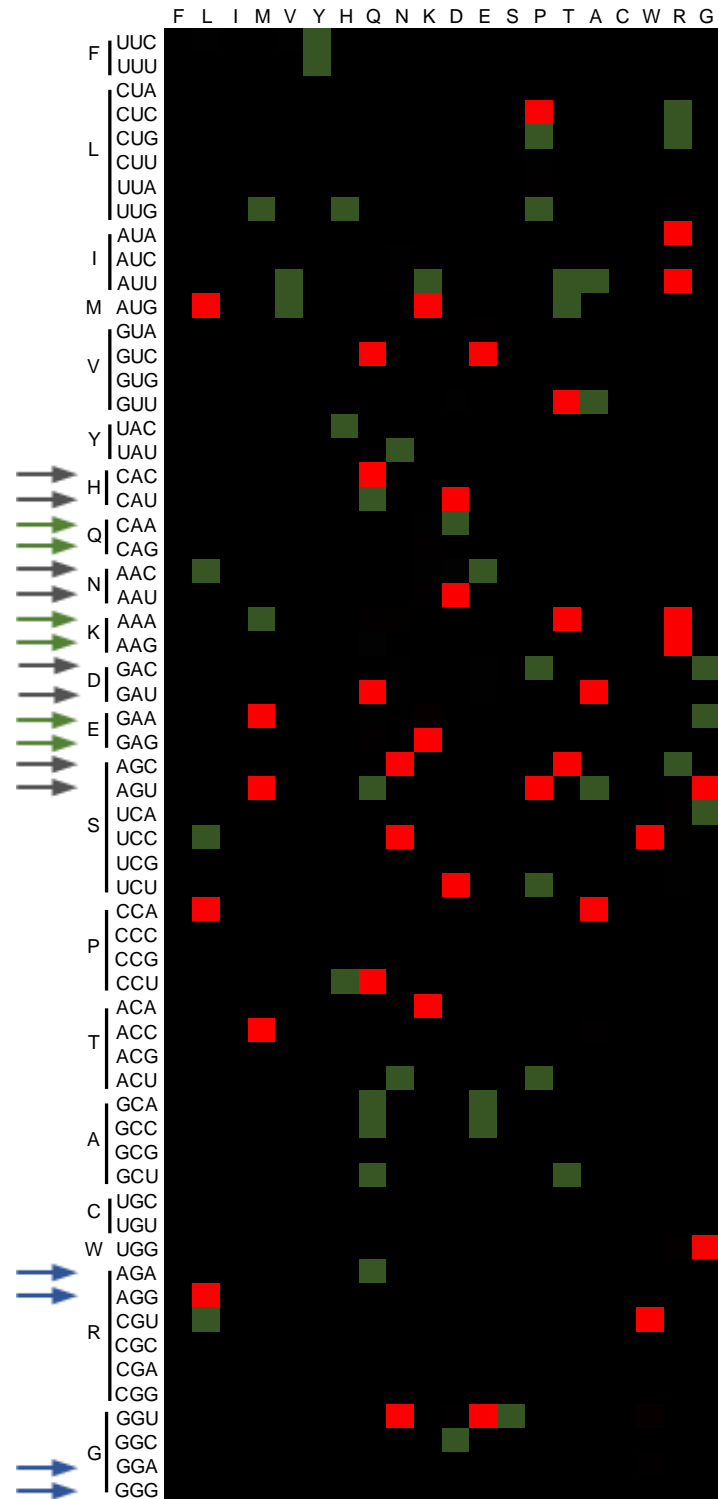
Annex IX.4. Plots show the relative abundance of peptides with amino acid misincorporations relative to the abundance of the WT peptide. Relative peptide abundances were calculated by dividing the area of each peptide with misincorporations at a specific codon site by the total area of all peptides for that specific codon site.

7. Annexes

↓ - Codons that pair with tRNAs with $mcm^S U_{34}$

↓ - Codons that pair with tRNAs with $mcm^E U_{34}$

↓ - Non-cognate codons that could pair with hypomodified tRNAs



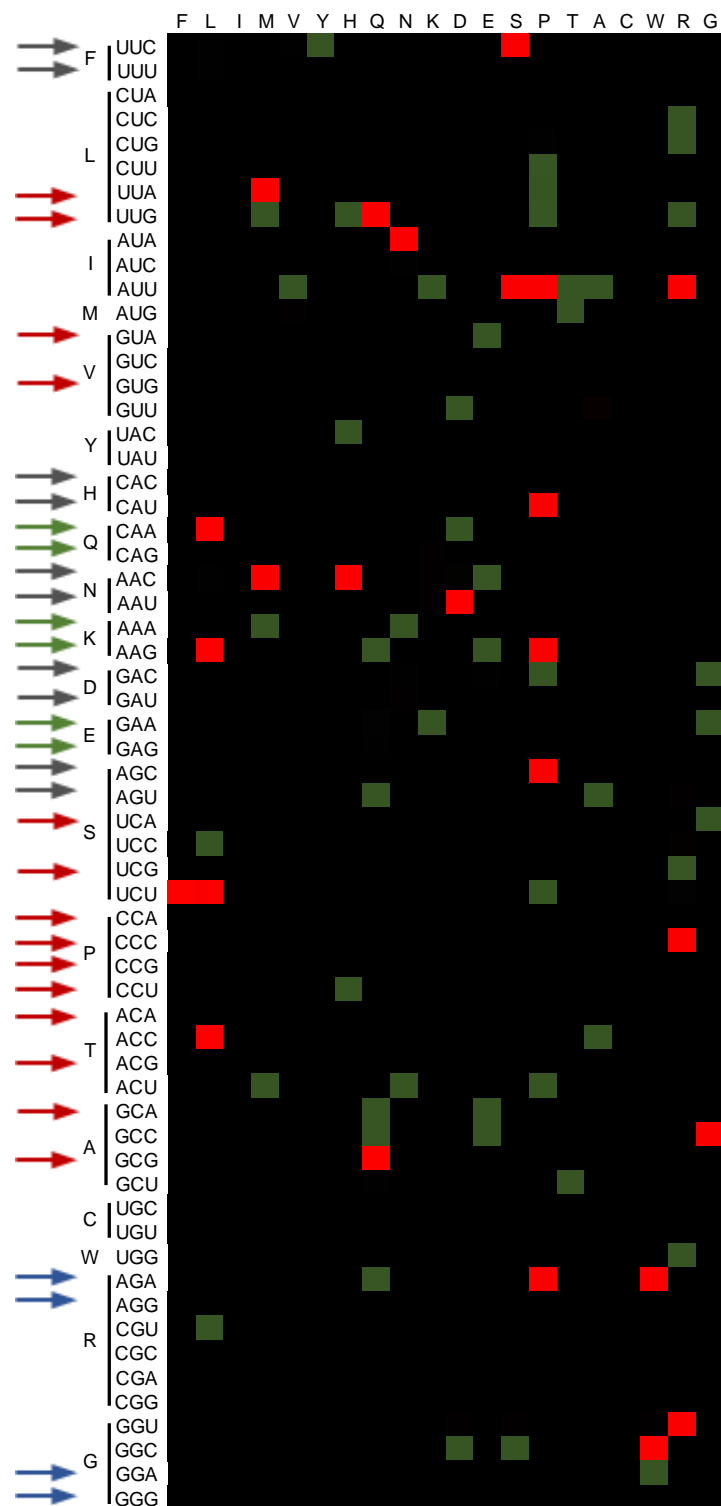
Annex IX.5. Amino acid misincorporations patterns observed in *Trm9Δ* relative to WT samples. The heat map shows the relative frequency of amino acid substitutions and the codons in which those substitutions occurred comparatively to WT. Over-represented codons are displayed in red and under-represented codons are displayed in green. Codons showing no difference from the genome average are displayed in black.

↓ - Codons that pair with tRNAs with $mcm^5S^2U_{34}$

↓ - Codons that pair with tRNAs with mcm^5U_{34}



↓ - Codons that pair with tRNAs with ncm^5U_{34}

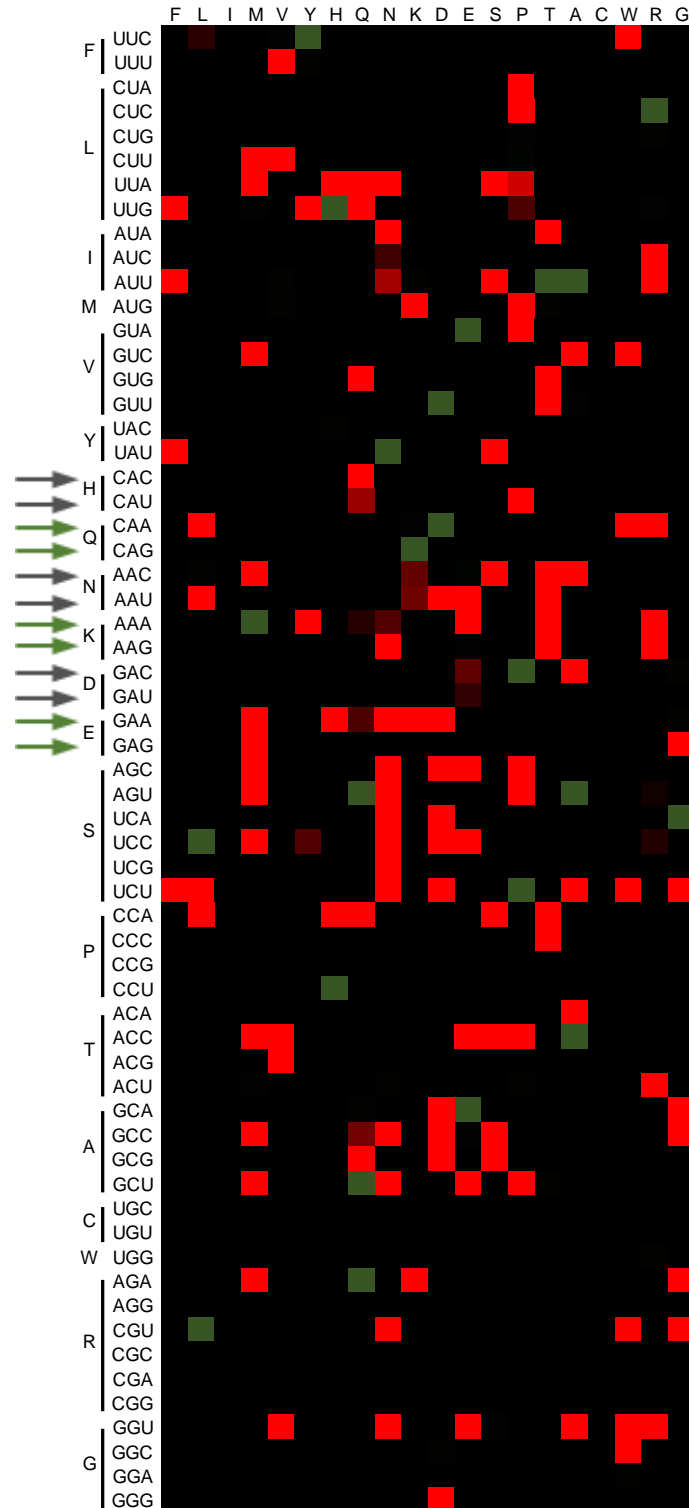
↓ - Non-cognate codons that could pair with hypomodified tRNAs



Annex IX.6. Amino acid misincorporations patterns observed in *Elp1Δ* relative to WT samples. The heat map shows the relative frequency of amino acid substitutions and the codons in which those substitutions occurred comparatively to WT. Over-represented codons are displayed in red and under-represented codons are displayed in green. Codons showing no difference from the genome average are displayed in black.

7. Annexes

 - Codons that pair with tRNAs with $mcm^5s^2U_{34}$
 - Non-cognate codons that could pair with hypomodified tRNAs



Annex IX.7. Amino acid misincorporations patterns observed in *Slm3Δ* relative to WT samples. The heat map shows the relative frequency of amino acid substitutions and the codons in which those substitutions occurred comparatively to WT. Over-represented codons are displayed in red and under-represented codons are displayed in green. Codons showing no difference from the genome average are displayed in black.

Annex X. Identification of human orthologues

Annex X.1. Identification of orthologues between human disease aggregates in Alzheimer's disease (Liao *et al.*, 2004; Wang *et al.*, 2005), Parkinson's disease (Xia *et al.*, 2009) and/or familial amyotrophic lateral sclerosis (Basso *et al.*, 2009) and yeast.

+ represents the presence of the human orthologue in the insoluble fraction of the mutant strain.

Disorder	Uniprot ID	Description	Yeast orthologue	Trm9Δ	Elp1Δ	Slm3Δ
β amyloid associated	Q93050	ATPase, H ⁺ -transporting, lysosomal V0 subunit A	VPH1, STV1			
	P21281	ATPase, H ⁺ -transporting, lysosomal V1 subunit B	VMA2	+	+	+
	P53675	Clathrin, heavy polypeptide 1	CHC1			
	Q14204	Dynein, heavy polypeptide 1	DYN1	+		+
	P08238	Heat shock 90-kDa protein 1, β	HSC82, HSP82		+	
	Q01813	Phosphofructokinase	PFK1, PFK2			+
	P22314	Ubiquitin-activating enzyme E1	UBA1			
	Q05193	Dynamin 1				
	P62258	14-3-3 ε	BMH2, BMH1			
	P63104	14-3-3 ζ				
	P31946	14-3-3 β/α				
	P31146	Coronin, actin-binding protein				
	Q01814	ATPase, Ca ²⁺ -transporting	PMC1	+		
	P07339	Cathepsin D	PEP4			
	Q9Y5K8	ATPase, H ⁺ -transporting, lysosomal V1 subunit D	VMA8			
	P36543	ATPase, H ⁺ -transporting, lysosomal V1 subunit E	VMA4			
	Q9UI12	Vacuolar ATPase subunit H				
	P08670	Vimentin				
	P14136	Glial fibrillary acidic protein (GFAP)				
	P02679	Fibrinogen γ				
	P10636	tau				
	P05067	Amyloid β-peptide				
	P01009	Antitrypsin				
	P02452	Collagen I, α-1 polypeptide				
P04080	Cystatin B					
P01034	Cystatin C					
tau associated	P60709	Actin, cytoplasmic 1	ACT1			
	P06733	α enolase	ENO1, ENO2, ERR3, ERR2		++	++
	P25705	ATP synthase α chain	ATP1			
	P06576	ATP synthase β chain	ATP2	+		
	Q13885	β tubulin	TUB2	+		+
	Q3ZCM7	β-tubulin 4Q	TUB2	+		+

7. Annexes

Q00610	Clathrin heavy chain 1	CHC1			
Q61Q15	Elongation factor 1- α 1				
P06744	Glucose 6-phosphate isomerase	PGI1		+	+
P11142	Heat shock cognate 71 kDa protein	SSA3, SSA2, SSA4			+
Q13509	Tubulin β -4 chain				
P38606	Vacuolar ATP synthase catalytic subunit A				
P04350	Hypothetical protein	TUB2	+		+
P00558	Phosphoglycerate kinase 1	PGK1			
P68366	Tubulin α -4 chain	TUB3, TUB1	++	++	+
P14618	Pyruvate kinase 3 isoform 2	CDC19, PYK2			
P04406	Glyceraldehyde-3-phosphate dehydrogenase	TDH3, TDH1, TDH2		+	
Q05193	Dynammin-1				
P28482	Mitogen-activated protein kinase 1	FUS3, KSS1	+		
P40926	Malate dehydrogenase	MDH1			
P12236	ADP, ATP carrier protein, liver isoform T2	PET9, AAC1, AAC3			
Q06830	Peroxisredoxin1	TSA2			
Q3MIH3	Ubiquitin A-52 residue ribosomal protein fusion product 1	RPL40A			
Q9HAV0	Guanine nucleotide-binding protein β subunit 4	STE4			
B3KRA9	Hexokinase				
P30041	Peroxisredoxin	PRX1			
P04908	H2A histone family, member A	HTA2, HTA1			
P62805	H4 histone family, member C	HHF1			
A6NIW5	Peroxisredoxin 2 isoform b				
B7Z2V7	Syntaxin binding protein 1				
Q9UPY8	Microtubule-associated protein RP/EB family member 3	BIM1	+		
P48047	ATP synthase oligomycin sensitivity conferral protein	ATP5			
Q6AWC5	Guanine nucleotide binding protein α				
P23528	Cofilin				
P09936	Ubiquitin carboxyl-terminal hydrolase isozyme L1				
Q16555	Dihydropyrimidinase related protein-2				
Q01082	Spectrin β chain				
Q99962	SH3-containing GRB2-like protein 2				
P40925	Cytosolic malate dehydrogenase				
P61978	Heterogeneous nuclear ribonucleoprotein K				
P07195	Lactate dehydrogenase B				
B4DGT1	Spectrin α chain				
P15924	Desmoplakin				
O00499	Myc box dependent interacting protein 1				
P08670	Vimentin				
Q92508	Hypothetical protein KIAA0233				
P05026	Sodium/potassium-transporting ATPase β -1 chain				
P00918	Carbonic anhydrase II				
B3KTM0	Microtubule-associated protein tau isoform 4				

	Q02413	Desmoglein 1 precursor				
	P07196	Similar to neurofilament, light polypeptide 68 kDa				
	P08758	Annexin A5				
	P02686	Myelin basic protein				
	Q8TC62	Septin 7				
	P04075	Fructose-bisphosphate aldolase A				
	Q86W61	Versican core protein precursor				
	Q9GZV7	Brain link protein-1 precursor				
	P09972	Aldolase C, fructose-bisphosphate				
	P02768	Similar to α -fetoprotein				
	Q92752	Tenascin-R				
	P17600	Synapsin I				
	Q16352	α -internexin				
	Q4W5L2	α -synuclein				
	B4DFN6	2',3'-cyclic nucleotide 3'-phosphodiesterase				
	A8K161	Calcium/calmodulin-dependent protein kinase type II α chain				
	P12277	Creatine kinase, B chain				
	P13073	Cytochrome c oxidase subunit IV isoform 1				
	P02792	Ferritin light chain				
	P47929	Galectin 7				
	P62937	Peptidyl-prolyl cis-trans isomerase A	CPR1, CPR5, CPR2, CPR3	+	+	+
	Q92777	Synapsin II				
α-synuclein associated	Q99798	Aconitase 2				
	O95782	Adaptor-related protein complex 2, α 1	APL3			
	P63010	Adaptor-related protein complex 2, β 1				
	P37840	α -synuclein				
	P38606	Atpase, lysosomal 70 kd, v1 subunit α				
	Q9ULU8	Calcium-dependent secretion activator				
	P06702	Calgranulin β				
	P16152	Carbonyl reductase 1				
	Q00610	Clathrin heavy chain 1	CHC1			
	P53621	Coatomer protein complex, subunit α	COP1			
	Q16555	Collapsin response mediator protein HCRMP-2				
	Q13616	Cullin 13	CDC53			
	O15075	Doublecortin-like kinase3				
	Q14203	Dynactin 1				
	O00429	Dynammin-like protein	DNM1			
	Q14204	Dynein, heavy polypeptide 1	DYN1	+		+
	Q5XPI4	E3 ubiquitin ligase kpc1, ring finger protein 1233				
	Q9UK22	F-box protein 23				
	P06396	Gelsolin				
	P06744	Glucose phosphate isomerase	PGI1		+	+
P04406	Glyceraldehyde-3-phosphate dehydrogenase	TDH3, TDH1, TDH2		+		
P09471	Guanine nucleotide binding protein α	GPA1, GPA2		+	+	

7. Annexes

	P08238	Heat shock protein 90 kda	HSC82, HSP82		+	
	P31939	Imp cyclohydrolase	ADE16, ADE17		+	
	Q02750	Mek1, mitogen-activated protein kinase kinase 1				
	P30044	Peroxiredoxin 53	AHP1	+	+	+
	Q15149	Plectin 1				
	Q13200	Proteasome 26s non-ATPase subunit 23	RPN1			
	P30101	Protein disulfide isomerase-associated 3	EUG1	+		
	P05771	Protein kinase c, β 1				
	Q13813	Spectrin, α				
	Q01082	Spectrin, β				
	P09936	Ubiquitin c-terminal hydrolase I1				
	P62988	Ubiquitin3				
	P22314	Ubiquitin-activating enzyme E1	UBA1			
	Q96FW1	Ubiquitin-specific protease otubain 13				
	Q96QK1	Vacuolar protein sorting 35	VPS35	+	+	+
	O75083	WD repeat-containing protein 1	AIP1		+	
	Familial ALS associated	P08553	Neurofilament triplet M protein (NFM)			
P19246		Neurofilament triplet H protein (NFH)				
P08551		Neurofilament triplet L protein (NFL)				
P08553		NFM				
P03995		Glial fibrillary acidic protein (GFAP)				
P08113		Endoplasmic reticulum chaperone protein				
Q01853		Transitional endoplasmic reticulum ATPase	CDC48			
P07901		Heat shock protein HSP 90 α	HSC82, HSP82		+	
Q91VD9		NADH-ubiquinone oxidoreductase 75 kDa subunit				
Q64521		Glycerol-3-phosphate dehydrogenase				
Q99KI0		Aconitase	ACO1		+	+
P20152		Vimentin				
P63017		Heat shock cognate 71 kDa protein (HSC70)	SSA2			
P09103		Protein disulfide-isomerase (PDI)	PDI1			
P46660		α -internexin				
O08553		Dihydropyrimidinase-related protein 2	DAL1	+		+
P52480		Pyruvate kinase M2	CDC19, PYK2			
P26443		Glutamate dehydrogenase 1	GDH3, GDH1		++	
Q03265		ATP synthase α chain (ATPase)	ATP1			
P20152		Vimentin				
P17182		α -enolase	ENO1, ENO2, ERR2, ERR3		++	++
P30275		Creatine kinase				
P15105		Glutamine synthetase	GLN1			
P15106		Glutamine synthetase				
P05201		Aspartate aminotransferase	AAT2		+	
Q9D6R2		Isocitrate dehydrogenase [NAD] subunit α	IDH2			
P63085		Mitogen-activated protein kinase 1 (ERK2)	FUS3, KSS1	+		
P05063	Fructose-bisphosphate aldolase C (aldolase)					

P16858	Glyceraldehyde-3-phosphate dehydrogenase (GAPDH)				
Q9D051	Pyruvate dehydrogenase E1+	PDB1			+
P62880	Guanine nucleotide-binding protein G(I)/G(S)/G(T) subunit β -2				
P16125	L-lactate dehydrogenase B chain (LDH)				
P14152	Cytosolic malate dehydrogenase				
P48036	Annexin A5				
P61982	14-3-3 protein γ				
P14602	Heat-shock protein β -1 (HSP27)				
P23927	α crystallin B chain				
P17742	Peptidyl-prolyl cis-trans isomerase A (CypA)	CPR1	+	+	+
P00441	SOD1	SOD1		+	
Q61292	Laminin subunit β -2				
Q60932	Voltage-dependent anion-selective channel protein 1 (VDAC1)	POR1, POR2			+